
Oil Production Greenhouse Gas Emissions Estimator

OPGEE v2.0b

User guide & Technical documentation

Hassan M. El-Houjeiri,^{1,*} Mohammad S. Masnadi,¹ Kourosh Vafi,^{1,*} James Duffy,²
Adam R. Brandt^{1,†}

With technical contributions from:

Jingfan Wang¹, Sylvia Sleep,³ Diana Pacheco,⁴ Zainab Dashnadi,³ Andrea Orellana,^{4,*}
Jacob Englander,¹ Scott McNally,^{1,*} Heather MacLean,⁴ Joule Bergerson³

¹ Department of Energy Resources Engineering, Stanford University

² California Air Resources Board, Alternative Fuels Section

³ Department of Chemical and Petroleum Engineering, University of Calgary

⁴ Department of Civil and Environmental Engineering, University of Toronto

* Prior affiliation, now employed elsewhere

[†]Corresponding author: abrandt@stanford.edu, +1 (650) 724 8251

June 5th, 2017

Funded by:

California Environmental Protection Agency, Air Resources Board

Contents

| | | |
|-----------|---|------------|
| 1 | Acknowledgements | 10 |
| I | Introduction and user guide | 11 |
| 2 | Introduction | 12 |
| 2.1 | Model motivation | 12 |
| 2.2 | OPGEE model goals | 13 |
| 2.3 | OPGEE model construction | 13 |
| 3 | User guide | 18 |
| 3.1 | Input worksheet | 18 |
| 3.2 | Process stage worksheets | 18 |
| 3.3 | Supplementary worksheets | 20 |
| 3.4 | Output gathering worksheets | 21 |
| 3.5 | Structure of each worksheet | 21 |
| 3.6 | Working with OPGEE | 22 |
| 3.7 | Inputs | 32 |
| II | Technical documentation | 34 |
| 4 | Process stage worksheets | 35 |
| 4.1 | Exploration emissions | 35 |
| 4.2 | Drilling & development | 38 |
| 4.3 | Production & extraction | 50 |
| 4.4 | Surface Processing | 87 |
| 4.5 | Maintenance operations | 109 |
| 4.6 | Waste treatment and disposal | 110 |
| 4.7 | Crude oil transport | 111 |
| 5 | Supplemental calculations worksheets | 115 |
| 5.1 | Gas balance | 115 |
| 5.2 | Steam generation for thermal oil recovery | 116 |
| 5.3 | Upgrading | 128 |
| 5.4 | Electricity | 131 |
| 5.5 | Drivers | 132 |
| 5.6 | Fuel cycle | 135 |
| 5.7 | Embodied emissions | 136 |

| | | |
|----------|--|------------|
| 5.8 | Emissions factors | 145 |
| 5.9 | Venting and fugitive emissions | 150 |
| 5.10 | Compressors | 161 |
| 5.11 | Flaring | 161 |
| 6 | Gathering worksheets | 169 |
| 6.1 | 'Energy Consumption' gathering worksheet | 169 |
| 6.2 | 'GHG Emissions' gathering worksheet | 170 |
| 7 | 'Active Field' gathering worksheet | 172 |
| 8 | Fundamental data inputs | 174 |
| 8.1 | Global warming potentials | 174 |
| 8.2 | Properties of water and steam | 174 |
| 8.3 | Properties of air and exhaust gas components | 175 |
| 8.4 | Compositions and properties of fuels | 175 |
| 9 | OPGEE limitations | 177 |
| 9.1 | Scope limitations | 177 |
| 9.2 | Technical limitations | 177 |
| 9.3 | Future work | 179 |
| A | Terminology: Acronyms and abbreviations | 180 |
| B | Mathematical terms and definitions | 182 |
| C | Tabulated sources for each production stage | 187 |
| D | Bulk assessment macro error correction | 194 |
| E | Changes and updates from previous versions of OPGEE | 198 |
| E.1 | Changes and updates from OPGEE v2.0a to OPGEE v2.0b | 198 |
| E.2 | Changes and updates from OPGEE v1.1 Draft E to OPGEE v2.0a . . . | 198 |
| E.3 | Changes and updates from OPGEE v1.1 Draft D to OPGEE v1.1 Draft E | 199 |
| E.4 | Changes and updates from OPGEE v1.1 Draft C to OPGEE v1.1 Draft D | 199 |
| E.5 | Changes and updates from OPGEE v1.1 Draft B to OPGEE v1.1 Draft C | 200 |
| E.6 | Changes and updates from OPGEE v1.1 Draft A to OPGEE v1.1 Draft B | 201 |
| E.7 | Changes and updates from OPGEE v1.0 to OPGEE v1.1 Draft A . . . | 202 |
| E.8 | Changes from OPGEE v1.0 Draft A to OPGEE v1.0 | 205 |

List of Figures

| | | |
|------|--|----|
| 2.1 | Schematic chart showing included stages within OPGEE. | 14 |
| 2.2 | Proposed workflow for improving emissions estimates using OPGEE. | 16 |
| 3.1 | Types of cells. <i>User Free</i> and <i>Default Free</i> cells can be changed, while <i>Locked</i> cells should not be changed due to possibility of compromising model functionality. | 22 |
| 3.2 | Data input section of the ' <i>Inputs</i> ' worksheet. | 27 |
| 3.3 | Input data section of ' <i>Production & Extraction</i> ' worksheet. User inputs are in column M, while defaults are kept as reference in column N. | 29 |
| 3.4 | Graphical results for an example crude oil. These results from ' <i>Active Field</i> ' Tables 1.1 and 1.2, Figures 1.1 and 1.2. | 31 |
| 3.5 | Logical structure of the assessment macro. | 33 |
| 4.1 | Drilling hole diameters for simple, moderate and complex well construction. | 40 |
| 4.2 | All GHGfrack results for drilling fuel consumption in US gallons of diesel (includes both rotary table + mud circulation). | 42 |
| 4.3 | GHGfrack results for drilling fuel consumption segmented by well complexity. Fuel consumption reported in US gallons of diesel (includes both rotary table + mud circulation). | 43 |
| 4.4 | GHGfrack results for drilling fuel consumption. Only simple wells are represented, and the results are segmented by efficiency and wellbore orientation. Fuel consumption reported in US gallons of diesel (includes both rotary table + mud circulation). | 44 |
| 4.5 | Fuel use in hydraulic fracturing as a function of fracturing volume. Each curve represents a different fracturing gradient value, ranging from 0.6 psi/ft to 1.0 psi/ft. | 46 |
| 4.6 | Standing and Katz [1] Natural Gas Mixture Z-Factor Chart. | 53 |
| 4.7 | Correlation of Upper Portion of Standing and Katz Z-Factor Chart. Source: [2]. | 54 |
| 4.8 | Correlation of Lower Portion of Standing and Katz Z-Factor Chart. Source: [2]. | 54 |
| 4.9 | Moody friction factor chart. Source: [3]. | 60 |
| 4.10 | An example of a linear pressure traverse curve (GLR= 0). | 61 |
| 4.11 | Natural gas use in mining operations | 67 |
| 4.12 | Electricity use in mining operations | 68 |
| 4.13 | Non-integrated bitumen mining operation | 71 |

| | | |
|------|---|-----|
| 4.14 | Upgrader-integrated bitumen mining operation | 72 |
| 4.15 | Distributions of global oilfield ages. Mean date of discovery (by count not by production-weighted average) is 1978.4. | 74 |
| 4.16 | Distributions of giant oilfield ages. Mean date of discovery (by production-weighted average) is 1960.2. | 75 |
| 4.17 | Distributions of global oilfield depths in bins of 500 ft depth. $N = 4489$ fields, mean = 7238 ft, SD = 3591 ft, median = 6807 ft. | 76 |
| 4.18 | Distributions of oilfield per-well productivity (bbl oil/well-d) for bins of 500 bbl/d, counted by numbers of countries (bar) and by fraction of production (dot) $N = 92$ countries. | 76 |
| 4.19 | Distributions of oilfield per-well productivity (bbl oil/well-d) for all countries with per-well productivities lower than 500 bbl/well-d, counted by numbers of countries (bar) and by fraction of production (dot) $N = 55$ countries. | 77 |
| 4.20 | Ratio of producers to injectors as a function of per-well productivity. Source: Various. | 77 |
| 4.21 | Distributions of major gas species across 135 samples from California associated gas producers. | 80 |
| 4.22 | Distributions of California GORs, binned by crude density. | 80 |
| 4.23 | Exponential WOR model fit with smart default parameters. The best fit to data gives $a_{WOR} = 1.706$ and $b_{WOR} = 0.036$. Regions are colored as follows: Alberta (red), Alaska (green), California (orange), Norway (blue) and UK (beige). | 82 |
| 4.24 | Schematic of associated gas treatment with four main branches. The lower 3 branches model post-breakthrough CO_2 enhanced oil recovery separation pathways [4]. | 90 |
| 4.25 | Process flow diagram for OPGEE upgrading module | 92 |
| 4.26 | Glycol dehydrator simple process flow diagram [5, p. 141]. | 96 |
| 4.27 | Amine simple process flow diagram [5, p. 112]. | 99 |
| 5.1 | Once-through steam generator with mass and energy balance terms. Lower case terms are defined per lbmol of input fuel. | 117 |
| 5.2 | Increase of crude contaminant load with increase in crude specific gravity (decrease in API gravity). Data from: Speight (1994) and Swafford (2009). | 120 |
| 5.3 | Gas turbine plus heat recovery steam generator model. Mass flows represented by m and energy flows represented by fuel lower heating value (LHV), electric power out (e) and enthalpy of gases (h). . . | 121 |
| 5.4 | Predicted turbine exit temperatures for variety of turbines from literature (y -axis) as compared to reported value from the literature (x -axis). | 122 |
| 5.5 | Distribution of SOR values for California and Alberta thermal EOR projects (steamflood, cyclic steam stimulation, steam-assisted gravity drainage). | 128 |
| 5.6 | Casing plan for wells of complex, intermediate, and simple design. Well depths here are illustrative, and all steel consumption intensities are computed per unit length of well (per ft.). See text for sources. | 139 |

| | | |
|------|---|-----|
| 5.7 | Diagram illustrating cement volume calculations (per unit depth). Cement is presented in grey, while earth is presented in green-brown. | 140 |
| 5.8 | Default OPGEE cementing plan. Default non-conductor, non-surface casing fill-up is twice reported minimum, or 600 ft. | 142 |
| 5.9 | Flowchart illustrating the logic of the flaring computation worksheet. | 162 |
| 5.10 | Rayleigh distribution fit to 6 wind speed datasets from western United States. Data source: NREL Western Wind Integration Dataset. | 166 |
| 5.11 | Example of OPGEE wind speed distribution for a 30 mph average windspeed input. | 167 |
| D.1 | The errors fixing/entries adjustment logic. | 195 |
| D.2 | The errors fixing/entries adjustment logic for non-GOR, gas compo- sition related entries. | 197 |

List of Tables

| | | |
|------|--|----|
| 2.1 | Emissions classification, order of magnitude emissions, and significance description. | 17 |
| 4.1 | Default inputs for exploration emissions | 37 |
| 4.2 | Hole diameters for different casing sections under three wellbore designs (in.) | 39 |
| 4.3 | Bottomhole depth for different segments (ft.) | 39 |
| 4.4 | Constants for quadratic fit of fracturing fuel consumption equation . | 46 |
| 4.5 | Land use GHG emissions for 30 year analysis period from field drilling and development in OPGEE for conventional oil operations [g CO ₂ eq./MJ of crude oil produced]. Data from Yeh et al [6]. | 47 |
| 4.6 | Land use GHG emissions for 150 year analysis period from field drilling and development in OPGEE for conventional oil operations [g CO ₂ eq./MJ of crude oil produced]. Data from Yeh et al [6]. | 48 |
| 4.7 | Default inputs for drilling calculations. | 49 |
| 4.8 | Comparison of Z-Factors for OPGEE Default natural gas, nitrogen, carbon dioxide, air, and oxygen During Compression to 20,000 PSIA. Note that air and oxygen are included for reference only, as OPGEE v2.0b does not include air- or oxygen-based EOR modeling. | 52 |
| 4.9 | Minimum Miscibility Pressure and API Gravity Default Correlation. Source: [7]. | 56 |
| 4.10 | Temperature Adjustment to Minimum Miscibility Pressure Default Correlation Source: [7]. | 56 |
| 4.11 | Reynold's number (Re) ranges of different flow patterns. Data from McAllister [8]. | 59 |
| 4.12 | Characteristics of operating mining projects | 64 |
| 4.13 | Non-integrated PFT mining energy intensities | 67 |
| 4.14 | Comparison between stand-alone mine energy consumption estimates based on COSIA mine template to integrated NFT mining and upgrading energy consumption reported by AER | 69 |
| 4.15 | Integrated NFT mining energy intensities | 70 |
| 4.16 | Mean and median injector to producer ratios. | 75 |
| 4.17 | Data on production, number of production wells, and number of injection wells by offshore field. | 78 |
| 4.18 | GOR values by crude oil API gravity bin. | 81 |
| 4.19 | Default inputs for production and extraction. | 84 |
| 4.20 | Description of OPGEE's Associated Gas Processing Schemes | 88 |

| | | |
|------|--|-----|
| 4.21 | Typical concentrations of process water pollutants. Table from Vlasopoulos et al [9]. | 104 |
| 4.22 | Categorization of water treatment technologies. Table based on table from Vlasopoulos et al. [9], with minor modifications | 105 |
| 4.23 | Default inputs for surface processing. | 107 |
| 4.24 | Default inputs for Transport. | 114 |
| 5.1 | Hydrogen constant a_H as a function of API gravity. | 120 |
| 5.2 | Gas turbine model results for hypothetical turbines A-D. These results serve as input data to OPGEE GT model. | 123 |
| 5.3 | Default inputs for steam injection calculations. | 125 |
| 5.4 | Indicators of SOR distributions for California and Alberta thermal EOR production. Units are bbl of cold water equivalent (CWE) per bbl of oil. | 127 |
| 5.5 | Inputs to OPGEE upgrading module from the Oil Sands Technology Upgrading Model (OSTUM) | 130 |
| 5.6 | Types and size ranges of the drivers embedded in OPGEE. | 132 |
| 5.7 | Default inputs for drivers calculations. | 134 |
| 5.8 | Cement blends modeled in OPGEE. ^a | 141 |
| 5.9 | Combustion technologies and fuels included in OPGEE. | 146 |
| 5.10 | ARB data used in the calculation of venting emissions factors (unit specified below). Source: [10]. | 147 |
| 5.11 | ARB data used in the calculation of fugitives emissions factors (unit specified below). Source: [10]. | 147 |
| 5.12 | ARB data for gas dehydrators, for systems with and without vapor recovery systems (VRS). Source: [11]. | 148 |
| 5.13 | An example of EPA emissions factors for oil and gas production components (g/unit-yr). Source: [12]. | 148 |
| 5.14 | Emissions data used in the estimation of operational venting. Data from California oil fields, 2007. Source: [10], except where otherwise noted. | 151 |
| 5.15 | Categorization of venting emissions sources by process stage. | 154 |
| 5.16 | Data used in the estimation of fugitives. Source: [10]. | 155 |
| 5.17 | Estimating the number of remaining components. | 155 |
| 5.18 | Speciation fractions for total hydrocarbon (THC) emissions calculated using API emissions factors [%]. | 156 |
| 5.19 | Categorization of fugitive emissions sources by process stage. | 157 |
| 5.20 | Default inputs for venting, flaring, and fugitive emissions. | 159 |
| 5.21 | Sources of flaring data and construction notes | 161 |
| 5.22 | Data requirements for utilizing field-specific flaring calculation. | 163 |
| 5.23 | Stoichiometric relationships for complete combustion. | 165 |
| 5.24 | Default inputs for venting, flaring, and fugitive emissions. | 168 |
| A.1 | Acronyms and abbreviations. | 180 |
| B.1 | Mathematical symbols and subscripts. | 183 |
| C.1 | Emissions sources from exploratory operations. For inclusion: 0 = not included, 1 = included. | 188 |

| | | |
|-----|--|-----|
| C.2 | Emissions sources from drilling operations. | 189 |
| C.3 | Emissions sources from production and extraction operations. | 190 |
| C.4 | Emissions sources from surface processing operations. | 191 |
| C.5 | Emissions sources from maintenance operations. | 191 |
| C.6 | Emissions sources from waste treatment and disposal operations. . . | 192 |
| C.7 | Emissions sources from transport. | 193 |

1 Acknowledgements

The construction and improvement of OPGEE has benefitted from significant technical and financial support.

Because OPGEE is an open-source project, we would like to acknowledge technical support, feedback, error corrections, and other useful suggestions from the following individuals: Jessica Abella (ICF International), Joule Bergerson (University of Calgary), Kevin Cleary (California Air Resources Board), John Courtis (California Air Resources Board), Trevor Demayo (Chevron), Cheryl Dereniwski (IHS), Jacob Englander (Stanford University), Jackie Forrest (IHS), Sebastian Galarza (International Council on Clean Transportation), Deborah Gordon (Carnegie Endowment for Global Peace), Gary Howorth (Energy Redefined), Johnathan Lillien (Chevron), Ella Lowry (Stanford University), Christopher Malins (International Council on Clean Transportation), Jeremy Martin (Union of Concerned Scientists), Simon Mui (Natural Resources Defense Council), Don O'Connor (S&T² Consultants), Jeff Rosenfeld (ICF International), Greg Schively (Booz Allen Hamilton), Timothy Skone (National Energy Technology Laboratory), Yuchi Sun (Stanford University), Luke Tonachel (Natural Resources Defense Council), Stefan Unnasch (Life Cycle Associates, LLC), Ann-Catarin Vaage (Statoil), Michael Wang (Argonne National Laboratory), Wojciech Winkler (European Commission, DG Climate).

Of course, all remaining errors and omissions remain the responsibility of the model authors.

We would like to acknowledge funding support for the development of OPGEE from the California Environmental Protection Agency, Air Resources Board (primary funder through research grants 10-418 and 13-408). We would like to acknowledge additional funding support for OPGEE development and application from: Carnegie Endowment for Global Peace; European Commission, Directorate General Climate; International Council on Clean Transportation; and Stanford University School of Earth Sciences.

Part I

Introduction and user guide

2 Introduction

The Oil Production Greenhouse gas Emissions Estimator (OPGEE) is an engineering-based life cycle assessment (LCA) tool that estimates greenhouse gas (GHG) emissions from the production, processing, and transport of crude petroleum. The system boundary of OPGEE extends from initial exploration to the refinery gate (see Figure 2.1).

This technical documentation introduces OPGEE and explains the calculations and data sources in the model. First, the overall goals and motivation for OPGEE are described. Then, the general structure of OPGEE is introduced with a brief explanation of the worksheets contained in the model. Next, each production stage is explained in detail, outlining the methods and assumptions used to generate estimates of energy use and emissions for that stage. Then supplemental calculation worksheets are outlined. Next, the gathering worksheets which collect and aggregate intermediate results are described. Lastly, we describe the worksheets that contain fundamental data inputs.

2.1 Model motivation

Current research suggests that GHG emissions from petroleum production can be quite variable [13–20]. Facilities will have low GHG emissions per unit of energy produced if they do not rely on energy intensive production methods and apply effective controls to fugitive emissions sources. In contrast, some crude oil sources can have higher GHG emissions if they rely on energy-intensive production methods.

The variability in crude oil production emissions is partly due to the use of energy-intensive secondary and tertiary recovery technologies [18, 21, 22]. Another major factor is significant variation in the control of venting, flaring and fugitive (VFF) emissions [23–25]. Other emissions arise from increased pumping and separation work associated with increased fluid handling in depleted oil fields (i.e., fields with a high water-oil ratio).

The existing set of general fuel cycle emissions models, exemplified by GREET and GHGenius [22, 26], cover a wide range of transport fuels, from biofuels to electric vehicles. These broad models have the advantage of being publicly available and transparent. Unfortunately, they lack process-level detail for any particular fuel cycle and only represent pathway averages. For example, conventional crude oil production in GREET is modeled using a common default production pathway, fuel mix, and energy efficiency. While these LCA tools have been useful to date, future regulatory approaches will require a more specific method of assessing the differences between crude oil sources.

Box 1.1. Goals of OPGEE

1. Build a rigorous, engineering-based model of GHG emissions from oil production operations.
2. Use detailed data, where available, to provide maximum accuracy and flexibility.
3. Use public data wherever possible.
4. Document sources for all equations, parameters, and input assumptions.
5. Provide a model that is free to access, use, and modify by any interested party.
6. Build a model that easily integrates with existing fuel cycle models and could readily be extended to include additional functionality (e.g. refining)

2.2 OPGEE model goals

The goals of OPGEE development are listed in Box 1.1.

First, OPGEE is built using engineering fundamentals of petroleum production and processing. This allows more flexible and accurate emissions estimations from a variety of emissions sources.

OPGEE is constructed using *Microsoft Excel* to ensure transparency and maximum accessibility by stakeholders, including industry, governments, and members of the public. OPGEE will be available for download from Stanford University servers, and servers of future institutions in which Adam Brandt is employed. This will ensure its future availability. Regular updates of the model are expected in intervals of 1-2 years.

Another goal of OPGEE is the generation of comprehensive documentation. Model functions and input data are documented within the *Excel* worksheet to allow effective use and modification of the tool by users. Additionally, this document serves to explain model calculations and assumptions and provides information on model data sources.

2.3 OPGEE model construction

2.3.1 Model functional unit

The functional unit of OPGEE is 1 MJ of crude petroleum delivered to the refinery entrance (a well-to-refinery, or WTR process boundary). This functional unit is held constant across different production and processing pathways included in OPGEE. This functional unit allows integration with other fuel cycle models that calculate refinery emissions per unit of crude oil processed, and to enable integration with refinery emissions models such as PRELIM [27]. The heating value basis can be chosen as lower or higher heating value (LHV or HHV), depending on the desired basis for the emissions intensity. The model defaults to LHV basis for best integration with GREET.

2.3.2 Model scope and focus

OPGEE includes emissions from all production operations required to produce and transport crude hydrocarbons to the refinery gate (see Figure 2.1 for model sys-

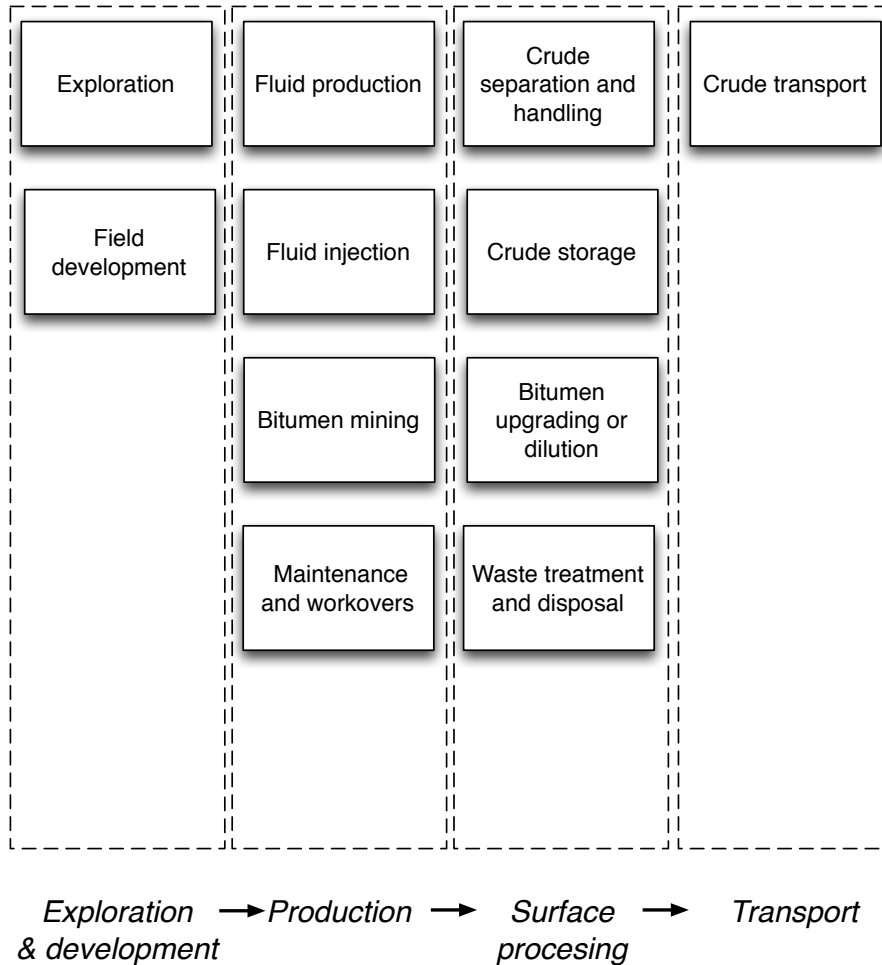


Figure 2.1: Schematic chart showing included stages within OPGEE.

tem boundaries). Included production technologies are: primary production (e.g. water injection), secondary production (e.g. water flooding), and major tertiary recovery technologies (also called enhanced oil recovery or EOR, e.g. CO₂ EOR). Bitumen mining and upgrading processes are also included.

2.3.3 Spreadsheet structure

OPGEE is modular in structure, with interlinked worksheets representing each production stage. Within each major production stage, a number of activities and processes occur (e.g., fluid production or fluid injection). Calculations take place sequentially and are numbered in a hierarchical fashion (see Box 2.1 for explanation of pointers to the model in this document).

2.3.4 Modeling detail and default specifications

OPGEE models oil production emissions in more detail than previous LCA models. For example, the energy consumed in lifting produced fluids (oil, water, and associated gas) to the surface is computed using the fundamental physics of fluid

lifting, accounting for friction and pump efficiencies.

Increased modeling detail results in an increase in the number of model parameters. All required inputs to OPGEE are assigned default values that can be kept as is or changed to match the characteristics of a given oil field or marketable crude oil blend. If only a limited amount of information is available for a given facility, most input values will remain equal to defaults. In contrast, if detailed field-level data are available, a more accurate emissions estimate can be generated.

For some processes and sub-processes, correlations or relationships are developed for defaults, which we call "smart defaults". For example, the amount of water produced with oil (water-oil-ratio, or WOR) affects the energy consumed in lifting, handling, and separating fluids. If the WOR is known, it can be inputted directly. However, in some regions, water production is not reported, so OPGEE includes a statistical relationship for water production as a function of reservoir age (see Section 4.3.3.7 for a description of the analysis underlying this smart default).

A workflow for updating and improving the data basis and accuracy of an emissions estimate using OPGEE is shown in Figure 2.2. This workflow represents one possible way that OPGEE could be used.

2.3.5 Emissions sources classification

Each process stage or sub-process in OPGEE can result in a variety of emissions sources. For example, the '*Drilling & Development*' process stage includes the terrestrial drilling sub-process. Terrestrial drilling could include the following emissions sources:

- Combustion emissions from drilling rig prime mover;
- Flaring emissions from drilling rig;
- Vents and other upset emissions from drilling rig;
- Combustion emissions from work performed in land clearing and site preparation;
- Biogenic emissions from ecosystem disturbance during development;
- Embodied emissions in cement and casing;
- Embodied emissions in other consumable materials (e.g., fracturing sand)

Note that these emissions sources are of significantly different magnitude and have different causation and potential methods of mitigation. In total, over 100 emissions sources are classified in OPGEE v2.0b across all process stages (e.g., all included processes and sub-processes). See Appendix C for a complete tabulation and classification of emissions sources. Model coverage is also shown in the '*Model Coverage*' tab of OPGEE v2.0b.

2.3.6 Emissions source significance cutoffs

It would be infeasible (and counter-productive) to attempt to estimate the magnitude of every emissions source listed in Appendix C. Fortunately, a small number

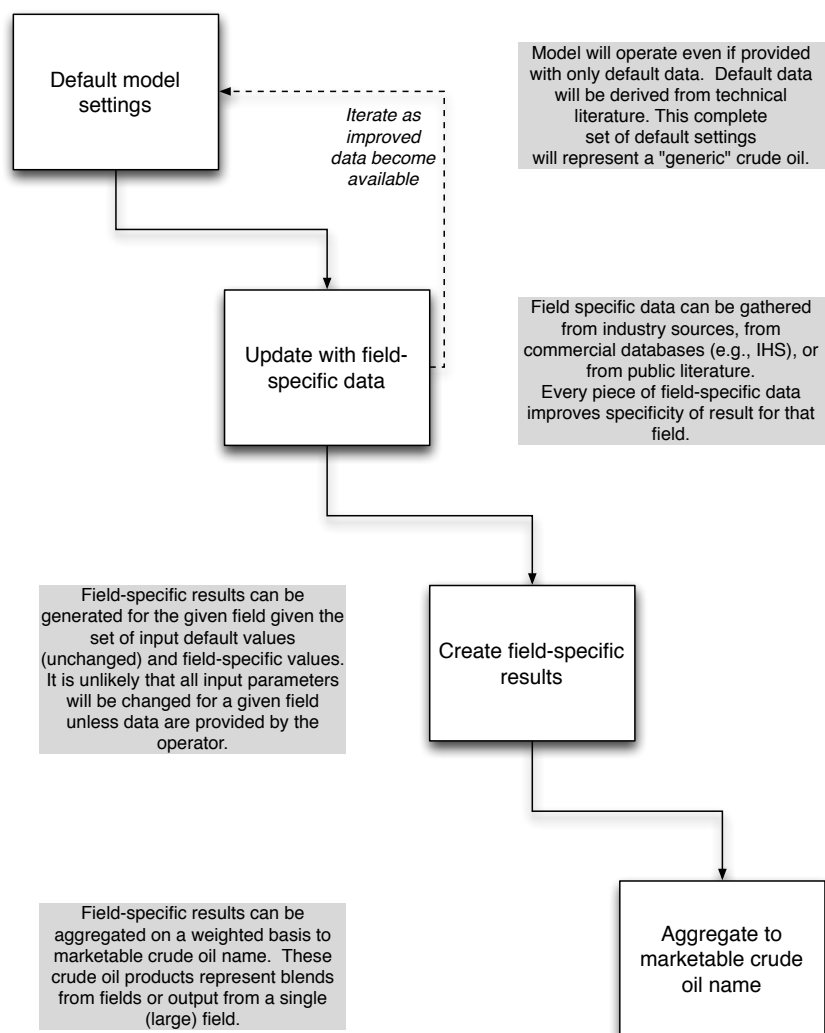


Figure 2.2: Proposed workflow for improving emissions estimates using OPGEE.

of emissions sources will result in most of the emissions from petroleum production operations.

For this reason, emissions sources included in the OPGEE system boundary are classified by estimated emissions magnitude. These emissions magnitudes are meant to represent *possible* emissions magnitudes from a source, not the actual emissions that would result from that source for any particular field. An order-of-magnitude estimation approach is used, with each source assigned a rating in “stars” from one-star (*) to four-star (****) corresponding to 0.01 to 10 g CO₂ eq. per MJ of crude oil delivered to the refinery gate. These classifications are explained in Table 2.1.

Emissions estimated to be one-star emissions (*) are not modeled in OPGEE due to insignificant magnitude. Since these small sources are known to have non-zero emissions, they are included in the overall emissions estimate by including a “small sources” term. Two-star (**) sources are included simply or are included in the small sources term. Often, two-star sources are minor in magnitude, but are

Results 2.8

Table 2.1: Emissions classification, order of magnitude emissions, and significance description.

| Class | Est. mag. [gCO ₂ /MJ] | Description |
|-------|-------------------------------------|--|
| * | 0.01 | Minor emissions sources not worthy of further study or estimation. This is the most common classification. One-star emissions are accounted for by adding a value for miscellaneous minor emissions. |
| ** | 0.1 | Minor emissions sources that are often neglected but may be included for physical completeness. |
| *** | 1 | Sources that can have material impacts on the final GHG estimate, and therefore are explicitly modeled in OPGEE. |
| **** | 10 | Sources that are large in magnitude (though uncommon). Examples include steam production for thermal oil recovery and associated gas flaring. These sources are significant enough to require their own dedicated OPGEE modules. |

modeled due to the need to model the physics and chemistry of crude oil production and processing.¹ Three-star (***) sources are explicitly modeled in OPGEE. Four-star sources (****) are modeled in detail with stand-alone modules to allow variation and uncertainty analysis.

2.3.7 Data sources

Because of the need for transparent data basis, OPGEE uses data from a variety of technical reference works. For example, emissions factors are derived from standard engineering references from the American Petroleum Institute (API) and Environmental Protection Agency (EPA) [28, 29]. A large number of technical references, journal articles, and fundamental data sources have been consulted during the construction of OPGEE, including:

- Exploration and drilling [29–36]
- Production and surface separations [5, 12, 28, 29, 37–64]
- Secondary and tertiary recovery [65–70]
- Water treatment and waste disposal [36, 59, 62, 71–74]
- Venting, flaring, and fugitive emissions [12, 37–39, 39–45, 75–79]
- Petroleum transport and storage [8, 42, 45, 55, 78, 80–83]

¹No strict criteria exist to determine the inclusion or exclusion of two-star sources. Modeler judgement is applied to determine the need for modeling these sources.

3 User guide

OPGEE is divided into four types of worksheets: (1) input sheets, (2) process stage worksheets, (3) supplementary worksheets, and (4) output gathering worksheets.

3.1 Input worksheet

'Inputs' worksheet Data are entered on the input worksheet in OPGEE v2.0b. This worksheet is labeled *'Inputs'* and is colored green. The user can input a simplified set of ≈ 50 data inputs on the *'Inputs'* worksheet. Data for hundreds of fields can be entered on the *'Inputs'* sheet. The data entered by the user are stored on the *'Inputs'* sheet without modification, so the *'Inputs'* sheet can be used to compile and store data for a variety of operations.

OPGEE v2.0b is run from the *'Inputs'* sheet. The user enters the starting field of analysis and the ending field of analysis and presses the "Run Assessment" button. See more detail about using the model below.

3.2 Process stage worksheets

Process stage worksheets form the core of OPGEE, and are where most model calculations occur. These worksheets have red-colored tabs.

3.2.1 *'Exploration' worksheet*

The *'Exploration'* worksheet contains pre-production emissions that occur during primary exploration for petroleum. These emissions are generally very small in magnitude when amortized over the productive life of an oil field, as they occur only at the outset of production. For this reason, these sources are classified as below the significance cutoff in OPGEE v2.0b. Exploration emissions are described in more detail in Section 4.1, and emissions sources from exploration are listed and classified in Table C.1.

3.2.2 *'Drilling & Development' worksheet*

The *'Drilling & Development'* worksheet includes emissions that occur during development of crude oil production facilities. Key sources include drilling of wells, hydraulic fracturing of wells, and land use impacts from land clearing and conversion. Drilling and development emissions tend to be relatively small because they only occur at the outset of production or sporadically during field life. Drilling and development emissions are described in more detail in Section 4.2, and emissions sources from drilling and development are listed and classified in Table C.2.

3.2.3 *'Production & Extraction' worksheet*

The *'Production & Extraction'* worksheet models the work required to lift fluids from the subsurface and to inject fluids into the subsurface. OPGEE includes the two most common lifting technologies: sucker-rod pumps and gas lift. Also included are the energy requirements of water flooding, gas flooding, and steam flooding. The lifting model used for calculating lifting energy is a single phase flow model which neglects gas slippage. Injection horsepower is calculated based on operating pressures and temperatures using fundamental physics. Production emissions are described in more detail in Section 4.3, and emissions sources from production are listed and classified in Table C.3.

3.2.4 *'Surface Processing' worksheet*

The *'Surface Processing'* worksheet models handling of crude, water, and associated gas with a set of common industry technologies. By defining default configurations and parameter values, the amount of data required is reduced. For example, in gas processing, default processes are assumed such as the amine-based acid gas removal (AGR), glycol-based gas dehydration units, or a dual membrane-amine AGR process used for CO₂ enhanced oil recovery associated gas processing. Process flow diagrams are included in the surface processing worksheet for improved readability. Surface processing emissions are described in more detail in Section 4.4, and emissions sources from surface processing are listed and classified in Table C.4.

3.2.5 *'Maintenance' worksheet*

The *'Maintenance'* worksheet includes venting and fugitive emissions associated with maintenance. These emissions occur during compressor blowdowns, well workovers and cleanups, and gathering pipeline maintenance. Maintenance emissions are described in more detail in Section 4.5, and emissions sources from maintenance are listed and classified in Table C.5.

3.2.6 *'Waste Disposal' worksheet*

The *'Waste Disposal'* worksheet includes emissions associated with waste disposal are within the system boundary of OPGEE. These sources are believed to be below the significance cutoff, so they are not explicitly modeled in OPGEE. Waste disposal emissions are described in more detail in Section 4.6, and emissions sources from waste disposal are listed and classified in Table C.6.

3.2.7 *'Transport' worksheet*

The *'Transport'* worksheet calculations allow variation in transport modes and in the distance travelled. Transport emissions are modeled using the method established in CA-GREET [84]. Transport emissions are described in more detail in Section 4.7, and emissions sources from transport are listed and classified in Table C.7.

3.3 Supplementary worksheets

Supplementary worksheets support calculations throughout OPGEE, including: calculating intermediate outputs in the process stage worksheets, compiling output in the gathering worksheets, and calculating results in the *'Active Field'* worksheet. Supplementary worksheets have blue-colored tabs.

'Gas Balance' worksheet This worksheet tracks produced gas composition from production to final user or sale to ensure that all produced gas is accounted for in the gas processing equipment, VFF emissions, and final gas sales. The *'Gas Balance'* worksheet is described in Section 5.1.

'Steam Generation' worksheet This worksheet is supplementary to the production and extraction worksheet and calculates in detail the natural gas consumed and electricity cogenerated (if applicable) during steam generation. The *'Steam Generation'* worksheet is described in Section 5.2.

'Upgrading' worksheet This worksheet provides a database of input data for modeling of crude oil upgrading for heavy oil and bitumen resources. The *'Drivers'* worksheet is described in Section 5.3.

'Electricity' worksheet This worksheet determines the offsite electricity mix and calculates the energy consumption in onsite electricity generation (other than electricity co-generated with steam). The *'Electricity'* worksheet is described in Section 5.4.

'Drivers' worksheet This worksheet provides a database of energy consumption for different types and sizes of prime movers (gas and diesel engines, gas turbines and electric motors). The *'Drivers'* worksheet is described in Section 5.5.

'Fuel Cycle' worksheet This worksheet retrieves and calculates the fuel cycle energy consumption and GHG emissions for the calculation of credits/debits from fuel exports/imports. The *'Fuel Cycle'* worksheet is described in Section 5.6.

'Emission Factors' worksheet This worksheet retrieves and builds emissions factors for the calculation of combustion and non-combustion GHG emissions from energy use and losses. The *'Emissions Factors'* worksheet is described in Section 5.8.

'Venting & Fugitives' worksheet This worksheet calculates in detail the GHG emissions associated with Venting and fugitives. The *'Venting & Fugitives'* worksheet is described in Section 5.9.

'Compressors' worksheet This worksheet performs detailed calculations for compressors located in the *'Surface Processing'* and *'Production & Extraction'* worksheets. The *'Compressors'* worksheet is described in Section 5.10.

'Flaring' worksheet This worksheet calculates in detail the GHG emissions associated with flaring. The *'Flaring'* worksheet is described in Section 5.11.

'Fuel Specs' worksheet This worksheet provides fuel specifications required for OPGEE calculations. The *'Fuel Specs'* worksheet is described in Section 8.

'Input Data' worksheet This worksheet provides other needed data inputs such as conversion factors and steam enthalpies. The *'Input Data'* worksheet is described in Section 8.

3.4 Output gathering worksheets

Output worksheets gather the information from the process stage calculations and compile them into summed energy consumption (including energy co-production credits) and summed GHG emissions (including any offsets from co-produced energy). Also included in the output worksheets is the worksheet where users input key parameters and display summary results. Output worksheets have brown-colored tabs.

‘Results’ worksheet The ‘Results’ worksheet compiles information for the analyzed crude, and represents the holding sheet for all changed parameters that are adjusted by OPGEE algorithms. The ‘Results’ sheet should be the place where the user obtains final results for large runs of multiple fields.

‘Active Field’ worksheet The ‘Active Field’ worksheet presents summary inputs and results in tabular and graphical form for the most recently processed field. It allows for detailed tracking and analysis of the results for an individual field. The ‘Active Field’ worksheet is described in Section 7. Importantly, the ‘Active Field’ worksheet serves as a holding place for information on the field currently under analysis during an OPGEE run, and logic on the sheet applies many of the “smart defaults” defined below. For this reason, the ‘Active Field’ worksheet should not be modified (at least without great care).

‘Energy Consumption’ worksheet The ‘Energy Consumption’ worksheet gathers data on energy consumption for sub-processes from all process worksheets. Each main process worksheet is included in the gathering table. All energy consumed is summed by type across all stages. This gross consumption is used to compute net consumption and energy imports and exports. The ‘Energy Consumption’ worksheet is described in Section 6.1

‘GHG Emissions’ worksheet The ‘GHG Emissions’ worksheet takes the energy quantities consumed in each stage and converts them to emissions using emissions factors. It also gathers any emissions associated with land use change and VFF emissions. Emissions are computed as $\text{gCO}_2\text{eq./d}$. The ‘GHG Emissions’ worksheet is described in Section 6.2.

3.5 Structure of each worksheet

Each process stage worksheet is divided into two main sections: (i) input data and (ii) calculations. The input data section is where the user enters the input parameters (e.g., API gravity, production volume). The input section of each worksheet has two data columns: *User* and *Default*, in columns M and N, respectively. The cells within the *User* column are the active cells, and are used to generate results. The cells within the *Default* column are used for reference, bookkeeping of default values, and generating defaults using correlations based on field data.

Below the input data section is the calculations section of a worksheet, where intermediate model outputs are calculated. These intermediate outputs are summarized and compiled by the gathering worksheets to provide the overall energy and emissions measures compiled in the ‘Outputs’ worksheet.

| | |
|-------------------|---------------------------|
| User free | Free to change |
| Default free | Do not change |
| User dependent | Reference |
| Default dependent | Reference - Do not change |

Figure 3.1: Types of cells. *User Free* and *Default Free* cells can be changed, while *Locked* cells should not be changed due to possibility of compromising model functionality.

3.5.1 Types of model cells

Four main types of cells exist in the calculation columns M and N: *User Free*, *User Locked*, *Default Free*, *Default Locked* (See Figure 3.1). As might be expected, locked cells should not be changed.¹ This is typically because locked cells contain formulas that draw on other cells and therefore should not be changed. “User Free” cells are cells that allow entry of user data.

3.6 Working with OPGEE

This section explains how to work with OPGEE. Box 2.1 shows how to best use this documentation in concert with the OPGEE model itself.

3.6.1 Primary interaction

The easiest way to use OPGEE (which this document calls “primary” interaction) is to input key parameters for a field or set of fields to the ‘*Inputs*’ sheet. These key parameters have the following characteristics:

- They have a significant effect on the GHG emissions from an oil and gas operation;
- They vary significantly across different operations and therefore could cause variability between different fields or projects;
- They are likely to be measured or are well-understood by operators.

The list of key inputs is a relatively small list of important factors. Other factors excluded from this list are left to process worksheets.

3.6.1.1 Controls on the ‘*Inputs*’ worksheet

The ‘*Inputs*’ worksheet is where key field parameters are entered for each field to be analyzed (see Figure 3.2). These key parameters are explained below. Inputs 1.1 - 1.8

Production methods Controls to turn on or off production methods including down- Inputs 1.1

¹Note: ‘locked’ cells are not locked via *Excel* password-protected locking mechanism, so they can be changed if desired by the user. However, this should be done with care, as the model can easily be rendered inoperable.

Box 2.1: Using OPGEE documentation and model together

OPGEE model documentation aligns with the model itself. Pointers to the model are contained in the right-hand margin of the model documentation in red, italic text. For example, a reference to the Production & Extraction worksheet calculation of gas-to-oil ratio (GOR), which is calculation number 1.1.4.1 on that worksheet (see Figure 3.3, Row 43), would be referred to in the right-hand margin as *Production & Extraction 1.1.4.1*

hole pump, water reinjection, gas reinjection, water flooding, gas lifting, gas flooding, steam flooding, oil sands mine (integrated with upgrader), and oil sands mine (non-integrated with upgrader).

- Downhole pump: This option is used to allow production when the naturally-occurring energy of the reservoir does not suffice to produce fluids at a desired wellhead pressure.
- Water reinjection: This option is used when injecting a fraction of the produced water. This option does not apply if the amount of water injected is more than the amount of water produced after treatment.
- Gas reinjection: This option is used when injecting a percentage of the amount of gas produced. This option does not apply if the amount of gas injected is more than the amount of gas remaining after processing and VFF losses. The remaining gas is shown in the 'Gas Balance' worksheet.
- Water flooding: This option is used when injecting an amount of water which is more than the amount of water produced. The amount of water injected is determined by the injection ratio (given in bbl water/bbl oil) and the fraction of water produced to reinjection/flooding must be set to 1.0. **The option of water reinjection must be turned OFF when the option of water flooding is turned ON.**
- Gas lifting: This option is used when gas is not injected into the reservoir, but injected into production string to reduce the pressure at the reservoir interface and induce production from the reservoir.
- Gas flooding: This option is used when injecting an amount of natural gas which is more than the amount of gas remaining after processing. The amount of gas injected is determined by the injection ratio (given in scf/bbl oil) and the fraction of remaining natural gas to reinjection must be set to 1.0. Alternately, this option can also be used when modeling EOR by flooding of nitrogen and carbon dioxide. **The option of gas reinjection must be turned OFF when the option of gas flooding is turned ON AND natural gas is selected as the flood gas.**
- Steam flooding: This EOR option is used when steam is injected to extract heavy crude oil. When this option is turned ON, steam-to-oil ratio (SOR) is needed to be entered or OPGEE will use its SOR default. The option of offshore field should be turned OFF when the option of steam flooding is turned ON.

- Oil sands mine (integrated or non-integrated with upgrader): The mining projects are mostly related to the Canadian oil sands. see section 4.3.2.14 for more details.

Field properties Field properties, including field location, field name, field age, field depth, oil production volume, number of producing wells, number of water injecting wells, production tubing diameter, productivity index, average reservoir pressure, average reservoir temperature, and whether the field is onshore (0) or offshore (1). *Inputs 1.2*

Fluid properties A variety of fluid properties, including API gravity of crude oil and composition of produced associated gas (N_2 , CO_2 , C_1 , C_2 , C_3 , C_4+ , and H_2S molar concentrations). *Inputs 1.3*

Production practices A variety of production practices or operating ratios. These include gas-to-oil ratio (GOR), water-to-oil ratio (WOR), water-injection ratio, gas lifting injection ratio, gas flooding injection ratio, the choice of flood gas (natural gas, N_2 , and CO_2), carbon dioxide enhanced oil recovery (CO_2 -EOR) related parameters (the percentage of the total injected CO_2 that is newly acquired, the source of CO_2 , and the percentage of the CO_2 sequestration credit assigned to the oilfield), steam-to-oil ratio (SOR), fraction of required electricity generated on site, fraction of remaining gas reinjected, fraction of water produced reinjected, fraction of steam generation via co-generation and volume fraction of diluent. WOR, GOR, and SOR are common parameters and self explanatory. Other less common parameters are explained below. *Inputs 1.4*

- Water injection ratio: The ratio of the amount of water injected in water flooding to the amount of oil produced. This is required only when the option of water flooding is turned ON.
- Gas lifting injection ratio: The ratio of the amount of gas injected for lifting to the amount of liquid (water + oil) produced. The amount of gas injected for gas lifting **does not** include gas injected into the reservoir. This is required only when the option of gas lifting is turned ON.
- Gas flooding injection ratio: The ratio of the amount of gas injected in gas flooding to the amount of oil produced. This is required only when the option of gas flooding is turned ON.
- Flood Gas: The choice flood gas (natural gas, N_2 , CO_2). This is required only when the option of gas flooding is turned ON.
- Percentage of total CO_2 injected that is newly acquired: The total amount of CO_2 injected consists of the sum of recycled CO_2 (that was previously injected, produced, and separated) and newly acquired CO_2 that is being injected for the first time. This is required only if the option of gas flooding is turned ON and CO_2 is the selected flood gas.
- Source of CO_2 : CO_2 can be acquired either from natural subsurface reservoirs or captured from anthropogenic sources such as power plants. This is required only if the option of gas flooding is turned ON and CO_2 is the selected flood gas.

- Percentage of sequestration credit assigned to the oilfield: Greenhouse gas emissions-related legislation may allow the oilfield to claim a sequestration credit for CO₂ sequestered during CO₂-EOR operations. If such a credit applies, then this parameter controls the proportion assigned to the oilfield. This is required only if the option of gas flooding is turned ON and CO₂ is the selected flood gas.
- Fraction of required electricity generated onsite: This parameter determines the fraction of the electricity required that is generated onsite not including electricity co-generation with steam generation. The fraction entered can be greater than 1.0, designating electricity export to the grid.
- Fraction of remaining gas reinjected: This parameter determines the fraction of gas remaining that is reinjected into the reservoir. In the case of methane gas flooding this fraction must be equal to 1.0 (the amount of gas injected is more than the amount of gas remaining).
- Fraction of water produced reinjected: This parameter determines the fraction of water produced after treatment that is reinjected into the reservoir. In the case of water flooding this fraction must be equal to 1.0 (the amount of water injected is more than the amount of water produced).
- Fraction of steam generation via co-generation: OPGEE allows the modeling of steam generation for thermal EOR with or without electricity co-generation. This parameter determines the share of steam generation via co-generation of electricity.

Processing practices Variables which represent the use of heater/treaters and stabilizer columns during oil phase separation, upgrader type, the choice of associated gas processing (AGR, dehydrator, demethanizer, and CO₂ EOR-related processing options), the ratio of gas flared to oil produced, and the ratio of gas vented to oil produced. Some parameters are explained below.

Inputs 1.5

- Heater/treater: Binary variables (0 or 1) are used to determine the use of a heater/treater in the oil-water separation process. 1 is used to turn ON the heater/treater and 0 is used to turn OFF the heater/treater. More detailed choices for heater/treaters are made in the 'Surface Processing' worksheet.
- Stabilizer column: Binary variables (0 or 1) are used to determine the use of a stabilizer column in the oil-gas separation process. 1 is used to turn ON the stabilizer column and 0 is used to turn OFF the stabilizer column. The stabilizer column is defined in section 4.4.2.2.
- Associated gas processing path: A set of 7 gas processing configurations are allowed to be chosen by setting value in this cell from 1 to 8. These options range from no gas processing (1) to extensive gas processing and CO₂ separation via cryogenic separation (8). Significant detail is provided on these gas processing paths below.
- Ratio of flaring to oil production: This is the ratio of gas flared to oil produced.

- Ratio of venting to oil production: This is the ratio of gas vented (not including operational venting or default leaks) to oil produced. **This ratio only includes venting used for gas disposal, as an alternative to flaring. It does not address normal operational vents and leaks.** Other default leaks are accounted in the *'Venting & Fugitives'* worksheet.
- Volume fraction of diluent: In some cases heavy crude is diluted after production using light hydrocarbons. This parameter determines the fraction of diluent or natural gas liquid (NGL) in diluted crude. The default case is the minimum NGL blend as determined by user inputs. The process model produces NGL in the demethanizer (if applicable), a fraction of which is blended as specified in the *'Surface Processing'* worksheet.

Land use impacts Parameters that determine the GHG emissions from land use change, *Inputs 1.6* including ecosystem carbon richness and relative disturbance intensity.

- Ecosystem carbon richness: Ecosystem carbon richness controls the amount of carbon emissions per unit of disturbed land, and varies from semi-arid grasslands (low potential carbon emissions) to forested (high potential carbon emissions).
- Field development intensity: The intensity of development can be chosen to be low, medium, or high. High intensity development resembles California thermal EOR operations, well production and injection wells are drilled on tight spacing. Low intensity development resembles conventional natural gas development or directional drilling from centralized drill pads, where the land disturbed per well is small.

Crude oil transport Parameters which determine transport modes and distances. This includes the fraction of crude oil transported by each mode of transport and the transport distance (one way) of each mode. The total fraction of all modes may exceed 1.0 because more than one transportation leg may be involved for transporting the crude oil from field to refinery. *Inputs 1.7*

Small emissions sources An added term to account for all emissions sources that are not explicitly included in OPGEE through calculations. Tables C.1 through C.7, as well as the *'Model Organization'* worksheet in OPGEE, describe which sources are explicitly included in the model. All sources that are not explicitly included are deemed to small to model, and are included in the small emissions sources term. *Inputs 1.8*

Parameters for multiple fields can be entered at a single time. After entry into *'Inputs'*, values for key parameters are propagated to other worksheets as needed for calculations. Therefore, if a key parameter (such as API gravity) is to be changed, it **must** be changed on the front *'Inputs'* worksheet so that it is changed identically in all calculations.

OPGEE provides defaults for all required input parameters; these can be replaced with user inputs where data are available. In some cases, OPGEE calculates 'smart default' values dynamically based on user inputs for other parameters. For instance, the default flaring volume is determined from NOAA data based on the specified field location [25]. These smart defaults can also be overruled by user inputs.

OPGEE 2.0_v108

Home Insert Page Layout Formulas Data Review View Developer

Font: Helvetica, 12, Bold, Italic, Underline, Color, Background Color, Text Color, Text Alignment, Wrap Text, Merge & Center, General, Number, Currency, Percentage, Decimals, Conditional Formatting, Format as Table, Cell Styles, Insert, Delete, Format, AutoSum, Fill, Sort & Filter, Clear

D2

| Data inputs | | Start field: | End field: | | | | | | | | | | | | |
|--|------------|--------------|---------------------|---------|---------|---------|-----------|------------|---------|-------------|----------|----------|-----------|----------|----------|
| Fields: | 1 | 108 | Run Assessment | | | | | | | | | | | | |
| 1 Inputs | | | | | | | | | | | | | | | |
| Variables | Unit | Default | Field 1 | Field 2 | Field 3 | Field 4 | Field 5 | Field 6 | Field 7 | Field 8 | Field 9 | Field 10 | Field 11 | Field 12 | Field 13 |
| | | Generic | Hassi R'M' Girassol | Kuito | Takula | Cossack | Azeri | Frade | Lula | Midale (So) | Hibernia | Bozhong | Huizhou 2 | Qin | |
| 1.1 Production methods | | | | | | | | | | | | | | | |
| Notes: Enter "1" where applicable and "0" where not applicable | | | | | | | | | | | | | | | |
| 1.1.1 Downhole pump | NA | 1 | 1 | 0 | 1 | 1 | 0 | 1 | 0 | 0 | 0 | 0 | 1 | 0 | |
| 1.1.2 Water reinjection | NA | 1 | 0 | 1 | 1 | 1 | 0 | 1 | 1 | 1 | 1 | 0 | 1 | 1 | |
| 1.1.3 Natural gas reinjection | NA | 0 | 1 | 1 | 0 | 0 | 0 | 0 | 0 | 1 | 1 | 1 | 1 | 0 | |
| 1.1.4 Water flooding | NA | 0 | 0 | 0 | 0 | 0 | 0 | 0 | 0 | 0 | 0 | 0 | 0 | 0 | |
| 1.1.5 Gas lifting | NA | 0 | 0 | 1 | 0 | 0 | 1 | 0 | 1 | 1 | 0 | 0 | 0 | 1 | |
| 1.1.6 Gas flooding | NA | 0 | 0 | 0 | 0 | 0 | 0 | 0 | 0 | 0 | 0 | 0 | 0 | 0 | |
| 1.1.7 Steam flooding | NA | 0 | 0 | 0 | 0 | 0 | 0 | 0 | 0 | 0 | 0 | 0 | 0 | 0 | |
| 1.1.8 Oil sands mine (integrated with upgrader) | NA | 0 | 0 | 0 | 0 | 0 | 0 | 0 | 0 | 0 | 0 | 0 | 0 | 0 | |
| 1.1.9 Oil sands mine (non-integrated with upgrader) | NA | 0 | 0 | 0 | 0 | 0 | 0 | 0 | 0 | 0 | 0 | 0 | 0 | 0 | |
| 1.2 Field properties | | | | | | | | | | | | | | | |
| 1.2.1 Field location (Country) | NA | Generic | Algeria | Angola | Angola | Angola | Australia | Azerbaijan | Brazil | Brazil | Canada | Canada | China | China | Chi |
| 1.2.2 Field name | NA | Generic | Hassi R'M' Girassol | Kuito | Takula | Cossack | Azeri | Frade | Lula | Midale (So) | Hibernia | Bozhong | Huizhou 2 | Qin | |
| 1.2.3 Field age | yr. | 35 | 48 | 12 | 15 | 35 | 27 | 17 | 4 | 3 | 60 | 15 | 23 | 25 | |
| 1.2.4 Field depth | ft | 7240 | 7309 | 3937 | | 188 | 9719 | 9075 | 6730 | 19737 | 4600 | 10065 | 10500 | | |
| 1.2.5 Oil production volume | bbld | 1500 | 180000 | 175000 | 50000 | 105000 | 60000 | 655700 | 16912 | 100000 | 5000 | 135483 | 90000 | 12403 | |
| 1.2.6 Number of producing wells | | 8 | 160 | 24 | 19 | 69 | 12 | 77 | 12 | 6 | 953 | | 88 | 10 | |
| 1.2.7 Number of water injecting wells | [-] | 5 | | 20 | 9 | 21 | 0 | 30 | 7 | 1 | 83 | | 36 | 4 | |
| 1.2.8 Production tubing diameter | in | 2.775 | | 8 | 6 | | 5 | | | | | | 3.5 | | |
| 1.2.9 Productivity index | bbld/psi-d | 3 | | 90.9 | | | 50 | | | | | | | | |
| 1.2.10 Reservoir pressure | psi | 1556.6 | 5874 | 3655 | | 1300 | 4000 | | 2900 | 8000 | 2600 | | 1450 | | |
| 1.2.11 Reservoir temperature | F | 150 | | | | | | | | | | | | | |
| 1.2.12 Offshore? | [0-1] | 0 | | | | | | | | | | | | | |
| 1.3 Fluid properties | | | | | | | | | | | | | | | |
| 1.3.1 API gravity | deg. API | 30 | 66.64 | 32 | 21 | 32 | 47.3 | 35 | 19 | 28 | 28.7 | 34.6 | 17.5 | 43.6 | |
| 1.3.2 Gas composition | | | | | | | | | | | | | | | |
| N ₂ | mol% | 2 | | | | | | | | | | | 1 | | |
| CO ₂ | mol% | 6 | | | | | | | | | | | 5.4 | | |
| C ₁ | mol% | 84 | | | | | | | | | | | 75 | | |
| C ₂ | mol% | 4 | | | | | | | | | | | 12.1 | | |
| C ₃ | mol% | 2 | | | | | | | | | | | 2.9 | | |

Ready

Introduction How to use Model coverage Inputs Results Active Field Energy Consumption GHG Emissions Exploration Drilling & Development Production & Extraction Surface Processing

100%

Figure 3.2: Data input section of the 'Inputs' worksheet.

3.6.2 Secondary interaction

If more detailed data are available for a given oil production operation, and more specific estimates are desired, secondary interaction can be pursued by changing parameters on process-stage specific worksheets and supplementary worksheets.

It should not be necessary to change these secondary input parameters in basic use of OPGEE. The secondary parameters include parameters with less effect on the resulting emissions, that are not highly variable across operations, or that are less likely to be known by model users. Examples include compressor suction pressure and temperature, type of prime mover, or pump efficiency. Note that some of these parameters (e.g., pump efficiency) have significant effects on model results, but are not believed to be highly variable across fields.

All secondary input parameters are free for the user to change in the input data sections of the process stage worksheets. Parameters that are classified as *User Locked* (see Figure 3.1 above) should not be changed because they are either calculated from other primary inputs or derived from the 'Inputs' worksheet.

Figure 3.3 shows the input data section of the 'Production & Extraction' worksheet. Moving left to right across the screen, features of interest include:

Parameters and sub-parameters In columns A through K, the names and descriptions of parameters and calculation results are numbered in a hierarchical fashion. Each parameter or calculation result has a unique number to allow ease of reference to the model. For example, the water specific gravity (2.1.2) is calculated using the concentration of dissolved solids (1.2.1.1).

User and default columns Columns M and N include the user and default inputs for the production calculations. Column M is always used in the final calculations. Column N is included for reference, and includes default values. Before any user input is changed, all user values are equal to default values.

Free and locked cells As shown in Figure 3.1 above, *User Free* and *Default Free* cells are included with light tones, while *User Locked* and *Default Locked* cells are included with dark tones. For example, in Figure 3.3 the highlighted cell M37 represents the mol% of methane (C₁) in the associated gas. Because this quantity is a key input parameter and is defined on the 'Inputs' worksheet, it is marked here as *User Locked*. Therefore, if the user wishes to change the gas composition, this should be done on the 'Inputs' worksheet where gas composition is classified as *User Free*.

Units In column O, units are listed for all input parameters, variables, and calculation results (where applicable).

User and default reference Columns Q and S are spaces to record the data sources of input parameters. Where applicable, the source of the default value is listed in the *Default reference* column. If a user changes a parameter to a non-default value, they can place any desired information about the source (such as author, page, dataset, vintage, data quality, expected uncertainty, etc.) in the *User reference* column.

Notes To the right of the default reference column is the notes column (not shown, column Y). The *Notes* column contains explanatory notes or other information that may be useful to the user.

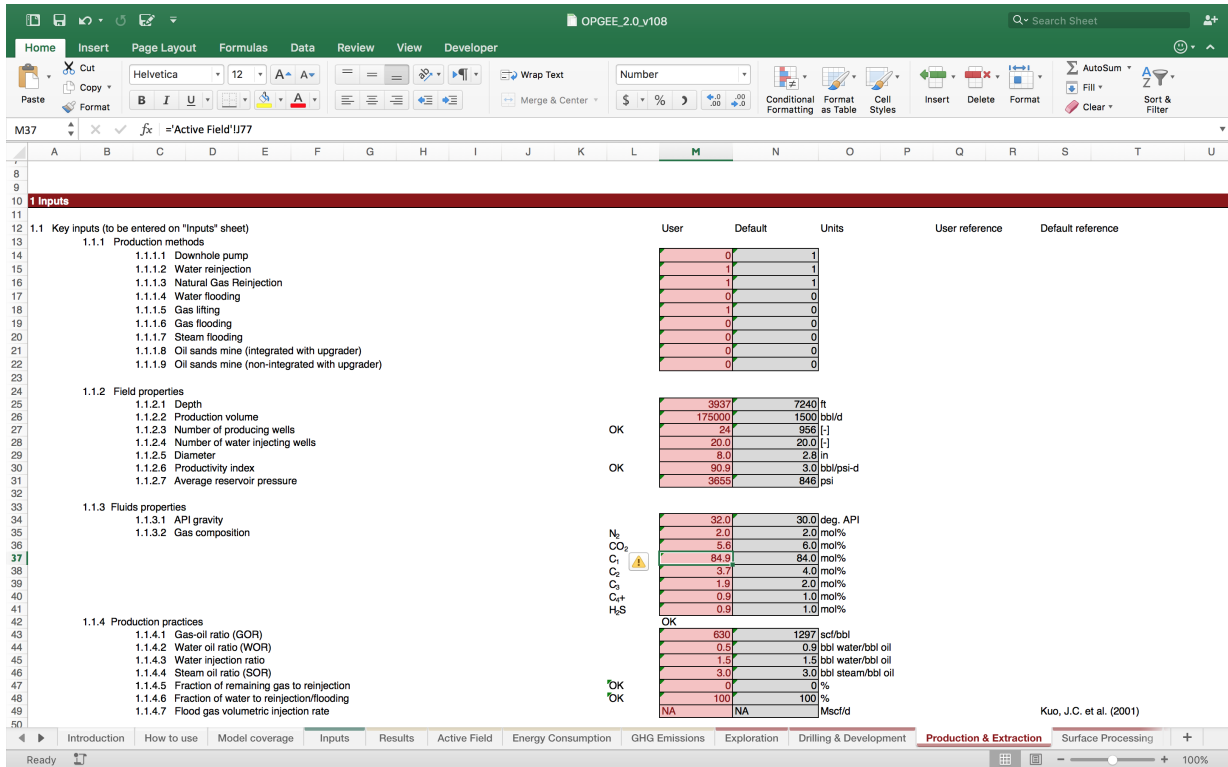


Figure 3.3: Input data section of 'Production & Extraction' worksheet. User inputs are in column M, while defaults are kept as reference in column N.

3.6.3 Checking for errors

It is possible to mistakenly enter data that are invalid, contradictory, or otherwise result in errors.

A summary indicator for model errors appears in the 'Results' worksheet as the "Overall Check." An overall check error is the result of an error in any of the fields that included in the model run, which appears as an error in the "Field by Field Check." To investigate an error in a specific field, the "End field" should be set equal to the field number of the field in question and the "Run Assessment" button should be clicked again. This will populate the 'Active Field' worksheet with the calculations regarding the error-causing field. Here, the error can be traced to a particular worksheet and cell by examining the 'Specific error checks.' Specific error checks can be debugged by moving to the worksheet and cell in question and tracing any logical or inputs errors that have flagged that error check. Common sources of errors include logical errors in pathway selection (e.g., more than one mutually exclusive technology selected) and input errors (e.g., gas composition sums to more than 100 mol%).

Hints for using OPGEE without errors are given in Box 2.2.

Results 2.14

Results 2.13

Active Field 4.1.1

- 7.1.29

Box 2.2: Hints for using OPGEE without errors

1. Do not change formulas in *User locked* or *Default locked* cells, as these can result in mis-calculation;
2. Always check error reports in 'Results' section 2.14 and, if necessary, section 2.13, for errors before considering results final;
3. Use care to collect physically realistic and consistent data where default values will be overwritten (e.g., if depth of field is greatly increased, operating pressure will often increase as well);
4. To ensure reproducibility of results, document any sources for user inputs in the 'User Reference' column;
5. Save individual field assessments as separate worksheets to prevent incorrect propagation of changed cells.

Model error check:

OK

Table 1.1: Summary GHG emissions

| GHG emissions [gCO ₂ eq/MJ] | |
|--|----------|
| Active field | Girassol |
| Exploration | 0.00 |
| Drilling | 0.04 |
| Production | 0.08 |
| Processing | 0.62 |
| Maintenance | 0.00 |
| Waste | 0.00 |
| VFF | 5.37 |
| Misc. | 0.50 |
| Transport | 0.93 |
| Offsite emissions | -0.29 |
| CO ₂ Sequestration | 0.00 |
| Net lifecycle emissio | 7.24 |

Notes: Copy highlighted column and paste 'as numbers' to generate a record

Figure 1.1: Summary GHG emissions

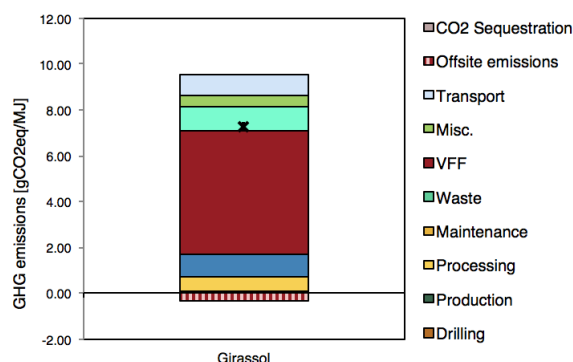


Figure 1.2: Summary energy consumption

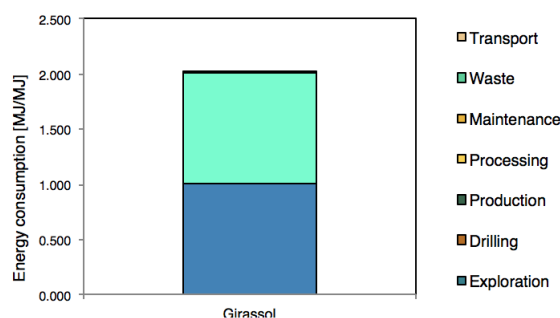


Table 1.2: Summary energy consumption

| Energy consumption [MJ/MJ] | |
|----------------------------|----------|
| Active field | Girassol |
| Exploration | 0.00 |
| Drilling | 0.00 |
| Production | 0.00 |
| Processing | 0.01 |
| Maintenance | 0.00 |
| Waste | 0.00 |
| Transport | 0.01 |
| Total | 0.024 |

Notes: Copy highlighted column and paste 'as numbers' to generate a record

Figure 3.4: Graphical results for an example crude oil. These results from 'Active Field' Tables 1.1 and 1.2, Figures 1.1 and 1.2.

3.6.4 Results

After the user enters data to the 'Inputs' sheet and clicks the Run Assessment button, OPGEE computes the resulting GHG emissions. The results are for the last field (End field) analyzed are stored in the 'Active Field' sheet, while the results from all fields are stored in the 'Results' in tabular form in gCO₂ equivalent GHG emissions per MJ LHV crude oil delivered to the refinery gate.² Emissions are broken down by stage (generally) or by type, with fugitive emissions for all process stages summed together for convenient interpretation as 'VFF' emissions. Total energy consumed per unit of energy delivered to the refinery gate is also presented in tabular and graphical form. These tabular and graphical results are illustrated in Figures 3.4.

Active Field Table

1.1

Results 2.1 - 2.14

Active Field Fig.

1.1

Active Field Table

1.2, Figure 1.2

²The heating value basis of the denominator crude oil can be changed so that emissions are calculated per MJ HHV of refinery input. This can be changed on the 'Fuel Specs' worksheet. See discussion below in Section 8.4.

3.7 Inputs

3.7.1 Further details regarding the Inputs sheet

OPGEE has a built-in capability to analyze a number of fields or oil production projects and bookkeep the results for comparison and further analysis.

The capability to analyze multiple fields simultaneously is provided by a Microsoft VBA macro. In addition to running a number of fields in sequence, the macro programmatically resolves significant errors that arise from input data inconsistencies. It also automates iterative calculations such as the reconfiguration of gas composition in the case of gas lift or setting gas export to zero by incrementally increasing gas reinjection.

At the top of the *'Inputs'* worksheet the user enters the fields to be assessed by entering the starting field and the ending field. In the input data section the user enters available data for each assessed field. When limited datasets are available, the assessment macro will complete the datasets by filling required inputs with defaults and smart defaults where applicable. The results are generated for all fields in one computational run. The macro is started by pressing the "Run Assessment" command button.

Inputs 1.1-1.8

3.7.2 Assessment macro description

Figure 3.5 shows the outer structure of the assessment macro. For every field under study, the macro first copies user entries into the (*'Active Field'*) worksheet. It then checks for empty user entries. For every empty user input, the macro copies the default value from the (*'Active Field'*) worksheet. In the case of "0" entry for the number of producing wells, a warning appears and prompts the user to enter a valid number of producing wells. When the data set of the field under study is complete, the macro copies the complete set of data into the (*'Active Field'*) worksheet, initiates the error correction and entry adjustments procedure, and returns the completed and corrected/adjusted set of data into the (*'Results'*) worksheet. Finally the macro copies the full data set back into the (*'Active Field'*) worksheet and returns the results into the (*'Results'*) worksheet. The same process is repeated for each field under study.

The assessment macro is capable of fixing errors, performing iterative calculations and adjusting input parameters where necessary. It is not practical to perform these computational tasks manually when assessing a large number of projects (100+). The macro ensures consistent treatment across all fields. Errors that are addressed in the macro include:

- Discrepancies between country-average default flaring rate and entered GOR (e.g., flaring module predicts more flaring than field has gas available);
- Discrepancies between default fugitive emissions of gaseous components and gas available from production;
- Requirement to iteratively solve for the gas composition in the wellbore in the case of gas lift;
- Error with productivity index resulting in negative bottomhole pressures;

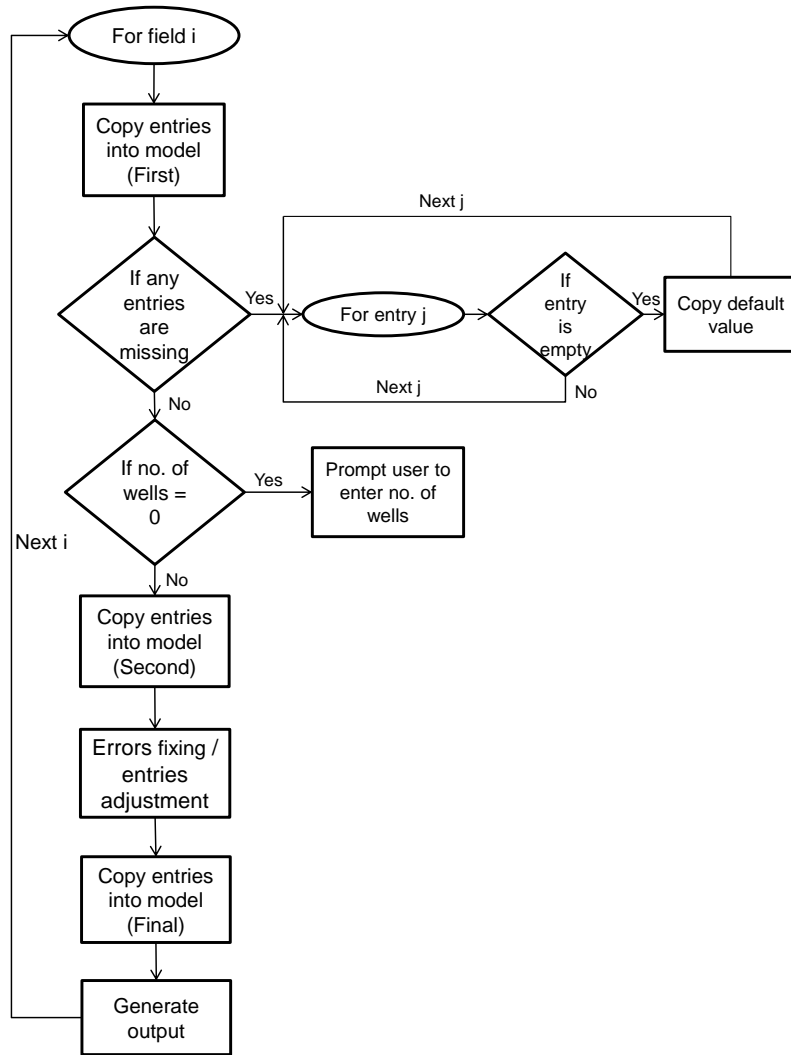


Figure 3.5: Logical structure of the assessment macro.

- Error resulting from very large frictional lifting penalties due to too-small default wellbore diameter;
- Requirement to iteratively solve for gas reinjected to result in 0 gas export.

Appendix D details the functioning of these error correction features.

Part II

Technical documentation

4 Process stage worksheets

This section explains the main assumptions and calculations for each process stage worksheet. Items discussed include user assumptions and choices, process calculation assumptions, calculations of input parameters, and calculations of intermediate outputs.

4.1 Exploration emissions

4.1.1 Introduction to petroleum exploration

Emissions from petroleum exploration occur during clearing of land for seismic surveys, operation of seismic survey equipment, drilling of exploratory wells, and from fugitive emissions during drilling operations. Offsite emissions occur due to other materials and services consumed during drilling (e.g., computing energy consumed during seismic data processing). A complete list of emissions sources, along with their categorization and estimated magnitude, is shown in Table C.1.

Required inputs for exploration emissions include the following terms gathered from the ‘*Active Field*’ worksheet:

Exploration 1.1

- Field depth [ft]
- Is field offshore [0-1]
- Field production rate [bbl/d]

Required inputs to be entered for secondary interaction on the ‘*Exploration Emissions*’ worksheet include:

*Exploration 1.2.1
- 1.2.5*

- Distance of travel for survey
- Weight of land survey vehicle
- Weight of ocean survey vehicle
- Dry holes drilled per field found
- Exploratory or scientific wells drilled after field discovery (non-producing)

The default values for these inputs are noted in Table 4.1.

4.1.2 Calculations for petroleum exploration

The survey vehicle energy consumption (e.g., seismic survey ship or seismic survey trucks) are calculated as:

$$E_{EXP} = \sum_j y_j m_j D_j U E_j \quad (j \in S, T) \quad (4.1)$$

$$[\text{mmBtu}] = [-] [\text{ton}] [\text{mi}] \left[\frac{\text{Btu}}{\text{ton-mi}} \right]$$

where y_j is a binary variable representing whether exploration mode S (ship-based exploration) or T (truck-based exploration) is performed $[-]$; m_j is the weight of exploration vehicle j $[\text{ton}]$, D_j is the distance traveled by exploration vehicle j $[\text{mi}]$, and $U E_j$ is the energy-specific effectiveness of transport type j $[\text{Btu}/\text{ton-mi}]$, as computed on the 'Transport' worksheet.

Transport 2.2

Energy consumed in drilling exploratory wells is computed using drilling energy intensity computed on the 'Drilling & Development' sheet.

Energy consumed in exploration is computed as a fraction of the total lifetime energy production assumed produced from the field. This quantity is derived in the 'Drilling & Development' sheet, as described below.

4.1.3 Defaults for petroleum exploration

Table 4.1 shows the default settings for petroleum exploration.

Table 4.1: Default inputs for exploration emissions

| Param. | Description | Eq. no. | Default | Literature range | Unit | Sources | Notes |
|--------|---|---------|---------|------------------|--------------|---------|-------|
| D_j | Distance exploration mode j travels (same for S and T) | - | 10,000 | - | [mi] | | a |
| m_S | Weight of exploration ship | - | 100 | - | [ton] | | b |
| m_T | Weight of exploration truck | - | 25 | - | [ton] | | c |
| UE_S | Effectiveness of exploration ship | - | 27 | | [Btu/ton-mi] | [84] | |
| UE_T | Effectiveness of exploration truck | - | 969 | | [Btu/ton-mi] | [84] | |

^a Simple assumption for distance of travel to remote exploration site. Distance traveled during actual survey is assumed by default to be small compared to distance to field location.

^b Simple assumption for weight of exploration ship

^c Simple assumption for weight of exploration truck

4.2 Drilling & development

4.2.1 Introduction to drilling & development

Drilling and development operations result in a variety of emissions. Well drilling and installation of production equipment results in on-site energy use (e.g., for rigs and other construction equipment) as well as indirect offsite energy use (e.g., embodied energy consumed to manufacture well casing). Drilling and development also results in land use impacts, which can release biogenic carbon from disturbed ecosystems and soils [6]. In addition, fugitive emissions can occur during the drilling process. A list of emissions sources, along with their categorization and estimated magnitude, is shown in Table C.2.

4.2.2 Calculations for drilling & development

Three aspects of field drilling and development are modeled in OPGEE v2.0b: drilling energy consumption, hydraulic fracturing energy consumption, and land use impacts. Other emissions from drilling and development are not explicitly modeled and therefore would be accounted for in the small sources term. The parameters and variables used in the drilling and development model equations are listed in Table 4.7.

Active Field 3.8

4.2.2.1 Emissions from drilling

Drilling oil wells consumes fuel. This fuel is consumed on site in prime movers (generally diesel engines) for a variety of purposes: to power mud pumps; apply torque to drill string; pull drill string; raise, lower and retrieve subsurface monitoring equipment; and pump cement.

Relationships for these functions are derived from the open-source drilling energy intensity model *GHGfrack* [85–87]. The *GHGfrack* model is developed with extensive documentation and validation efforts [85, 86].

In order to develop correlations for use in OPGEE v2.0b, we ran a number of cases in *GHGfrack*. First, three well complexity settings are designed in *GHGfrack* (see Figure 4.1). These well complexity designs are also used in the ‘*Embodied Emissions*’ worksheet, as described below. The *Simple* well design has one string of surface casing and one string of production casing. The *Moderate* well design has one string of surface casing, one string of intermediate casing, and one string of production casing. The *Complex* well design has one string of surface casing, two strings of intermediate casing, and one string of production casing. These wellbore designs are derived from examples in industry texts [34]. For each casing design an appropriate set of true vertical depth (TVD) values is chosen based on well complexity. *Simple* wells are assumed to range between 0 ft and 12,000 ft deep, *Moderate* wells are between 4,000 and 16,000 feet deep, while *Complex* wells are between 12,000 and 20,000 feet deep. Each TVD is incremented in segments of 1000 ft.

Drilling & Development 1.2

Each well casing design plan is designed for four wellbore diameters, called *Small*, *Medium*, *Large* and *Extra-large*. The diameters (hole diameter not casing diameter) for each of these cases is listed for each well complexity in Table 4.2. These hole diameters are chosen from API casing-hole size charts [34, Figure 11.22]. The resulting depth ranges for each casing string section are given in Table 4.3.

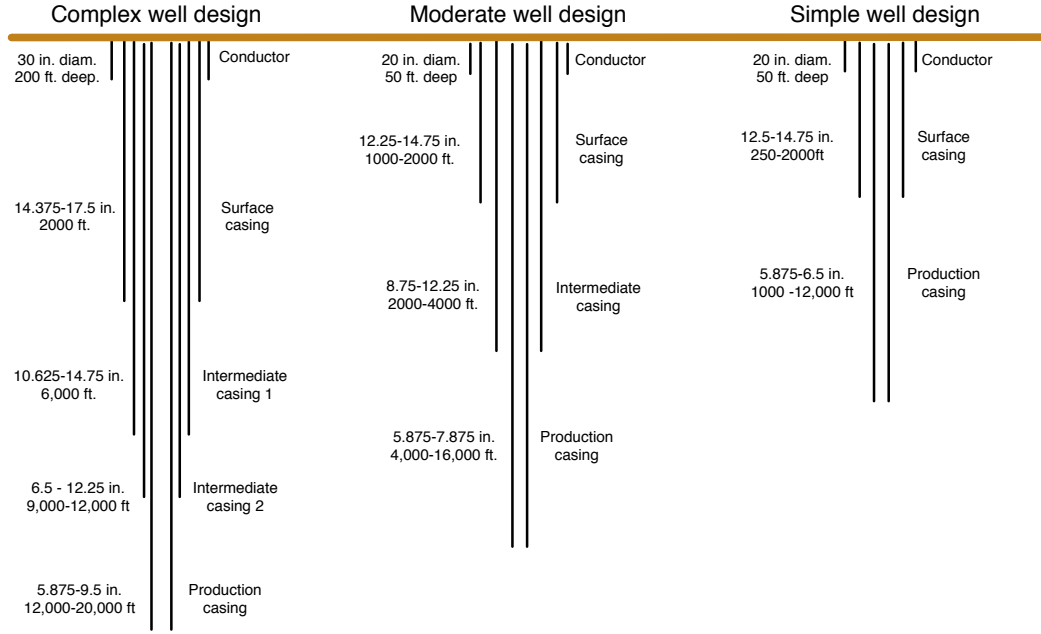


Figure 4.1: Drilling hole diameters for simple, moderate and complex well construction.

In addition, the energy efficiencies of rotary table/drill string torque provision and mud pump work are varied. The moderate efficiency settings for these terms are 45% and 65% respectively [86]. The low and high efficiency settings are 40% and 50% for the rotary table and 60% and 70% for the mud pumps, respectively.

The resulting energy consumption for rotary table and mud circulation uses are therefore modeled as:

$$E_D = E_D^{rt} + E_D^{mp} \quad (4.2)$$

Where E_D^{rt} is the energy consumed in rotary table work provision and E_D^{mp} is the energy consumed in mud circulation pumps.

The energy consumption for rotary table work E_D^{rt} is computed using the torque and torque factors as noted in GHGfrack documentation [86]:

$$E_D^{rt} = BHP^{rt} \times t, \quad (4.3)$$

or,

$$E_D^{rt} = \frac{2\pi TN}{33,000\eta} \times t, \quad (4.4)$$

where BHP^{rt} , is the brake horsepower required by the rotary table [hp], and t is the amount of time that the rotary table is operating [h]. BHP is computed using the torque T [ft-lb_f], rotational speed N [rpm], and overall electro-mechanical efficiency of the rotary table drive system η [-]. The value 33,000 is a unit conversion factor. These values are set equal to GHGfrack defaults in all results presented below. If the user wishes to change torque or other rotary table inputs, please use the GHGfrack model directly.

The energy consumption for mud circulation is computed using the overall pressure drop in the mud circulation system [86]:

$$E_D^{mp} = BHP^{mp} \times t, \quad (4.5)$$

or,

$$E_D^{mp} = \frac{\Delta P_{mp} Q}{1714 \eta} \times t, \quad (4.6)$$

where ΔP_{mp} is the pressure drop that must be overcome by the mud pump [psi], Q is the mud flowrate [gal. per min.], t is the time of mud pump operation [h] and 1714 is a conversion factor.

This pressure drop ΔP_{mp} is made up of a series of terms, including:

$$\Delta P_{mp} = \Delta P_{fric} + \Delta P_{dynamic} + \Delta P_{dm} - \Delta P_{hydrostatic} + \Delta P_{other} \quad (4.7)$$

where subscripts refer to different pressure drop terms. The *fric* pressure drop is due to friction in drill string and annulus, modeled using a set of laminar and turbulent pipe and annulus flow models using different assumptions regarding non-Newtonian nature of drilling fluids (see *GHGfrack* documentation [85, 86]). The *dm* term corresponds to energy imparted on the mud motor and converted to rotational motion of the bit. In developing results for OPGEE, all *GHGfrack* mud circulation settings are left at *GHGfrack* defaults. If the user wishes to mud circulation inputs, please use the *GHGfrack* model directly.

Given overall energy term E_D , we can compute fuel use in drilling as follows:

$$F_D = \frac{E_D \eta_{gs}}{LHV_{di}} \quad (4.8)$$

where F_{DD} is the fuel use in drilling and development [gal], η_{gs} is the efficiency of the drilling prime mover (diesel engine) [-], and LHV_{di} is the lower heating value of diesel fuel [mmBtu/gal].

A number of other *GHGfrack* settings are required. For simplicity, in each model run, the drill pipe outer diameter (OD) [in] is set equal to 2.5 in. smaller than the smallest casing string inner diameter (ID). In all cases, the drill pipe ID is set equal 0.5 in. smaller than the drill pipe OD. The drill collar OD is set equal to 1.5 in. smaller than the smallest casing string ID. The drill collar ID is set equal 0.5 in. smaller than the drill collar OD. Also, in each well design, the last segment is set to an inclination angle of either 0° (vertical) or 90° (horizontal). We do not apply a slanted transition zone (i.e., a 45° zone).

Given all of the above variables, a total of 816 *GHGfrack* model runs are computed using an automated macro. The resulting depths and fuel consumption quantities for all runs are illustrated in Figure 4.2.

As can be seen, there is a wide range of energy consumption values for each depth. To further understand drivers of emissions, we then segment these results into results from simple, moderate, and complex wells (Figure 4.3).

We can further segment these results by separating vertical and horizontal wells and by noting the effect of rotary table and mud pump efficiency. This process is illustrated in Figure 4.4 for the case of simple wells only.

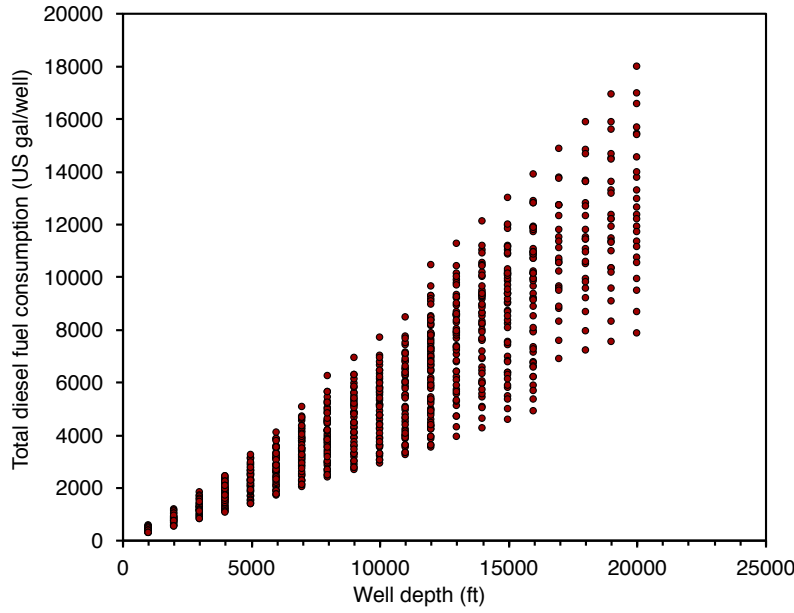


Figure 4.2: All GHGfrack results for drilling fuel consumption in US gallons of diesel (includes both rotary table + mud circulation).

Using these segmented results, we construct a drilling intensity factor per-foot of drilled well for vertical wells. Because the results in Figure 4.4 are largely linear within a given efficiency setting and well geometry, we can use a linear model segmented by well category. Fuel intensity factors FI [gal diesel fuel/ft.] are constructed separate for each “line” in Figure 4.4 as follows: vertical wells are segmented by well-complexity, well diameter, and assumed efficiency setting. A linear slope is computed to estimate the fuel intensity factor FI by summing the total fuel use across all wells in a given well complexity-well size category and summing the total distance drilled across all wells in that category:

$$FI_D^{v,cat} = \frac{\sum_{i \in cat} F_D^i}{\sum_{i \in cat} D_v^i} \quad (4.9)$$

where i is the index for wells, $i \in cat$ represents the subset of all wells i that are included in a given well-complexity, well diameter, and efficiency setting category. D_v^i is the vertical distance drilled (TVD) for each vertical well in the particular category. These tabulated fuel intensity factors FI are included in OPGEE and selected using logic for each field depending on field well construction practices.

To compute the excess fuel required to drill horizontal wells, we compare each horizontal well to the vertical well of the same total drilling distance and compute the additional fuel use associated with making each well have a horizontal segment. This additional fuel use can then be divided for each well by the length of the horizontal segment. This gives a horizontal well fuel intensity factor FI :

$$FI_D^{h,cat} = \frac{\sum_{i \in cat} (F_D^{i,h} - F_D^{i,v})}{\sum_{i \in cat} D_h^i} \quad (4.10)$$

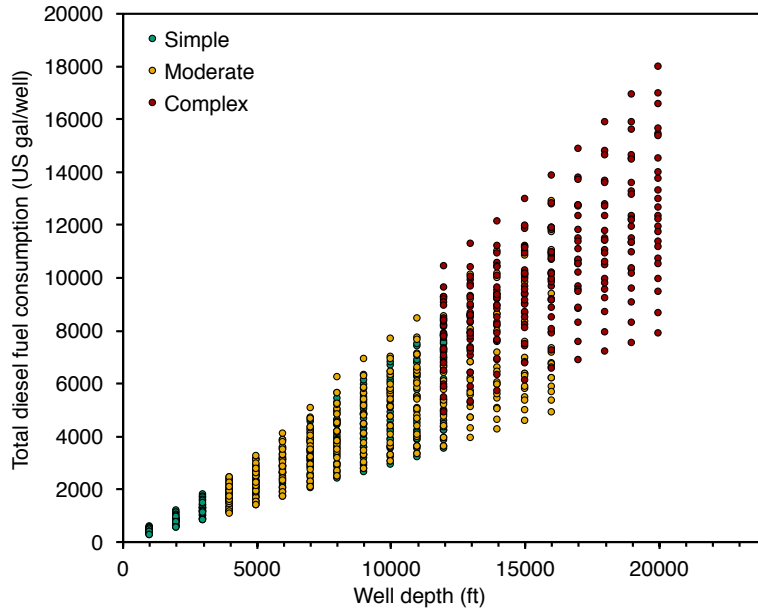


Figure 4.3: GHGfrack results for drilling fuel consumption segmented by well complexity. Fuel consumption reported in US gallons of diesel (includes both rotary table + mud circulation).

Where $F_D^{i,h}$ is the fuel consumed in the horizontal version of well i and $F_D^{i,v}$ is the fuel consumed in the vertical version of the same well i [gal diesel]. The horizontal distance D_h for a given well is the distance of the terminal well segment (horizontal). This computation results in an incremental fuel consumption per ft. of horizontal well drilled [gal/ft. horizontal].

Using these two factors, we can compute the total fuel required to drill a horizontal or vertical well i using a single expression:

$$F_D^i = D_v^i \left(FI_D^{v,i} \right) + f_h D_h^i \left(FI_D^{v,i} + FI_D^{h,i} \right) \quad (4.11)$$

where f_h is the fraction of wells [0-1] with horizontal segment of length D_h [ft].

Drilling energy consumption must be amortized over the producing life of a well. Also, drilling and development energy must account for drilling of water injection wells. The lifetime productivity of wells varies by orders of magnitude, depending on the quality of the oil reservoir and its size. We include three cases for the productivity of wells from prior studies of embodied energy in oilfield operations [88]. Three options are allowed, corresponding to “low”, “medium”, and “high” per-well cumulative productivity. These settings correspond approximately to average production in the US, global average, and OPEC average productivity. Numerical values are 150 kbbbl/well, 800 kbbbl/well and 7,000 kbbbl/well, respectively [88, Supporting Information Table S1].

The energy intensity of drilling per unit of energy produced is therefore calculated as follows:

$$ei_D = \frac{F_D N_W LHV_{di}}{Q_{o,tot} LHV_o} \quad [\text{mmBtu/mmBtu}] \quad (4.12)$$

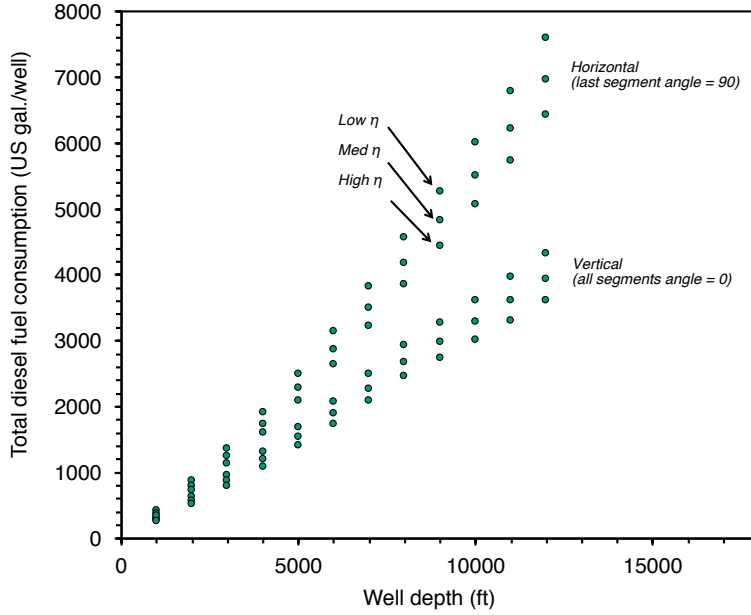


Figure 4.4: GHGfrack results for drilling fuel consumption. Only simple wells are represented, and the results are segmented by efficiency and wellbore orientation. Fuel consumption reported in US gallons of diesel (includes both rotary table + mud circulation).

where ei_{DR} = energy intensity of drilling [mmBtu/1000 ft]; h_W = average well depth [1000 ft]; $Q_{o,tot}$ = total lifetime productivity per well drilled [bbl oil/well]; and LHV_o = lower heating value of the crude produced [mmBtu LHV/bbl].

The energy intensity of drilling tends to be small when amortized over total well productivity, with values on order 10^{-6} to 10^{-2} mmBtu/mmBtu.

4.2.2.2 Emissions from hydraulic fracturing

The practice of hydraulic fracturing can consume large amounts of energy. This is because modern high-volume multi-stage hydraulic fracturing requires injecting large amounts of fluid at high pressures. *GHGfrack* models the injection of hydraulic fracturing fluids by accounting for the pressure required for fracturing:

$$\Delta P_{hf} = \Delta P_{fracture} + \Delta P_{fric} - \Delta P_{hydrostatic} \quad (4.13)$$

where $\Delta P_{fracture}$ is the fracturing pressure required to overcome the fracturing gradient [psi], ΔP_{fric} is the frictional pressure drop during injection [psi], and $\Delta P_{hydrostatic}$ is the contribution from the hydrostatic head of water in the wellbore [psi].

As in the case of mud pump injection energy, the energy requirements of hydraulic fracturing are calculated from the pressure drop as follows:

$$E_D^{hf} = \frac{\Delta P_{hf} Q_{hf}}{1714 \eta} \times t, \quad (4.14)$$

and the fuel consumption due to hydraulic fracturing is computed similarly to the

fuel consumption due to drilling:

$$F_D^{hf} = \frac{E_D^{hf} \eta_{gs}}{LHV_{di}}. \quad (4.15)$$

We compute the fuel consumption due to hydraulic fracturing using *GHGfrack* for numerous cases and use the results to create simple correlations for use in OPGEE. We use a number of default *GHGfrack* assumptions during the runs, including:

- Injection string ID = 5 in.
- Horizontal lateral length = 5000 ft.
- Fracturing fluid density = 9.0 lbm/gal.
- Viscosity = 1 cp
- Pipe roughness = 0.00008 in
- Length of fracturing stage = 300 ft
- Number of computational segments = 10
- Pump efficiency = 65%
- Injection time = 48 hr

In order to generate the relationships used in OPGEE, we vary two key inputs to the *GHGfrack* hydraulic fracturing module: (1) amount of fracturing fluid injected, and (2) fracturing gradient. In these runs, the fracturing gradient is varied from 0.6 psi/ft to 1.0 psi/ft in increments of 0.05 psi/ft. Also, in these runs the amount of fluid injected is varied from 1 to 5×10^6 gallons in increments of 1×10^6 gallons. Therefore, a total of 45 *GHGfrack* fracturing simulations are performed.

The results from these *GHGfrack* simulations are shown in Figure 4.5. We fit quadratic functions to each set of results from the same fracturing gradient value. In each case, the r^2 value is ≥ 0.999 . The resulting quadratic function coefficients are used in OPGEE to predict hydraulic fracturing energy use in a particular field based on the volume of fracturing fluid injected. The equation used is:

$$F_D^{hf} = aV_{hf}^2 + bV_{hf} + c \text{ [gal diesel]} \quad (4.16)$$

where a , b and c are fitting constants unique to each fracturing gradient. The results for the fitting constants a , b and c are shown in Table 4.4.

Table 4.4: Constants for quadratic fit of fracturing fuel consumption equation

| Fracturing gradient [psi/ft] | <i>a</i> | <i>b</i> | <i>c</i> |
|------------------------------|----------|----------|----------|
| 0.60 | 588.55 | -488.77 | 1184.50 |
| 0.65 | 599.49 | -246.27 | 1349.20 |
| 0.70 | 511.30 | 575.63 | 964.32 |
| 0.75 | 499.47 | 924.06 | 1012.50 |
| 0.80 | 566.77 | 1090.40 | 1101.60 |
| 0.85 | 570.18 | 1378.20 | 1162.60 |
| 0.90 | 523.67 | 1882.70 | 1233.90 |
| 0.95 | 664.49 | 1512.60 | 1922.70 |
| 1.00 | 477.57 | 3025.40 | 752.02 |

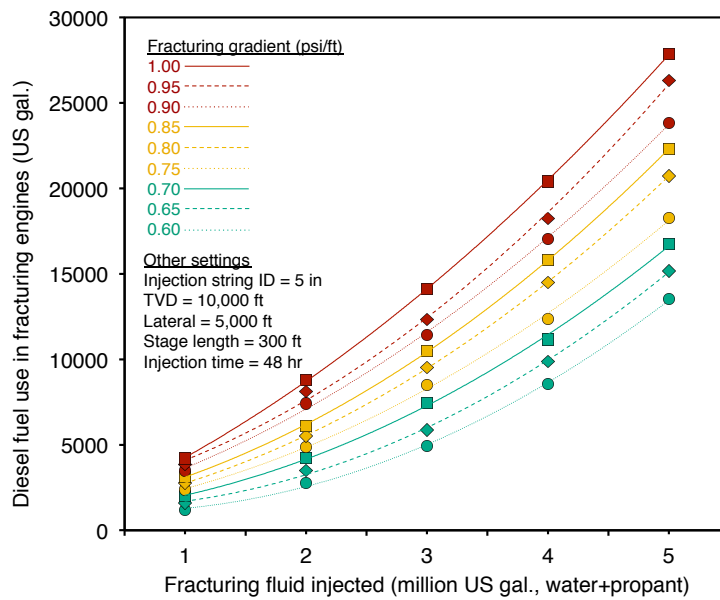


Figure 4.5: Fuel use in hydraulic fracturing as a function of fracturing volume. Each curve represents a different fracturing gradient value, ranging from 0.6 psi/ft to 1.0 psi/ft.

Table 4.5: Land use GHG emissions for 30 year analysis period from field drilling and development in OPGEE for conventional oil operations [g CO₂ eq./MJ of crude oil produced]. Data from Yeh et al [6].

| | Low carbon stock (semi-arid grasslands) | | | Moderate carbon stock (mixed) | | | High carbon stock (forested) | | |
|---------------|--|--------------|--------------|----------------------------------|--------------|--------------|---------------------------------|--------------|--------------|
| | Low int. | Med. int. | High int. | Low int. | Med. int. | High int. | Low int. | Med. int. | High int. |
| Soil carbon | 0.03 | 0.13 | 0.35 | 0.22 | 0.57 | 1.93 | 0.40 | 1.01 | 3.51 |
| Biomass | 0.00 | 0.00 | 0.00 | 0.34 | 0.68 | 1.47 | 0.68 | 1.36 | 2.94 |
| Foregone seq. | 0.00 | 0.00 | 0.00 | 0.01 | 0.01 | 0.01 | 0.01 | 0.01 | 0.02 |

4.2.2.3 Emissions from land use impacts

Land use impacts during drilling and field development are included in OPGEE for three categories: soil carbon that is oxidized upon disturbance of land, biomass carbon that is oxidized due to biomass disturbance, and emissions from foregone sequestration, due to the fact that biomass carbon sequestration is slowed on cleared land. For each of these impacts, emissions estimates from Yeh et al. [6] are included. Yeh et al. measured impacts over a 150 year period, which is not in alignment with other analyses that use 30 year land use impact calculations. For this reason, calculations from Yeh et al. were modified to reduce the timeframe for analysis to 30 years, reducing the amount of regrowth possible [89].

The user has the option to choose a 30 year or 150 year analysis timeframe. The default analysis timeframe is set to 30 years.

In order to estimate land use GHG emissions, three settings are required. First, the crude production method must be chosen. The options for crude production method include conventional production via wellbore (primary, secondary, and tertiary recovery of conventional and heavy hydrocarbons, including in situ recovery of bitumen) and mining-based production of bitumen.

Next, the carbon richness of the ecosystem is specified. Options include low, moderate, and high carbon richness. Low carbon richness estimates are derived from California production in the semi-arid to arid central valley of California [6]. The high carbon richness estimates are derived from forested regions in Alberta (e.g., rocky mountain foothills) [6]. Moderate carbon richness is considered a mixed ecosystem with carbon richness between these ecosystems.

Lastly, the intensity of field development must be specified. High intensity field development corresponds to high fractional disturbance, such as in a field drilled on tight spacing. Low intensity field development corresponds to a sparsely developed field with little fractional disturbance. Moderate field development occurs between these two extremes. Work by Yeh et al. [6] can be consulted for satellite images of low and high field development intensity.

Emissions associated with each choice are shown in Table 4.6 in units of gCO₂eq GHGs per MJ of crude oil produced.

4.2.3 Defaults for drilling & development

Default values for drilling & development calculations are shown in Tables 4.7 and 4.6.

Drilling & Development 1.3,2.3

Emissions Factors Tables 1.6,1.7

Drilling & Development 1.2.13

Drilling & Development 1.1.3,1.1.4

Drilling & Development 1.1.10

Drilling & Development 1.1.11

Emissions Factors Tables 1.6,1.7

Table 4.6: Land use GHG emissions for 150 year analysis period from field drilling and development in OPGEE for conventional oil operations [g CO₂ eq./MJ of crude oil produced]. Data from Yeh et al [6].

| | Low carbon stock (semi-arid grasslands) | | | Moderate carbon stock (mixed) | | | High carbon stock (forested) | | |
|---------------|--|--------------|--------------|----------------------------------|--------------|--------------|---------------------------------|--------------|--------------|
| | Low int. | Med. int. | High int. | Low int. | Med. int. | High int. | Low int. | Med. int. | High int. |
| Soil carbon | 0.03 | 0.13 | 0.35 | 0.10 | 0.35 | 1.50 | 0.16 | 0.57 | 2.65 |
| Biomass | 0.00 | 0.00 | 0.00 | 0.01 | 0.09 | 0.33 | 0.02 | 0.17 | 0.65 |
| Foregone seq. | 0.00 | 0.00 | 0.00 | 0.02 | 0.03 | 0.05 | 0.03 | 0.05 | 0.09 |

Table 4.7: Default inputs for drilling calculations.

| Param. | Description | Eq. no. | Default | Literature range | Unit | Sources | Notes |
|-------------|--|---------|---------|------------------|-----------------------|---------|-------|
| D_v | Vertical depth of wells | | 7240 | 100-20,000 | [ft] | | a |
| D_h | Length of horizontal segment of well | - | 5000 | 1000-10,000 | [ft] | | a |
| f_h | Fraction of wells with horizontal segment | - | 0 | 0 - 1 | [fraction horizontal] | | |
| FI_D^h | Horizontal drilling incremental fuel intensity | - | 0.380 | 0.218 - 0.459 | [gal/ft. horizontal] | [86] | b |
| FI_D^v | Vertical drilling fuel intensity | - | 0.404 | 0.226 - 0.724 | [gal/ft.] | [86] | b |
| N_W | Number of total wells, prod. and inj. | - | 13 | - | [Wells] | - | c |
| $Q_{o,tot}$ | Cumulative production per well over life of well | - | 800 | 150 - 7,000 | [kbbbl/well] | [88] | d |
| LHV_{di} | Lower heating value of diesel fuel | - | 128.5 | 128.5 | [mBtu/gal] | [84] | e |
| LHV_o | Lower heating value of crude oil | - | 5.51 | 5.15 - 6.18 | [mmBtu/bbl] | [90] | e |

^a Low and high drilling efficiency constants found from fitting data. Default set to low intensity.

^b Exponential increase with drilling depth. Low intensity drilling actually has slightly higher growth rate.

^c Default well depth chosen to be depth of field h . Range of field depths is large in practice.

^d Cumulative production per well from Brandt [88].

^e Lower heating value of crude depends on density and composition, we use relationship from Schmidt [90].

4.3 Production & extraction

4.3.1 Introduction to production & extraction

The production and extraction process transports reservoir fluids from the subsurface reservoir to the surface. Emissions from crude oil production and extraction mainly occur from fuel combustion for lifting and injection drivers, along with other smaller sources such as fugitive emissions from wellbores.

As production from a field proceeds the reservoir pressure will decrease. To maintain economic viability, artificial lift equipment is used to enhance production rates. Most commonly, energy is added to the reservoir fluids through the use of a downhole pump [91, p. 2]. Another method is gas lifting, which entails injecting gas into the production string to decrease the density of the column of oil and water in the production tubing.

In addition to artificial lifting, water can be injected into the reservoir to support reservoir pressure and increase oil recovery [68, p. 1]. Enhanced oil recovery (EOR) methods include gas flooding and steam injection.

Most common artificial lifting and improved oil recovery techniques are included in OPGEE. These include: downhole pump, gas lift, water flooding, gas flooding, and steam injection. In the *‘Inputs’* worksheet the user is prompted to choose a combination of techniques applicable to the modeled operation.

A complete list of emissions sources from production, along with their estimated magnitude, is shown in Table C.3. A list of all of the equation parameters, including their default values and sources, is included in Table 4.19.

4.3.2 Calculations for production and extraction

Energy for lifting is required to overcome the pressure traverse, i.e., the pressure drop between the subsurface reservoir and the surface wellhead. The pressure traverse arises due to two factors: (i) flow against gravity, and (ii) frictional losses. The pressure required for lifting is calculated by adding the wellhead pressure to the pressure traverse and subtracting the wellbore pressure. The artificial lifting methods that can be chosen in OPGEE are: (i) downhole pump, and (ii) gas lift. The pressure required for lifting is equal to the discharge pressure of the downhole pump. The power required to generate the required discharge pressure depends on the discharge flow rate and pump efficiency. Finally the energy required to drive the pump is calculated based on the power requirement (expressed as brake horsepower).

The calculation of the energy required in water injection- and gas injection-based EOR uses the user inputs for injection volume and discharge pressure. Smart defaults are in place to help assign the discharge pressure taking into account the well depth and frictional losses.

The energy required for steam flooding requires rigorous modeling of steam generation. An additional complexity is caused by the modeling of electricity co-generation at steam projects. These calculations are explained in Section 5.2, which covers steam generation emissions.

In the case of gas lift, if the user enters the volume of gas injected and the discharge pressure, OPGEE will compute the compression energy. However, OPGEE is not sensitive to changes in the gas lift, i.e. the dynamics between the volume of

gas lift and the lifting head are not considered. The calculation of these dynamics is beyond the scope of a linear GHG estimator. This requires a two phase flow model, which is not included in OPGEE v2.0b.

Default values for production and extraction calculations are shown in Table 4.19.

4.3.2.1 Oil specific gravity

The specific gravity of crude oil is usually reported as API gravity, measured at 60 °F. The API gravity is related to the specific gravity γ_o by:

$$^{\circ}\text{API} = \frac{141.5}{\gamma_o} - 131.5 \quad [-] \quad (4.17)$$

Production & Extraction 2.1.1

where API gravity and γ_o are dimensionless measures. The specific gravity is the ratio of the oil density to the density of water [8, p. 478].

4.3.2.2 Gas specific gravity

The specific gravity of associated gas is calculated as [91, p. 10]:

$$\gamma_g = \frac{\rho_{gsc}}{\rho_{asc}} \quad [-] \quad (4.18)$$

Production & Extraction 2.1.4

where ρ_{gsc} = gas density at standard conditions [lbm/ft³]; and ρ_{asc} = air density at standard conditions [lbm/ft³]. Standard temperature is 60 °F; standard pressure is 14.7 psia [5, p. 35]. The gas density at standard conditions is calculated using:

$$\rho_{gsc} = \frac{p_b \text{MW}_g}{RT_b} \quad \left[\frac{\text{lbm}}{\text{ft}^3} \right] \quad (4.19)$$

where MW_g = molecular weight of the associated gas mixture [lbm/lbmol]; p_b = base pressure [psia]; and T_b = base temperature [°R]; R = gas constant [ft³-psia/lbmol-°R]. The molecular weight is calculated from the molecular weights and molar fractions of the gas constituents.

4.3.2.3 Water specific gravity

The specific gravity of produced water at standard conditions is calculated using [54, p. 481]:

$$\gamma_w = 1 + C_{sd} 0.695 \times 10^{-6} \quad [-] \quad (4.20)$$

Production & Extraction 2.1.2

where C_{sd} = concentration of dissolved solids (also known as TDS) [mg/L]. The constant 0.695×10^{-6} has units of [L/mg].

4.3.2.4 Gas compression ratio

The total gas compression ratio is calculated using:

$$R_C = \frac{p_d}{p_s} \quad [-] \quad (4.21)$$

Table 4.8: Comparison of Z-Factors for OPGEE Default natural gas, nitrogen, carbon dioxide, air, and oxygen During Compression to 20,000 PSIA. Note that air and oxygen are included for reference only, as OPGEE v2.0b does not include air- or oxygen-based EOR modeling.

| P (psia) | T (F) | Natural Gas (OPGEE Default Composition) | Carbon Dioxide | Nitrogen | Air | Oxygen |
|-------------|----------|---|----------------|----------|----------|----------|
| | | Z-Factor | Z-Factor | Z-Factor | Z-Factor | Z-Factor |
| 125.0 | 656.7 | 0.991 | 1.001 | 0.976 | 1.000 | 0.998 |
| 447.4 | 697.8 | 0.977 | 1.008 | 0.935 | 1.005 | 0.998 |
| 1601.4 | 744.4 | 0.955 | 1.040 | 0.830 | 1.032 | 1.008 |
| 5731.6 | 794.5 | 1.089 | 1.202 | 0.792 | 1.179 | 1.100 |

where P_d = discharge pressure [psia]; and P_s = suction pressure [psia].

Multi-stage compression applies when $R_C > 5$ [8, p. 295]. The compression of gas generates significant amount of heat, but compressors can only handle a limited temperature change. Multiple stage compressors allow cooling between stages making compression less adiabatic and more isothermal. OPGEE sets the compression ratio for each of the N stages equal to the N^{th} root of the total compression ratio [8, p. 295]:

Production & Extraction 2.5.1

$$\text{If } \frac{p_d}{p_s} < 5, \text{ then } R_C = \frac{p_d}{p_s}, \text{ otherwise if } \left(\frac{p_d}{p_s}\right)^{\frac{1}{2}} < 5, \text{ then } R_C = \left(\frac{p_d}{p_s}\right)^{\frac{1}{2}}, \dots \quad (4.22)$$

where p_d = discharge pressure [psia]; and p_s = suction pressure [psia].

The number of stages is determined from the calculation of the compression ratio, as shown in eq. (4.22). OPGEE allows a maximum of 5 stages of compression.

4.3.2.5 Gas compressibility factor (Z-factor)

Compression-related calculations account for the compressibility factor (z-factor) of the gas being compressed. The Z-factor of a gas measures the degree to which its properties differ from ideal gas behavior and is dependent on pressure and temperature conditions.

For compression of nitrogen (N_2) [92], carbon dioxide (CO_2) [93], air [94], or oxygen (O_2) [95], OPGEE refers to z-factor data generated using the National Institute of Standards and Technology's REFPROP thermodynamic software package, which uses equations of state to generate compressibility factors [96].

Input data Table 2.7

Table 4.8 depicts Z-factors for the compression stages for the compression of all five flood gases from the OPGEE default 1st stage inlet suction pressure of 125 psia to an extremely high reservoir pressure of 20,000 psia for flooding purposes. For the natural gas the table uses OPGEE's default flood gas composition. Deviations from ideality are largest for carbon dioxide and air, which are more compressible than natural gas, nitrogen, or oxygen.

The experimentally-determined Standing and Katz hydrocarbon Z-factor correlation chart (Figure 4.6 [1]) presents compressibility factors for a hydrocarbon gas mixture based on its pseudoreduced temperature and pseudoreduced pressure [1].

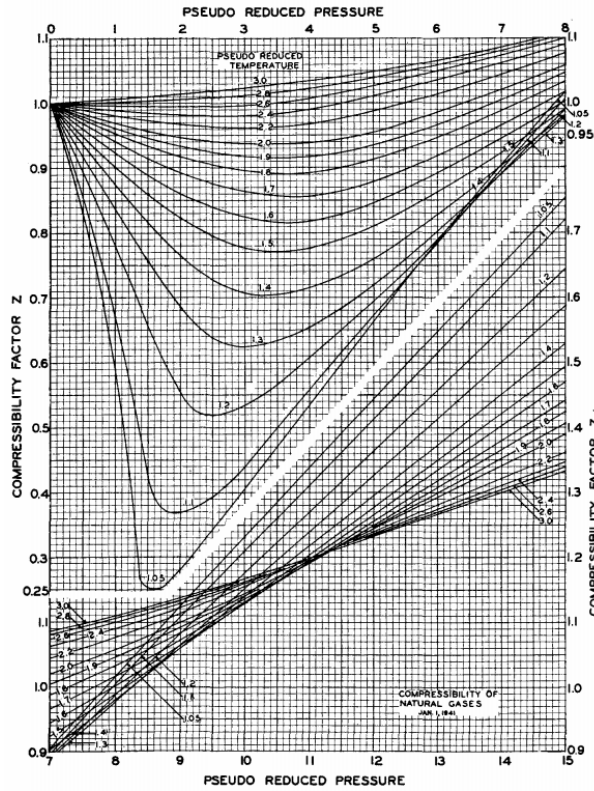


Figure 4.6: Standing and Katz [1] Natural Gas Mixture Z-Factor Chart.

The pseudoreduced parameters of a gas mixture are calculated using [97, p. 111]:

$$T_{pr} = \frac{T}{T_{pc}} \quad (4.23)$$

and

$$P_{pr} = \frac{P}{P_{pc}} \quad (4.24)$$

where T_{pr} = pseudoreduced temperature of the hydrocarbon mixture; T = temperature of the hydrocarbon mixture; T_{pc} = pseudocritical temperature of the hydrocarbon mixture; P_{pr} = pseudoreduced pressure of the hydrocarbon mixture; P = pressure of the hydrocarbon mixture; and P_{pc} = pseudocritical temperature of the hydrocarbon mixture.

The pseudocritical temperature and pressure of a gas mixture are easily determinable approximations of the true critical parameters [97, p. 111]. OPGEE uses a mixing rule to calculate the pseudocritical parameters based on the critical temperatures and pressures of the components of the gas mixture, weighted according to the specific composition of the mixture [98].

The presence of carbon dioxide (CO_2) or hydrogen sulfide (H_2S) in a hydrocarbon gas mixture impart acidic (sour) qualities that alter the pseudocritical parameters and must be accounted for. OPGEE accounts for the presence of hydrogen sulfide (up to 74% of the gas composition) or carbon dioxide (up to 54% of the gas composition) using a correction factor to adjust the pseudocritical temperature and pressure [99].

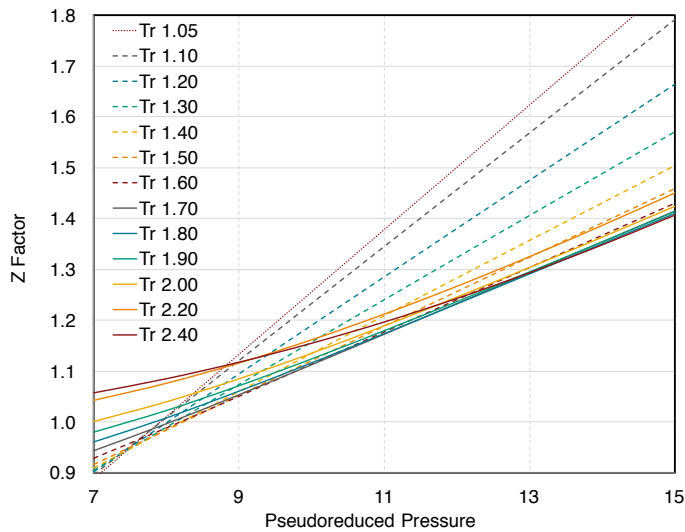


Figure 4.7: Correlation of Upper Portion of Standing and Katz Z-Factor Chart. Source: [2].

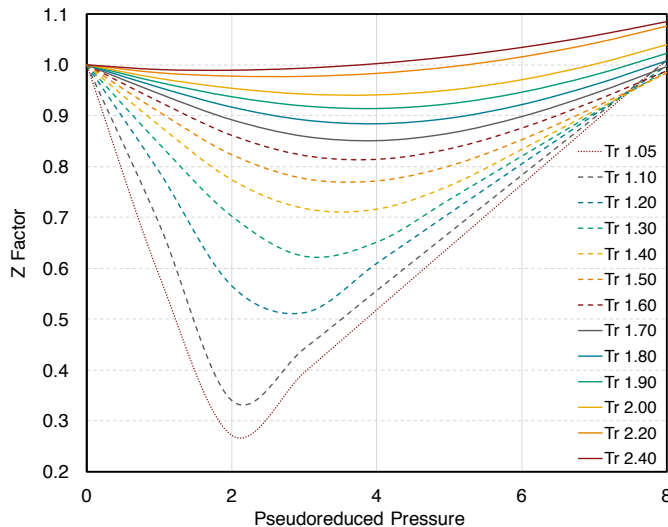


Figure 4.8: Correlation of Lower Portion of Standing and Katz Z-Factor Chart. Source: [2].

When hydrocarbon gas mixtures are compressed, OPGEE uses a correlation of the Standing and Katz chart to calculate an approximate Z-factor for each stage of compression [2]. The correlations for the upper and lower portions of the chart are

presented in Figure 4.7 and Figure 4.8, respectively.

4.3.2.6 Gas compressor suction temperature

When multiple stage compressors are used the gas must be cooled between stages to reduce the adiabatic work of compression. The discharge temperature at a given compressor stage is calculated using [66, p. 105]:

$$\frac{T_d}{T_s} = \left(\frac{p_d}{p_s} \right)^{\left[\frac{z_s (C_{p/v} - 1)}{C_{p/v}} \right]} \quad [-] \quad (4.25)$$

where T_d = discharge temperature [$^{\circ}\text{R}$]; T_s = suction temperature [$^{\circ}\text{R}$]; $C_{p/v}$ = ratio of specific heats at suction conditions; and z_s = suction z-factor.

The suction temperature of the subsequent compressor is estimated assuming 80% interstage cooling (imperfect cooling) so that:

$$T_{s2} = \lambda_{\Delta T} (T_d - T_s) + T_s \quad [^{\circ}\text{R}] \quad (4.26)$$

where T_{s2} = suction temperature of stage 2 compressor [$^{\circ}\text{R}$]; and $\lambda_{\Delta T}$ = fraction of temperature increase remaining after cooling, 0.2 [fraction]. The default of $\approx 80\%$ interstage cooling is taken from an example of imperfect cooling in [100, Table 7].

Production & Extraction 2.5.3

4.3.2.7 Gas flooding

Introduction to gas flooding Gas flooding can be performed with natural gas, molecular nitrogen (N_2), carbon dioxide (CO_2), air, or oxygen (O_2). Note that OPGEE v2.0b does not include air or oxygen flooding, so any parameters there are included for reference only. If gas flooding via N_2 injection is chosen, the work of air separation must be accounted for. Industrial capacity N_2 plants have specific work on the order of 0.25 kWh/ Nm^3 [101]. The largest N_2 separation plant in the world serves to provide N_2 for injection into the Cantarell field in Mexico [102]. This facility has compression horsepower of 500,500 hp to supply 1,200 MMSCF/d of N_2 at ≈ 1700 psia.

Production & Extraction 2.8

OPGEE computes gas flooding work to take gas from 125 psia to reservoir injection pressure.

Production & Extraction 2.7.4

Subtracting this work from the reported consumption at Cantarell, we arrive at specific work of ≈ 0.15 kWh/ Nm^3 for only the air separation component. Depending on the reservoir pressure, OPGEE will then add to this separation work the work to compress N_2 to required pressure. The work for gas injection compressors is modeled as noted above. If reinjected produced natural gas is assumed, then no separation work for N_2 production is required.

OPGEE calculates the reservoir injection pressure based on the choice of the flood gas. If a gas other than CO_2 is the flood gas, then the reservoir injection pressure is calculated as:

$$P_{inj} = P_{res} + 500 + 14.7 \quad [\text{psia}] \quad (4.27)$$

where P_{inj} = reservoir injection pressure [psia] and P_{res} = reservoir pressure [psig]. The term 14.7 converts [psig] to [psia].

Table 4.9: Minimum Miscibility Pressure and API Gravity Default Correlation. Source: [7].

| API Gravity [$^{\circ}$ API] | Minimum Miscibility Pressure [psia] |
|-------------------------------|-------------------------------------|
| <27 | 4,000 |
| 27-30 | 3,000 |
| >30 | 1,200 |

Table 4.10: Temperature Adjustment to Minimum Miscibility Pressure Default Correlation Source: [7].

| Reservoir Temperature [$^{\circ}$ F] | Adjustment [psia] |
|---------------------------------------|-------------------|
| 120 | 0 |
| 120-150 | +200 |
| 150-200 | +350 |
| 200-250 | +500 |

CO₂ flooding and minimum miscibility pressure OPGEE assumes that CO₂ injection is performed to achieve a miscible gas flood. If CO₂ is the flood gas, then the reservoir injection pressure must reach the minimum miscibility pressure (MMP). The MMP is the minimum pressure necessary for CO₂ and oil to form a single fluid phase, which increases recovery rates and is the basis of miscible gas flooding. Many factors influence the MMP, such as reservoir temperature, the presence of other chemical species such as H₂S, and the density and composition of the oil [103].

The default MMP value is estimated using a correlation from the NPC (National Petroleum Council) based on the API gravity and reservoir temperature [7]. However, actual MMP values are usually available for miscible CO₂ flood projects and the actual data should be used whenever possible.

The API gravity of the oil is used to generate an initial estimate, as shown in Table 4.9. The reservoir temperature adjustment is then applied to the initial estimate as shown in table 4.10.

If CO₂ is the flood gas and the MMP is higher than the standard reservoir injection pressure determined in Equation (4.27), then the flood gas compressor injects at the MMP. If the standard reservoir injection pressure calculated in Equation (4.27) is higher than the MMP, then the flood gas compressor injects at the standard reservoir injection pressure.

4.3.2.8 CO₂ Enhanced oil recovery and sequestration parameters

CO₂ sequestration calculation In the early stage of a CO₂ flood project, newly acquired CO₂ will account for the entirety of the injected CO₂. As the injected CO₂ proceeds through the reservoir, a proportion of it will be trapped in the reservoir by factors such as blockage by surrounding rocks of low permeability or by trapping within water in the reservoir. The portion of CO₂ that is not immediately trapped will be produced and injected again following its separation from the oil and/or associated gas stream, if applicable, as described in the Surface Processing section. Thus, following CO₂ breakthrough the injected CO₂ will consist of two portions: 1) a newly acquired, never-injected portion and 2) a previously-injected and recycled portion.

An individual molecule of CO₂ injected for EOR may thus transit the reservoir and the surface processing facilities multiple times before it is trapped within the

reservoir. OPGEE assumes that a molecule of newly acquired CO₂ will ultimately be sequestered within the reservoir. An example demonstrating this process is the EOR project at the Denver Unit of the Wasson Field in the Texas Permian Basin, where Occidental Petroleum has injected CO₂ since the early 1980s [104]. In a presentation submitted to California's Energy Commission, Occidental Petroleum depicts an accounting of the volume of CO₂ acquired, injected, produced, trapped, recycled, and lost to venting and fugitive emissions during a 25-year period at the Denver Unit flood [105]. Occidental Petroleum indicates that 115 million metric tons of CO₂ were supplied to the project; their material balance calculations indicated that essentially an equivalent amount was sequestered in the reservoir. Venting and fugitives accounted for the loss of 0.3% of the cumulative volume of produced or recycled CO₂ [105].

OPGEE accounts for loss of CO₂ due to terminal blow-down operations or long-term leakage from the reservoir. These factors decrease the overall sequestration rate and are included in the 'GHG Emissions' gathering worksheet section. The gross (before deduction of aforementioned losses) daily CO₂ is calculated as follows:

First, the volumetric injection rate of CO₂ is calculated as:

$$Q_{CO2} = R_{inj,fg} \cdot Q_o \cdot \frac{1[\text{Mscf}]}{1000[\text{scf}]} \left[\frac{\text{Mscf}}{\text{d}} \right] \quad (4.28)$$

where Q_{CO2} = the volumetric injection rate of CO₂ [Mscf/d]; $R_{inj,fg}$ = the gas flooding injection ratio [scf/bbl]; and Q_o = the oil production rate [bbl/d].

Second, the CO₂ gross sequestration rate S is calculated as:

$$S_{CO2} = Q_{CO2} \cdot f_{CO2,new} \cdot \frac{1000[\text{scf}]}{1[\text{Mscf}]} \cdot \frac{0.117[\text{lb}]}{1[\text{scf}]} \cdot \frac{453.6[\text{g}]}{1[\text{lb}]} \left[\frac{\text{g}}{\text{d}} \right] \quad (4.29)$$

where S_{CO2} = the gross sequestration rate of CO₂ [scf/d]; Q_{CO2} = the volumetric injection rate of CO₂ [Mscf/d]; and $f_{CO2,new}$ is the proportion of newly acquired CO₂ that has not previously been injected [-].

Long-term leakage rate of sequestered carbon CO₂ that is sequestered over the course of an EOR project must remain sequestered for long-term periods to have a significant impact on climate change mitigation. For this reason, considering the long-term stability of carbon storage is necessary for lifecycle assessment of CO₂-EOR. Many CO₂-EOR projects are located in extensively developed petroleum fields with large amounts of abandoned wells through which previously sequestered CO₂ could migrate and leave the reservoir. Research has investigated the role that these wells may play in allowing trapped CO₂ to leave the reservoir. For example, Kang et al. collected methane emissions data from abandoned wells in Pennsylvania; they concluded that the permeability of such wells was sufficiently low that they present only a "small" risk of allowing leakage of sequestered CO₂ [106].

Computational analyses of reservoir fluid flow have estimated long-term leakage rates through oil and gas wells of CO₂ sequestered by injection into saline aquifers. In one example, Celia et al. [107] used the properties of an area in Alberta, Canada with deep brine aquifers that have the potential to serve as CO₂ sequestration sites. The area also contains many oil and gas wells that could potentially allow the loss of trapped CO₂. After estimating the properties of the geological

Production & Extraction 2.7.11

layers and the oil and gas wells in the target area, Celia et al modeled CO₂ injection into the deep aquifers and subsequent migration over 50 years. Celia et al. found that CO₂ leakage rates through the oil and gas wells were nearly always below 1% [107].

An Intergovernmental Panel on Climate Change's (IPCC) report by Benson, et al. [108] analyzed the general prospects of CO₂ sequestration and long-term leakage in underground geological formations, which include oil and gas reservoirs in the context of EOR operations. Benson et al. indicated — with the stipulation that sequestration sites must be "appropriately selected and managed" — that leakage rates are "likely" to be below 1% over a 1,000 year period; they defined "likely" as a 66%-90% probability [108]. During a 100 year period, Benson, Cook et al stated that is "very likely" (90%-99%) that CO₂ leakage rates would be below 1% [108].

Lastly, NETL's 2013 life-cycle analysis of CO₂ EOR assumes that 100-year leakage rates are between 0% to 1% and its base case value is a 0.5% leakage rate [4]. OPGEE adopts this value for its default long-term CO₂ leakage rate of 0.5%. OPGEE temporally collapses the proportion of CO₂ lost to long-term reservoir leakage and models it occurring at the time of injection.

Blow-down and venting of CO₂ in terminal stage of operation OPGEE allows the user to model an oilfield operator's decision to conduct a blow-down procedure on a CO₂ flood in the final stage of the project. Blow-down entails ceasing CO₂ injection and sealing the injector wells while maintaining production from the producer wells. Additional oil would be recovered during this terminal-stage pressure decline; CO₂ could be vented following its separation from the produced oil [109].

Leach et al. [110] reviewed the literature to determine whether blow-down procedures are commonly used during the final stage of CO₂ EOR floods. While Leach et al. [110] found a handful of sources indicating that blow-down operations typically occur, their analysis of EOR-specific technical materials did not reveal references to blow-down. For this reason the OPGEE default is that 0% of sequestered CO₂ is lost because of terminal stage blow-down and venting. If the user chooses to select a positive blow-down percentage, then it is considered in the overall life-cycle calculations in the 'GHG Emissions' gathering worksheet section. An actual blow-down procedure would be a process taking place over weeks and months. OPGEE temporally collapses the blow-down procedure and models it occurring at the time of injection.

Production & Extraction 1.2.9.3

4.3.2.9 Well pressure traverse

The pressure traverse is the total pressure required to lift the crude oil mixture against gravity and overcome friction and kinetic losses. This is equal to the pressure drop along the well tubing from the wellbore to the wellhead. This pressure drop has two main components: (i) the elevation component, which is the pressure drop due to gravity; and (ii) the friction component, which is the pressure drop due to liquid contact with the inner walls of the well tubing.

The first step in the estimation of the pressure traverse is the calculation of the total head as:

$$h_{tot} = h_{el} + h_f \quad [\text{ft}] \quad (4.30)$$

Production & Extraction 1.2.2.2.1

Table 4.11: Reynold's number (Re) ranges of different flow patterns. Data from McAllister [8].

| Flow pattern | NRe [-] |
|-----------------|--------------------------|
| Laminar flow | $Re < 2000$ |
| Transition flow | $2000 \leq Re \leq 4000$ |
| Turbulent flow | $Re > 4000$ |

where h_{tot} = total head [ft]; h_{el} = well depth [ft]; and h_f = friction head [ft]. The friction head is calculated using the Darcy formula [8, p. 447]:

$$h_f = \frac{f h_{el} v_{l,W}^2}{2 D_P g_c} \quad [\text{ft}] \quad (4.31)$$

where f = Moody friction factor [-]; h_{el} = well depth [ft]; $v_{l,W}$ = pipeline flow velocity [ft/s]; D_P = pipeline diameter [ft]; and g_c = gravitational constant, 32.2 [lbm-ft/lbf-s²]. A major determinant of friction losses is the pipeline diameter or production tubing diameter (D_P). API production tubing diameters range from 1.05 to 4.5 inches ID; the API system is a petroleum industry standardized measuring system [53, p. 106].

A Moody friction factor chart is shown in Figure 4.9 [3]. f varies with the Reynold's Number (Re) and/or pipeline roughness, depending on whether the flow regime is laminar or turbulent [8, p. 481]. Table 4.11 shows the Re ranges of different flow patterns.

The Moody friction factor is estimated using simplifications for the default case as follows: Water and oil are assigned viscosities of 1 and 10 cP, respectively. The viscosity of the oil-water mixture is assigned the volume-weighted viscosity of the two fluids.¹

The Reynolds number, Re, is calculated as follows [111, p. 46]:

$$Re = \frac{1.48 Q_l \rho_l}{D_P \mu_l} \quad (4.32)$$

where Q_l is the total liquid production rate [bbl/d]; ρ_l is the liquid density (oil-water mixture) [lbm/ft³]; D_P is the wellbore production diameter [in], and μ_l is the fluid viscosity [cP]. Roughness of commercial steel of 0.0018 in is assumed [112], for a relative roughness r of 0.0006. The approximate friction factor is calculated as follows [112, p. 625]:

$$f = \left(\frac{-1}{1.8 \log \left(\left[\frac{6.9}{N_{re}} \right] + \left[\frac{r}{3.7} \right]^{1.11} \right)} \right)^2 \quad (4.33)$$

This equation gives a friction factor f of 0.02 for default conditions. The friction factor is a user input on the 'Production & Extraction' worksheet and can be adjusted by the user.

¹This simplification does not account for the complexity of oil-water mixture viscosity, but is used as a first-order approximation. Heavy oil can have very high viscosities as well.

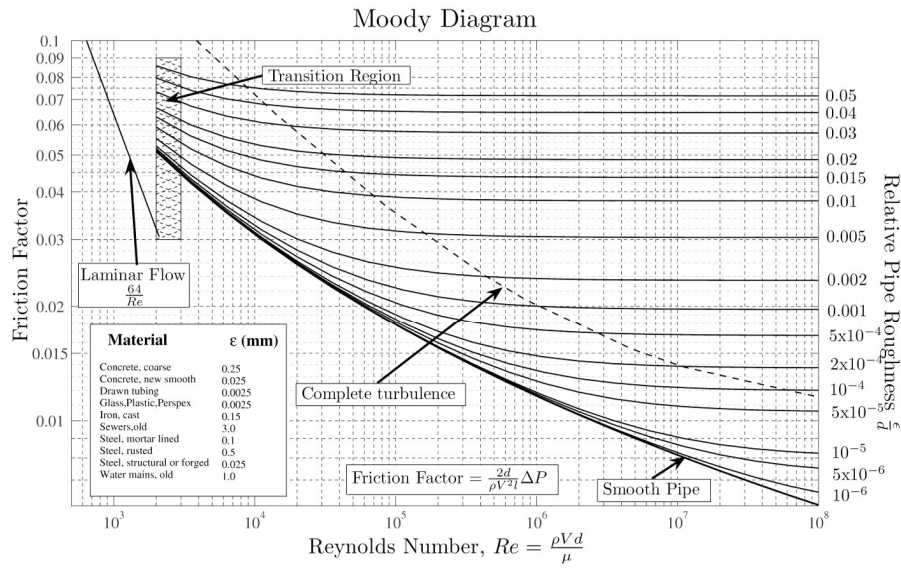


Figure 4.9: Moody friction factor chart. Source: [3].

The pipeline flow velocity is calculated as:

$$v_{l,w} = \frac{Q_{l,w}}{A_p} \quad [\text{ft/s}] \quad (4.34)$$

where $Q_{l,w}$ = wellbore flow rate or liquid production per well [ft^3/s]; and A_p = the cross sectional area of the pipe [ft^2]. The wellbore flow rate is calculated as:

$$Q_{l,w} = \frac{Q_l}{N_w} \quad [\text{ft}^3/\text{s}] \quad (4.35)$$

where Q_l = total rate of liquid production [ft^3/s]; and N_w = number of producing wells. The total rate of liquid production is calculated as:

$$Q_l = Q_o(1 + \text{WOR}) \quad [\text{ft}^3/\text{s}] \quad (4.36)$$

where Q_o = total rate of oil production [bbl/d]; WOR = water-to-oil ratio [bbl/bbl]. The total rate of liquid production is converted from [bbl/d] to [ft^3/s].

The pressure traverse is estimated using the total head as [8, Table 1, p. 455]:

$$p_{trav,tot} = 0.43 h_{tot} \gamma_l \quad [\text{psi}] \quad (4.37)$$

where $p_{trav,tot}$ = total pressure traverse [psi]; 0.43 = fresh water gradient at 60 °F [psi/ft] [68, p. 25]; h_{tot} = total head [ft]; and γ_l = the specific gravity of the crude oil mixture [-], calculated as:

$$\gamma_l = \gamma_o \lambda_o + \gamma_w \lambda_w \quad [-] \quad (4.38)$$

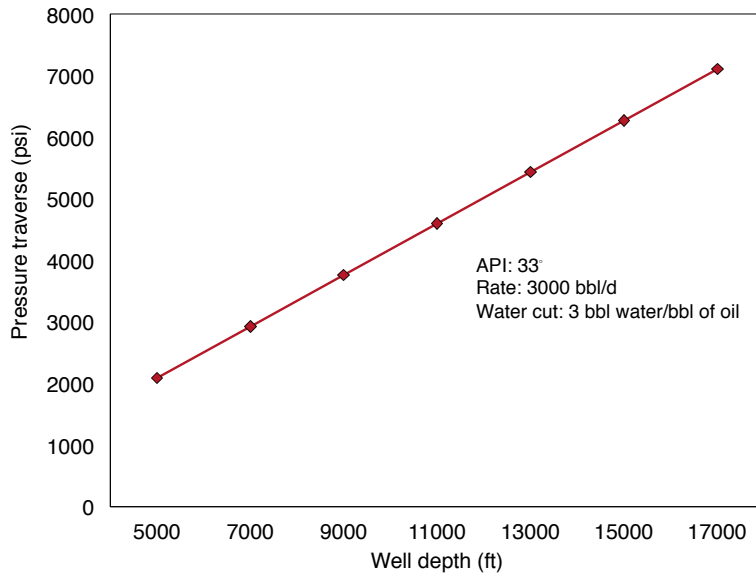


Figure 4.10: An example of a linear pressure traverse curve (GLR= 0).

where γ_o = the specific gravity of oil [-]; γ_w = the specific gravity of water [-]; λ_o = fraction of oil [fraction]; and λ_w = fraction of water [fraction]. The fraction of oil is calculated as:

$$\lambda_o = \frac{Q_o}{Q_o(1 + \text{WOR})} \quad [-] \quad (4.39)$$

The elevation component of the pressure traverse is estimated using a linear one phase flow model where the gas-to-liquid ratio is equal to zero (GLR= 0) and the temperature and pressure effects are ignored. Figure 4.10 shows an example of a linear pressure-traverse curve for a particular production rate and fluid properties. The slope of the curve is the relative density of the flowing oil-water mixture. For GLR>0 the relationship becomes non-linear and the pressure traverse becomes less sensitive to changes in the well depth with increasing GLR [53, p. 27]. However, the generation of a non-linear relationship requires the application of the multi-phase flow correlations which requires an iterative, trial-and-error solution to account for the changes in flow parameters as a function of pressure. Due to the complexity of this approach, we do not implement multi-phase flow in OPGEE v2.0b.

4.3.2.10 Pressure for lifting

The second step after estimating pressure traverse is the calculation of the pressure for lifting which is the pressure required by artificial means (e.g., pump) to lift the oil-water mixture to the surface at the desired wellhead pressure. The pressure for lifting is calculated as:

$$p_{\text{lift}} = (p_{\text{trav,tot}} + p_{\text{wh}}) - p_{\text{wf}} \quad [\text{psi}] \quad (4.40)$$

where p_{lift} = pressure for lifting [psi]; $p_{tav,tot}$ = total pressure traverse [psi]; p_{wh} = wellhead pressure [psi]; and p_{wf} = bottomhole pressure [psi]. The wellbore pressure is calculated from the average reservoir pressure by subtracting the pressure drawdown. The pressure drawdown is the difference between the reservoir pressure and the bottomhole pressure [91, p. 22].

The productivity index, PI, is defined as [91, p. 23]:

$$PI = \frac{Q_{l,W}}{(p_{res} - p_{wf})} \left[\frac{\text{bbl liquid}}{\text{psi-d}} \right] \quad (4.41)$$

where PI = well productivity index [bbl liquid/psi-d]; $Q_{l,W}$ = liquid production per well [bbl liquid/d]; p_{res} = average reservoir pressure [psi]; and p_{wf} = wellbore pressure [psi]. The increase in production requires an increase in pressure drawdown at a constant productivity index. In OPGEE a default productivity index of 3.0 [bbl liquid/psi-d] is assumed to calculate the pressure drawdown. The user has to control the inputs to satisfy the condition of $p_{wf} \geq 0$. The pressure for lifting can either be applied by a downhole pump or by gas lift; in OPGEE these methods may be used individually or simultaneously.

4.3.2.11 Pump brake horsepower

The brake horsepower (BHP) is calculated using the pump discharge flow rate and the pumping pressure as [68, p. 27]:

$$BHP_P = \frac{1.701 \times 10^{-5} Q_d \Delta p}{\eta_P} \quad [\text{hp}]$$

This is equivalently expressed as:

$$BHP_P [\text{hp}] = \frac{\frac{1[\text{hp}]}{1714[\text{gpm-psi}]} \frac{42[\frac{\text{gal}}{\text{bbl}}]}{24[\frac{\text{hr}}{\text{d}}]} \frac{1[\frac{\text{min}}{\text{hr}}]}{60[\frac{\text{min}}{\text{hr}}]} Q_d \left[\frac{\text{bbl}}{\text{d}} \right] \Delta p [\text{psi}]}{\eta_P} \quad (4.42)$$

where BHP_P = brake horsepower [hp]; Q_d = pump discharge rate [bbl/d]; Δp = pumping pressure [psi]; and η_P = pump efficiency [%]. The term 1714 is a dimensionless factor that converts between [hp] and [gpm-psi]. The pumping pressure is the difference between pump discharge and suction pressures. The default suction pressure is 0 psi. In the case of a downhole pump the pumping pressure is equal to the pressure for lifting as calculated in eq. (4.40).

4.3.2.12 Compressor brake horsepower

OPGEE assumes use of a reciprocating compressor. The ideal isentropic horsepower is calculated using [66, p. 105]:

$$-W_N = \left\{ \frac{C_{p/v}}{(C_{p/v} - 1)} \right\} \left(3.027 \cdot \frac{14.7}{520} \right) T_s \left\{ \left(\frac{p_d}{p_s} \right)^{\frac{z_s(C_{p/v}-1)}{C_{p/v}}} - 1 \right\} \left[\frac{\text{hp-d}}{\text{MMscf}} \right] \quad (4.43)$$

where W_N = adiabatic work of compression of N^{th} stage [hp-d/MMscf] (-W denotes work output); $C_{p/v}$ = ratio of specific heats [-]; T_s = suction temperature [$^{\circ}\text{R}$];

Production & Extraction 2.2.3

Production & Extraction 2.5.6, 2.6.5, 2.7.6

p_s = suction pressure [psia]; p_d = discharge pressure [psia]; and z_s = suction z-factor. The constant 3.027 has a unit of [hp-d/MMscf-psia]. Standard temperature (520 [°R]) and pressure (14.7 [psia]) are used as the initial values.

The total work of compression of the multiple stage compressor is multiplied by the compressor discharge rate and divided by the compressor efficiency to calculate the brake horsepower requirement as:

$$\text{BHP}_C = \sum_{N=1}^S \frac{W_N Q_d}{\eta_C} \quad [\text{hp}] \quad (4.44)$$

Production
& Extraction
2.5.8, 2.6.7, 2.7.8

where Q_d = compressor discharge rate [MMscf/d]; η_C = compressor efficiency [fraction]; and S = number of compressor stages.

4.3.2.13 Driver fuel consumption

The total brake horsepower requirement (BHP) is used to determine the driver size. A database of drivers of different types and sizes (natural gas engine, diesel engine, electric motor, etc.) is built in the 'Drivers' supplementary worksheet using technical worksheets of engine and motor manufacturers such as Caterpillar and General Electric [113, 114]. Natural gas fueled drivers, for example, range from 95 hp engine to 20,500 hp turbine. The appropriate driver is retrieved from a database based on the chosen driver type and the required driver size. Finally the fuel consumption of the component (pump, compressor, etc.) is calculated as:

Production & Ex-
traction 3.1

$$E_j = \text{BHP}_j \cdot e_D \cdot \frac{24}{10^6} \quad \left[\frac{\text{MMBtu}}{\text{d}} \right] \quad (4.45)$$

where E_j = component fuel consumption [MMBtu/d]; and e_D = driver fuel consumption [Btu/hp-hr]. The type of fuel consumed (i.e. natural gas, diesel, etc.) is determined by the chosen type of driver.

The driver fuel consumption is required for the calculation of energy consumption of various production components. This includes sucker-rod pumps, electric submersible pumps, water injection pumps, and gas compressors.

4.3.2.14 Bitumen mining

There are seven mining projects currently operating in the Canadian oil sands as of late 2015. The characteristics of each mining operation are summarized in Table 4.12. One of the main differences between oil sands mines is the bitumen froth treatment technology used. Once oil sands material is mined it is transported to a separation facility where hot water is added to produce an oil sands slurry. The slurry is brought to an extraction facility where gravity drainage is used to remove larger solids and produce a bitumen froth, a mixture of bitumen, fine solids, and water. This bitumen froth undergoes froth treatment, in which a light hydrocarbon (either naphthenes or paraffins) acts as a solvent and separates bitumen from other material contained in the bitumen froth. Older projects (those constructed prior to 2002) all employ naphthenic froth treatment (NFT), while projects constructed from 2002 onwards (with the exception of the CNRL Horizon project which employs NFT) employ paraffinic froth treatment (PFT).

Table 4.12: Characteristics of operating mining projects

| Mine | Start-up year | Capacity (bbl/d) | Type of sep. | Int. upgr. | Notes |
|-----------------------|---------------|------------------|--------------|------------|---|
| Suncor | 1967 | 490,000 | NFT | Yes | Upgrader also processes bitumen produced from Suncor Firebag in situ project. |
| Syncrude Mildred Lake | 1978 | 150,000 | NFT | Yes | Upgrader also processes bitumen produced at Syncrude Aurora mine. |
| Syncrude Aurora | 2001 | 200,000 | NFT | No | Waste heat from Syncrude Mildred Lake upgrader used in Syncrude Aurora mine. |
| CNRL Horizon | 2008 | 250,000 | NFT | Yes | |
| Shell Muskeg River | 2002 | 155,000 | PFT | No | Bitumen transported to stand-alone Shell Scotford upgrader. |
| Shell Jackpine | 2010 | 100,000 | PFT | No | Bitumen transported to stand-alone Shell Scotford upgrader. |
| Imperial Kearn | 2013 | 220,000 | PFT | No | Only mine that produces diluted bitumen. |

The bitumen produced at NFT facilities is of lower quality, containing a higher percentage of asphaltenes and more residual water and solids. Bitumen produced at NFT mines must therefore go through upgrading to synthetic crude oil (SCO) and cannot be diluted and sent directly to refineries, as is the case for bitumen produced at PFT facilities. Generally NFT mines include an upgrader located at the mine site. Because natural gas and electricity consumed for the mine and the upgrader are delivered to the site altogether, the facilities share a common cogeneration system and a significant amount of waste heat from the upgrader is used in the bitumen separation process.

Disentangling use by mining operations alone is challenging given the complex nature of operations. Importantly, the Alberta Energy Regulator (AER) reports natural gas and electricity consumption for integrated mining and upgrading facilities together without specifying the quantities of natural gas and electricity consumed for mining alone. The exception to this is the Syncrude Aurora (NFT) project, as bitumen produced at that site is transported to the Syncrude Mildred Lake (NFT) project for upgrading at the Mildred Lake upgrading facility. Also, the Suncor upgrader located at the mine site also upgrades bitumen produced at Suncor's Firebag in situ project. Bitumen produced by the stand-alone Shell Muskeg River and Jackpine (PFT) mines is upgraded at the stand-alone Shell Scotford upgrader, however as the upgrader is located off-site the energy consumption for the mines is reported separately from the upgrading process. The Imperial Kearn project is the only mining project that produces diluted bitumen (known as dilbit) that is sent directly to refineries without undergoing any intermediate upgrading. Of all the mining projects, the Suncor upgrader produces some diesel fuel that is combusted as a fuel on-site.

Public Data Available Data are available from a number of public sources. First, the AER publishes monthly Statistical Reports on oil sands operations. Most useful are ST39: *Alberta Mineable Oil Sands Plant Statistics*, which was published from 1970-2002 and 2008-2014 [115]; as well as ST43: *Alberta Oil Mineable Oil Sands Plant Statistics - Annual*, which was published in years 2003-2007 [116]. These statistical

reports tabulate monthly energy consumption, flared/wasted fuels, and electricity, bitumen, and SCO production for each oil sands project. Some projects operated by the same company receive fuel at one mine and then deliver fuel to the other mine and so report the total fuel consumption under the mine that receives the fuel (e.g., Syncrude's Mildred Lake and Aurora projects) rather than reporting the fuel consumption for each project separately [117].

Definitions provided by AER for energy consumption reported in the AER's ST39 and ST43 reports include definitions of some potentially ambiguous data [117]:

- SCO Fuel Use: The total volume of SCO combusted as fuel at the facility.
- SCO Plant Use: The total volume of SCO used at the facility for uses other than fuel.
- Bitumen Flared/Wasted: The total volume of unrecovered crude bitumen from spills, upgrading slops, tanks dewatering etc.

Note that diesel fuel consumption for each project is collected by the AER but not reported in any of the AER's reports [117]. One project, Suncor, does report that the upgrader produces diesel fuel that is used as fuel on site for mining operations. This use is reported under the AER as SCO fuel consumption [115].

Another important data source are engineering "templates" generated by the Canada's Oil Sands Innovation Alliance (COSIA). COSIA has published two mine templates that contain material and energy flow diagrams for the two froth treatment technologies (naphthenic froth treatment and paraffinic froth treatment) employed in the oil sands [118, 119]. For each froth treatment technology, energy and material flows are presented for two possible oil sands ore qualities: low grade ore at 9 wt.% bitumen, and high grade ore at 12 wt.%. The COSIA Mine Templates provide approximate energy consumption values for a representative mining project based on existing oil sands operations but not representative of any currently operating oil sands project.

A last source of data is the Alberta Environmental Monitoring, Evaluation, and Reporting Agency (AEMERA), which has published estimates of fugitive GHG emissions from mine face, tailings ponds, and 'other' (e.g., emissions from pipe fitting and equipment leaks, releases from pressure relief valves, tanks, and sewage lagoons) for each oil sands company operating a mining project from January 1st, 2011 to December 31st, 2014 [120]. The fugitive GHG emissions generated by AEMERA are developed from figures reported by companies to the Government of Alberta under the Specified Gas Emitters Regulation (AB, 2007). The estimated fugitive CH₄ emissions from oil sands mine face and tailings ponds reported by AEMERA are close to the numbers reported elsewhere [121, 122].

In order to capture the range of mining projects, OPGEE models two template mining operations:

- an upgrader-integrated mine using naphthenic froth treatment (NFT) separation technology;
- A stand-alone mine using paraffinic froth treatment (PFT) separation technology.

As can be seen in Table 4.12 above, the integrated mine and upgrader using NPT separation is more indicative of older large-scale mining projects developed in the 1970s and 1980s, such as the Suncor and Syncrude operations. Additionally, the more recently developed CNRL Horizon project is an integrated NFT mine. The non-integrated mine with PFT separation is more representative of modern developments such as Albion Sands (Shell), Aurora (Syncrude), Jackpine (Shell), and Kearl (Imperial).

Public natural gas and electricity consumption literature data available, AER facility-reported data and COSIA Mine Template ranges, is presented in Figures 4.11 and 4.12, respectively, below. Production-weighted average energy consumption is reported for both 2014 and over the project life based on the AER data reported for each facility. The shaded regions represent the natural gas consumption for NFT and PFT mines presented in the COSIA Mine Template for low grade and high grade ore. Note that no corresponding graph can be created for diesel consumption due to lack of consistent reporting of diesel use in AER datasets.

There is some challenge in interpreting reported public data. First, note that natural gas consumption reported by AER for Suncor, Syncrude Mildred Lake, and CNRL Horizon mines includes natural gas consumed in on-site upgraders. Similarly, electricity consumption reported by AER for Suncor, Syncrude Mildred Lake, and CNRL Horizon mines include electricity consumed in on-site upgraders. Lastly, the Shell Muskeg River mine receives the majority of natural gas that is consumed at Shell Jackpine mine, meaning that per-mine consumption at each Shell mine is between the two reported values (high for Muskeg River and very low for Jackpine). The separation of stand-alone vs. integrated upgrading mines, is discussed more fully below.

Modeling of non-integrated PFT mining operations The non-integrated mining operation is illustrated in Figure 4.13. The energy imports to the stand-alone mining operation include diesel imports, electricity imports, and natural gas imports. Some mining operations co-generate power on site and may also export power. The mine takes in raw bitumen ore and exports diluted bitumen for shipment to upgraders or direct shipment to refineries.

The default values for energy use in non-integrated PFT mining operations are computed as follows:

- Natural gas consumption is modeled using the AER 2014 production-weighted average for three stand-alone PFT projects (Shell Muskeg River, Shell Jackpine, and Imperial Kearl).
- Electricity consumption is modeled using the AER 2014 production-weighted average for three stand-alone PFT projects (Shell Muskeg River, Shell Jackpine, and Imperial Kearl).
- Diesel consumption is estimated as the average of COSIA reported high and low ranges of diesel consumption, as reported for low-grade (9 wt.% and high-grade (12 wt.%) ores respectively. The range from the COSIA templates is used as the range of diesel consumption rate.
- Diluent blending rates are modeled using AER 2014 production-weighted averages from the stand-alone PFT projects (Shell Muskeg River, Shell Jack-

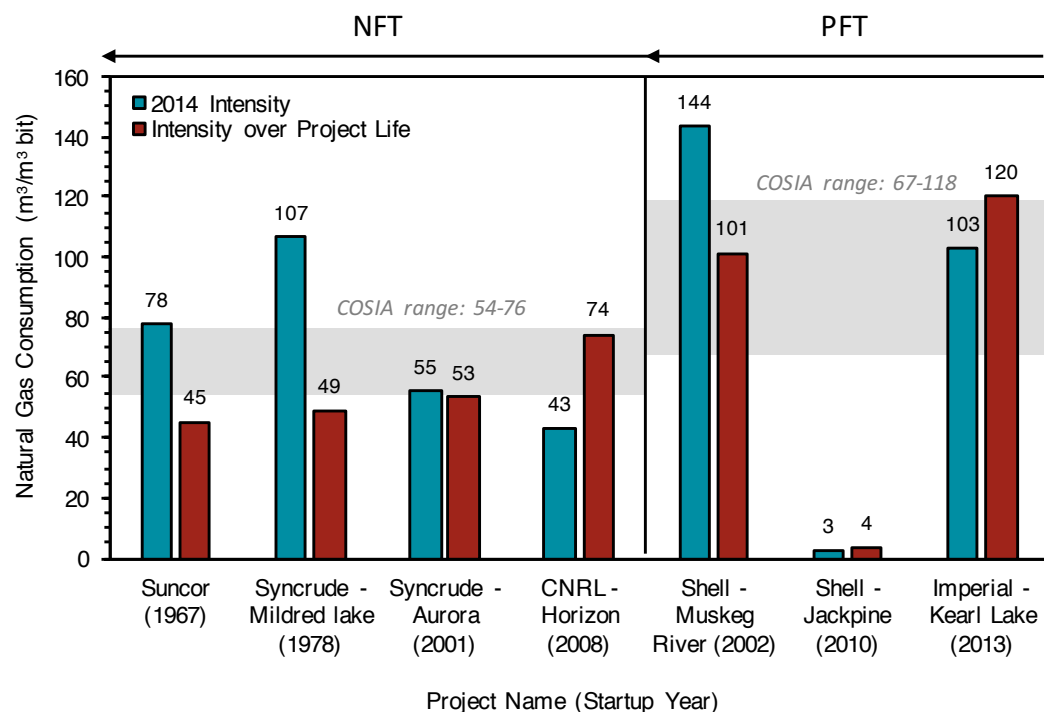


Figure 4.11: Natural gas use in mining operations

Table 4.13: Non-integrated PFT mining energy intensities

| Fuel | OPGEE value | AER avg. | PW | COSIA avg. | COSIA range | Notes |
|--------------------------|-------------|----------|----|------------|-------------|-------|
| Natural gas | 85 | 85 | | 93 | 67 – 118 | |
| Electricity cons. | 125 | 125 | | 114 | 99 – 130 | |
| Electricity gen. | 77 | 77 | | 114 | 96 – 132 | |
| Frac. elect. gen. onsite | 0.6 | 0.6 | | 1.0 | 1.0 – 1.0 | |
| Diesel | 12.5 | - | | 12.5 | 9 – 16 | a |
| Diluent | 25.4% | 25.4% | | - | - | |

^a COSIA Mine Template ranges presented for low (9%) and high (12%) grade ore.

pine, and Imperial Kearl). Volumetric blending rates over all months averaged 25.4% diluent in dilbit. The range over 2014 was from 24.3% to 26.5%. Although Kearl dilutes bitumen with SCO (creating “syn-bit”) the dilution fraction was nearly identical to those of Muskeg River and Jackpine.

Table 4.13 gives results as used in OPGEE, results for the AER production-weighted average, COSIA template average, and COSIA template range.

Proposed modeling of integrated NFT mining operations The integrated mining operation is illustrated in Figure 4.14. The net flows across the process boundary are roughly equivalent to the stand-alone mining operation, with some exceptions. First, large volumes of diluent are not used to reduce the viscosity of bitumen, as upgrading the bitumen to SCO renders it ready for pipeline transport. Also, two new co-products can be exported from the system: process gas and coke. Therefore, emissions credits should be given for these fuels if they are exported. Lastly, new internal flows between upgrader and mine include heat recovered from up-

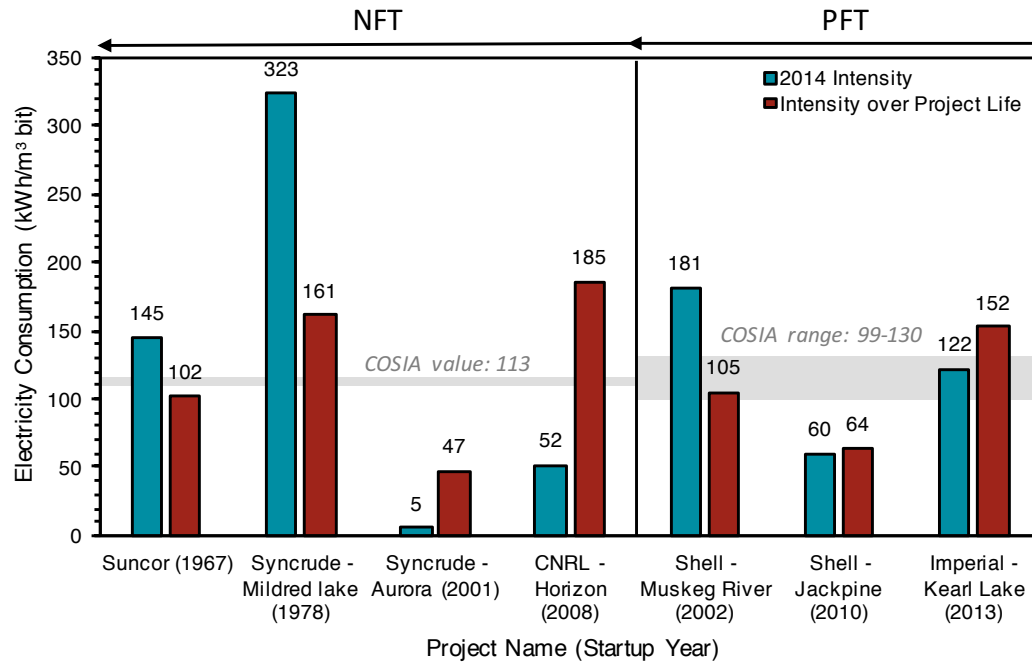


Figure 4.12: Electricity use in mining operations

grader operations that is used in mine ore separations, as well as upgrader product streams (distillate fuels) that are consumed in mining trucks. New internal consumption at the upgrader can include coke and process gas.

Due to sharing of waste heat at integrated mining and upgrading projects, some efficiency is gained through process integration. Suncor and Jacobs (2012) estimate that 30 percent of total natural gas required at a project can be reduced by using low-grade waste heat from an integrated upgrader for the bitumen extraction process.

Updated OPGEE default values for stand-alone NFT mines are taken directly from the COSIA NFT Mine Template [119]. The efficiency factor from Suncor and Jacobs [123] is multiplied by the COSIA stand-alone mining natural gas consumption to approximate the natural gas consumed solely by the mine at an integrated mining and upgrading facility. These values are compared to the energy consumption for integrated mining and upgrading projects in Table 4.14. The remaining energy for integrated projects not attributed to mining is approximately that consumed in the upgrading process. For example, if we compare Suncor and Syncrude natural gas consumption (total) less that estimated used in upgrading, we get values approximately equal to the COSIA stand-alone NFT mine less a 30% integration benefit ($40\text{--}45 \text{ m}^3 \text{ per m}^3$).

Table 4.14: Comparison between stand-alone mine energy consumption estimates based on COSIA mine template to integrated NFT mining and upgrading energy consumption reported by AER

| Fuel | OPGEE value ^a | COSIA SA NFT ^b | AER reported ^c | | Upgrading est. ^d | |
|-------------------|--------------------------|---------------------------|---------------------------|----------|-----------------------------|----------|
| | | | Suncor | Syncrude | Suncor | Syncrude |
| Natural gas cons. | 45 | 65 (54 – 76) | 78 | 77 | 30 | 37 |
| Electricity cons. | 113 | 113 | 145 | 166 | 30 | 63 |

^a Natural gas consumption for mining portion of an integrated mining and upgrading project calculated by subtracting the percentage of natural gas Suncor and Jacobs [123] estimate will be saved through sharing of waste heat.

^b Includes mining energy consumption estimates provided in COSIA Mine Templates for a representative stand-alone NFT mine.

^c 2014 operating data reported in AER Statistical Report ST39. Suncor and Syncrude projects have on-site upgraders so AER data is reported for both mining and upgrading.

^d Estimate of energy consumed from upgrading calculated by subtracting the estimated energy consumed for mining in integrated projects from the mining and upgrading energy consumption reported to the AER. The values presented in the table for upgrading are per m³ of SCO produced by the on-site upgrader (17,200,000 m³ and 15,200,000 m³ for Suncor and Syncrude upgraders, respectively), whereas the energy consumption values for mined bitumen presented in the table are per m³ of bitumen produced.

^e The range presented in the table for natural gas consumption from the COSIA Mine Template for NFT projects is based on the low and high estimates for natural gas consumption for high grade and low grade oil sands ore, respectively. The same values for electricity consumption are reported for low and high grade ore in the NFT COSIA Mine Template (113 kWh/m³ bitumen).

Table 4.15: Integrated NFT mining energy intensities

| Fuel | OPGEE value | AER avg. | PW | COSIA avg. | COSIA range | Notes |
|--------------------------|-------------|----------|----|------------|-------------|----------|
| Natural gas | 45 | - | | 65 | 54 – 76 | <i>a</i> |
| Electricity cons. | 113 | - | | 113 | 113 – 113 | |
| Electricity gen. | 114 | - | | 114 | 96 – 132 | |
| Frac. elect. gen. onsite | 1 | - | | 1.0 | 0.8 – 1.2 | |
| Diesel | 11 | - | | 11 | 9 – 13 | <i>b</i> |

^a Note from Table 4.14 above that the COSIA stand-alone NFT mine consumption must be reduced by the heat integration benefit. That is, OPGEE value of 45 m³ per m³ bitumen should be compared to 65 × (1.0 – 0.3) [119]

^b COSIA Mine Template ranges presented for low (9%) and high (12%) grade ore.

In order to enable self-consistent treatment of integrated mining and upgrading, the following conventions are applied:

- Integrated mining and upgrading operations use the same upgrading models described below in Section 5.3.
- Any benefits associated with upgrading integration result in less net consumption of mining consumables that flow across conventional mine boundary (i.e., diesel, electricity, natural gas).
- Emissions associated with on-site use of fuels by upgrader are calculated on the upgrading sheet.

These conventions allow for computation of the benefits of integrated mining and upgrading operations, while also maintaining computations of emissions impacts of operations.

The default values for energy use in upgrader-integrated NFT mining operations are therefore computed as follows:

- Natural gas consumption is modeled using COSIA stand-alone NFT mine less a 30% integration benefit. This is approximately equal to the reported values of Suncor and Syncrude less estimated upgrading consumption.
- Electricity consumption is modeled using COSIA electricity use at a stand-alone NFT mine. No integration benefit applicable.
- Diesel consumption is estimated as the average of COSIA reported high and low ranges of diesel consumption, as reported for low-grade (9 wt.%) and high-grade (12 wt.%) ores respectively.

For both integrated and non-integrated mining operations, the emissions and energy use are tracked simply. For example, diesel fuel use in non-integrated mining operations is computed as:

$$Q_{di}^{MN} = Q_{db}^{MN} I_{di}^{MN} \quad (4.46)$$

where Q_{di}^{MN} is diesel consumed in non-integrated mining operations [gal/d], Q_{db}^{MN} is diluted bitumen output from the non-integrated mining operation [bbl/d], and I_{di}^{MN} is the diesel fuel intensity of non-integrated mining operations [gal/bbl]. This

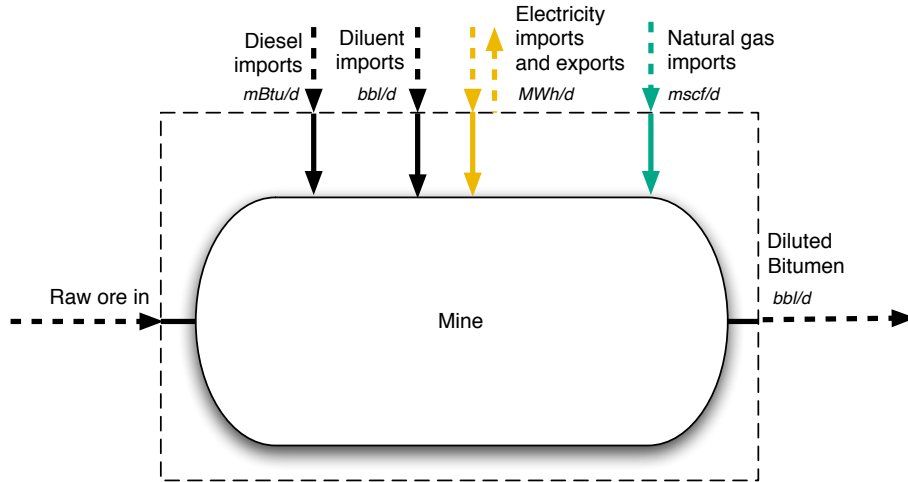


Figure 4.13: Non-integrated bitumen mining operation

quantity of diesel fuel consumed can then be converted into an energy consumption rate:

$$E_{di}^{MN} = Q_{di}^{MN} LHV_{di} \quad (4.47)$$

where LHV_{di} is the lower heating value of diesel fuel [mBtu LHV/gallon]. This quantity can then be gathered on the 'Energy Consumption' gathering sheet and used to compute emissions on the 'GHG Emissions' gathering sheet.

Similar quantities are computed for all main inputs to non-integrated mining operations by using intensities of electricity use (I_{el}^{MN}) and natural gas (I_{ng}^{MN}). For the case of integrated mining and upgrading operations, the relevant intensities for diesel, electricity, and natural gas are similarly named (I_{di}^{MI} , I_{el}^{MI} , and I_{ng}^{MI} respectively). Recall via convention above that consumption of coke or refinery process gas is computed as part of upgrading operations in Section 5.3.

After these mine-type-specific calculations are performed, the overall consumption due to mining is then computed using binary variables from the 'Active Field' sheet. For the case of diesel energy consumption:

$$E_{di} = y^{MN} E_{di}^{MN} + y^{MI} E_{di}^{MI} \quad (4.48)$$

where y^{MN} and y^{MI} represent binary variables for mining-non-integrated and mining-integrated, respectively.

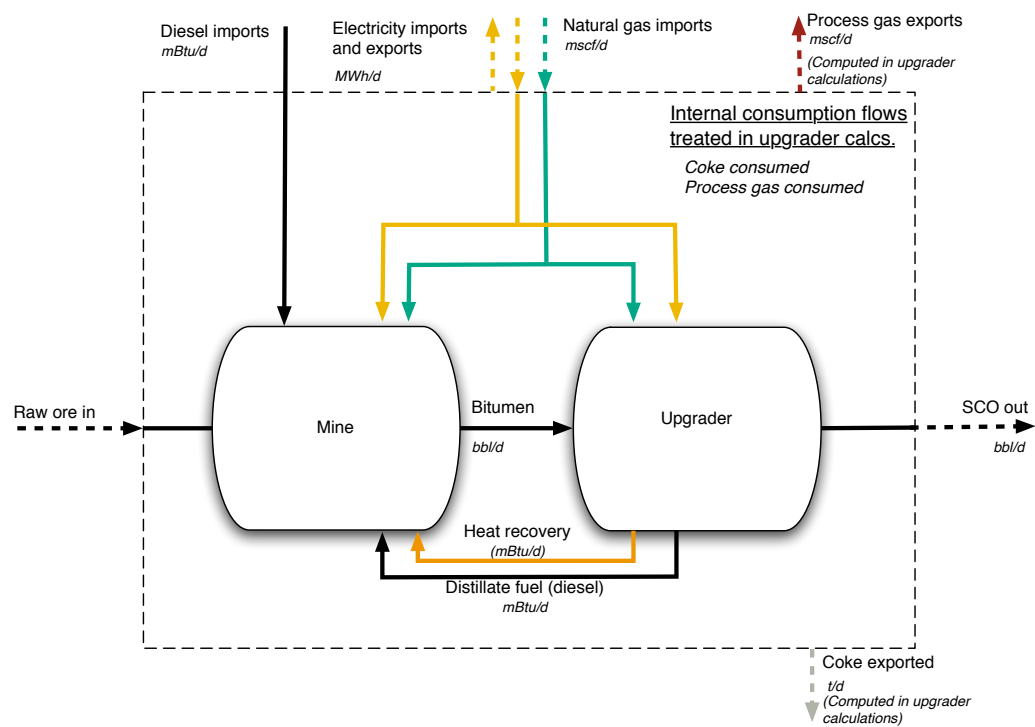


Figure 4.14: Upgrader-integrated bitumen mining operation

4.3.3 Production and extraction defaults

Default values for production and extraction equations are shown in Table 4.19. The data basis for smart defaults for production and extraction modeling are described below.

4.3.3.1 Default field age

Field age data were collected for global oil fields. A total of 6,502 global oil fields were collected from the Oil & Gas Journal 2010 *Worldwide Oil Field Production Survey* [124]. A total of 4837 of these fields had reported discovery dates. No data are available on date of first production, although this will most commonly occur less than 5 years after discovery.

The histogram of field discovery dates is shown in Figure 4.15. Because the dataset has poor coverage of field-specific production data, a production-weighted average age figure was not thought to provide an accurate representation of the true production-weighted age distribution, so this was not calculated. The mean date of discovery in the dataset was 1972.1. If a conservative 3 year development timeline is assumed, an average of 35 years has elapsed between 1975 and 2010.

Active Field 2.2.3

However, many of these fields are likely small fields that do not supply large quantities of oil to the global export markets. It is known that giant oilfields are somewhat older on average than the general field population [125–128]. A database of 116 giant oilfields was collected (defined as all producing over 100 kbbl/d in the year 2000) [126, Appendix A]. In total, these 116 fields produced $\approx 32,000$ kbbl/d, or some 43% of global oil production in 2000.

These giant fields have a count distribution and production-weighted average age distribution that are somewhat older than the complete set of global fields. Figure 4.16 shows these distributions. The production-weighted average discovery year of the sample was 1960.2, for an average age of 40 years since discovery at the time of production data collection (weighted by year 2000 production data). Data on giant oilfield production in 2010 are not available. Due to the general global slowdown in the discovery of giant fields since the 1970s, it is likely that the age distribution of giant oilfields has not shifted in step with advancing years. Therefore, the production-weighted average age for large fields is likely now greater than 40 years.

4.3.3.2 Default field depth

Field depth data were collected for a large number of global oil fields [124]. A total of 6,502 global oil fields were collected from the Oil & Gas Journal 2010 *Worldwide Oil Field Production Survey*. Of these fields, 4,489 fields had depth data presented. For fields where a range of depths was presented, the deeper depth is used.

The distribution of depths by number of fields per depth range is presented in Figure 4.17. Because of sporadic reporting of production data in the same dataset, a production-weighted depth figure was not thought to provide an accurate representation. The mean depth for these 4,489 fields is 7,238, or $\approx 7,240$ ft. The standard deviation is 3,591 ft. The depth distribution has a longer right (deep) tail than left (shallow) tail, so the mean is somewhat larger than the median (median = 6,807 ft).

Active Field 2.2.4

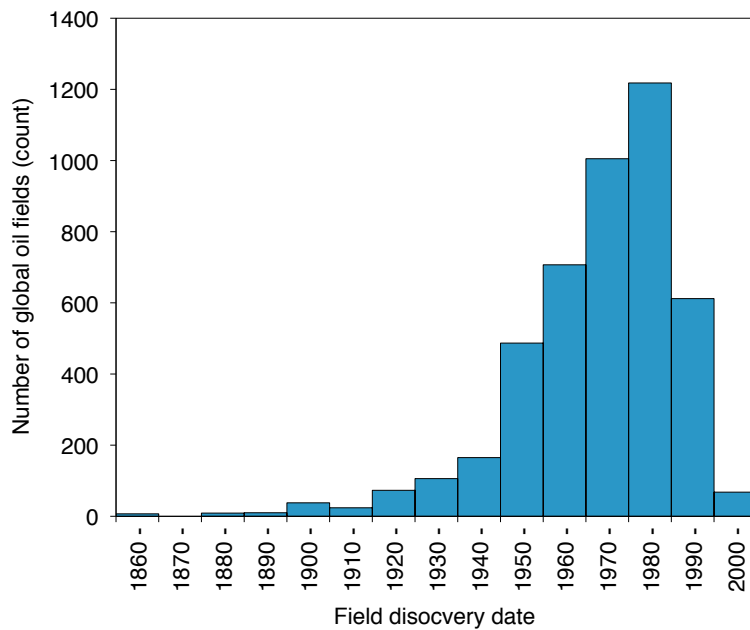


Figure 4.15: Distributions of global oilfield ages. Mean date of discovery (by count not by production-weighted average) is 1978.4.

4.3.3.3 Default production per well

Country-level oil production data and numbers of producing wells were collected for a large number of oil producing countries. Data from a total of 107 oil producing countries were collected from the *Oil & Gas Journal 2010 Worldwide Oil Field Production Survey* [129]. Production data and operating well counts for 2008 were collected from 92 of these 107 countries.

The distribution of per-well productivities for all countries is shown in Figure 4.18. A majority of oil producing countries produced less than 500 bbl/well-d. Weighting these well productivities by country-level share of global production, we see a very similar distribution.

Because of the large number of countries producing less than 500 bbl/well-d, we plot the distribution for countries under 500 bbl/well-d (see Figure 4.19). For the 55 countries with per-well productivity less than 500 bbl/well-d, the most common productivity by number of countries was the 0-25 bbl/well-d. However, when weighted by total production, the most common productivity bin is 75-100 bbl/well-d.

In 2008, the world produced 72822 kbbbl/d from 883691 wells, for an average per-well productivity of 82 bbl/well. However, the very low productivity of the US oil industry (representing ≈ 512000 wells) pulls down this average significantly. Non-US producers averaged a per-well productivity of 183 bbl/well-d, which is used as default well productivity in OPGEE.

Active Field 2.2.6

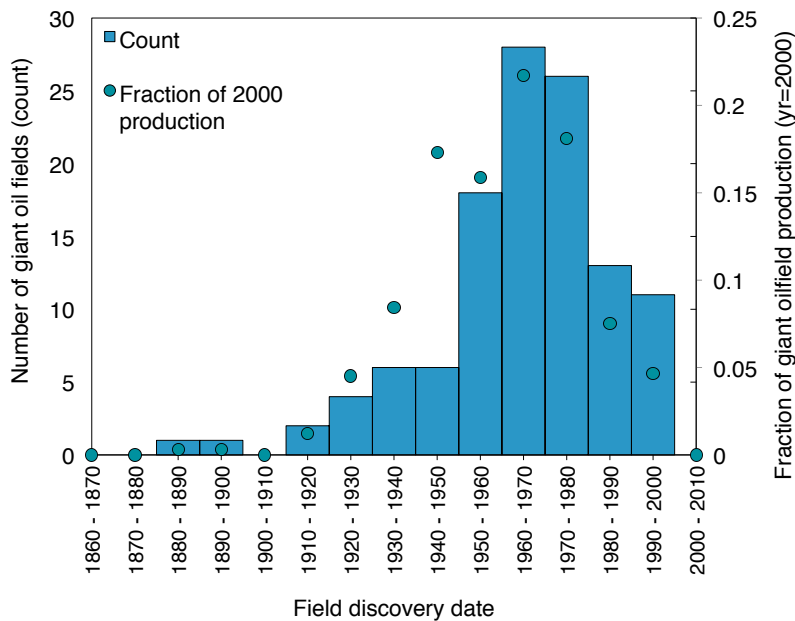


Figure 4.16: Distributions of giant oilfield ages. Mean date of discovery (by production-weighted average) is 1960.2.

Table 4.16: Mean and median injector to producer ratios.

| Prod. well productivity | Mean | Median |
|-------------------------|-------|--------|
| 0-10 bbl/d | 0.193 | 0.143 |
| 10 - 100 bbl/d | 0.326 | 0.254 |
| 100 - 1000 bbl/d | 0.578 | 0.532 |
| > 1000 bbl/d | 0.716 | 0.831 |

4.3.3.4 Default number of injector wells

The default number of injector wells is a smart default based on the number of producing wells. To model this relationship, data from California, Alaska, and a variety of offshore fields was collected [130, 131]. Data from offshore fields is provided in Table 4.17 below. Per-well productivity across these fields ranges from less than 10 bbl/d to over 10,000 bbl/d.

A strong relationship is seen between the productivity of producing wells and the number of injection wells required. Highly productive wells require a significantly larger number of injectors. Figure 4.20 shows the relationship between the per-well productivity of a field and the ratio of injectors to producers.

From these data, a relationship was generated for the mean and median ratio for each logarithmic bin of production well productivity (see Table 4.16). Median values for each bin are used to define the smart default for the number of injector wells.

Active Field 2.2.7

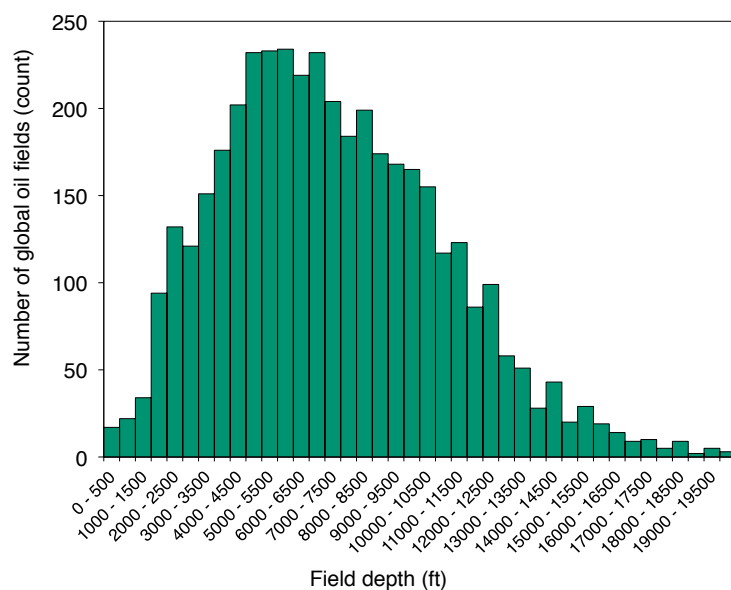


Figure 4.17: Distributions of global oilfield depths in bins of 500 ft depth. $N = 4489$ fields, mean = 7238 ft, SD = 3591 ft, median = 6807 ft.

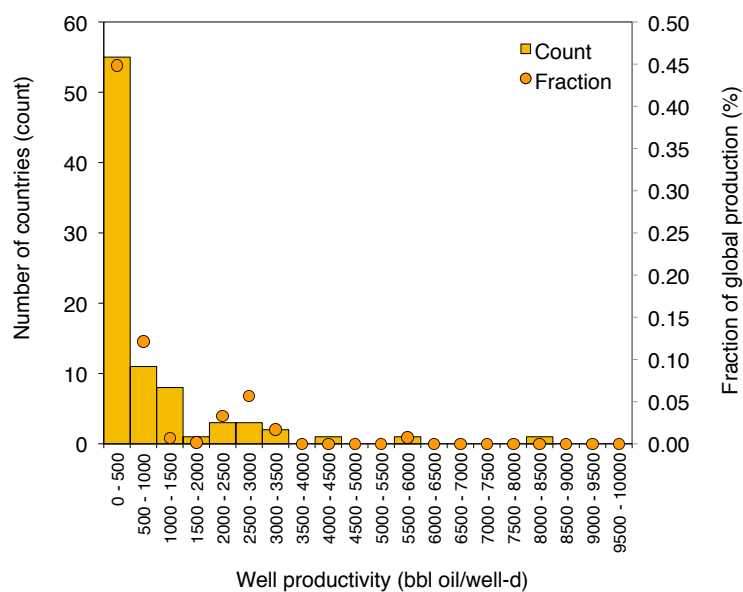


Figure 4.18: Distributions of oilfield per-well productivity (bbl oil/well-d) for bins of 500 bbl/d, counted by numbers of countries (bar) and by fraction of production (dot) $N = 92$ countries.

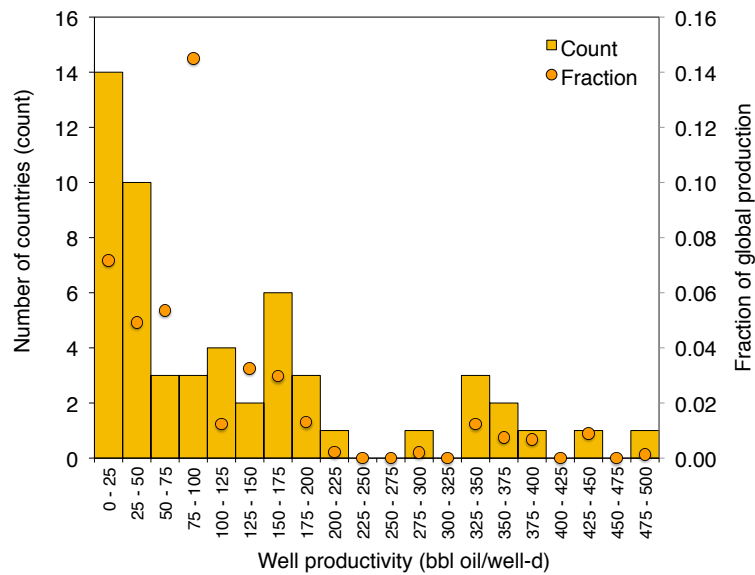


Figure 4.19: Distributions of oilfield per-well productivity (bbl oil/well-d) for all countries with per-well productivities lower than 500 bbl/well-d, counted by numbers of countries (bar) and by fraction of production (dot) $N = 55$ countries.

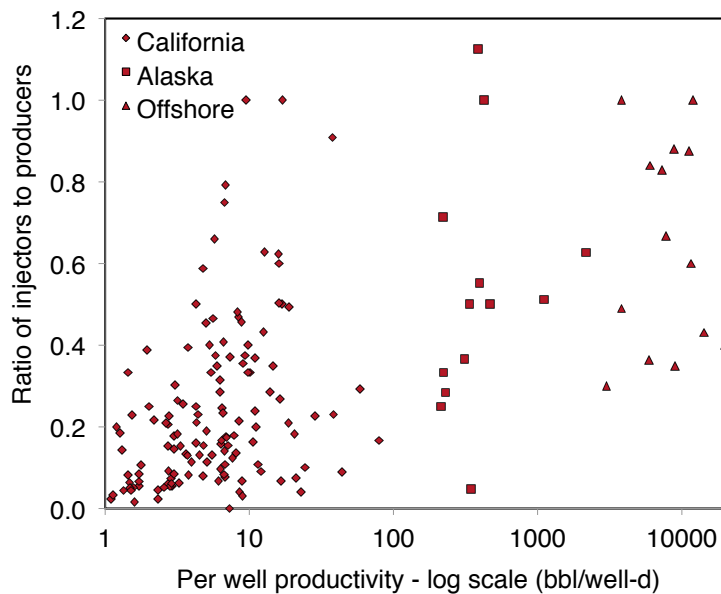


Figure 4.20: Ratio of producers to injectors as a function of per-well productivity. Source: Various.

Table 4.17: Data on production, number of production wells, and number of injection wells by offshore field.

| Field | Prod. wells | Inj. wells | Prod. (bbl/d) | References |
|----------------|----------------|---------------|------------------|---|
| Dalia | 37 | 31 | 240000 | http://www.offshore-technology.com/projects/dalia/ |
| Gimboa | 3 | 4 | 14000 | http://www.statoil.com/en/OurOperations/TradingProducts/CrudeOil/Crudeoilassays/PagPa/Gimboa.aspx http://www.offshore-technology.com/projects/gimboa/ |
| Girassol | 23 | 13 | 240000 | http://www.offshore-technology.com/projects/girassol/ |
| Plutonio | 20 | 20 | 240000 | http://www.offshore-technology.com/projects/greater_plutonio/ |
| Hungo | 30 | 26 | 130000 | http://www.exxonmobil.com/crudeoil/about_crudes_hungo.aspx http://www.fluor.com/projects/Pages/ProjectInfoPage.aspx?prjid=93 |
| Kissanje | 25 | 21 | 150000 | http://www.exxonmobil.com/crudeoil/about_crudes_kissanje.aspx http://www.ogj.com/articles/print/volume-103/issue-38/special-report/kizomba-b-attains-production-capacity-early.html |
| Mondo | 17 | 17 | 65000 | http://www.exxonmobil.com/crudeoil/about_crudes_mondo.aspx http://www.offshore-technology.com/projects/kizomba/ |
| Pazflor | 25 | 22 | 220000 | http://www.exxonmobil.com/crudeoil/about_crudes_pazflor.aspx |
| Azeri | 58 | 25 | 823000 | http://www.offshore-technology.com/projects/pazflor-fpsol/ |
| Albacora Leste | 16 | 14 | 180000 | http://crudemarketing.chevron.com/crude/central_asian/azeri.aspx http://www.bp.com/genericarticle.do?categoryId=9029616&contentId=7067613 |
| Bijupira | 9 | 6 | 70000 | Albacora Leste Field Development Project, Offshore Technology Conference, 2006 (OTC 17925) |
| Frade | 11 | 4 | 65000 | http://www.offshore-technology.com/projects/bijupira/ |
| Jubarte | 20 | 7 | 180000 | http://www.offshore-technology.com/projects/fradefieldcamposbasi/ |
| Lula | 5 | 2 | 100000 | http://www.epcengineer.com/ http://subseaiq.com/data/Project.aspx?project_id=764&AspxAutoDetectCookieSupport=1 |
| Marlim | 102 | 50 | 390000 | http://subseaiq.com/data/Project.aspx?project_id=274 |
| Marlim Sul | 41 | 34 | 300000 | http://www.offshore-technology.com/projects/marlimpetro/ |
| Polvo | 10 | 3 | 30000 | http://uk.reuters.com/article/2011/06/02/petrobras-platform-idUKN0227875420110602 |
| Roncador | 40 | 24 | 460000 | http://subseaiq.com/data/Project.aspx?project_id=371 |
| Sapinhoa | 10 | 10 | 120000 | http://www.offshore-mag.com/articles/print/volume-68/issue-3/production-operations/devon-breaks-new-ground-at-polvo.html |
| | | | | http://subseaiq.com/data/Project.aspx?project_id=348 |
| | | | | http://www.offshore-technology.com/projects/guaraoilfield/ |

4.3.3.5 Default gas composition

The default gas composition for associated gas from oil production is derived from reported gas composition data from 135 California oil fields [10]. Species concentration distributions for major gas species is shown in Figure 4.21. In order to remove outliers, all compositions with methane concentration less than 50% were removed from the dataset (17 data points removed out of 135). The resulting mean compositions were rounded and used in OPGEE for default gas composition.

Active Field 2.3.2

4.3.3.6 Smart default for GOR

The gas-oil ratio (GOR) varies over the life of the field. The amount of gas able to be evolved from crude oil depends on its API gravity, the gas gravity, and the temperature and pressure of the crude oil [97, p. 297]. As the reservoir pressure drops, increasing amounts of gas evolve from the liquid hydrocarbons (beginning at the bubble point pressure if the oil is initially undersaturated) [97]. This tends to result in increasing producing GOR over time. Also, lighter crude oils tend to have a higher GOR.

Because of this complexity, a static single value for GOR is not desirable. However, all data required to use empirical correlations for GOR is not likely to be available for all crude oils modeled. Therefore we use California producing GORs to generate average GORs for three crude oil bins.

Active Field 2.4.1

Crude oils are binned by API gravity into heavy ($< 20^\circ\text{API}$), medium (≥ 20 , $< 30^\circ\text{API}$), and light crude ($\geq 30^\circ\text{API}$). Each California oil field is assigned an average API gravity using the following procedure:

1. API gravity by pool is collected from DOGGR datasets [132–134] and digitized.
2. If a range of API gravities is given for a single pool, the high and low specific gravities are averaged to obtain a single specific gravity value per pool, which is then converted back to API gravity.
3. The above steps give a set of single API values by pool. Each field has between 1 and 17 pools that have data in DOGGR field properties datasets.
4. Each field is assigned an average API gravity using the following method:
a) if a single pool API value is given for the field, that is used; b) if multiple pool API gravities are given, and production data are available by pool, the pools are weighted by production level in 2009 DOGGR annual data (again by first converting to specific gravity then converting back to API gravity).
5. The above procedure results in a single API gravity for each field in California.

The associated gas GOR for 179 California oil fields was compiled for 2009 [135, 136]. These data are binned as above based on their weighted average API gravity value. Outliers with GOR in excess of 10,000 scf/bbl were removed. The distributions, mean, and median values for each crude bin were generated (see Figure 4.22 for plot of distributions and Table 4.18 for listing of mean and median GORs by bin).

The mean GORs are used to assign a smart default for each bin.

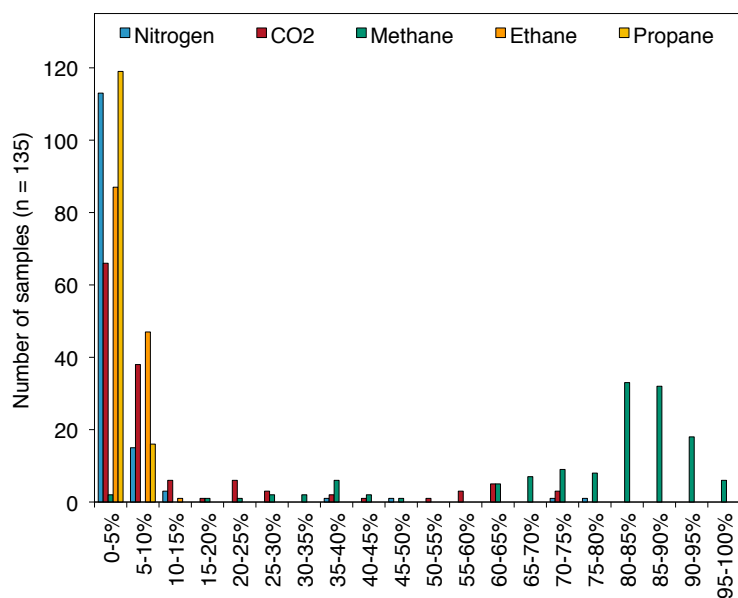


Figure 4.21: Distributions of major gas species across 135 samples from California associated gas producers.

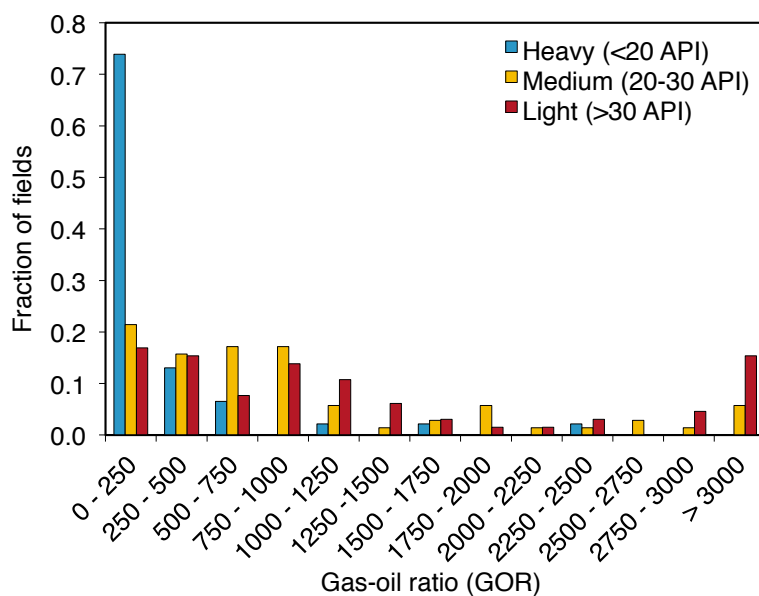


Figure 4.22: Distributions of California GORs, binned by crude density.

Table 4.18: GOR values by crude oil API gravity bin.

| Crude bin | Num. fields [#] | Gravity range [°API] | Avg. gravity [°API] | Mean GOR [scf/bbl] | Median GOR [scf/bbl] |
|-----------|--------------------|-------------------------|------------------------|-----------------------|-------------------------|
| Heavy | 45 | < 20 | 15.3 | 227 | 8 |
| Medium | 69 | ≥ 20, ≤ 30 | 24.3 | 908 | 621 |
| Light | 65 | > 30 | 35.0 | 1297 | 877 |

4.3.3.7 Default water oil ratio (WOR)

A smart default for the water oil ratio as a function of field age was generated using data from large fields in various world regions.

Active Field 2.4.2

Data on oil and water production were extracted from reports issued by California Division of Oil, Gas and Geothermal Resources (DOGGR), Alberta Energy Resources Conservation Board (ERCB), Alaska Oil and Gas Conservation Commission (AOGCC), United Kingdom Department of Energy and Climate Change (DECC), and the Norwegian Petroleum Directorate (NPD). For the Norwegian fields, water production data were not available prior to the year 2000. For Alberta fields, data were not available prior to 1962. Only data for the first 60 years of production were included. Only California fields contained data beyond 55 years, and therefore we excluded these years to avoid possibly atypical depleted field behavior in California from significantly affecting the least squares fit.

Because the majority of crude oil that is marketed globally originates from larger oil fields, fields that have produced less than 100 million m³ (630 million bbl) of crude oil were excluded. Also excluded from the analysis were fields that produce heavy crude using steam injection.

Additionally, a small number of fields were excluded because of apparent data anomalies or unusual events that may have affected oil or water production. Both the Redwater field in Alberta and the Ninian field in UK North Sea were excluded for data anomalies. These fields have highly unusual water production data that can only be plausibly attributed to data entry error. Also, the Elk Hills field in California was excluded because it was part of the National Petroleum Reserve for many years and the Piper field in the UK was excluded because oil production was halted for several years. In total, data from 24 giant oil fields (10 onshore and 14 offshore) were included in the analysis. The largest and the only super-giant field to be included is Prudhoe Bay.

The default WOR is represented by an exponential function:

$$WOR(t) = a_{WOR} \exp[b_{WOR}(t - t_0)] - a_{WOR} \left[\frac{\text{bbl water}}{\text{bbl oil}} \right] \quad (4.49)$$

where a_{WOR} = fitting constant for the initial WOR in time = t_0 [bbl water/bbl oil]; b_{WOR} = exponential growth rate [1/y]; t_0 = initial year of production (or year of discovery if year of first production unavailable) [y]; and t = year being modeled (independent variable) [y]. Note that the pre-exponential a_{WOR} is subtracted to force WOR to start at 0 when $t = t_0$. This model was fit to the collected data using a nonlinear least-squares fit from multiple starting points to ensure robustness. The results of fitting this model to the smart default fit values, compared to oil

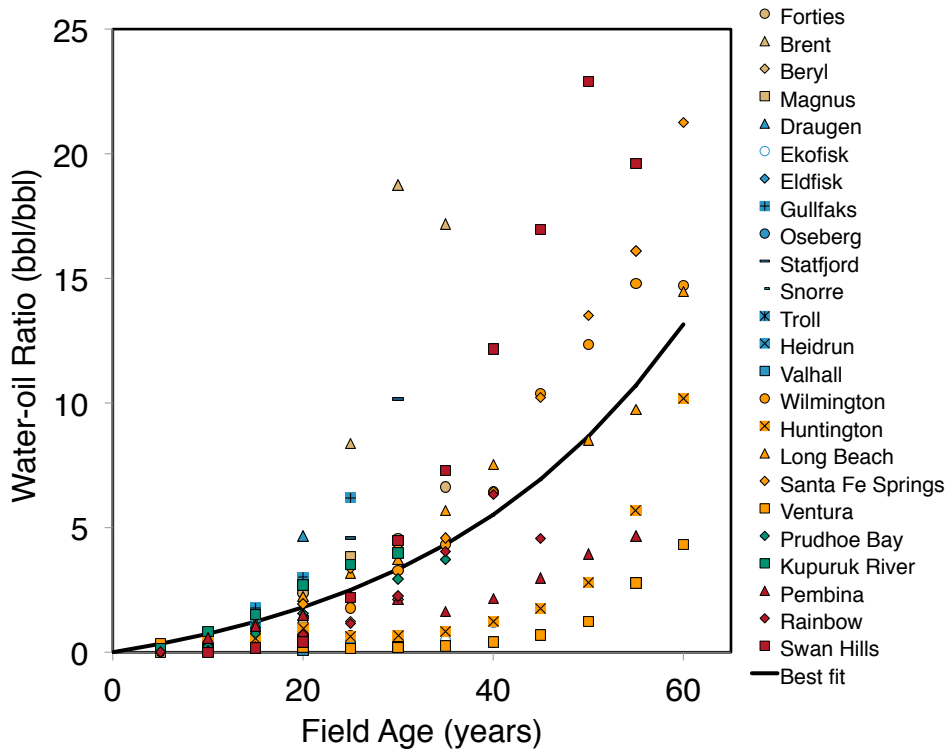


Figure 4.23: Exponential WOR model fit with smart default parameters. The best fit to data gives $a_{WOR} = 1.706$ and $b_{WOR} = 0.036$. Regions are colored as follows: Alberta (red), Alaska (green), California (orange), Norway (blue) and UK (beige).

fields from a variety of world regions, is shown in figure 4.23. The resulting fit gives $a_{WOR} = 1.706$ and $b_{WOR} = 0.036$.

4.3.3.8 Default waterflooding volume

The volume of water injected in a waterflooding project is meant to maintain reservoir pressure. As a default value, OPGEE assumes that the surface volume is replaced, such that the total oil produced plus the water produced is reinjected, or the injection per bbl = 1 + WOR.

Active Field 2.4.3

4.3.3.9 Default flood gas injection ratio

This is the ratio of the volume of flood gas injected [scf] to the volume of oil produced [bbl]. The volume of the oil is measured after bulk processing has removed the associated gas. The default flood gas injection ratio value depends on the choice of flood gas. If natural gas is selected as the flood gas, then the default ratio is calculated as follows:

Active Field 2.4.5

$$R_{fl} = 1.5 \cdot GOR \left[\frac{\text{scf gas}}{\text{bbl oil}} \right] \quad (4.50)$$

where R_{fl} = flood gas injection ratio [scf/bbl] and GOR is the gas-oil-ratio [scf/bbl].

If N_2 is selected as the flood gas, then R_{fl} is 1,200 scf/bbl. This is based on the immiscible nitrogen flood operation at the Cantarell field in Mexico to maintain reservoir pressure. As described in the Gas flooding section, the field operating equipment is designed to inject 1,200 MMscf/d [102]. In 2008, the injection rate was approximately 1,200 MMscf/d and the field was producing approximately 1.2 million bbl/d, leading to a default ratio of 1,200 scf/bbl [137].

If CO_2 is selected as the flood gas, then default R_{fl} is 10,000 scf/bbl. As with all injection ratios, R_{fl} changes over the life cycle of the flood project. It can also vary based on the specific reservoir engineering strategies selected by the operator. An example comes from DiPietro and Murrell (2013), who presented data from Kinder Morgan indicating that the injection ratio during the overall lifespan of an anonymous representative project was 6,000 scf/bbl.

Another example is provided by Pyo et al. [138], who reviewed the performance of a CO_2 flood at the Joffre Viking Pool in Alberta, Canada that had been active for approximately 30 years. The overall flood gas injection ratio during the life of the project was 10,800 scf/bbl; the ratios for the individual injector-producer well patterns within the field varied from 3,500 to 24,900 scf/bbl.

The OPGEE default flood gas injection ratios are presented only as representative values that provide an order-of-magnitude estimate. Actual field data should be obtained when possible.

4.3.3.10 Proportion of injected CO_2 that is newly acquired

The OPGEE default for the proportion of CO_2 that is newly acquired (not previously injected) is 41%. This figure is from the Malone et al. [139] discussion of an offshore CO_2 flood project at Weeks Island, Louisiana over an 9-year period (based on dates in the original reference by Johnston [140]). As with the flood gas injection ratio, actual data should be used if possible.

Table 4.19: Default inputs for production and extraction.

| Param. | Description | Eq. no. | Default | Literature range | Unit | Sources | Notes |
|------------------|--|---------|--------------------------------------|------------------|------------------------------|----------------|-------|
| ρ_{API} | API gravity | (4.17) | - | - | [-] | [59, p. 47] | |
| A_P | Pipeline cross sectional area | - | $\pi \left(\frac{D_P}{2} \right)^2$ | - | [ft ²] | | |
| BHP _P | Pump brakehorse power | (4.42) | - | - | [hp] | [68, p. 27] | |
| BHP _C | Compressor brakehorse power | (4.44) | - | - | [hp] | | |
| BHP _j | Component <i>j</i> brakehorse power | - | - | - | [hp] | | |
| C_{sd} | Concentration of dissolved solids | - | 5000 | - | [mg/L] | [9] | |
| C_P/v | Ratio of specific heats | - | 1.28 | 1.16-1.40 | [-] | [8, p. 320] | a |
| D_P | Well diameter | - | 2.78 | 1.04-4.50 | [in] | [53, p. 121] | |
| η_P | Pump efficiency | - | 65% | 70% | [-] | [68, p. 27] | b |
| η_C | Compressor efficiency | - | 70% | 75-85% | [-] | [66, p. 105] | c |
| E_j | Fuel consumption of component <i>j</i> | (4.45) | - | - | [MMBtu/d] | | |
| e_D | Driver fuel consumption | - | var. | Section 5.5 | [Btu/hp-hr] | | d |
| f | Friction factor | (4.33) | 0.02 | ≤ 0.1 | [-] | | e |
| γ_o | Oil specific gravity | - | 0.84 | 0.8-1.05 | [-] | [90] | |
| γ_g | Gas specific gravity | (4.18) | - | - | [-] | [91, p. 10] | |
| γ_w | Water specific gravity | (4.20) | - | - | [-] | [54, p. 1-481] | |
| γ_l | Liquid mixture specific gravity | (4.38) | - | - | [-] | [91] | |
| g_c | Gravitational constant | - | 32.2 | - | [lbm-ft/lbf-s ²] | | |
| h | Well depth | - | 7240 | - | [ft] | Figure 4.17 | |
| h_{tot} | Total head | (4.30) | - | - | [ft] | | |
| h_{el} | Elevation head | - | h | - | [ft] | | |
| h_f | Frictional head | (4.31) | - | - | [ft] | [8, p. 447] | |
| I_{di}^{MI} | Diesel intensity, integrated mine | - | - | - | [gal/bbl SCO] | | |
| I_{di}^{MN} | Diesel intensity, non-integrated mine | - | - | - | [gal/bbl dilbit] | | |
| I_{el}^{MI} | Electricity intensity, integrated mine | - | - | - | [kWh/bbl SCO] | | |
| I_{el}^{MN} | Electricity intensity, non-integrated mine | - | - | - | [kWh/bbl dilbit] | | |
| I_{ng}^{MI} | Natural gas intensity, integrated mine | - | - | - | [scf/bbl SCO] | | |
| I_{ng}^{MN} | Natural gas intensity, non-integrated mine | - | - | - | [scf/bbl dilbit] | | |
| λ_o | Volume fraction of oil | (4.39) | $1 - \lambda_o$ | - | [-] | | |
| λ_w | Volume fraction of water | - | var. | - | [-] | | |
| MW _g | Gas molecular weight | - | - | - | [lbm/lbmol] | [5, p. 35] | f |

Continued on next page...

Continued from previous page

| Param. | Description | Eq. no. | Default | Literature range | Unit | Sources | Notes |
|-----------------|---|---------|---|------------------|------------------------|---|-------|
| μ_l | Fluid viscosity | - | var. | - | [cP] | | |
| Nre | Reynolds number | (4.32) | - | - | [unitless] | [111] | |
| N_W | Number of producing wells | - | $\frac{Q_l[\text{bbl/d}]}{183[\text{bbl/well-d}]}$ | - | [-] | Section 4.3.3.3 | |
| p_b | Base pressure | - | 14.7 | - | [psi] | [5, p. 35] | |
| p_d | Flow discharge pressure | - | var. | - | [psi] or [psia] | | |
| p_s | Compressor suction pressure | - | 125 | - | [psia] | | |
| $p_{Hrac, tot}$ | Total pressure traverse | (4.37) | - | - | [psi] | [8, p. 455] | g |
| p_{lift} | Pressure for lifting | (4.40) | - | - | [psi] | | |
| p_{wh} | Wellhead pressure | - | 1000 | - | [psi] | [5, p. 80] | |
| p_{res} | Reservoir pressure | - | $0.5 \left(\frac{\mu(t)}{2.31[\text{ft/psi}]} \right)$ | - | [psi] | | |
| p_{wf} | Bottomhole pressure | - | - | - | [psi] | | |
| PI | Well productivity index | (4.41) | 3 | - | [bbl liquid/psi-d] | | |
| $Q_{l,W}$ | Wellbore flow rate | (4.35) | - | - | [ft ³ /s] | | |
| Q_d | Discharge flow rate | - | var. | - | [bbl/d] or [MMscf/d] | | |
| Q_{MI} | Rate diesel fuel consumption, integrated mine | (4.46) | - | - | [gal/d] | | |
| $Q_{di, MIN}$ | Rate diesel fuel consumption, non-integrated mine | (4.46) | - | - | [gal/d] | | |
| Q_l | Total rate of liquid production | (4.36) | - | - | [ft ³ /s] | | |
| Q_o | Total rate of oil production | - | 1500 | - | [bbl/d] | | |
| Q_{db} | Rate of diluted bitumen production | - | 1500 | - | [bbl/d] | | |
| Q_{SCO} | Rate of synthetic crude oil production | - | 1500 | - | [bbl/d] | | |
| r | Relative pipe roughness | - | 0.0006 | - | [unitless] | [112] | |
| R_C | Compression ratio | (4.21) | - | - | [-] | | |
| ρ_{gsc} | Gas density at standard conditions | (4.19) | - | - | [lbm/ft ³] | [5, p. 35] | |
| ρ_{asc} | Air density at standard conditions | - | 0.0764 | - | [lbm/ft ³] | [91, p. 10] | |
| T_b | Base temperature | - | 520 | - | [°R] | [5, p. 35] | |
| T_d | Compressor discharge temperature | (4.25) | - | - | [°R] | [66, p. 105] | |
| T_s | Compressor 1 suction temperature | - | 656.7 | - | [°R] | | |
| T_{s2} | Compressor 2 suction temperature | (4.26) | - | - | [°R] | | |
| $v_{l,W}$ | Pipeline flow velocity | (4.34) | - | - | [ft/s] | [91] | h |
| WOR | Water-to-oil ratio | - | Section 4.3.3.7 | - | [bbl water/bbl oil] | | |
| y^{MI} | Integrated mining operation? | (4.48) | 0 | - | [0-1] | | |
| y^{MN} | Non-integrated mining operation? | (4.48) | 0 | - | [0-1] | | |
| Z | Compressibility factor | - | Section 4.3.2.5 | - | [-] | [92], [93], [94], [95], [96], [97, p. 111], [98], [99], [2] | |

Continued on next page...

4.4 Surface Processing

4.4.1 Introduction to Surface processing

Surface processing of crude oil includes all production steps required after lifting the crude oil from the subsurface and before it is transported to the refinery. This includes oil-water-gas separation, treatment and stabilization of crude oil, and treatment of produced gas. The particular field processing scheme selected for an oilfield varies based on field parameters such as API gravity and operational factors such as limitations on energy inputs [59, p. 65]. The choice to conduct CO₂ EOR flooding will also affect the associated gas processing choice.

In OPGEE it is not possible to account for all variations in surface processing. The goal is to include frequently applied processes in the industry, while still retaining some flexibility to model varying operating modes and processing schemes.

A complete list of emissions sources from surface processing, along with their estimated magnitude, is shown in Table C.4. A list of all equation parameters and their default values (if applicable) and data sources is included in Table 4.23.

4.4.2 Calculations for surface processing

4.4.2.1 Crude oil dehydration

Removing free water from crude oil can be accomplished by passive chemical and gravitational methods that do not use heat. Because no fuel is used in passive gravitational separation techniques, they do not cause significant GHG emissions. However, based on the properties of the oil, gravity separation techniques may not be sufficient to produce crude oil with the desired water content required for transport and sales. Additional treatment may be provided by a heater/treater, which may be turned ON or OFF in OPGEE, to remove entrained water remaining after passive separation.

Inputs 1.5.1

To exploit heat capacity differences between water and oil [59, p. 303], OPGEE assumes that oil entering a heater/treater contains only entrained water. The free water proportion that was not separated prior to the application of heat is assumed to be negligible (1-2%) [141, Section 5.4.2].

The first step in the calculation of the heat duty of the heater/treater is the calculation of the volume of heated water, which is equal to the volume of the entrained water:

Surface
Processing 2.1.1

$$Q_{w,heat} = Q_{w,ent} \left[\frac{\text{bbl}}{\text{d}} \right] \quad (4.51)$$

where $Q_{w,heat}$ = volume of heated water [bbl/d]; $Q_{w,ent}$ = volume of water entrained in oil emulsion, [bbl/d]. The volume of water entrained $Q_{w,ent}$ is calculated from the fraction of water entrained in oil emulsion as:

Surface
Processing
1.1.2.1.1

$$Q_{w,ent} = \lambda_{w,ent} \frac{Q_o}{1 - \lambda_{w,ent}} \left[\frac{\text{bbl}}{\text{d}} \right] \quad (4.52)$$

where $\lambda_{w,ent}$ = fraction of water entrained in oil emulsion [-]; and Q_o = rate of oil production [bbl/d]. Once the volume of heated entrained water is calculated, the heat duty is calculated using:

Surface
Processing 2.1.1.3

Table 4.20: Description of OPGEE's Associated Gas Processing Schemes

| Path # | Path Description | Path Components |
|--------|-------------------------------------|--|
| 1 | None | None |
| 2 | Minimal | Glycol dehydrator |
| 3 | Acid gas | Glycol dehydrator + amine process |
| 4 | Wet gas | Glycol dehydrator + demethanizer |
| 5 | Acid wet gas | Glycol dehydrator + amine process + demethanizer |
| 6 | Dry acid gas reinjection | |
| 7 | CO ₂ EOR: Membrane/amine | Glycol dehydrator + compressor + membrane + amine process + demethanizer |
| 8 | CO ₂ EOR: Ryan-Holmes | Dehydrator + Ryan-Holmes process + demethanizer |

$$\Delta H_{CD} = \Delta T_{CD} (Q_o C_{p_o} + Q_{w,heat} C_{p_w}) (1 + \epsilon_{CD}) \left(\frac{1}{10^6} \right) \left[\frac{\text{MMBtu}}{\text{d}} \right] \quad (4.53)$$

where ΔH_{CD} = heat duty [MMBtu/d]; C_{p_o} = specific heat of oil [Btu/bbl-°F]; C_{p_w} = specific heat of water [Btu/bbl-°F]; ΔT_{CD} = difference between treating and feed temperatures [°F]; and ϵ_{CD} = heat loss [fraction]. Default values are 90 and 165 °F for feed and treating temperatures, respectively; 150 and 350 Btu/bbl-°F for specific heats of oil and water, respectively; and 0.02 for heat loss [59, p. 136 and 303].

4.4.2.2 Crude oil stabilization

Following the removal of water content, stabilization is the next phase of the bulk separation process. This involves the removal of dissolved natural gas [59, p. 159]. The default type of stabilizer in OPGEE is a high-pressure stabilizer (100 psi) which requires a higher reboiler temperature compared to a low-pressure stabilizer. The use of a stabilizer column is an important assumption because a heat source is required to provide the required temperature. OPGEE assumes a direct-fired heater.

The stabilizer column heat duty is calculated as:

$$\Delta H_S = \Delta T_S Q_o C_{p_o} (1 + \epsilon_S) \left(\frac{1}{10^6} \right) \left[\frac{\text{MMBtu}}{\text{d}} \right] \quad (4.54)$$

where ΔH_S = heat duty [MMBtu/d]; C_{p_o} = specific heat of oil [Btu/bbl-°F]; ΔT_S = difference between reboiler and feed temperatures [°F]; and ϵ_S = heat loss [fraction]. The default values are 120 and 344 °F for feed and reboiler temperatures, respectively; 150 Btu/bbl-°F for the specific heat of oil; and 0.02 for heat loss [59, p. 136, 161, 163].

4.4.2.3 Overview of associated gas processing

After phase separation in the fluid separator, the associated gas is processed in a selected gas processing path. OPGEE allows the user to choose from eight gas processing paths to simulate a variety of field conditions and production choices, presented in Table 4.20.

Path 1 (None) is chosen in case the associated gas requires no processing. Path 5 (Acid wet gas) includes use of a glycol dehydrator, amine acid gas removal unit, and a demethanizer and is the default gas processing path. Paths 2, 3, and 4 allow the user to turn OFF one or more of the processing components of Path 5. Paths 6

Surface
Processing 2.1.2.2

and 7 represent processing of associated gas during CO₂ flooding for EOR. Paths 6 to 8 represent CO₂ EOR options. Path 6 is simple dehydration and reinjection of mixed acid gases and hydrocarbons. Pathways 7 and 8 adapt CO₂ EOR-related modeling performed by the Department of Energy's NETL [4, 142–144].

Figure 4.24 is a simplified depiction of the associated gas processing paths in OPGEE containing four main branches. The upper branch is the standard processing train and contains a glycol dehydrator, amine AGR unit, and a demethanizer — each of which can be turned ON or OFF. Gas processing paths 2–5 fall within the upper trunk. The middle and lower trunks are the CO₂ EOR-specific paths. Pre-breakthrough CO₂ EOR separation is modeled using Processing Paths 1–5 within the upper branch (before breakthrough, injected CO₂ is not present in the associated gas stream).

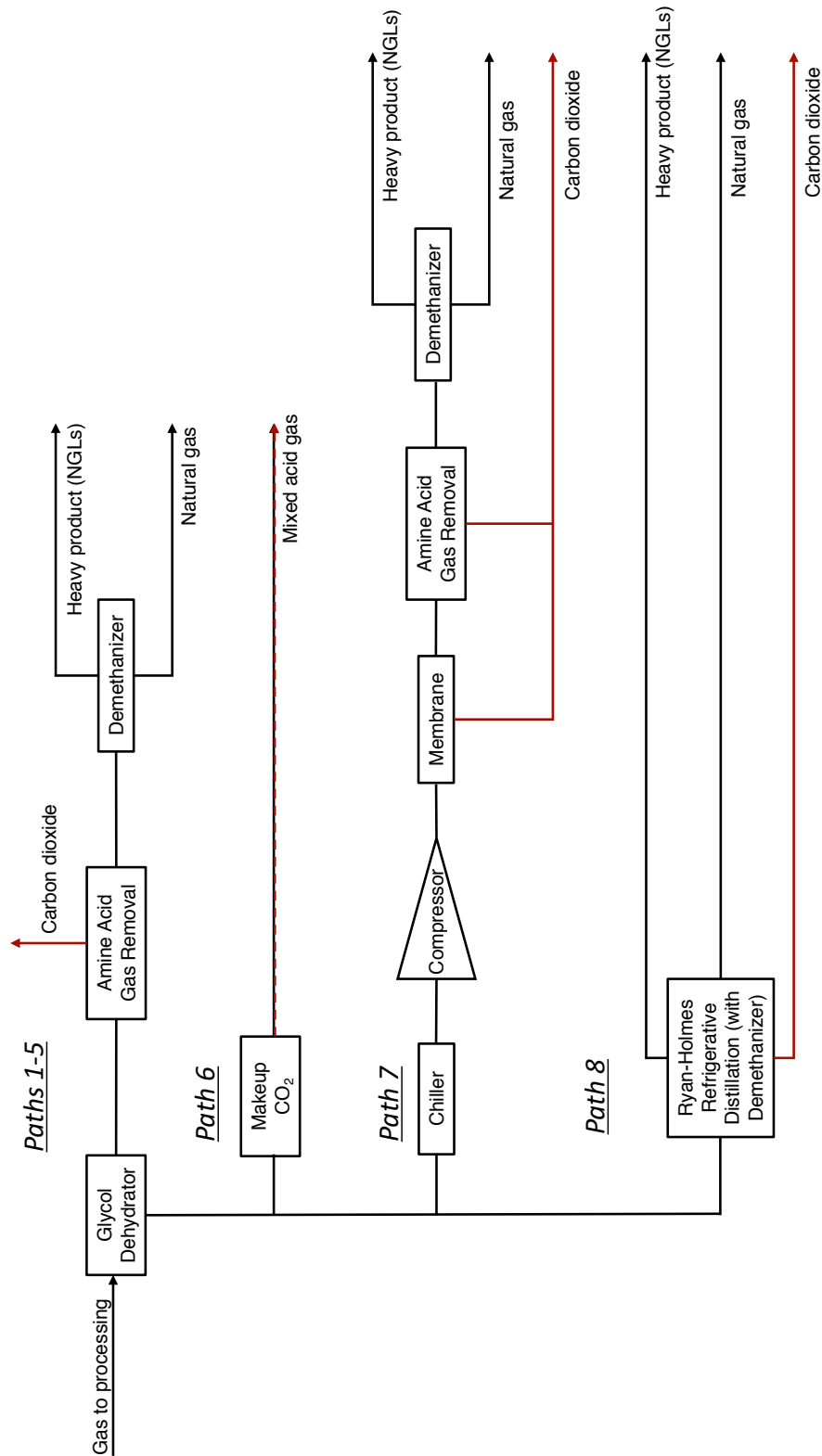


Figure 4.24: Schematic of associated gas treatment with four main branches. The lower 3 branches model post-breakthrough CO₂ enhanced oil recovery separation pathways [4].

4.4.2.4 *Heavy crude and bitumen upgrading*

Very heavy crude oils ($\text{API}^\circ \leq 12$) are often upgraded before transport. This is due to the heavy, viscous character of the crude which prevents flow at ambient conditions. This also results from the need to align heavy crude characteristics more closely to refinery input specifications. As a result, significant capacity in crude heavy oil and bitumen upgrading exists. Approximately 1 million bbl/d of bitumen upgrading capacity exists in Canada, while ≈ 0.5 million bbl per day of upgrading capacity exists in Venezuela.

Crude oil upgrading is modeled OPGEE using results from the OSTUM model, supplemented with reported data from Canadian regulators [145]. The results for crude upgrading in OPGEE are most applicable to the case of Canadian bitumen upgrading, as data from these operations was used in the development of OSTUM. Applying the OPGEE upgrading module to other heavy crude upgrading operations is subject to greater uncertainty.

Crude oil upgrading operations are illustrated in process flow form in Figure 4.25

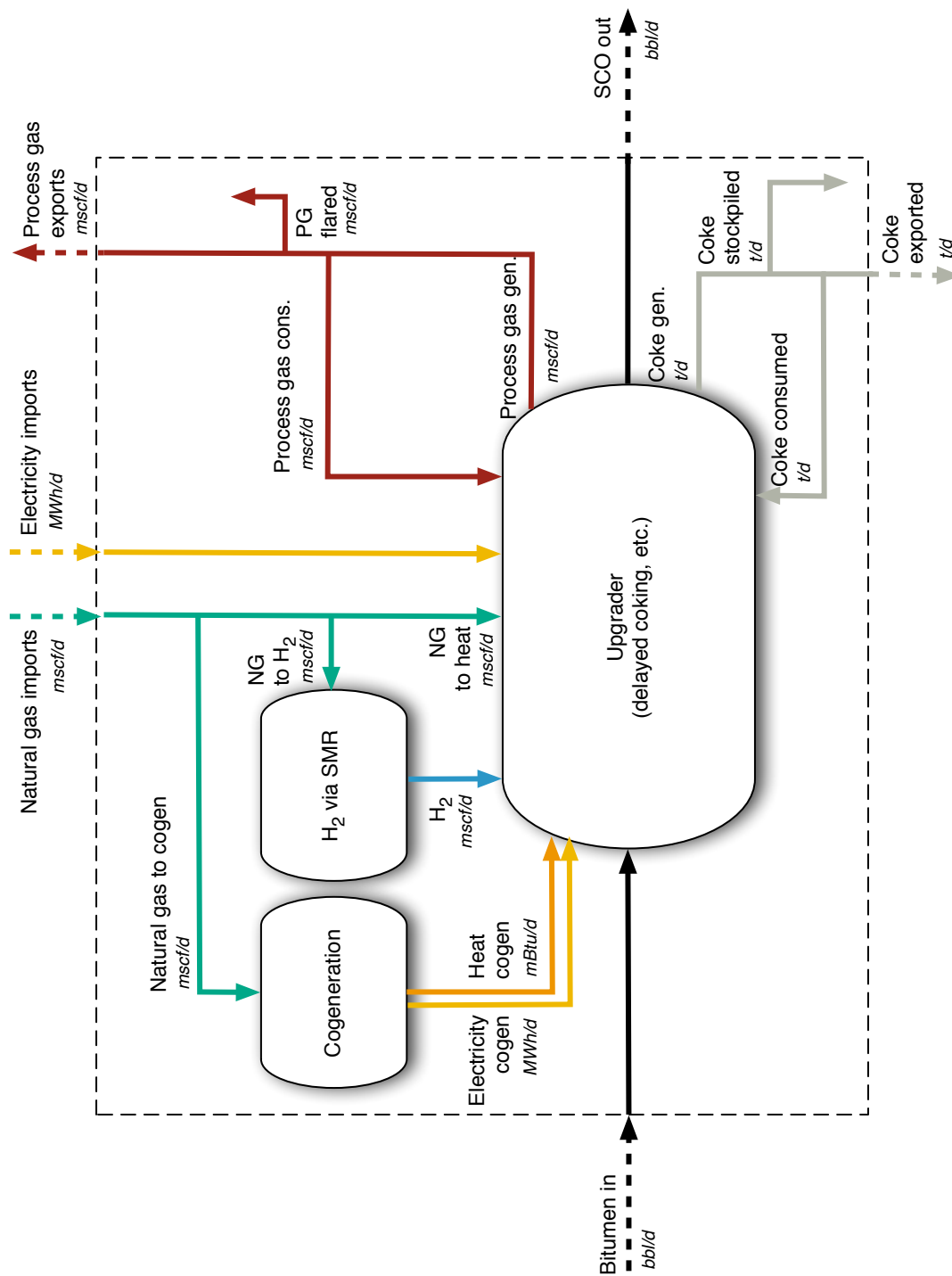


Figure 4.25: Process flow diagram for OPGEE upgrading module

The quantity “SCO out”, or Q_{sco} is given by user in the inputs sheet. The required bitumen input rate Q_{bit}^{in} is determined using the SCO yield factor:

$$Q_{bit}^{in} = \frac{Q_{sco}}{Y_{sco}} \quad (4.55)$$

where Y_{sco} is the volumetric yield of SCO per volume of bitumen input [bbl SCO/bbl bitumen].

In addition to SCO, two other by-products are generated during upgrading of bitumen: process gas and coke. The generation of process gas is given by a process gas yield factor:

$$Q_{pg} = Q_{sco} Y_{pg} \quad (4.56)$$

where Y_{pg} is the process gas yield factor [scf process gas per bbl of SCO output]. The generation of coke is given by a coke yield factor:

$$Q_{ck} = Q_{sco} Y_{ck} \quad (4.57)$$

where Y_{ck} is the coke yield factor [kg coke per bbl of SCO output].

These two byproducts can be handled in one of three ways:

- Self-use in processing and upgrading facilities
- Disposal or rejection on site (flaring of process gas and stockpiling or land-filling of coke)
- Sales on secondary fuels markets

These uses are computed using three disposition fractions. Terms f_{pg}^{su} , f_{pg}^{fl} , and f_{pg}^{sl} for the case of process gas self-use, flaring, and sales, respectively. For coke, the equivalent terms are f_{ck}^{su} , f_{ck}^{sp} , and f_{ck}^{sl} , corresponding to self-use, stockpiling, and sales, respectively. For each by-product these terms must sum to 1.

Hydrogen consumption by the upgrader is given by a hydrogen intensity factor:

$$Q_{H2} = Q_{sco} I_{H2} \quad (4.58)$$

where I_{H2} is the H_2 intensity [scf H_2 per bbl of SCO]. The natural gas consumption associated with generating H_2 is therefore given by:

$$Q_{ng,H2} = \frac{Q_{H2} LHV_{H2}}{\eta_{H2} LHV_{ng}} \quad (4.59)$$

where LHV_{H2} is the lower heating value of hydrogen [Btu LHV/scf H_2], η_{H2} is the lower-heating-value-basis efficiency of H_2 generation [Btu LHV H_2 /Btu LHV NG], and LHV_{ng} is the lower heating value of natural gas [Btu LHV/scf NG].

Similarly, the electricity requirement of upgrading is given by an electricity intensity factor:

$$Q_{el} = Q_{sco} I_{el} \quad (4.60)$$

where I_{el} is the electricity intensity [Btu e- per bbl of SCO]. This electricity is either generated on site using cogeneration, or purchased externally. The fraction of electricity generated on site f_{el} is entered by the user on the 'Inputs' sheet.

The need for process steam for upgrading is met by a combination of heat generated during co-generation of electricity (if used) and through a steam boiler. The need for steam is given by a steam intensity factor:

$$Q_{ws} = Q_{SCO} I_{ws} \quad (4.61)$$

where I_{ws} is the steam intensity [Btu steam enthalpy per bbl of SCO produced]. This steam need is therefore met by steam cogeneration and conventional steam boilers:

$$Q_{ws} = Q_{el} f_{el} \frac{\eta_{HRSG}}{\eta_{GT}} + Q_{ng,ws} \eta_{ws} \quad (4.62)$$

where η_{HRSG} is the efficiency of steam generation from cogeneration HRSG [Btu steam enthalpy per Btu LHV NG input to turbine], η_{GT} is the efficiency of gas turbine [Btu e- per Btu LHV NG input to turbine], and η_{ws} is the efficiency of a supplemental steam boiler [Btu steam enthalpy per Btu LHV of NG input].

The inputs for these values, derived from the OSTUM model and public data sources, are described below in the discussion of the 'Upgrading' worksheet.

4.4.2.5 Gas dehydration

In addition to the sweetening process, natural gas often must be dehydrated to prevent issues such as condensation and hydrate formation that could negatively affect the gas processing and distribution process [5, p. 139]. The default dehydration method in OPGEE is liquid triethylene glycol (TEG) desiccant, which contacts the natural gas and absorbs water from it; heat is then applied to separate the water from the TEG [5, p. 140].

The dehydration process involves operational venting of some natural gas and water [5, p. 140]; dehydrator venting is discussed in the Venting & Fugitives section (see Section 5.9). A schematic of the glycol dehydrator is shown in Figure 4.26.

The first step in the estimation of the TEG reboiler duty is the calculation of the rate of water removed using the assumed weight of water vapor in the inlet and exit gases as:

$$\Delta M_{w,rem} = M_{w,in} - M_{w,out} \left[\frac{[\text{lb H}_2\text{O}]}{\text{MMscf}} \right] \quad (4.63)$$

where $\Delta M_{w,rem}$ = water removed [lb H₂O/MMscf]; $M_{w,in}$ = water in inlet gas [lb H₂O/MMscf]; $M_{w,out}$ = water in outlet gas [lb H₂O/MMscf]. The weights of water vapor in the inlet and exit gases are user inputs. The default values are 52 and 7 lb H₂O/MMscf, respectively [5, p. 160]. The weight of water removed is converted to rate of water removal ($\Delta Q_{w,rem}$) in lb H₂O/d by multiplying with the gas flow rate, MMscf/d.

The reboiler duty per weight of water removed is calculated as [5, p. 158]:

$$\Delta H_{GD} = 900 + 966 q_{TEG} \left(\frac{1}{10^6} \right) \left[\frac{\text{MMBtu}}{\text{lb H}_2\text{O}} \right] \quad (4.64)$$

Surface
Processing
2.2.2.1.3

Surface
Processing
2.2.2.2.1

where ΔH_{GD} = specific reboiler heat duty [MMBtu/lb H₂O]; and q_{TEG} = TEG circulation rate [gal TEG/lb H₂O] removed. The heat duty is converted to MMBtu/d by multiplying by the rate of water removed, lb H₂O/d, as calculated in eq. (4.63).

The default TEG concentration assumed is 99 wt% [5, p. 155] and the default TEG circulation rate q_{TEG} is 2 gal TEG/lb H₂O removed [5, p. 147].

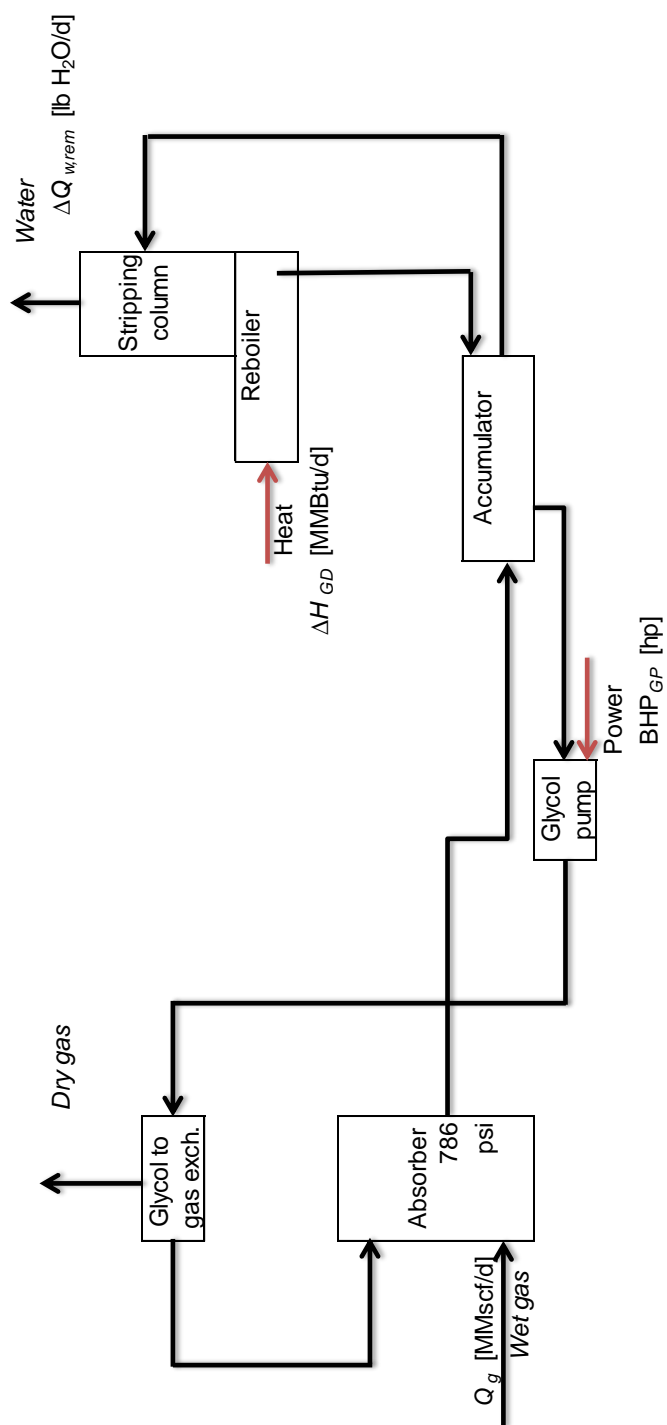


Figure 4.26: Glycol dehydrator simple process flow diagram [5, p. 141].

The glycol pump in the gas dehydration process is assumed to be electric by default. The horsepower is calculated using the conventional brake horsepower equation:

$$\text{BHP}_{\text{TEG}} = \frac{Q_{\text{TEG}} \cdot \Delta p}{1714 \eta_{\text{TEG}}} \quad [\text{hp}] \quad (4.65)$$

where BHP_{TEG} = TEG pump brake horsepower [hp]; Q_{TEG} = TEG circulation rate [gpm]; Δp = pumping pressure [psi]; and η_{TEG} = TEG pump efficiency [-]. The pumping pressure is the difference between pump discharge and suction pressures. The default pump suction pressure is 0 psi. The TEG pump discharge pressure is equal to contactor operating pressure. The default contactor operating pressure is 786 psi [5, p. 160]. The TEG circulation rate in gpm is calculated as:

$$Q_{\text{TEG}} = q_{\text{TEG}} \Delta Q_{w,\text{rem}} \left(\frac{1}{24 \cdot 60} \right) \quad [\text{gpm}] \quad (4.66)$$

where q_{TEG} = TEG circulation rate [gal TEG/lb H₂O removed]; and $\Delta Q_{w,\text{rem}}$ = rate of water removal [lb H₂O/d]. The calculation of the rate of water removal is shown in eq. (4.63).

4.4.2.6 Acid gas removal

A major element of associated gas treatment is acid gas removal (AGR). Associated gas from petroleum may naturally contain CO₂ and H₂S, which are acidic gases. Their concentrations are limited by regulations and thus they must be removed if necessary [146, p. 211-213].

In addition to containing naturally-occurring acid gases, associated gas may contain additional CO₂ injected during carbon dioxide enhanced oil recovery operations. In the period immediately following commencement of carbon dioxide flooding, the produced fluids will not contain any additional, non-native carbon dioxide. But as CO₂ mixes with the reservoir fluids and proceeds away from injector wells it will eventually begin to be produced along with the other reservoir fluids. Associated gas from a mature CO₂ flood project may contain very high levels of carbon dioxide. An example of this process is provided by the flood at the SACROC unit in Texas' Permian Basin, which commenced in 1972. Based on the specifications of the initial acid gas processing units installed in 1973 and 1974, the associated gas contained approximately 24% CO₂. The CO₂ content of the associated gas stream rose to 40% twelve years after carbon dioxide flooding began [147]. By 2002 the carbon dioxide content had risen to 85% [148].

The large variation in the percentage of CO₂ and the overall volume of gas over the course of a carbon dioxide enhanced recovery project may require modifications to the separation process. The initial SACROC gas treatment facilities used monoethanolamine or potassium carbonate chemical separation processes [148]. As CO₂ percentage and gas volumes increased, the operators adopted a dual treatment process that added filtration through a selectively permeable membrane in addition to the chemical separation unit [147].

Besides chemical-based and membrane separation technologies, a refrigerated distillation method known as the Ryan-Holmes process is another means of removing CO₂ from associated gas streams. OPGEE incorporates three different acid

Surface

Processing 2.2.2.3

Surface

Processing

2.2.2.1.5

gas separation modules: an amine-based process, a membrane-amine dual process, and the Ryan-Holmes refrigerative process.

The second step after the separation of individual phases is the treatment of associated gas. Treatment of associated gas starts with acid gas removal (AGR, also called gas sweetening). There are more than 30 natural gas sweetening processes. OPGEE assumes that the amine process is used. The batch and amine processes are used for over 90% of all onshore wellhead applications with amines being preferred when lower operating costs justifies the higher equipment cost. The chemical cost of batch processes may be prohibitive [5, p. 99].

In the amine process an aqueous *alkanolamine* solution is regenerated and used to remove large amounts of sulfur and CO₂ when needed. The model scheme allows the user to choose between the commonly used amine solutions (MEA, DEA, DGA, etc.). Each amine solution is characterized by a K value which is inversely proportional to both the acid gas removal rate (pick up) and amine concentration [5, p. 115]. When choosing an "other" amine solution, the user must enter a K value. The default contactor operating pressure is the median value of the pressures reported in the calculation of the contact tower diameter [149] [5, p. 117]. A schematic of the amine process is shown in Figure 4.27. The user has the option of turning OFF the AGR unit in the gas processing scheme.

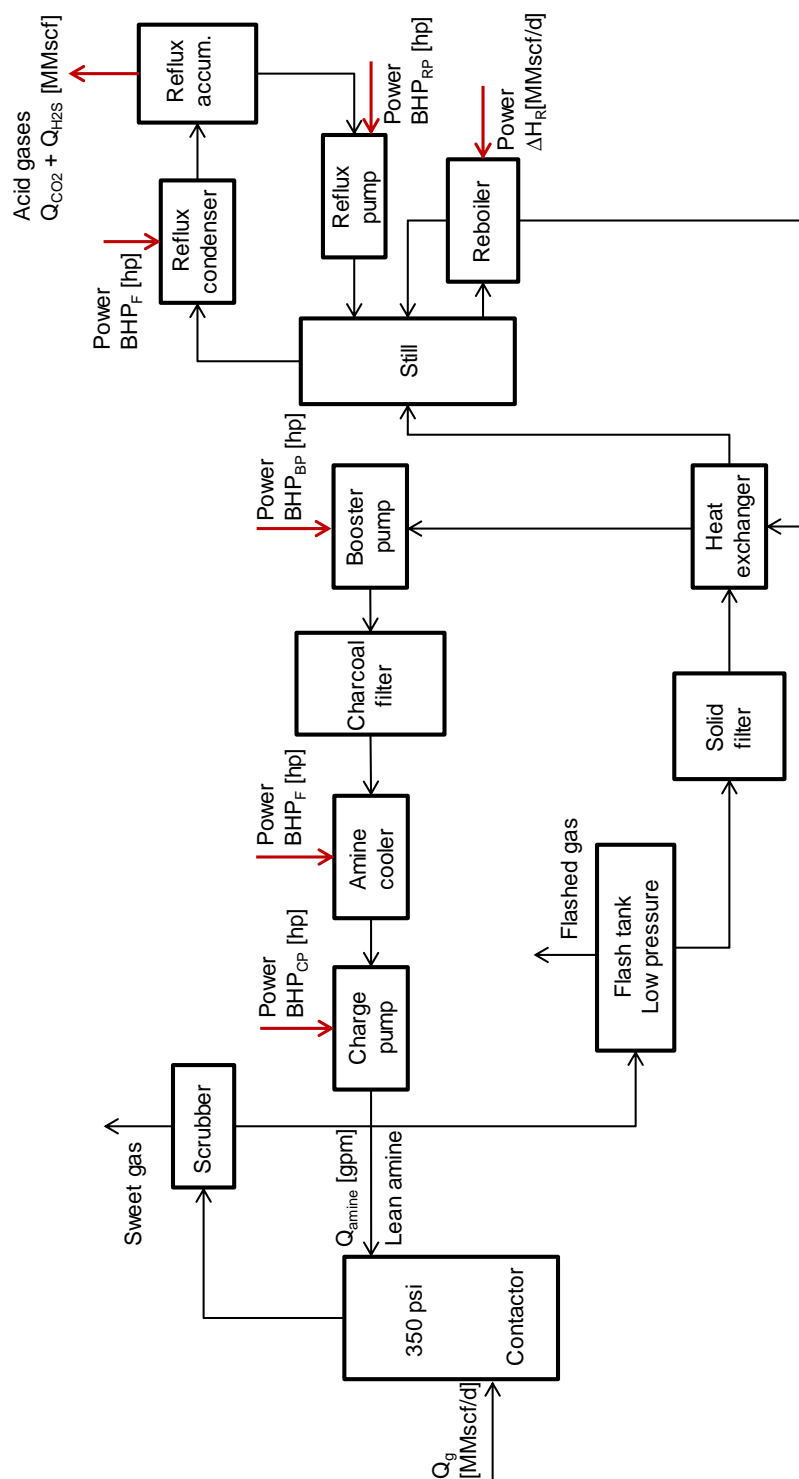


Figure 4.27: Amine simple process flow diagram [5, p. 112].

The inlet gas flow rate of the gas processing stage in the gas balance (see 'Gas Balance' worksheet) is calculated as:

$$Q_g = Q_o \cdot \text{GOR} \left(\frac{1}{10^6} \right) - Q_F \quad \left[\frac{\text{MMscf}}{\text{d}} \right] \quad (4.67)$$

Surface
Processing 2.2.1
Figure

where Q_g = inlet gas flow rate [MMscf/d]; Q_o = rate of oil production [bbl/d]; Q_F = flaring rate [MMscf/d]; and GOR = gas-to-oil ratio [scf/bbl]. The inlet gas flow rate is used in the calculation of the amine circulation rate in eq. (4.69). Although the accumulation of gases to flare likely occurs at various points throughout the process, OPGEE assumes that the gas flared is removed before gas processing occurs. This allows for OPGEE to account for "early field production" or production in locations without a gas market. For these situations, no surface processing exists and all produced gas is flared.

The amine reboiler in OPGEE is a direct fired heater that uses natural gas. The reboiler duty is: (i) the heat to bring the acid amine solution to the boiling point, (ii) the heat to break the chemical bonds between the amine and acid gases, (iii) the heat to vaporize the reflux, (iv) the heat load for the makeup water, and (v) the heat losses from the reboiler and still [5, p. 117].

The heat duty of the amine reboiler can be estimated from the circulation rate of the amine solution as [5, p. 119—originally Jones and Perry, 1973]:

$$\Delta H_R = \frac{24 \cdot 72000 \cdot Q_{\text{amine}}}{10^6} 1.15 \quad \left[\frac{\text{MMBtu}}{\text{d}} \right] \quad (4.68)$$

Surface
Processing 2.2.1.4

where ΔH_R = heat duty [MMBtu/d]; and Q_{amine} = amine flow rate [gpm]. A gallon of amine solution requires approximately 72000 Btu for regeneration [150]. A safety factor of 15% is added for start up heat losses and other inefficiencies. The flow rate of the amine solution can be estimated using the following equation [5, p. 115]:

$$Q_{\text{amine}} = 100 K (Q_{\text{H}_2\text{S}} + Q_{\text{CO}_2}) \quad [\text{gpm}] \quad (4.69)$$

Surface
Processing 2.2.1.1.1

where Q_{amine} = amine flow rate [gpm]; K = amine solution K value [gpm-d/100MMscf]; $Q_{\text{H}_2\text{S}}$ = H₂S removal [MMscf/d]; and Q_{CO_2} = CO₂ venting from AGR unit [MMscf/d]. The venting of CO₂ from the AGR unit is calculated in the 'Gas Balance' worksheet. The rate of H₂S removal is calculated as:

$$Q_{\text{H}_2\text{S}} = x_{\text{H}_2\text{S}} \cdot Q_g \quad \left[\frac{\text{MMscf}}{\text{d}} \right] \quad (4.70)$$

where $x_{\text{H}_2\text{S}}$ = molar fraction of H₂S [-]; and Q_g = inlet gas flow rate [MMscf/d]. The calculation of the inlet gas flow rate is shown in eq. (4.67). The molar fraction of H₂S is determined from the composition of associated gas.

In OPGEE all H₂S remaining in the associated gas is removed in the AGR unit. Removed H₂S is calculated in eq. (4.70) by multiplying the inlet gas flow rate with the molar percent of H₂S. Also all the CO₂ removed is vented and that is calculated in the 'Gas Balance' worksheet.

Other equipment in the amine regeneration system that consume power and energy include the reflux condenser and the amine cooler. There also are reflux, booster, and circulation pumps. The reflux condenser and the amine cooler are air-cooled, forced-draft heat exchangers. In OPGEE both services are combined into one structure with a common fan.

The motor size of the amine cooler fan can be estimated from the amine circulation rate as [5, p. 118]:

$$\text{BHP}_F = 0.36 \cdot Q_{\text{amine}} \quad [\text{hp}] \quad (4.71)$$

where BHP_F = fan brake horsepower [hp]; and Q_{amine} = amine circulation rate [gpm].

The heat duty of the reflux condenser is approximately twice the heat duty of the amine cooler [5, p. 117]. Therefore the motor size of the 'common' fan is estimated by multiplying the brake horsepower of the amine cooler by 3.

Similarly motor sizes of pumps can also be estimated from the amine circulation rate as [5, p. 118]:

$$\text{BHP}_{RP} = 0.06 \cdot Q_{\text{amine}} \quad [\text{hp}] \quad (4.72)$$

$$\text{BHP}_{BP} = 0.06 \cdot Q_{\text{amine}} \quad [\text{hp}] \quad (4.73)$$

$$\text{BHP}_{CP} = 0.00065 \cdot Q_{\text{amine}} \cdot p_d \quad [\text{hp}] \quad (4.74)$$

where BHP_{RP} = reflux pump brake horsepower [hp]; BHP_{BP} = booster pump brake horsepower [hp]; BHP_{CP} = circulation pump brake horsepower [hp]; and p_d = pump discharge pressure [psi]. The circulation pump discharge pressure = 50 psi over contactor operating pressure [5, p. 121]. The default contactor operating pressure as mentioned earlier is 350 psi.

4.4.2.7 CO₂ Enhanced oil recovery pathway: membrane-amine dual process

Gas Processing Path 7 includes the same amine-based AGR unit described in the Acid gas removal section, but also incorporates a selectively permeable membrane that reduces the CO₂ content of the gas stream prior to its transit through the amine process.

In addition treatment in the glycol dehydrator, the associated gas stream is cooled in an electric chiller to preserve the functionality of the membrane [4]. The default temperatures of the gas streams entering and exiting the chiller are 59 °F and 35 °F, respectively [142].

The electricity consumption rate of the chiller is calculated as [142]:

$$E_c = 3.44 \cdot \left(\frac{Q_c}{6.11} \right) \cdot \frac{(T_I - T_O)}{56} \quad [\text{MW}] \quad (4.75)$$

where E_c = chiller electricity consumption rate [kWh/d]; Q_c = mass flow rate of the chiller feed stream [mmkg/d]; T_I = temperature of the chiller feed stream [K]; and T_O = temperature of the chiller exit stream [K].

Equation 4.75 linearly scales the refrigeration compressor load in a gas separation process in the NETL chiller module [142] in which 6.11 mmkg/d is the mass flow rate of the feed stream, 56 K is the temperature drop resulting from the refrigeration process, and 3.44 [MW] is the compressor load.

After exiting the chiller, the feed stream is compressed to reach a pressure sufficient to traverse the selectively permeable membrane. The compressor's energy calculations and operational assumptions are identical to the compressors described in the Production & extraction section. The membrane removes 67% of

Surface
Processing
2.2.1.3.1

Surface
Processing 2.2.1.2

Surface
Processing 2.2.6

the CO₂ in the feed stream; it is assumed that the post-membrane carbon dioxide stream is 100% pure [142]. The post-membrane natural gas-rich stream still contains 33% of the original CO₂, which then proceeds to an amine-based process which operates as described in the Acid gas removal section. The pure CO₂ streams exiting the amine-process and the membrane are united and ultimately reinjected into the reservoir.

4.4.2.8 CO₂ Enhanced oil recovery pathway: Ryan-Holmes process

Gas Processing Path 8 models the Ryan-Holmes separation process, which uses controlled compression and refrigeration to take advantage of the differing boiling points of the components of the feed gas stream; it includes a demethanizer. The process splits the feed stream into a CO₂ stream (assumed to be 100% pure), a natural gas stream, and a heavy product NGL stream [151]. OPGEE incorporates NETL's Ryan-Holmes process module which includes energy consumption for natural gas-fired compressors, a natural gas-fired oil heater, and a diesel-fired backup engine [144]. The default temperature of the feed stream entering the Ryan-Holmes process is 81 °F [144].

The energy consumption of each component of the Ryan-Holmes process is calculated as follows:

The natural gas consumption rate of the turbines is calculated as [144]:

$$E_t = \frac{Q_{RH}}{45} \cdot 25,800 \cdot \frac{24[\text{hrs}]}{1[\text{d}]} \cdot \frac{1[\text{Mscf}]}{1,000[\text{scf}]} \left[\frac{\text{Mscf}}{\text{d}} \right] \quad (4.76)$$

where E_t = turbine natural gas consumption rate [Mscf/d] and Q_{RH} = volumetric flow rate of the Ryan-Holmes feed stream [MMscf/d]. Equation 4.76 linearly scales the turbine natural gas consumption rate based on the 45 MMscf/d feed stream throughput in the NETL Ryan-Holmes model, in which the turbines consume a total of 25,800 scf/hr [144].

The natural gas consumption rate of the compressors is calculated as [144]:

$$E_c = \frac{Q_{RH}}{45} \cdot 110,519 \cdot \frac{24[\text{hrs}]}{1[\text{d}]} \cdot \frac{1[\text{Mscf}]}{1,000[\text{scf}]} \left[\frac{\text{Mscf}}{\text{d}} \right] \quad (4.77)$$

where E_c = compressor natural gas consumption rate [Mscf/d]; Q_{RH} = volumetric flow rate of the Ryan-Holmes feed stream [MMscf/d]. Equation 4.77 linearly scales the compressor natural gas consumption rate based on the 45 MMscf/d feed stream throughput in the NETL Ryan-Holmes model, in which the compressors consume a total of 110,519 scf/hr [144], [152].

The natural gas consumption rate of the oil heater is calculated as [144]:

$$E_h = \frac{Q_{RH}}{45} \cdot 14,589 \cdot \frac{24[\text{hrs}]}{1[\text{d}]} \cdot \frac{1[\text{Mscf}]}{1,000[\text{scf}]} \left[\frac{\text{Mscf}}{\text{d}} \right] \quad (4.78)$$

where E_h = oil heater natural gas consumption rate [Mscf/d]; Q_{RH} = volumetric flow rate of the Ryan-Holmes feed stream [MMscf/d]. Equation 4.78 linearly scales the oil heater natural gas consumption rate based on the 45 MMscf/d feed stream throughput in the NETL Ryan-Holmes model, in which the hot oil heater consumes 14,589 scf/hr [144].

Surface
Processing 2.2.5

The diesel consumption rate of the backup engine is calculated as [144]:

$$E_e = \frac{Q_{RH}}{45} \cdot 57 \cdot \frac{2.63}{24} \quad \left[\frac{\text{gal}}{\text{d}} \right] \quad (4.79)$$

where E_e = backup engine consumption rate [gal/d] and Q_{RH} = volumetric flow rate of the Ryan-Holmes feed stream [MMscf/d]. Equation 4.78 linearly scales the oil heater natural gas consumption rate based on the 45 MMscf/d feed stream throughput in the NETL Ryan-Holmes model in which the hot oil heater consumes diesel at a rate of 57 gal/d. The default usage rate rate of the backup engine is 2.63 hr/d [144].

4.4.2.9 Gas demethanizer

The demethanizer splits the natural gas stream into a pipeline quality natural gas stream and a natural gas liquids (NGL) stream. The main sources of GHG emissions from the demethanizer unit are the refrigeration system and compressor shaft power and the heat duty of the fractionation column reboiler, if supplemental heat is required. These are calculated using energy factors which are generated from a default configuration [153]. The independent demethanizer unit described below is included in Gas Processing Paths 4 and 5. Gas Processing Path 7 (Ryan-Holmes) includes an integrated demethanizer.

In the default OPGEE demethanizer configuration, the compressor system is assumed to operate upstream of the demethanizer; the resulting feedstream pressure is 60 bar [153]. The refrigeration duty is assumed to be proportional to the amount of gas condensed. A heat recovery system allows the cold gas that remains to be warmed back up in exchange with incoming gas. The energy factors of the compressor and refrigeration system are 0.58 [bhp-hr/kmol_{FEED}] and 3.6 [bhp-hr/kmol_{COND}], respectively. As seen in the demethanizer literature, OPGEE assumes that the reboiler heat duty is provided by heat exchangers from the incoming feed stream. Under this configuration the demethanizer is assumed to condense 90.2% of ethane and 100% of propane and butane [153], which is then assumed to be exported as LPG. These fractions can be changed on the 'Surface Processing' worksheet. The gas feed measure is in gram moles as reported in the demethanizer unit synthesis report. The gas feed moles is calculated from the 'Gas Balance' worksheet using the gas composition of the demethanizer feed. The refrigeration brake horse power is calculated as:

$$\text{BHP}_{RS} = \frac{1}{24} \cdot e_{RS} \cdot Q_{gin} \quad [\text{hp}] \quad (4.80)$$

where BHP_{RS} = refrigeration system shaft brakehorse power [hp]; e_{RS} = energy factor [bhp-hr/kmol_{COND}]; and Q_{gin} = demethanizer gas condensed [kmol/d]. The compressor work is calculated similarly. The molar amount of the gas feed and gas condensed is calculated in the 'Surface Processing' worksheet.

The energy consumption of the compression and refrigeration system is calculated using the fuel consumption of an appropriate NG turbine as determined by the power demand. GHG emissions are calculated using emissions factors of NG turbine from the 'Emissions Factors' worksheet.

Surface Processing
1.2.2.3.2

Surface
Processing
1.2.2.3.1

Surface
Processing 2.2.3.1

Table 4.21: Typical concentrations of process water pollutants. Table from Vlasopoulos et al [9].

| Pollutants | Concentration (mg/l) |
|------------------------------|----------------------|
| Oil and grease | 200 |
| Boron | 5 |
| Total dissolved solids (TDS) | 5000 |
| Sodium | 2100 |

OPGEE allows flexibility in the gas processing scheme; the demethanizer unit can be turned OFF in fields with dry associated gas or where NGL recovery is not economic by selecting Gas Processing Paths 1, 2, or 3.

4.4.2.10 Water treatment

Oil production generates a significant amount of produced water, which can be contaminated with hydrocarbons, salts, and other undesirable constituents; Table 4.21 [9, p. 59] presents a typical profile. The pollutant profile varies with factors such as reservoir geology [9]. The fraction of water produced is determined by the WOR. After cleaning, produced water is reinjected, discharged to the local environment, or injected into aquifers.

Process water from oil production can be treated in a variety of different ways. The technologies in OPGEE are grouped into 4 different treatment stages according to the categorization of water treatment technologies as shown in Table 4.22 [154]. This categorization and the energy consumption of each technology in kWh per m³ of water *input* (converted to kWh per bbl of water) was adopted from Vlasopoulos et al. [9].

The user can set up a water treatment system composed of 1-4 stages of treatment with one option from each treatment stage as shown in Table 4.22, which also describes the pollutants targeted by each stage. The technology combinations are selected according to the target water qualities that must be achieved.

The model scheme has two treatment trains: (i) one for the treatment of process water generated from oil production and (ii) another for the treatment of imported water, such as sea water, if applicable.

The user can set up a treatment train by switching on/off the treatment technologies listed under each treatment stage. One option is allowed for each treatment stage. Based on the user selections, OPGEE retrieves the corresponding electricity consumption and calculates the total electricity consumption:

$$E_{tot} = e_{s1}Q_{w1} + e_{s2}Q_{w2} + e_{s3}Q_{w3} + e_{s4}Q_{w4} \quad \left[\frac{\text{kWh}}{\text{d}} \right] \quad (4.81)$$

where E_{tot} = total electricity consumption [kWh/d]; $e_{s,N}$ = electricity consumption of stage N [kWh/ bbl of water input]; and $Q_{w,N}$ = water feed into stage N [bbl of water/d].

For the produced water treatment train the water feed of stage 1 is equal to the water flow in the well stream as calculated in eq. (4.82). The default volume losses are assumed 0% for all treatment technologies except for wetlands which is assumed to be 26% [9]. The water feed of stages 2-4 is calculated as:

Surface
Processing 2.3.1

Surface
Processing 2.3.1
Figure

Table 4.22: Categorization of water treatment technologies. Table based on table from Vlasopoulos et al. [9], with minor modifications

| Name | Signifier |
|--------------------------------|-----------|
| Stage 1 | |
| Dissolved air flotation | DAF |
| Hydrocyclones | HYDRO |
| Stage 2 | |
| Rotating biological contactors | RBC |
| Absorbents | ABS |
| Activated sludge | AS |
| Trickling filters | TF |
| Air stripping | AIR |
| Aerated lagoons | AL |
| Wetlands | CWL |
| Microfiltration | MF |
| Stage 3 | |
| Dual media filtration | DMF |
| Granular activated carbon | GAC |
| Slow sand filtration | SSF |
| Ozone | OZO |
| Organoclay | ORG |
| Ultrafiltration | UF |
| Nanofiltration | NF |
| Stage 4 | |
| Reverse osmosis | RO |
| Electrodialysis reversal | EDR |
| Warm lime softening | WLS |

$$Q_{w,N} = Q_{w,(N-1)}[1 - \epsilon_{V,(N-1)}] \left[\frac{\text{bbl of water}}{d} \right] \quad (4.82)$$

where $\epsilon_{V,(N-1)}$ = volume loss in stage $N - 1$ [fraction].

For the imported water treatment train, if applicable, the same calculations apply but the water feed is calculated backwards starting from stage 4 where the output is equal to the amount of water supplied to the process in excess of the output from the produced water train. The volume losses are set to be direct user inputs in the mass balance to avoid circular references.

The energy consumption value for warm lime softening (WLS) is taken from documents outlining the processing configurations for Canadian SAGD operations [155].

4.4.3 Defaults for surface processing

Defaults for surface operations are shown in Table 4.23.

Table 4.23: Default inputs for surface processing.

| Param. | Description | Eq. no. | Default | Literature range | Unit | Sources | Notes |
|-----------------------|---|---------|------------------------|------------------|-------------------------------|---------------|-------|
| BHP_F | Fan brakehorse power | (4.71) | - | - | [hp] | [5, p. 118] | |
| BHP_{RP} | Reflux pump brakehorse power | (4.72) | - | - | [hp] | [5, p. 118] | |
| BHP_{BP} | Booster pump brakehorse power | (4.73) | - | - | [hp] | [5, p. 118] | |
| BHP_{CP} | Circulation pump brakehorse power | (4.74) | - | - | [hp] | [5, p. 118] | |
| BHP_{TEG} | TEG pump brakehorse power | (4.65) | - | - | [hp] | [8, p. 455] | |
| BHP_{RS} | Refrigeration brakehorse power | (4.80) | - | - | [hp] | [153] | |
| C_{p0} | Specific heat of oil | - | 150 | - | [Btu/(bbbl ^o F)] | [59, p. 136] | |
| C_{pw} | Specific heat of water | - | 350 | - | [Btu/(bbbl ^o F)] | [59, p. 136] | |
| E_{tot} | Total electricity consumption | (4.81) | - | - | [Kwh/d] | | |
| $e_{s1} \dots e_{s4}$ | Electricity consumption by stage | - | - | - | [Kwh/d] | | |
| ϵ_j | Fraction of heat loss in unit j | - | 0.02 | - | [-] | [59, p. 136] | a |
| $\epsilon_{V,(N-1)}$ | Fraction of volume loss in stage $N-1$ | - | var. | - | [-] | [9] | |
| η_P | Pump efficiency | - | 0.65 | - | [-] | | |
| $\lambda_{w,rem}$ | Fraction of water removed below fire tube | - | 0.4 | - | [-] | [59, p. 136] | |
| GOR | Gas-to-oil ratio | - | Section 4.3.3.6 | - | [scf/bbl] | | |
| ΔH_R | Amine process reboiler heat duty | (4.68) | - | - | [MMBtu/d] | [5, p. 119] | |
| ΔH_{GD} | Glycol dehydrator reboiler heat duty | (4.64) | - | - | [MMBtu/d] | [5, p. 158] | |
| ΔH_{FR} | Fractionation reboiler heat duty | - | 0 | - | [MMBtu/d] | [153] | |
| K | Amine solution K value | - | 2.05 | 0.95-2.05 | [gpm-d/100MMscf] | [5, p. 115] | b |
| $\lambda_{w,ent}$ | Fraction of water entrained in oil | - | 0.14 | - | [-] | [59, p. 136] | c |
| q_{TEG} | TEG circulation rate | - | 2 | - | [gal TEG/lb H ₂ O] | [5, p. 147] | |
| p_d | Pump discharge pressure | - | 786 | - | [psi] | [5, p. 160] | |
| $\Delta Q_{w,rem}$ | Rate of water removal | - | $Q_g \Delta M_{w,rem}$ | - | [lb H ₂ O/d] | | |
| Q_{amine} | Amine flow rate | (4.69) | - | - | [gpm] | [5, p. 115] | |
| Q_{CO_2} | Volume of CO ₂ removed | - | var. | - | [MMscf/d] | 'Gas Balance' | |
| $Q_{w,ent}$ | Volume of entrained water | (4.52) | - | - | [bbl/d] | [59, p. 136] | |
| Q_F | Flaring volume | - | Section 5.11.1 | - | [MMscf/d] | | |
| Q_g | Inlet gas flow rate | (4.67) | - | - | [MMscf/d] | | |
| Q_{H_2S} | Volume of H ₂ S removed | - | var. | - | [MMscf/d] | 'Gas Balance' | |
| $Q_{w,heat}$ | Volume of heated water | (4.51) | - | - | [bbl/d] | 'Gas Balance' | |
| Q_o | Volume of oil production | - | 1500 | - | [bbl/d] | [59, p. 136] | |

Continued on next page...

Continued from previous page

| Param. | Description | Eq. no. | Default | Literature range | Unit | Sources | Notes |
|-----------------------|--|---------|---------|------------------|-----------------------------|-------------------|-------|
| Q_{TEG} | TEG circulation rate in gpm | (4.66) | - | - | [gpm] | | |
| Q_w | Volume of produced water | (4.82) | - | - | [bbl/d] | | |
| $Q_{w1} \dots Q_{w4}$ | Water feed by stage | (4.82) | - | - | [bbl water/d] | | |
| ΔT_{CD} | Crude dehyd. temp. difference | - | 75 | - | [°F] | [59, p. 136] | |
| ΔT_S | Crude stabilizer temp. difference | - | 224 | - | [°F] | [59, p. 161, 163] | |
| $\Delta M_{w,rem}$ | Weight of water removed | (4.63) | - | - | [lb H ₂ O/MMscf] | | |
| $M_{w,in}$ | Weight of water in inlet gas | - | 52 | - | [lb H ₂ O/MMscf] | [5, p. 160] | |
| $M_{w,out}$ | Weight of water in outlet gas | - | 7 | - | [lb H ₂ O/MMscf] | [5, p. 160] | |
| WOR | Water-to-oil ratio | (4.49) | - | - | [bbl water/bbl oil] | | |
| $Chiller_{IN}$ | Temperature of feedstream entering chiller unit | - | 59 | - | [°F] | [142] | |
| $Chiller_{OUT}$ | Temperature of feedstream exiting chiller unit | - | 35 | - | [°F] | [142] | |
| RH_{IN} | Temperature of feedstream entering Ryan-Holmes process | - | 81 | - | [°F] | [144] | |
| RH_{backup} | Usage rate of Ryan-Holmes backup engine | - | 2.63 | - | [hrs/d] | [144] | |

a - This is a user input. No defaults are available for most of the treatment technologies. The default for wetlands (CWL) where volume losses are significant is 26% [9].
b - It is assumed that heat exchange with the inlet stream provides the heat duty.
c - The default is monoethanolamine (MEA).

4.5 Maintenance operations

4.5.1 Introduction to maintenance operations

Emissions from maintenance include venting and fugitives associated with compressor blowdowns, well workovers and cleanups, separator cleaning and repair, and gathering pipeline maintenance and pigging. Other maintenance emissions are believed to be below the significance cut-off and are not included.

4.5.2 Calculations for maintenance operations

Emissions from maintenance operations are classified in Table C.5. Emissions from maintenance operations are either very small (e.g., embodied energy consumed in maintenance parts) or are tracked in the '*Venting & Fugitives*' worksheet (see Section 5.9). For this reason, OPGEE does not perform specific maintenance emissions calculations in the separate '*Maintenance*' worksheet.

4.5.3 Defaults for maintenance operations

Defaults used in the calculation of emissions from maintenance operations are discussed in Section 5.9.

4.6 Waste treatment and disposal

4.6.1 Introduction to waste treatment and disposal

Emissions from waste disposal occur during routine oilfield maintenance operations (e.g., disposal of residual hazardous waste products) due to clean up operations, or due to one-time events such as decommissioning of oilfield equipment. Emissions occur offsite due to the energy demands of waste disposal and the transport requirements for moving waste to waste treatment or disposal sites. A complete list of emissions sources, along with their categorization and estimated magnitude, is shown in Table C.6.

4.6.2 Calculations for waste treatment and disposal

Because waste treatment emissions only occur sporadically, they are likely to be small when amortized over the producing life of an oil field. For this reason, emissions from waste treatment are considered below the significance cutoff in OPGEE v2.0b.

Possible exceptions could be the treatment and disposal of fracturing fluids and fracturing flow-back water, due to the large volumes produced. Future versions of the model may include these factors.

4.6.3 Defaults for waste treatment

Waste treatment emissions default to 0 gCO₂/MJ. Any waste treatment emissions are assumed to be captured in the small sources emissions default parameter. *Active Field 3.6*

4.7 Crude oil transport

4.7.1 Introduction to crude oil transport

Crude oil transport includes all activities associated with moving crude oil from a production facility to a refinery. In the case of land transport, this generally involves transport via pipeline to the refinery. Pipelines are powered by natural gas, oil, or electric-powered drivers. In some instances, rail transport is used for over-land transport. In the case of inter-continental trade, crude oil is transported to a loading dock, loaded onto a tanker or barge, transported via ship over water, unloaded at the destination, and finally transported to a refinery. Transport emissions occur due to energy consumption by transport equipment and due to fugitive emissions from loading and unloading operations. In OPGEE, transport emissions are modeled using methods and data from CA-GREET [84]. Transport emissions calculations allow for variations in transport modes, distance travelled, and fuel mix in each mode.

4.7.2 Calculations for crude oil transport

OPGEE crude oil transport calculations use sets of transport modes, transport propulsion technologies in each mode (most commonly one technology per mode), and transport fuels. Emissions are tracked per species of GHG. Transport modes include tanker (*T*), barge (*B*), pipeline (*P*), rail (*R*), and truck (*TR*). Pipelines include two propulsion technologies: turbines (*GT*) and reciprocating engines (*RE*). Fuels used in transport include diesel fuel (*di*), residual oil (*ro*), natural gas (*ng*), and electricity (*el*).

The effectiveness crude oil transport [Btu/ton-mi] is calculated for a variety of modes using a similar general form. Each mode has an effectiveness *U*. For example, tanker transport effectiveness U_T is calculated as:

$$U_T = \frac{\eta_T l_T P_T}{v_T C_T} \left[\frac{\text{Btu}}{\text{ton-mi}} \right] = \frac{\left[\frac{\text{Btu}}{\text{hp-hr}} \right] [-] [\text{hp}]}{\left[\frac{\text{mi}}{\text{hr}} \right] [\text{ton}]}, \quad (4.83)$$

Crude
Transport
2.2

where U_T = specific energy intensity of crude oil transport via tanker [Btu/ton-mi]; η_T = efficiency of tanker transport [Btu/hp-hr]; l_T = load factor of tanker (different on outbound and return trip) [-]; P_T = tanker power requirements [hp]; v_T = tanker velocity [mi/hr]; and C_T is tanker capacity [ton/tanker]. Barge and truck transport effectiveness U_B and U_{TR} are calculated in an analogous fashion.

For the case of pipeline and rail transport, the calculation is simpler. For pipeline transport the effectiveness is calculated as follows:

$$U_P = \sum_{j \in GT, RE} \lambda_{Pj} U_{Pj} \left[\frac{\text{Btu}}{\text{ton-mi}} \right] = [-] \left[\frac{\text{Btu}}{\text{ton-mi}} \right] \quad (4.84)$$

Crude
Transport
2.2

where λ_{Pj} = fraction of each pipeline pumping technology *j* [-]; and U_{Pj} = effectiveness of pipeline transport for technology *j* [Btu/ton-mi]. For rail transport, only one technology exists, so no summation is required.

Back haul trips are calculated using GREET factors for the energy intensity of return trips [26]

The energy-specific transport energy intensity is calculated from the transport effectiveness using the energy density of crude oil. For example, in the case of tanker transport:

$$e_T = U_T \frac{1}{LHV_o} \rho_w \gamma_o \frac{1}{2000} \quad (4.85)$$

Crude
Transport
2.4

$$\left[\frac{\text{Btu}}{\text{MMBtu-mi}} \right] = \left[\frac{\text{Btu}}{\text{ton-mi}} \right] \left[\frac{\text{bbl}}{\text{MMBtu}} \right] \left[\frac{\text{lb}}{\text{bbl water}} \right] \left[\frac{\text{lb/bbl oil}}{\text{lb/bbl water}} \right] \left[\frac{\text{lb}}{\text{ton}} \right] \quad (4.86)$$

where UE_T = crude oil transport intensity per unit of energy transported [Btu/MMBtu-mi], LHV_o = crude lower heating value [MMBtu/bbl]; ρ_w = density of water [lb/bbl]; γ_o = crude specific gravity [-]; and $1/2000$ = conversion factor between lb and ton.

Calculating emissions of GHG species associated with the consumption of a given energy type in a given device is performed via multiplication with the appropriate emissions factor. For example, in the case of tanker emissions:

$$EM_{Ti} = e_T \sum_k \lambda_{Tk} EF_{Tki}, \quad (k \in di, ro, ng) \quad (4.87)$$

$$\left[\frac{\text{g}}{\text{MMBtu-mi}} \right] = \left[\frac{\text{Btu}}{\text{MMBtu-mi}} \right] [-] \left[\frac{\text{g}}{\text{Btu}} \right]$$

Crude
Transport
Table 2.4

where EM_{Ti} = emissions of species i from tankers [g/MMBtu-mi]; λ_{Tk} = fraction of fuel k used in tankers [-]; and EF_{Tki} = emissions factor for fuel k , species i consumed in tankers [g/Btu]. Other modes are calculated similarly.

The total CO₂ equivalent emissions are then computed by weighting by gas global warming potential (GWP). Again, for the case of tanker transport:

$$EM_T = \sum_i EM_{Ti} GWP_i, \quad \left[\frac{\text{g CO}_2 \text{ eq.}}{\text{MMBtu-mi}} \right] = \left[\frac{\text{g}}{\text{MMBtu-mi}} \right] \left[\frac{\text{g CO}_2 \text{ eq.}}{\text{g}} \right] \quad (4.88)$$

Crude
Transport
Table 2.4

where GWP_i = GWP of species i .

The total energy consumption from transport is computed using the distances and fractions of transport, along with the mode-specific energy intensity of transport:

$$E_{TR} = \sum_j \lambda_j D_j UE_j \quad (j \in T, B, P, R) \quad (4.89)$$

$$\left[\frac{\text{Btu}}{\text{MMBtu}} \right] = [\text{mi}] \left[\frac{\text{Btu}}{\text{MMBtu-mi}} \right] [-]$$

Crude
Transport
3.1

where D_j = distance of crude oil transport in mode j [mi]; UE_j = energy-specific transport effectiveness for mode j [Btu/MMBtu-mi]; and λ_j = fraction of crude oil transported in mode j . The sum of fractional transport shares λ_j can be greater than 1, because some crude may be transported via both pipeline and tanker, for example.

The total emissions are calculated identically:

$$EM_{TR} = \sum_j \lambda_j D_j EM_j \quad (j \in T, B, P, R) \quad (4.90)$$

$$\left[\frac{\text{g CO}_2 \text{ eq.}}{\text{MMBtu}} \right] = [\text{mi}] \left[\frac{\text{g CO}_2 \text{ eq.}}{\text{MMBtu-mi}} \right] [-]$$

Crude
Transport
3.2

where EM_j are the emissions from mode j on a CO₂-equivalent basis.

4.7.3 Defaults for crude oil transport

Defaults for crude oil transport are generally taken from the CA-GREET model, with some modifications and simplifications applied. Defaults for surface operations are given below in Table 4.24.

Table 4.24: Default inputs for Transport.

| Param. | Description | Eq. no. | Default | Literature range | Unit | Sources | Notes |
|------------------|--|----------------|-------------------------------|------------------|----------------------------------|------------|-------|
| C_j | Transport capacity of mode j | - | 'Transport' Table 2.1 | | [ton] | [26] | |
| e_m | Energy intensity of transport in mode j by energy unit transported | (4.85) | - | - | [Btu/MMBtu-mi] | | |
| EF_{jki} | Emissions factor for fuel k , species i , mode j | - | 'Emissions Factors' Table 1.5 | | [g/MMBtu] | | a |
| EM_{ji} | Emissions of species i by mode j | (4.87) | - | - | [g/MMBtu-mi] | | |
| EM_j | Emissions of all GHGs in CO ₂ eq. units by mode j | (4.88) | - | - | [g CO ₂ eq./MMBtu-mi] | | |
| E_{TR} | Total energy use in transport | (4.89) | - | - | [Btu/MMBtu] | | a |
| EM_{TR} | Total emissions from in transport | (4.90) | - | - | [g/MMBtu] | | a |
| η_j | Efficiency of transport mode j | - | 'Transport' Table 2.3 | | [Btu/hp-hr] | [26] | |
| $GW P_i$ | Global warming potential for species i | - | 'Input data' Table 2.1 | | [gCO ₂ eq./g] | | |
| γ_o | Specific gravity of crude oil | - | 0.876 | 0.8-1.05 | [-] | [90] | |
| I_j | Load factor of mode j | - | 'Transport' Table 2.3 | | [%] | [26] | |
| $\lambda_{j1/2}$ | Fraction of technology j_2 used in mode j_1 | - | 'Transport' Table 2.6 | | [%] | [26], Est. | |
| λ_{jk} | Fraction of fuel k used in mode j | - | 'Transport' Table 2.7 | | [-] | Est. | a |
| P_j | Power consumption of mode j | - | 'Transport' Table 2.2 | | [hp] | [26] | |
| ρ_w | Density of fresh water | - | 350.4 | - | [lb/bbl] | [156] | |
| U_j | Transport effectiveness in mode m | (4.84); (4.83) | - | - | [Btu/ton-mi] | [26] | |
| $U_{j1/2}$ | Transport effectiveness of propulsion tech j_2 used in mode j_1 | - | 'Transport' Table 2.5 | | [Btu/ton-mi] | [26] | |
| v_j | Velocity of mode j | - | 'Transport' Table 2.3 | | [mi-hr] | [26] | |

^a Default crude oil shipment distance in CA-GREET is 750 mi for a one-way trip [26].

5 Supplemental calculations worksheets

5.1 Gas balance

This worksheet tracks the gas balance across the process stages and ensures that gas is conserved in the system. Due to the complexity of allocating VFF emissions some simplifications were made to the overall structure of the system.

The gas-oil-ratio is the volume of natural gas that separates from oil during bulk separation divided by the post-bulk-separation oil volume [5]. The GOR is used to calculate the volume of the produced gas stream based on the volume of oil. Fugitives from active wells, well cellars, and well maintenance events (such as well workovers and cleanups) are assumed to occur upstream from surface separation. Therefore these emissions sources do not affect the volume and composition of the initial produced gas stream in the gas balance.

Gas Balance Table
1.1

The flaring of associated gas is assumed to occur upstream of the gas processing stage. Although the accumulation of gases to flare likely occurs at various points throughout the process, the flared gas is modeled as being flared before gas processing in OPGEE. This allows for an added flexibility in OPGEE to account for early field production or production in locations without a gas market. For these situations, no surface processing occurs and all produced gas is flared.

Gas Balance Table
1.3

Gas processing is presented in the gas balance as multiple process stages, some of which include fugitive and operational venting calculations. These emissions do not include the venting from crude oil storage tanks. The associated gas GOR is computed at the last stage in the surface oil-gas separator.

A user control is placed at the composition of the inlet gas to the gas processing stage to ensure that the total fugitives and venting of associated gas components (i.e., CO₂, CH₄, and C₂+) are conserved in the gas stream. In the event of "ERROR" the user has to increase either the molar fraction of the gas component or the GOR.

The output flows from the gas balance sheet consist of 1) Pipeline quality natural gas, 2) Natural gas liquids (NGL), and, in the case of the CO₂ EOR processing paths, a 3) CO₂ stream. Based on the nature of the associated gas stream and the user's processing choices, some of these paths may contain zero volumes. The product NGL left after the use of NGL as a process fuel is either added to the crude oil output to increase its market value or exported. The export of NGL incurs a GHG emissions credit. The user determines the proportion of each gas component that is condensed in the demethanizer in the 'Surface Processing' worksheet. The default assumption is 50% ethane, 100% propane, and 100% butane.

The volume of lifting gas, if applicable, is subtracted from the volume of product gas stream to calculate the volume of gas remaining for use as a process fuel and/or re-injection into the reservoir for pressure maintenance. Any product gas left after supplying the process fuel requirements and gas re-injection is exported.

5.2 Steam generation for thermal oil recovery

5.2.1 Introduction to steam generation

Steam injection for thermal enhanced oil recovery (TEOR) is practiced globally, with significant operations in California, Alberta, Indonesia, and Venezuela [157]. Steam injection reduces the viscosity of heavy crude oils by multiple orders of magnitude, even with relatively small temperature increases [21, 67, 70, 158, 159]. This viscosity reduction results in improved flow characteristics and improved reservoir sweep [70]. Many fields that would not produce economic volumes of hydrocarbons without steam injection become large producers after steam injection.

5.2.2 Calculations for steam generation

Steam generation for thermal oil recovery is modeled using three technologies: steam generation via once-through steam generators (OTSG) (Figure 5.1), and steam and electricity co-production via gas turbine and heat recovery steam generator (HRSG) combination (5.3), and steam generation via solar thermal technology.

Steam Generation
1.1.6

5.2.2.1 Steam system properties

The quantity of steam required is given by the oil production rate and the steam oil ratio:

Steam Generation
2.1.1

$$Q_{ws} = SOR\rho_w Q_o \quad \left[\frac{\text{lbm water}}{\text{d}} \right] \quad (5.1)$$

Where Q_{ws} = steam required to be generated per day [lbm water/d]; SOR = steam oil ratio [bbl steam as cold water equivalent/bbl oil]; ρ_w = density of water [lbm/bbl]; and Q_o = quantity of oil produced [bbl/d]. Steam quantities are measured as volume of cold water equivalent.

The enthalpy of steam generated ($h_{ws} = h_{ws}(p_{ws}, T_{ws})$) at steam quality X_{ws} , steam pressure p_{ws} , saturated steam temperature T_{ws} is given by:

Steam Generation
2.1.11

$$h_{ws} = h_{ws,g}X_{ws} + h_{ws,f}(1 - X_{ws}) \quad \text{where} \quad h_{ws} = h_{ws}(p_{ws}, T_{ws}) \quad \left[\frac{\text{Btu}}{\text{lbm}} \right] \quad (5.2)$$

Steam temperature T_{ws} [°F] is tabulated for saturated steam as a function of saturation pressure p_{ws} [psia] (assuming that pressure is the controlled variable) [160]. Because we are using steam tables rather than direct computation, steam pressure is rounded before lookup. $h_{ws,g}$ = enthalpy of vapor phase water at p_{ws} [Btu/lbm] while $h_{ws,f}$ = enthalpy of saturated water at p_{ws} [Btu/lbm].

Input Data Table
5.3

Steam is generated at sufficient pressure to ensure that it will flow into the sub-surface (eliminating the need for wellhead compressors). Due to friction and thermal losses in piping and wellbore, the steam pressure drops before reaching the reservoir:

Steam Generation
1.2.8

$$p_{ws} = p_{res}\epsilon_p \quad [\text{psia}] \quad (5.3)$$

where ϵ_p = pressure loss factor which is ≥ 1 [psia generator/psia reservoir]. Chilingarian et al. [50, p. 228] note that 10-50% of the pressure in the steam at steam

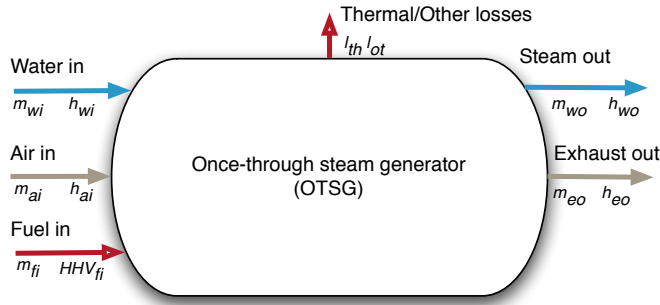


Figure 5.1: Once-through steam generator with mass and energy balance terms. Lower case terms are defined per lbmol of input fuel.

generator outlet can be lost by the time the steam reaches the reservoir. The default assumption is loss of 10% of steam pressure, so $\epsilon_p = 1.1$. In addition, DOE guidebooks on practical implementation of EOR suggest that chokes are used at the wellhead to control steam flow-rate, and that the choke upstream pressure is about 1.7 times the choke downstream pressure. Both of these losses are incorporated in computing steam generator outlet pressure.

Pressure is provided by reciprocating positive displacement pumps with 90% mechanical efficiency and 97% volumetric efficiency (compressibility and slip through seals). [161, Fig. 27]. Thus, overall pressure provision has a default efficiency of 87.3%.

Steam quality X_{ws} [lbm vapor/lbm steam] is governed by the needs of the project. Higher steam qualities impart more energy into the formation, but steam quality is limited by the steam generator configuration. OTSGs cannot generate 100% quality steam because of deposition of solids in boiler tubes. In practice, $\approx 20\%$ of water mass is left in fluid state to carry solutes ($X_{ws} \approx 0.8$) [162].

The enthalpy increase of water is given by the difference between water inlet enthalpy and exit enthalpy:

$$\Delta h_{ws} = h_{ws} - h_{w,in} \quad \left[\frac{\text{Btu}}{\text{lbm water}} \right] \quad (5.4)$$

Where $h_{w,in}$ is water inlet enthalpy [Btu/lbm] for compressed water enthalpy at inlet water pressure $p_{w,in}$ and inlet water temperature $T_{w,in}$ [160]. Inlet pressure is assumed equal to required steam outlet pressure (e.g., no pressure drop in boiler).

5.2.2.2 Once-through steam generator modeling (OTSG)

Once-through steam generators are modeled [21, 162], as shown in Figure 5.1. Fuel inputs include pipeline quality natural gas, produced gas, or produced crude oil. A binary choice is required for gaseous or liquid fuels. For gaseous fuels, a mixture of produced gas and purchased gas is allowed.

The operating conditions of combustion must be specified. These include the inlet air temperature $T_{a,in}$ [°F], the outlet exhaust temperature $T_{e,out}$ [°F] and the excess air in combustion $R_{a,comb}$ [mol O₂/ mol stoichiometric O₂].

Steam Generation

2.1.7

Steam Generation

2.1.12

Input Data Table

5.4

Steam Generation

2.2

Gaseous fuel combustion for steam generation The gas species tracked in the OTSG are described below in Section 8.4. For an arbitrary fuel makeup, the composition, average molar mass, and lower heating value (LHV) are calculated.

Steam Generation
2.2.3

OTSG inlet air composition, combustion stoichiometry, and excess air ratio are used to compute the mass of air required per lbmol of fuel consumed. For each reactive species, the reactants needed per mol of input fuel are computed:

Fuel
Specs
Table 2.3

$$N_i = \frac{x_{a,i}}{x_{a,O_2}} \left(x_{f,C} + \frac{x_{f,H}}{4} \right) \quad \left[\frac{\text{lbmol}}{\text{lbmol fuel}} \right] \quad (5.5)$$

where N_i = number of moles of air species i [mol]; $x_{a,i}$ = mole fraction of species i in air [mol/mol]; $x_{f,C}$ = mol of carbon per mol of fuel (e.g., 2 for C_2H_6) [mol/mol]; and $x_{f,H}$ = mol of hydrogen per mol of fuel [mol/mol]. The sum over all species i gives air required for stoichiometric combustion, which is multiplied by the excess air ratio $R_{a,comb}$ to get real air requirements:

Steam Generation
2.2.3

$$N_a = R_{a,comb} \sum_{i=1}^n N_i \quad \left[\frac{\text{lbmol air}}{\text{lbmol fuel}} \right] \quad (5.6)$$

Where $R_{a,comb}$ = ratio of combustion air to stoichiometric air [lbmol air / min lbmol air for combustion]. In this case there are n species present in air.

At constant pressure the change in enthalpy with temperature is given as:

$$\delta h = C_p \delta T \quad \left[\frac{\text{Btu}}{\text{lbmol}} \right] \quad (5.7)$$

Specific heat capacity C_p as a function of T can be defined for gas species i as [163, Table A-2E]:

$$C_{p,i} = a_i + b_i T + c_i T^2 + d_i T^3 \quad \left[\frac{\text{Btu}}{\text{bmol} \cdot ^\circ\text{R}} \right] \quad (5.8)$$

Which can be integrated between outlet and inlet temperatures

$$h_i = \int_{T_{ref}=300}^T C_{p,i} dT = a_i T + \frac{b_i}{2} T^2 + \frac{c_i}{3} T^3 + \frac{d_i}{4} T^4 + e_i \quad \left[\frac{\text{Btu}}{\text{lbmol}} \right] \quad (5.9)$$

where e_i is a constant of integration. OPGEE sets $h = 0$ at $T_{ref} = 300$ K to solve for e_i . Terms a through d are given in OPGEE for N_2 , O_2 , CO_2 , SO_2 , air, $H_2O_{(v)}$ and fuel inputs (approximated as CH_4) [163].

Steam Generation
2.2.4
Input Data
Table 4.1 - 4.6

For example, inlet air enthalpy is computed using the inlet air temperature:

$$h_{a,in} = \sum_{i=1}^n \left(a_i T_{a,in} + \frac{b_i}{2} T_{a,in}^2 + \frac{c_i}{3} T_{a,in}^3 + \frac{d_i}{4} T_{a,in}^4 + e_i \right) \quad \left[\frac{\text{Btu}}{\text{lbmol air}} \right] \quad (5.10)$$

where again we have $i \in 1 \dots n$ components in air.

The outlet lbmol of all gases per lbmol of fuel consumed are computed assuming complete combustion (e.g., no unburned hydrocarbons, no CO produced), and no reactions with nitrogen.

Steam Generation
2.2.3

The enthalpy of OTSG outlet exhaust $h_{e,out}$ is computed with eq. (5.10), using user input OTSG exhaust outlet temperature $T_{e,out}$. In practice, efficient steam generation is achieved by reducing $T_{e,out}$ to as low as practicable, thus removing as

Steam Generation
2.5.1.4

much heat as possible from OTSG combustion products. $T_{e,out}$ has a lower limit due to the need to avoid condensing corrosive flue gas moisture onto heat transfer tubes [162].

A wide range of exhaust gas temperatures is cited. Buchanan et al. cite ideal (minimum) exhaust gas temperatures of 266 °F [130 °C] or higher [164, p. 78]. Other sources cite temperatures of 350 °F [159, p. 36], 400 °F [50, p. 227] and even greater than 550 °F for older Russian units [158, p. 181]

In some cases, the exhaust gas temperature is limited by the approach to the inlet water temperature. In SAGD operations hot produced water is used as inlet water, and $T_{e,out}$ comes to within 15 °C of the inlet water temperature. An air pre-heater would allow utilization of this excess energy if hot produced fluids are used for water source [164].

In addition to losses from flue gas exhaust, other losses occur in an OTSG. We lump all thermal losses into a thermal shell loss term. For simplicity, it is assumed that 4% of fuel enthalpy is lost as thermal shell loss ϵ_{th} [Btu/lbmol fuel consumed]. Other losses (start up inefficiencies, fouling, etc.) ϵ_{ot} are assumed $\approx 1\%$ of the fuel LHV [Btu/lbmol fuel consumed]. These total losses are supported by references, which cite losses of approximately 4% [162].

The enthalpy available for transfer to the incoming water is given by the difference between incoming enthalpy sources (incoming combustion air, fuel inputs) and outgoing enthalpy sources (hot exhaust, shell losses, other losses):

$$\Delta h_{comb} = LHV + h_{a,in} - h_{e,out} - \epsilon_{th} - \epsilon_{ot} \quad \left[\frac{\text{Btu to water}}{\text{lbmol fuel}} \right] \quad (5.11)$$

The efficiency of steam generation η_{OTSG} (LHV basis) can be computed by comparing the enthalpy imparted on steam to the higher heating value of the fuel inputs:

$$\eta_{OTSG} = \frac{\Delta h_{comb}}{LHV} \quad \left[\frac{\text{Btu to steam}}{\text{Btu fuel}} \right] \quad (5.12)$$

Using the enthalpy provided to steam and Δh_{comb} , the total fuel consumption rate required per day can be computed.

$$m_f = \frac{Q_{ws} \Delta h_{ws}}{\Delta h_{comb}} \quad \left[\frac{\text{lbmol fuel}}{\text{d}} \right] \quad (5.13)$$

Liquid fuels for steam generation Liquid fuels can be used for steam generation. In general, these are produced heavy crude oils that are consumed on site for steam generation. This was common practice in California TEOR developments until the 1980s, when air quality impacts stopped the practice.

Because liquid fuels do not have consistent molar compositions, computations generate lbm of fuel consumed. The heating value of crude oil as a function of API gravity is tabulated [90]. The bulk chemical composition of crude oil is calculated [90, p. 41]. The mass fraction hydrogen w_H as a function of crude specific gravity sg is given as:

$$w_H = a_H - 15\gamma_o \quad [\text{mass frac. H}] \quad (5.14)$$

Where a_H is a constant that varies with crude API gravity (and therefore specific gravity) as show in Table 5.1.

Steam Generation
2.2.7.2

Steam Generation
2.6.3

Steam Generation
2.2.7.4

Steam Generation
2.2.8.1

Fuel Specs
Table 1.1

Fuel Specs
Table 1.2

Table 5.1: Hydrogen constant a_H as a function of API gravity.

| API gravity | a_H |
|-------------|-------|
| 0 - 9 | 24.50 |
| 10 - 20 | 25.00 |
| 21 - 30 | 25.20 |
| 31 - 45 | 25.45 |

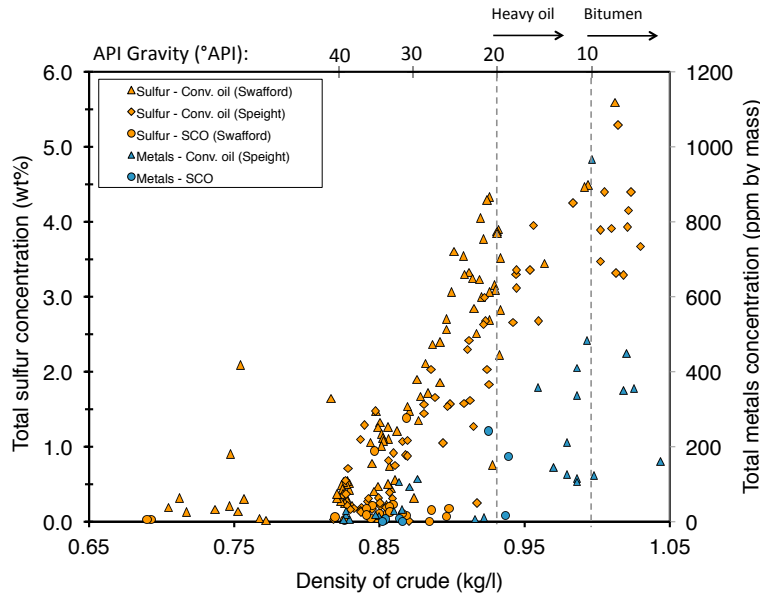


Figure 5.2: Increase of crude contaminant load with increase in crude specific gravity (decrease in API gravity). Data from: Speight (1994) and Swafford (2009).

The mass fraction of sulfur and other contaminants decreases with increasing API gravity, as seen in Figure 5.2 [165, Ch. 8, tables 3, 4] [165, Ch. 7, tables 2, 3, and 19] [166]. We therefore include default values of w_S that vary with API gravity from 5 wt.% (API gravity 4-5) to 0.5 wt.% (API gravity greater than 35). Nitrogen and oxygen content $w_N + w_O$ is assumed constant at 0.2 wt.% and in element balance it is assumed to be entirely made up of N. Mass fraction carbon w_C is calculated by difference using above mass fractions. Using the relative molar proportions of C, H, S, and N, the stoichiometric oxygen demand per carbon atom is computed assuming complete combustion.

Using the oxygen requirement for combustion and the excess air ratio $R_{a,comb}$, the lbmol of air required is computed similarly to eq. (5.6) above. The inlet air enthalpy for combustion is computed using eq. (5.10) above. The outlet exhaust composition is computed via element balance assuming complete oxidation (including S to SO_2). The outlet exhaust enthalpy is computed as in eq. (5.10) for gaseous fuels combustion. The energy balance for combustion of liquid fuels is computed as in eq. (5.11).

Forced air blower in OTSG Combustion air is forced through the OTSG unit with a blower. The power rating of the default OTSG blower is taken from COSIA

Fuel Specs
Table 1.2

Steam Generation
2.2.3

Steam Generation
2.2.8.3

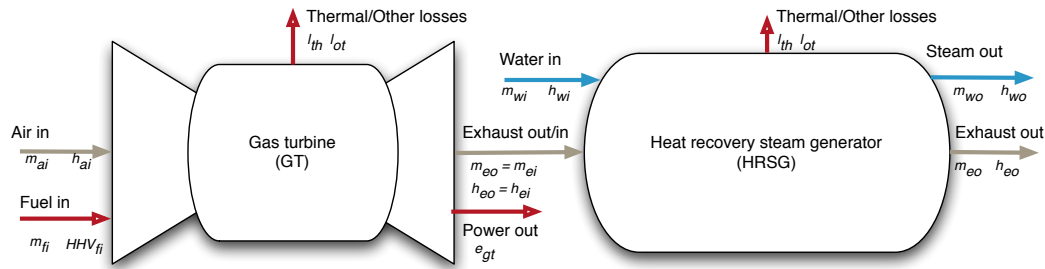


Figure 5.3: Gas turbine plus heat recovery steam generator model. Mass flows represented by m and energy flows represented by fuel lower heating value (LHV), electric power out (e) and enthalpy of gases (h).

documents outlining energy consumption and mass balances of a moderate-sized Steam-Assisted Gravity Drainage (SAGD) facility. The COSIA OTSG has a combustion duty rating of 1488 mmBtu/h and an air blower power consumption rate of 3.7 MW. This results in a consumption intensity of 0.139 bhp per mmBtu/d of OTSG consumption capacity.

High and medium pressure boiler feedwater pump The OTSG boiler must generate steam at pressures high enough to overcome frictional loss in the surface and subsurface piping as well as to allow flow into the reservoir. The required pressure is supplied to the recycled produced water and makeup water depending on the mass fraction of each water stream. This pressure is assumed supplied by an electrically-driven pump of large capacity. For fields with low producing pressure, this consumption term is small.

5.2.2.3 Gas turbine with heat recovery steam generator

Cogeneration is used to co-produce electricity and steam for thermal oil recovery. These systems combine a gas turbine (GT) with a heat recovery steam generator (HRSG) to produce steam from the exhaust gas of the gas turbine (see Figure 5.3). OPGEE allows the usage of supplemental gas firing in the post-turbine exhaust stream, sometimes called “duct firing”, to allow for increased steam generation per unit of power output.

Steam Generation
2.3

Gas turbine modeling The chemical kinetics software tool Cantera [167] is used with MATLAB to compute the efficiency, losses, and turbine exit temperature for four hypothetical gas turbines labeled A, B, C, and D. The general method is as follows:

- Fuel and air compositions are specified in OPGEE for purchased natural gas (95% CH₄, 3% C₂H₆, 1.5% C₃H₈, and 0.5% inert) and air (dry air with 2% moisture).
- The LHV of the fuel is computed assuming complete combustion.
- Using the excess air fraction for a given turbine, the amount of O₂ (and therefore air) required relative to stoichiometric air requirements is used to compute relative air and fuel inputs into a mixture. The masses of fuel inputs $m_{f,in}$ and air inputs $m_{a,in}$ are normalized to a 1 kg mixture, as is default in Cantera.

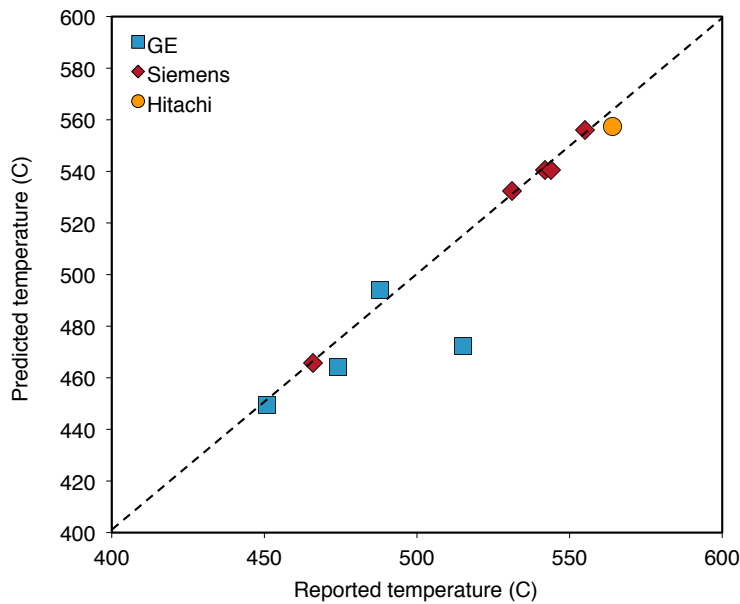


Figure 5.4: Predicted turbine exit temperatures for variety of turbines from literature (*y-axis*) as compared to reported value from the literature (*x-axis*).

- The fuel and air mixture is equilibrated using the assumption of adiabatic combustion.
- The enthalpy of products of adiabatic combustion is recorded as h_e , or the mass-specific exhaust enthalpy after combustion.
- The enthalpy of products of combustion is computed when returned to initial conditions (300 K, 101.325 kPa) to compute the reference enthalpy $h_{e,atm}$.
- The difference between the enthalpy of hot combustion products and the reference enthalpy of completely cool exhaust is partitioned into losses (pressure and temperature losses due to real machine imperfections), work provided by turbine (W_{GT}), and enthalpy of hot exhaust ($h_{e,out}$).
- The resulting temperature of hot exhaust gases is computed.

The gas turbine model was tested against reported gas turbine data. Data for turbine heat rate, power output, turbine exhaust mass flow rate, and turbine exhaust temperature were collected for commercial turbines from Siemens, GE, and Hitachi [168–170]. The code assumes consistent 4% thermal and other losses ($\epsilon_{th} + \epsilon_{ot}$) for each turbine. Results show excellent agreement between predicted turbine exhaust temperature and manufacturer-reported turbine exhaust temperatures (Figure 5.4).

The GT model is used to model four hypothetical turbines A - D, using characteristics similar to those specified by Kim [171]. The results from our code are used to generate required inputs for turbines A-D including turbine exhaust temperature [F], turbine efficiency [Btu e- per Btu LHV fuel input], turbine specific power

Input data
Table 3.1

Table 5.2: Gas turbine model results for hypothetical turbines A-D. These results serve as input data to OPGEE GT model.

| Parameter | Unit | Turb. A | Turb. B | Turb. C | Turb. D |
|------------------------|---|---------|---------|---------|---------|
| Turbine exhaust temp. | [°F] | 932.0 | 947.9 | 950.0 | 1074.1 |
| Turbine efficiency | $\left[\frac{\text{Btu e-}}{\text{Btu LHV}} \right]$ | 0.205 | 0.237 | 0.280 | 0.324 |
| Turbine specific power | $\left[\frac{\text{Btu e-}}{\text{lb exhaust}} \right]$ | 69.5 | 85.4 | 108.0 | 155.7 |
| Turbine excess air | $\left[\frac{\text{Mol O}_2 \text{ real}}{\text{Mol O}_2 \text{ stoich.}} \right]$ | 4.00 | 3.75 | 3.50 | 2.80 |
| Turbine loss | $\left[\frac{\text{Btu loss}}{\text{Btu LHV}} \right]$ | 0.041 | 0.036 | 0.032 | 0.027 |

[Btu e-/lb exhaust], turbine excess air [lbmol O₂ / lbmol stoichiometric O₂], and turbine loss factor [Btu/Btu LHV fuel input]. These results are shown in Table 5.2.

Using turbine efficiency and turbine loss from Table 5.2, energy balances for each turbine are computed. Using turbine excess air ratios from Table 5.2, total air requirements per lbmol of fuel input to gas turbine are computed. Inlet air enthalpy is computed as shown in eq. (5.10). Moles of combustion products are computed via stoichiometric relationships. Using turbine exhaust temperature, turbine exhaust composition, and relationships from eq. (5.10), the enthalpy of gas turbine exhaust is computed.

The enthalpy of the gas turbine exhaust is the useful energy input to the HRSG. Steam production via the HRSG is modeled analogously to that of the OTSG.

Forced air blower in HRSG It is assumed that no forced air blower is required in an HRSG due to the high exit velocities of turbine exhaust.

Duct firing Duct firing increases the amount of steam generated from the gas turbine exhaust stream by heating the exhaust stream through supplemental combustion in the inlet of the HRSG. Because GTs operate with large amounts of excess air (air input = 2-3 times stoichiometric requirement), large amounts of residual oxygen remain the GT exhaust.

Duct firing is turned on at the top of the steam generation sheet.. If duct firing is selected, the GT exhaust temperature remains as selected from input data, but the effective HRSG inlet temperature is assumed to increase to 1300 °F [172, Table 5, Case 2]. The computed additional fuel required to duct fire to the desired temperature is computed using the composition of HRSG inlet gas to compute the effective heat capacity of the gas, which gives an approximate additional fuel needed to raise temperature (thus avoiding an iterative calculation). If very different conditions are selected (e.g., turbine or post-duct firing temperature), this approximate fuel consumption factor should be adjusted by the user.

Duct firing increases the efficiency of the HRSG, but this efficiency gain is somewhat offset by the loss of exported electricity per unit of steam generated. This reduces the co-production credit received by the cogeneration system and negates some of the potential GHG intensity reductions associated with duct firing.

5.2.2.4 Solar thermal steam generation

Solar thermal steam generation is modeled to allow for partial displacement of natural gas in steam generation thermal needs. The fraction of steam generated using solar thermal is provided by the user on the 'Inputs' sheet. That fraction of

Steam Generation

2.3.1

Steam Generation

2.3.5

Steam Generation

3.3.5.1

Steam Generation

2.3.5

Steam Generation

1.2.7.2.3

Steam Generation

2.3.8.4

Steam Generation

2.4

Inputs 1.4.13

steam is then provided by the solar thermal system at no cost of natural gas. Solar thermal pumping work for solar HTF circulation is calculated assuming that HTF pumping scales similarly to air blower work for OTSG steam generation (personal communication, John O'Donnell GlassPoint energy).

Steam Generation

Reasonable fractions of energy displaced by solar thermal are around 15-25% in the absence of thermal storage or modification of steam injection schedule [173–175]. If steam injection schedule is modified to only inject steam during daytime solar hours, then the fraction of steam generated with solar thermal can approach complete NG displacement.

2.4.2.2

5.2.3 Defaults for steam injection

5.2.3.1 General default parameters

Parameters and variables in the steam injection model are listed below in Table 5.3.

Table 5.3: Default inputs for steam injection calculations.

| Param. | Description | Eq. no. | Default | Lit. range | Unit | Sources | Notes |
|---------------------|--|---------|-----------|--------------|---------------------------------|------------|-------|
| a_H | Crude hydrogen fraction constant | - | Table 5.1 | - | [lbm H / lbm crude oil] | [90] | |
| $a_i \dots e_i$ | Species-specific heat capacity constants | - | var. | - | [various] | [163] | |
| C_p | Heat capacity at constant pressure | (5.8) | - | - | [Btu/lbmol-°R] | | |
| η_{OTSG} | OTSG efficiency | (5.12) | - | - | [Btu steam / Btu LHV fuel] | | |
| ϵ_{th} | Thermal losses from OTSG | - | 0.04 | - | [Btu/BtuL fuel] | [162] | |
| $\epsilon_{oil,ng}$ | Other losses from OTSG fueled with natural gas | - | 5000 | - | [Btu/lbmol fuel] | [162] | c |
| $\epsilon_{oil,co}$ | Other losses from OTSG fueled with crude oil | - | 250 | - | [Btu/lbm fuel] | [162] | c |
| ϵ_{us} | Steam pressure loss factor | - | 1.25 | 0.1 - 0.5 | [frac.] | [50] | d |
| λ_{ng} | Fraction natural gas | - | 1 | 0 - 1 | [frac] | - | b |
| λ_{pg} | Fraction processed associated gas | - | 0 | 0 - 1 | [frac] | - | b |
| $h_{a,in}$ | Inlet air enthalpy | (5.10) | - | - | [Btu/lbmol] | | |
| $h_{e,out}$ | Enthalpy of OTSG exhaust | (5.10) | - | - | [Btu/lbmol] | | |
| $h_{us,f}$ | Enthalpy of liquid phase water in steam | - | var. | 180 - 730 | [Btu/lbm] | | |
| $h_{us,g}$ | Enthalpy of vapor phase water in steam | - | var. | 1090 - 1205 | [Btu/lbm] | | |
| h_{us} | Enthalpy of injected steam (< 100% quality) | (5.2) | - | - | [Btu/lbm] | | |
| $h_{w,in}$ | Inlet water enthalpy | - | 9.8 | - | [Btu/lbm] | | |
| Δh_{us} | Change in water enthalpy upon boiling | (5.4) | - | - | [Btu/lbm] | | |
| Δh_{comb} | Heat available from combustion to water | (5.11) | - | - | [Btu / lbmol fuel] | | |
| h_i | Enthalpy of species i | (5.9) | - | - | [Btu / lbmol] | | |
| LHV | Lower heating value of fuel | - | var. | - | [Btu LHV / lbmol fuel] | | |
| N_i | Number of moles of air species i | (5.5) | - | - | [lbmol] | | |
| N_a | Number of moles of air for real combustion | (5.6) | - | - | [lbmol] | | |
| $p_{w,in}$ | Inlet water pressure | - | $= p_s$ | - | [psia] | | |
| p_{us} | Steam pressure | (5.3) | - | - | [psia] | | |
| Q_o | Quantity of oil produced | - | 1000 | - | [bbl oil / d] | | |
| Q_{us} | Steam required | (5.1) | - | - | [lbm water / d] | | |
| $R_{a,comb}$ | Excess air combustion ratio | - | 1.2 | 1.075 - 1.25 | [lbmol air / lbmol air stoich.] | - | e |
| ρ_w | Density of water | - | 350.4 | - | [lbm / ft ³] | [156] | f |
| γ_o | Crude specific gravity | (4.17) | - | - | [-] | | |
| SOR | Ratio of steam injected to oil produced | - | 3.0 | 2.5 - 6 | [bbl water / bbl oil] | | g |
| $T_{a,in}$ | Inlet air temperature | - | 540 | 500 - 560 | [°R] | [130, 176] | h |

Continued on next page...

Continued from previous page

| Param. | Description | Eq. no. | Default | Lit. range | Unit | Sources | Notes |
|-------------|---------------------------------------|---------|---------|------------|----------------------|-----------|-------|
| $T_{e,out}$ | Temperature of OTSG exhaust | - | 810 | 725 - 910 | [°R] | [various] | i |
| $T_{w,in}$ | Inlet water temperature | - | 40 | - | [°F] | | j |
| T_{ws} | Steam temperature | - | var. | - | [°F] | | |
| w_H | Mass fraction hydrogen in crude | (5.14) | - | - | [lbm H / lbm oil] | | |
| $x_{a,i}$ | Mole fraction of species i in air | - | var. | - | [lbmol/lbmol] | | m |
| x_C | Moles of carbon per mole of fuel | - | var. | - | [lbmol/lbmol] | | a |
| x_H | Moles of hydrogen per mole of fuel | - | var. | - | [lbmol/lbmol] | | a |
| X_s | Steam quality | - | 0.8 | - | [lbm vap./lbm steam] | [70] | k |
| y_{ng} | Binary variable: gaseous fuel in OTSG | - | 1 | 0 or 1 | [y/n] | - | l |
| y_{co} | Binary variable: crude oil in OTSG | - | 0 | 0 or 1 | [y/n] | - | l |

a - See 'Fuel specs' Table 2.3 for combustion factors for gas inputs.
b - Assumption: Gas is purchased due to typical low GORs for heavy crudes.
c - Assumption to account for incomplete combustion, fouling, warm up and cool-down, and other real-world inefficiencies.
d - Piping friction losses can represent 10-50% of the steam pressure developed at the outlet of the steam generator." [50, p. 228]
e - Conservative assumption for input excess air. Can be lower with special combustion equipment.
f - Fresh water input
g - Common SOR for efficient TEOR project. Range is quite variable, especially in early years of steam injection.
h - Equal to 300 K. Chosen for ease of gas turbine modeling.
i - Equal to 350 °F. Reported range is wide in literature. See [50, 158, 159, 164].
j - Assumption for cool water inlet.
k - Most commonly cited steam quality. Other qualities cited include 75%.
l - Assumption: Most steam generation in California and Alberta is natural gas fired.
m - See 'Input Data' Table 2.4 for air composition.

Table 5.4: Indicators of SOR distributions for California and Alberta thermal EOR production. Units are bbl of cold water equivalent (CWE) per bbl of oil.

| | Mean - SOR_t | Mean - SOR_i |
|-------------------|----------------|----------------|
| California - 2009 | 3.32 | 4.29 |
| California - 2010 | 3.41 | Unk. |
| Alberta - 2009 | 3.58 | NA |
| Alberta - 2010 | 3.32 | NA |

5.2.3.2 Default for steam-oil-ratio (SOR)

Because the SOR is a key parameter driving GHG emissions from thermal oil production operations, we examine default values for SOR in more detail.

SOR data are collected for California and Alberta thermal oil recovery operations for 2010 and 2011 [130, 136, 176–178].

For California operations, incremental SOR is calculated for 2009 using volumes of steam injected and reported incremental production due to steam injection. ‘Total’ SOR is also calculated for 2009 using total production by field and total steam injection. For 2010, only monthly data are available, so incremental production data are not available. Therefore, only total SOR is reported.

For Alberta operations, data on bitumen produced and steam injected were collected for 24 thermal recovery projects (SAGD and CSS). No data were available on incremental rather than total production, and it is not clear what incremental production figures would represent bitumen operations where non-enhanced production would be very small.

Production volumes are binned by SOR for both regions and reported in Figure 5.5. Averages for SOR are presented in Table 5.4. The default SOR in OPGEE v2.0b is a conservative 3.0 bbl CWE per bbl oil.

5.2.3.3 Defaults for SAGD operations

Default data for Canadian SAGD operations are taken from a variety of public sources. The overall approach to collecting data inputs for OPGEE is use the COSIA template (Base case, warm lime softening- OTSG) [155] wherever possible to provide default input data to OPGEE to estimate emissions for SAGD operations [155]. When the template does provide the required data, we supplement that data with AER company reported data including statistical reports [115] and in situ performance presentations [179] and expert feedback when no public data is available.

Production method SAGD and CSS projects use gas lift or mechanical lift (downhole pump) and steam flooding for oil production. In mechanical lift, electric submersible pump (ESP), progressive cavity pump (PCP) and rod pump are used. OPGEE calculations can be modified based on the characteristics of these pump types. In the COSIA SAGD reference facility, mechanical lift via ESP, with downhole pressure of 2.2 MPa, is used [155].

Gas handling properties: GOR, flaring, and venting These gas volume parameters are reported as a dimensionless value in AER statistical reports [115]. We assume that the value is in m^3 gas per m^3 bitumen, and convert to the desired unit (scf/bbl

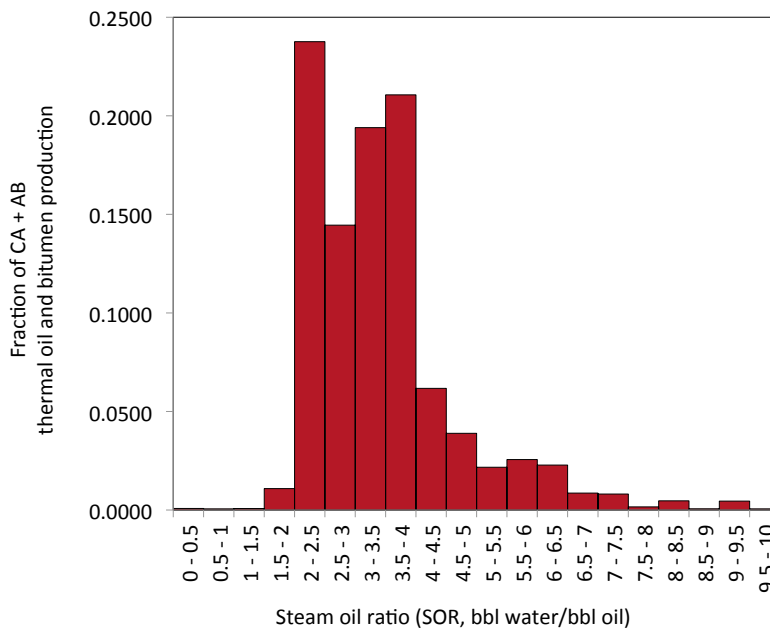


Figure 5.5: Distribution of SOR values for California and Alberta thermal EOR projects (steamflood, cyclic steam stimulation, steam-assisted gravity drainage).

bitumen). The resulting values for all three gas volumes are much lower than conventional defaults, which is expected due to small quantities of associated gas in bitumen deposits.

Field properties: productivity index, pressure, depth The difference between reservoir pressure and the injection downhole pressure is reported around 350 kPa for the Firebag project [179]. Using this value and other Firebag project data, productivity index (PI) is calculated around 22 bbl/(psi-d). This default is reasonable for SAGD projects in general due to the fact that at SAGD conditions, even large changes in PI do not affect the results significantly. The default high pressure steam system operates at 1400 psia [155]. Field depth of in situ extraction in current SAGD operations is 1300-2000 ft [155].

Steam generation technology Default steam generation technology from the COSIA template is a once-through-steam generator fired with (primarily) purchased gas. The OTSG requires forced air blowers and boiler feedwater pumps to increase pressure of both produced water and makeup water. The water is treated before boiling in a warm lime softener/evaporator.

5.3 Upgrading

The 'Upgrading' supplemental worksheet contains tabulated data on upgrading operations that are used in the 'Surface Processing' worksheet to compute the energy use and emissions from crude hydrocarbon upgrading. The values of energy consumption for upgrading are estimated using the Oil Sands Technology Upgrading

Model (OSTUM) produced by the University of Toronto and University of Calgary [145].

The OSTUM model is run for three different upgrading configurations. These three refinery configurations include:

- Delayed coking
- Hydroconversion
- Hydroconversion and fluid coking

These three refinery configurations resemble real-world refinery configurations used at the Suncor, Scotford, and Syncrude upgraders respectively.

In each upgrading configuration, a bitumen blend modeled as the Borealis Heavy Blend (BHB) is modeled as the input hydrocarbon feedstock. In each upgrading configuration, a light-sweet synthetic crude oil is produced, with characteristics similar to the premium SCO product produced by real-world upgraders. The properties of the output SCO blends are as follows:

- Delayed coking: Sweet SCO with API gravity = 33.2 °API, S = 0.18 wt%, and N = 692.3 ppm by mass. This SCO is similar to Suncor Synthetic A.
- Hydroconversion: Sweet SCO with API gravity = 31.1 °API, S = 0.03 wt%, and N = 77.6 ppm by mass. This SCO is similar to Premium Albion Synthetic.
- Hydroconversion and fluid coking: Sweet SCO with API gravity = 31.1 °API, S = 0.11 wt%, and N = 623.2 ppm by mass. This SCO is similar to Syncrude Sweet Premium.

The assumed heating value of process gas in OSTUM is nearly identical to the heating value of natural gas assumed by default in OPGEE (982 Btu/ft³ LHV).

The resulting intensities in OSTUM are given below in Table 5.5

Table 5.5: Inputs to OPGEE upgrading module from the Oil Sands Technology Upgrading Model (OSTUM)

| | Delayed coking | Hydroconversion | Hydroconversion and fluid coking | Units |
|--|----------------|-----------------|----------------------------------|-------------------------------------|
| Process gas (PG) yield per bbl SCO output | 501 | 341 | 650 | [scf/bbl SCO] |
| - Fraction PG to self use | 0.650 | 0.800 | 0.943 | [0-1] |
| - Fraction PG exported | 0.300 | 0.190 | 0.032 | [0-1] |
| - Fraction PG flared | 0.050 | 0.01 | 0.025 | [0-1] |
| Coke yield per bbl SCO output | 43 | 0 | 30 | [kg/bbl SCO] |
| - Fraction coke to self use | 0.106 | 0.000 | 0.207 | [0-1] |
| - Fraction coke exported | 0.000 | 0.000 | 0.000 | [0-1] |
| - Fraction coke stockpiled | 0.894 | 1.000 | 0.793 | [0-1] |
| Electricity intensity | 5.451 | 17.25 | 19.98 | [kWh/bbl SCO] |
| - Fraction electricity self generated w/ cogen | - | - | - | [0-1] |
| Hydrogen (H2) intensity | 845 | 1644 | 1283 | [scf H2/bbl SCO] |
| - H2 generation efficiency | 0.7 | 0.7 | 0.7 | [LHV H2/LHV NG] |
| - NG requirements for H2 | 323.6 | 629.6 | 491.2 | [scf NG/bbl SCO] |
| Cogen turbine efficiency | 0.31 | 0.31 | 0.31 | [Btu e- per Btu NG LHV] |
| Cogeneration steam efficiency | 0.40 | 0.40 | 0.40 | [Btu steam enthalpy per Btu NG LHV] |
| Steam requirements of upgrading | 113.8 | 247.1 | 240.8 | [mBtu steam enthalpy/bbl SCO] |
| Steam boiler efficiency | 0.8 | 0.8 | 0.8 | [Btu steam enthalpy/Btu NG LHV] |
| SCO/bitumen ratio | 0.834 | 1.02 | 0.865 | [bbl SCO/bbl bitumen] |

5.4 Electricity

The ‘*Electricity*’ supplemental worksheet calculates the energy consumption of on-site electricity generation. The ‘*Electricity*’ worksheet does not include electricity co-generation in steam generation system. Available generation technologies include natural gas generator set, natural gas turbine, and diesel generator set. The user enters the capacity of onsite electricity generation as a fraction of the electricity required. The fraction of electricity above 1.0 is exported. In the ‘*Electricity*’ worksheet the amount of electricity generated onsite is calculated as:

$$E_{el,gen} = f_{el} \cdot E_{el,req} \quad \left[\frac{\text{MMBtu}}{\text{d}} \right] \quad (5.15)$$

where $E_{el,gen}$ = onsite electricity generation [MMBtu/d]; f_{el} = fraction of required electricity generated onsite; and $E_{el,req}$ = electricity required. The electricity required is calculated in the ‘*Energy Consumption*’ worksheet.

The energy consumption of the generator is calculated from the appropriate driver in the ‘*Drivers*’ worksheet as:

$$e_{GS} = \frac{e_D}{0.75\eta_G} \quad \left[\frac{\text{Btu}}{\text{kWh}} \right] = \frac{\left[\frac{\text{Btu}}{\text{bhp-hr}} \right]}{\left[\frac{\text{bkW}}{\text{bhp}} \right] [-]} \quad (5.16)$$

where e_{GS} = energy consumption of generator set [Btu/kWh]; η_G = efficiency of the electricity generator (not including driver) [-]; and e_D = driver energy consumption [Btu/bhp-hr]. The appropriate driver is determined by the required size based on the electricity generation capacity as calculated in eq. (5.15).

Once the onsite electricity generation, $E_{el,gen}$, and the energy consumption of the electricity generator, e_{GS} , are calculated the total energy consumption of onsite electricity generation is calculated as:

$$E_{EG} = E_{el,gen} \cdot 0.000293 \cdot e_{GS} \quad \left[\frac{\text{MMBtu}}{\text{d}} \right] = \left[\frac{\text{MMBtu}}{\text{d}} \right] \left[\frac{\text{kWh}}{\text{Btu}} \right] \left[\frac{\text{Btu}}{\text{kWh}} \right] \quad (5.17)$$

where E_{EG} = energy consumption of onsite electricity generation [MMBtu/d].

In addition to calculating the energy consumption of onsite electricity generation, this worksheet determines the grid electricity mix and the allocation method of credits from electricity export (see Section 5.6 on the ‘*Fuel Cycle*’ worksheet). The user is allowed to choose between two allocation methods for credit from electricity export: (i) allocation by substitution of grid electricity, and (ii) allocation by substitution of natural-gas-based electricity. The default allocation method is the substitution of natural-gas-based electricity. This method prevents achieving unreasonably large credits from operations with significant power generation.

Table 5.6: Types and size ranges of the drivers embedded in OPGEE.

| Type | Fuel | Size range [bhp] |
|----------------------------|-------------|------------------|
| Internal combustion engine | Natural gas | 95 - 2,744 |
| Internal combustion engine | Diesel | 1590 - 20,500 |
| Simple turbine | Natural gas | 384 - 2,792 |
| Motor | Electricity | 1.47 - 804 |

5.5 Drivers

Drivers (also known as prime movers) of pumps, compressors, and onsite electricity generators come in different types and sizes. Drivers in OPGEE include natural gas driven engines, natural gas turbines, diesel engines, and electric motors. The size and energy consumption of the driver is required to convert power requirements (e.g., downhole pump brake horsepower) into energy consumption as explained in Section 4.3.2.13. A database of drivers specifications of different types and sizes is included in OPGEE. Table 5.6 shows the types and size ranges of the drivers included in OPGEE.

Specifications of natural-gas-driven engines and diesel-driven engines are taken from Caterpillar technical worksheets [113]. Specifications of natural gas turbines are taken from Caterpillar-subsidiary Solar Turbines technical worksheets [180]. Specifications of electric motors are taken from General Electric technical worksheets [114]. Data were reported in original sources in different forms and with different levels of completeness.

The data for each driver model was converted into [bhp] for power and [Btu/bhp-hr] for energy consumption. In some cases the data on engine power was given in [bhp] and energy consumption is given in [Btu/bhp-hr], so no conversion is required. In other cases only data on the electricity generator set is given. The generator set includes an engine and an electricity generator. The brake horsepower of the engine is calculated from the electric power of the generator set as:

$$P_D = \frac{P_{GS}}{\eta_G} \cdot 1.34 \quad [\text{bhp}] = \frac{[\text{ekW}]}{[-]} \left[\frac{\text{bhp}}{\text{bKW}} \right] \quad (5.18)$$

where P_D = driver brake horsepower [bhp]; P_{GS} = electric power of the electricity generator set [ekW]; and η_G = efficiency of the electricity generator (not including engine) [-]. For the calculation of the electric power [ekW] of the electricity generator sets Caterpillar assume an electricity generator (without engine) of efficiency 96% [181, p. 4]. Accordingly η_G in eq. (5.18) is equal to 0.96 [-].

In the case where the overall efficiency of the electricity generator set is given, but the energy consumption of the engine component is not, the latter is calculated as:

$$e_D = \frac{3.6}{\eta_{GS}} \eta_G \quad \left[\frac{\text{MJ}}{\text{bKW-hr}} \right] = \frac{\left[\frac{\text{MJ}}{\text{bKW-hr}} \right]}{[-]} [-] \quad (5.19)$$

$$e_D = \frac{e_D \cdot 947.8}{1.34} \quad \left[\frac{\text{Btu}}{\text{bhp-hr}} \right] = \frac{\left[\frac{\text{MJ}}{\text{bKW-hr}} \right] \left[\frac{\text{Btu}}{\text{MJ}} \right]}{\left[\frac{\text{bhp}}{\text{bKW}} \right]}$$

where e_D = driver energy consumption [Btu/bhp-hr]; η_{GS} = efficiency of generator set (engine + generator) [-]; η_G = efficiency of generator (without engine) [-].

The diesel engines energy consumption is reported in the technical worksheets in the form of gallons per hour [gal/hr]. This is converted into [Btu/bhp-hr] by:

$$e_D = \frac{e_D \cdot 137,380}{P_D} \left[\frac{\text{Btu}}{\text{bhp-hr}} \right] = \frac{\left[\frac{\text{gal}}{\text{hr}} \right] \left[\frac{\text{Btu}}{\text{gal}} \right]}{[\text{bhp}]} \quad (5.20)$$

where e_D = driver energy consumption [Btu/bhp-hr]; P_D = driver brake horsepower [bhp]. The driver brake horsepower, P_D , is calculated from the electric power [kW] of the given generator set as shown in eq. (5.18).

The calculation used to convert the efficiency of electric motors from the General Motors technical worksheets into energy consumption in [Btu/bhp-hr] is very similar to the calculation of the energy consumption of the engine component from the overall efficiency of the generator set in eq. (5.19):

$$e_D = \frac{3.6}{\eta_M} \left[\frac{\text{MJ}}{\text{kWh}} \right] = \frac{\left[\frac{\text{MJ}}{\text{kWh}} \right]}{[-]} \quad (5.21)$$

where e_D = driver energy consumption [Btu/bhp-hr]; η_M = electric motor efficiency [-]. The energy consumption is converted to [Btu/bhp-hr] as shown in eq. (5.19).

OPGEE retrieves the energy consumption of the appropriate driver based on the user input and the required size.

Table 5.7: Default inputs for drivers calculations.

| Param. | Description | Eq. no. | Default | Literature range | Unit | Sources | Notes |
|-------------|---|---------|---------|------------------|--------------|-------------|-------|
| e_D | Driver energy consumption | (5.19) | - | - | [Btu/bhp-hr] | | a |
| η_M | Electric motor efficiency | - | var. | 0.84-0.96 | [-] | [114] | b |
| η_{GS} | Efficiency of electricity generator set | - | var. | 0.36-0.40 | [-] | [113] | c |
| η_G | Efficiency of electricity generator (no engine) | - | 0.96 | - | [-] | [181, p. 4] | d |
| P_D | Driver brakehorse power | (5.18) | - | - | [bhp] | | |
| P_{GS} | Electric power of elect. gen. set | - | var. | 275-2000 | [ekWh] | [113] | e |

^a The cited equation is for gas drivers. Energy consumption of diesel and electricity drivers is calculated in eq. (5.20) and (5.21), respectively.

^b Motor efficiency ranges from 0.84 to 0.96 for commonly applied motor size ranges [114].

^c Literature range cited only for gas generator sets with gas engine sizes ranging from 1535-2744 [bhp].

^d Standard electricity generator efficiency [181, p. 4].

^e Literature range cited for diesel generator sets [113].

5.6 Fuel cycle

For fuels consumed in OPGEE, the upstream or “fuel cycle” energy consumption and GHG emissions are required to calculate the indirect energy consumption and GHG emissions of imported fuel. For example, if purchased electricity is used on site, the emissions associated with generating and transporting that purchased electricity must be accounted for and added to the direct emissions burden. Similarly, any co-products that are sold separately from the produced oil (e.g., natural gas, electricity, NGL) must be assigned a co-production credit for emissions avoided from the system that they displace. The approach here can therefore be described as a co-product emissions assessment via system boundary expansion rather than via allocation between products [182, 183]. In all cases, the energy consumption and GHG emissions of the displaced production system is calculated from CA-GREET [84].

For the calculation of credit from the export of natural gas or natural gas liquid (NGL), the natural gas production system is displaced. For NGL export, the natural gas production system is displaced because NGL is a byproduct of gas production and does not have an independent fuel cycle. Credit is not given for avoided gas transport emissions, because it is assumed that the gas will be transported to a remote consumer.

For the calculation of credit from electricity exports, the boundary of the system is extended to the user “plug”: the displaced system includes electricity generation and transport to the end user. This choice was made because exported electricity will naturally flow to the nearest consuming entity and not require long-distance transport. OPGEE calculates the energy consumption and GHG emissions of electricity generation based on the grid electricity mix (entered in the ‘*Electricity*’ worksheet) using CA-GREET data of different electricity sources (natural gas, biomass, etc).

For regions with significantly different fuel cycle characteristics than those represented in CA-GREET, the user can and should modify the inputs on the ‘*Fuel Cycle*’ worksheet.

5.7 Embodied emissions

Embodied emissions are emissions that occur during the production, processing, and transport of materials used oilfields. In OPGEE, the following embodied emissions are included:

- Embodied emissions in wellbore steel
- Embodied emissions in wellbore cement
- Embodied emissions in surface piping
- Embodied emissions in surface processing equipment
- Embodied emissions in on-site storage infrastructure
- Embodied emissions in pipeline infrastructure
- Embodied emissions from fracturing sand and water procural
- Embodied emissions from transporting above materials to oilfield site

We first discuss the datasets used to determine embodied emissions per unit of each required material. We then discuss methods of calculating the amount of materials consumed in each of these sources below.

5.7.1 Datasets for calculating embodied emissions from consumed materials

Two datasets are used to determine the GHG intensity of materials consumed in oilfield operations. The resulting tabulated data are included in the *'Input data'* worksheet, and compiled into the *'Embodied Emissions'* worksheet depending on the dataset selected by the user. We include data from the EcoInvent v.3.0 dataset [184] and the GREET model, version GREET2_2012 [185].

*Embodied
Emissions 1.3*

5.7.1.1 EcoInvent v3.0

The EcoInvent v.3.0 dataset was used to determine emissions for a variety of materials consumed within oilfield construction and operation. The materials included in OPGEE are listed in the *'Input Data'* worksheet. The EcoInvent v.3.0 dataset was accessed in April 2014. For each material of interest, two datasets were accessed. First, the unit process data (UPR) dataset was accessed for each material. The UPR data represent direct flows between the process of interest and other processes in the “technosphere”, as well as flows between that process and the natural environment (both flows into and out of the process from the environment).

*Embodied
Emissions 1.3*

Next, full life cycle impact data were gathered for each material, in the form of life cycle inventory (LCI) data. These data were gathered using the EcoInvent default co-product accounting scheme (allocation). For each material, LCI data represent 1000s of possible flows between the economy and the natural environment, summed across all processes in the economy.

Because the desired impacts to be measured include *all* impacts across the economy, we base OPGEE emissions intensities on the LCI results, not the UPR results. For each product, primary energy consumption in the form of crude oil, natural

gas, and hard coal are tabulated. For each product, the following gas emissions rates (mass basis) are tabulated: CO₂, CH₄, non-methane volatile organic compounds (NMVOC), and N₂O. For each gas flow rate, EcoInvent partitions emissions to air using the following emissions location categories:

*Embodied
Emissions 1.3*

- Urban air, close to ground
- Non-urban air, or from high stacks
- Lower stratosphere + upper troposphere
- Unspecified emissions location
- Non-urban air
- Unspecified

For each mass flow rate, emissions from all relevant atmospheric categories are summed. Each species tracked may also be partitioned into various sources. Because we do not want to include general non-fossil emissions sources, the following sources were summed for each species.

- CO₂: Fossil carbon dioxide and carbon dioxide from soil or biomass stock. Non-fossil carbon dioxide (e.g., CO₂ from ethanol manufacture) is not included.
- CH₄: Fossil methane and methane emissions from soil. Unlabeled methane sources are not included.
- NMVOC: Sum of NMVOC emissions. Origins not partitioned.
- N₂O: Sum of dinitrogen monoxide emissions. Origins not partitioned.

For each product included in OPGEE, a functional unit of 1 kg was used in EcoInvent. Emissions intensities are also converted to g/lbm of material.

In order to choose the material production process, by default we use ROW (rest of world) or GLO (global) processes where possible. Because OPGEE is a global model, we prefer to use these ‘generic’ values rather than country-specific values. Specifically, each material input is documented below:

- Sand: The “gravel and sand quarry operation ROW” with output of 1 kg of sand was used. No specific entry was available for hydraulic fracturing proppant sand.
- Cement: The “cement production, Portland, RoW” process is used, with a functional unit of 1 kg of cement. Mitchell suggests [34, p. 382] that “almost all drilling cements are made of Portland cement, a calcined (burned) blend of limestone and clay.” The types of cement included in SPE documents are ASTM type I, II, III, and IV, which correspond to API classes A, C, G, H.
- Pipe manufacture: the “drawing of pipe, steel, RoW” process is used, with a functional unit of 1 kg of pipe manufactured. Mitchell and Miska [35, p. 387] suggest that most casing is manufactured via seamless production, which is a drawing mechanism. In EcoInvent, the pipe drawing process is modeled as a multiple of the wire drawing process.

- Gravel: the “gravel production, crushed, RoW” process is used, with a functional unit of 1 kg of gravel.
- Hematite: the “iron mine operation, crude ore, 46% Fe’, GLO” is used. The functional unit is 1 kg of ore.
- Steel: the “steel production, converter, unalloyed, ROW” and “steel production, converter, low-alloyed, ROW” are used, with 1 kg of steel functional unit in each case. Mitchell suggests that “almost without exception, casing is manufactured of mild (0.3 carbon) steel, normalized with small amounts of manganese. Strength can also be increased with quenching and tempering.” [34, p. 288].
- Bentonite clay: the “bentonite quarry operation, RoW” process is used, with a functional unit of 1 kg bentonite.
- Calcium chloride: the “soda production, solvay process, RoW” is used, with a functional unit of 1 kg calcium chloride.
- Sodium chloride: the “market for sodium chloride, powder, GLO” is used, with a functional unit of 1 kg sodium chloride.
- Monoethanolamine: the “market for monoethanolamine, GLO” is used, with a functional unit of 1 kg MEA.
- Triethylene glycol: the “market for triethylene glycol, GLO” process is used, with a functional unit of 1 kg TEG.

5.7.1.2 GREET2_2012

The GREET vehicle emissions model, GREET2, contains embodied emissions for a variety of materials. We use version GREET2_2012, accessed in April 2014 [185]. From the GREET worksheet ‘Mat_Sum’, the energy intensity (mmBtu/lb of material product) and emissions intensity (g/lb of product) were collected. In addition, emissions from cement production are taken from the ‘Cement_Concrete’ worksheet, for the same model outputs. Because GREET2 focuses on materials used in automobile manufacture, some inputs are not available (e.g., bentonite clay for cementing). These missing materials are given emissions of 0 g/lb in the current version of OPGEE when GREET is selected as the source of data inputs.

*Embodied
Emissions 1.3*

Because OPGEE GWP-weighting values are taken from GREET, the aggregate GREET GHGs figure is used for each material input.

5.7.2 Embodied emissions in wellbore steel

In order to estimate the amount of steel required per foot of well constructed, three “illustrative” wells are modeled in OPGEE: a complex well, a moderate well, and a simple well. The complex well design scheme is from Mitchell and Miska [35], for a deepwater GOM well. The moderate and simple well designs are from Nguyen [186]. The default well configuration is the moderate well configuration, with depths for some casing strings drawn from the overall depth of the well. A blank ‘User defined’ well type is also included for cases where specific well casing

*Embodied
Emissions 2.2.2*

*Embodied
Emissions 2.2.2*

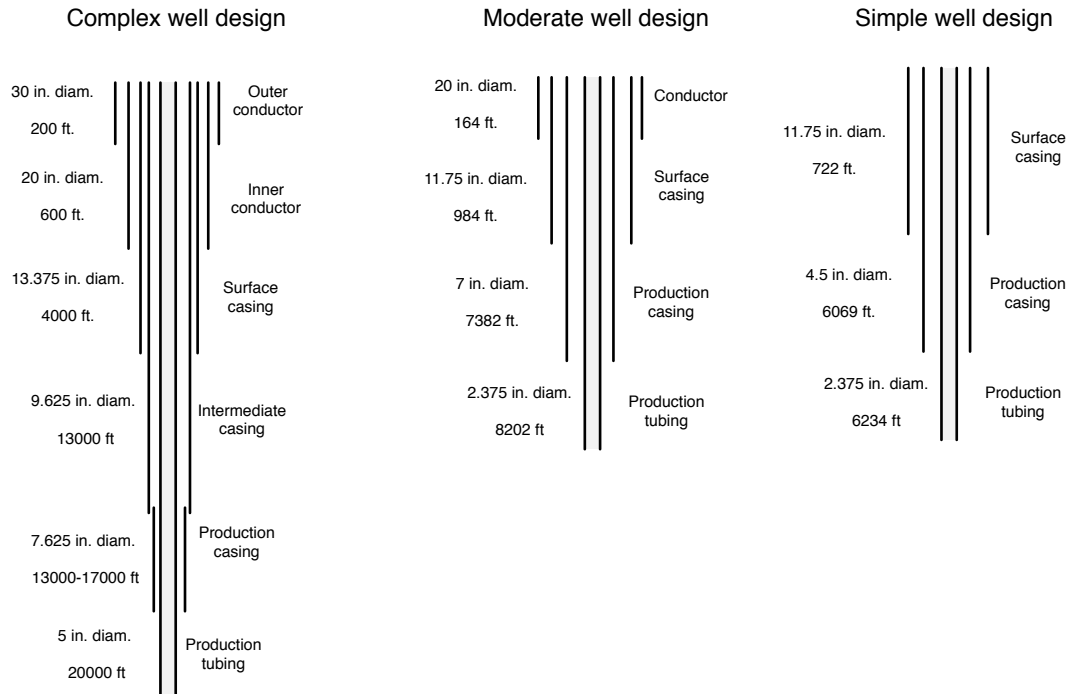


Figure 5.6: Casing plan for wells of complex, intermediate, and simple design. Well depths here are illustrative, and all steel consumption intensities are computed per unit length of well (per ft.). See text for sources.

geometry data are known (likely uncommon).

The casing plan for each of these wells is shown in Figure 5.6. For each casing diameter, the appropriate hole diameter was chosen from the literature [35, Figure 7.18]. Only commonly used bit/casing combinations were used, with tight clearance designs avoided. The smallest common bit diameter was used for each casing size. The diagram used does not give bit sizes for 24 or 30 inch casing, so we assume 6 inch excess hole diameter, as reported for 20 inch casing.

*Embodied
Emissions 2.2.1*

The mass of steel per unit length of casing is taken from Mitchell [34, Table 7.10]. Each casing outer-diameter size is listed in the literature with 1 to 10 inner diameters. The minimum, maximum, and average of all reported weights are used in OPGEE. OPGEE defaults to the average casing mass. No data were available on the mass per unit length of 30 in. diameter conductor casing, so data from GE were used [187], along with a steel density of 0.3 lbm/in³. Some casing sizes (e.g., 18.625 in. and 20 in.) only report one thickness, so min, max, and average value are identical.

*Embodied
Emissions 2.3.1*

Similarly, the production tubing mass per unit length is taken from the API tubing table for production tubing of nominal diameter 0.75 to 4.5 in [188]. For production tubing, many of the same grades have the same weight per unit length.

*Embodied
Emissions 2.3.2*

The resulting mass of steel per unit of well length [lbm/ft] is calculated for each casing and tubing layer. These per-unit length mass estimates are then compiled into aggregate steel use intensities per foot of simple, moderate, and complex well designs [lbm/ft]. The total steel used per production and injection well is also computed using these information.

*Embodied
Emissions 2.3.3
Embodied
Emissions 2.3.6*

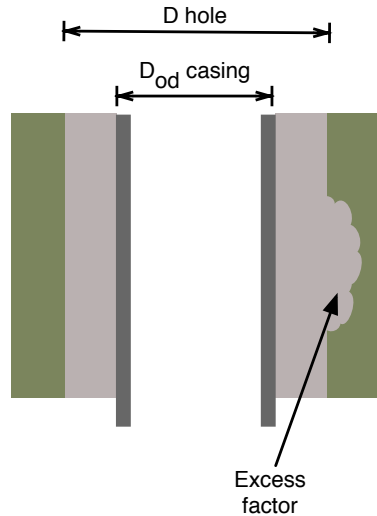


Figure 5.7: Diagram illustrating cement volume calculations (per unit depth). Cement is presented in grey, while earth is presented in green-brown.

5.7.3 Embodied emissions in wellbore cement

Wellbore diameters are collected for each casing diameter. The outer-diameter of each casing string, along with the drill bit diameter, are used to compute the volume of void space per unit length of the well [ft³/ft] (see Figure 5.7) using the cross-sectional area to be filled:

$$A_{fill} = \pi \left(\left(\frac{D_{hole}}{2} \right)^2 - \left(\frac{D_{cas,out}}{2} \right)^2 \right) \quad (5.22)$$

The appropriate hole diameter for a given casing diameter was obtained from the literature [35, Figure 7.18]. Only commonly used bit/casing combinations were used, with tight clearance designs avoided. The nominal void volume is increased by a cement excess factor of 1.75, which represents additional cement required due to cement infiltration and excess hole enlargement or hole roughness created during drilling [35, Example 4.5], see Figure 5.7.

Four cement slurry compositions are modeled in OPGEE, based on API Class A cement [35, Table 4.2]. These compositions are low density, moderate density, high density, and high strength slurry blends. Slurry blend composition is calculated using method of Mitchell and Miska [35, Examples 4.3, 4.4, 4.5]. The properties of cement additives are provided by Mitchell and Miska, including data on bulk weight, specific gravity, and absolute volume [35, Table 4.4], as are water requirements per additive [35, Table 4.5]. Properties of these cement blends are presented in Table 5.8.

The amount of cement required varies with the casing string being cemented. The following assumptions are applied to estimate the vertical extent of cementing in each well casing segment:

- Well conductor casing is cemented along its entire length (for stability and groundwater protection);

*Embodied
Emissions 2.2.1*

*Embodied
Emissions 2.2.1*

*Embodied
Emissions 2.4.1*

Table 5.8: Cement blends modeled in OPGEE.^a

| Cement type: | Low density | Moderate density | High density | High strength |
|--------------------------------|------------------------|------------------|--------------|---------------|
| Additives: | 16% bentonite, 5% NaCl | 3% bentonite | 5% hematite | 2% CaCl |
| lb/sack of cement | | | | |
| - Class A cement | 94.00 | 94.00 | 94.00 | 94.00 |
| - Bentonite | 15.04 | 2.82 | 0.00 | 0.00 |
| - Hematite | 0.00 | 0.00 | 4.70 | 0.00 |
| - Calcium chloride | 0.00 | 0.00 | 0.00 | 1.88 |
| - Sodium chloride | 4.70 | 0.00 | 0.00 | 0.00 |
| - Water | 108.29 | 58.19 | 37.63 | 43.32 |
| kg/kg slurry | | | | |
| - Class A cement | 0.42 | 0.61 | 0.69 | 0.68 |
| - Bentonite | 0.07 | 0.02 | 0.00 | 0.00 |
| - Hematite | 0.00 | 0.00 | 0.03 | 0.00 |
| - Calcium chloride | 0.00 | 0.00 | 0.00 | 0.01 |
| - Sodium chloride | 0.02 | 0.00 | 0.00 | 0.00 |
| - Water | 0.49 | 0.38 | 0.28 | 0.31 |
| Slurry density | | | | |
| - lb/gal | 12.39 | 14.48 | 16.58 | 15.75 |
| - kg/l | 1.49 | 1.74 | 1.99 | 1.89 |
| Slurry yield | | | | |
| - ft ³ /sack cement | 2.34 | 1.43 | 1.10 | 1.18 |
| - l/kg cement | 1.56 | 0.95 | 0.73 | 0.78 |

^a - See Mitchell and Miska [35, Example 4.3], Example 4.3 for overall methodology. Other composition data from [35, Example 4.4, 4.5]

- Surface casing is cemented along its entire length to prevent groundwater contamination;
- All other casing strings are assumed cemented to 300 ft. vertical fill-up (min), 600 ft. vertical fill-up (default), or filled in their entirety (max.). Minimum vertical extent of cementing is given in Mitchell and Miska [35, Section 4.5.11].

These assumptions are illustrated in Figure 5.8.

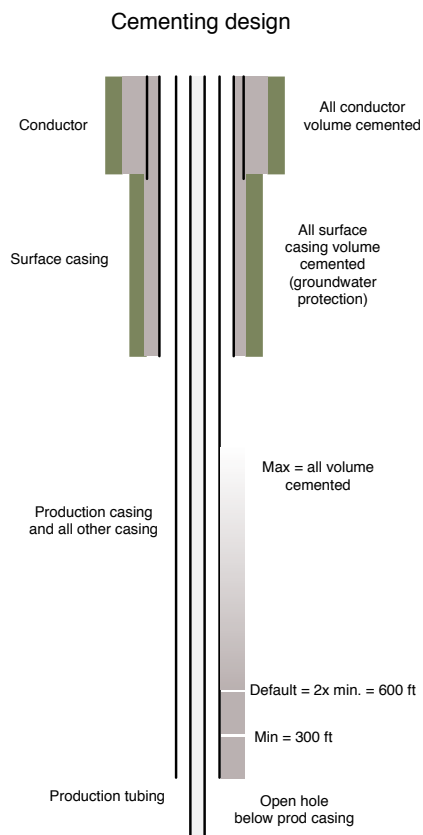


Figure 5.8: Default OPGEE cementing plan. Default non-conductor, non-surface casing fill-up is twice reported minimum, or 600 ft.

5.7.4 Embodied emissions in surface piping

Surface piping requirements will be highly dependent on the layout of the particular oilfield of interest. Data from the “Oilfield Data Handbook” [189, p.26] on surface pipe weight per unit length provide data on weight per pipe foot for standard (STD) and extra-strength (XH) pipes. Nominal diameters of 0.5 in. to 16 in. are included, with weights ranging from 0.8 to 80 lb/ft.

*Embodied
Emissions 3.1*

OPGEE defaults are set to 3 in. average diameter of surface piping, extra-strength (10.25 lbm steel/ft). OPGEE default surface piping per well is set to 2000 ft./well. If field-specific data are available on amounts of surface piping, these data should be used in preference to defaults.

*Embodied
Emissions 3.2.1
Embodied
Emissions 3.2.4*

5.7.5 Embodied emissions in fracturing materials

Materials requirements for fracturing are assumed (in the current version of OPGEE) to include only fracturing water and sand. We therefore currently neglect all other fracturing chemicals.

The water requirements of fracturing are set by default to 2 million gallons per well, a number near the median value observed in a recent study of the Bakken formation [190]. Across all studied Bakken wells, about 1.1 lb of sand was injected per gallon of fracturing water, which we use to estimate a default fracturing sand loading of 2.2 million lbs of sand per well. If well-specific data are available, or if regional or play-specific estimates for these quantities are available, those should be used in preference to defaults.

*Embodied
Emissions 2.5.1

Embodied
Emissions 2.5.4*

5.7.6 Embodied emissions in surface processing equipment

Three types of surface processing equipment are modeled to understand steel requirements: oil-water-gas separators, acid gas removal (AGR) units, and gas dehydration units.

5.7.6.1 Oil-water-gas separators

Horizontal, three-phase separators are assumed to be used to separate oil, water and gas. Three-phase separator data are tabulated from an equipment provider [191]. Working pressures of 720, 1000, 1200 and 1440 psig are tabulated, with liquid capacities ranging from 720 to 3170 bbl/d. Gas capacities range from 10.6 to 62.0 MMSCF/d, varying with the pressure of outlet gas, separator size and separator working pressure. The mass of each separator is tabulated from vendor specifications.

*Embodied
Emissions 3.3.1*

The wellhead pressure entered into the ‘Production & Extraction’ worksheet is used to select the proper separator working pressure. The number of separators needed is computed by dividing the total liquids production of the field (oil + water) by the liquid throughput capacity of each of the sizes of separators available at the desired pressure. It is assumed that the smallest number of large separators will be the most economical option, so by default this is selected. OPGEE checks to ensure that gas throughput capacity of these separators is sufficient to process the associated gas that is produced by the field. Given the number of separators and

*Embodied
Emissions 3.3.2

Embodied Emissions 3.3.5 - 3.3.7
Embodied
Emissions 3.3.8*

the required pressure and size of separators, the required total mass of separators is computed. Separator mass is assumed to be made of steel.

5.7.6.2 Acid gas removal

Acid gas removal contactor columns assume a 20-tray system, with a tray spacing of 18 in. [5, p.116], for a total contactor tower height of 30 ft. Correlations for sizing acid gas removal contacting towers are gathered from the technical literature [5]. For different gas pressures and gas flow rates, the required contactor tower diameter is computed using correlations from Manning and Thompson [5]. The log-log relationship plotted in the literature is converted to an exponential relationship, where for each operating pressure, the required contactor inner diameter is computed as:

$$D_{abs} = a_{abs} Q_{pg}^{b_{abs}} \quad (5.23)$$

Where D_{abs} is the absorber diameter [in.], a and b are fitting constants, and Q_{pg} is the flow rate of processed gas [MMscf/d], defined as associated gas less well-bore fugitives and flaring. The required inner diameter is combined with assumed steel thickness to compute the mass of the shell. The mass of contactor trays and auxiliary piping is assumed by default to equal the mass of the shell.

Detailed correlations for acid gas removal regenerator column sizing were not found in the public literature. Therefore, the mass of the desorber unit is assumed by default to equal the mass of the absorption column.

5.7.6.3 Gas dehydration

Vendor information on glycol dehydration absorption units is tabulated, with sizes (inner or outer diameter) given for various throughputs and operating pressures [192]. The required wall thickness is computed using ASME Standard B31.3 [49, eq. 9.27] for given diameters and pressures, and the required size of unit is computed using required gas processing throughput Q_{pg} (defined above). The estimated wall thickness is rounded up to the nearest 0.1 in. and used to compute the mass of steel required.

Glycol reboiler specifications are taken from vendor specifications [192]. The required wall thickness is computed using ASME Standard B31.3 [49, eq. 9.27] for given diameters, rated at assumed maximum operating pressure of 1000 psig. Given the glycol circulation rate the reboiler inner and outer diameters are computed. The required volume of steel is then computed, and doubled to estimate requirements for piping, support, exhaust, skid, and other auxiliary components.

5.7.7 Embodied emissions in on-site storage infrastructure

Crude oil and produced water storage tanks are assumed to meet API standard 12F specifications [193]. While larger custom tanks may be built on site in some instances, for simplicity, we assume standard tank dimensions. Tank capacity is chosen, which dictates height, outside diameter, shell and top/bottom steel thickness. From these parameters, assuming 0.25 in. thick steel (specific weight of 10.2 lb./ft²), the weight of each tank type is calculated.

To limit interrupted delivery due to equipment downtime, on-site storage of 3 days worth of produced oil and produced water is assumed. By default, the largest API 12F tank size is chosen (750 bbl, 15.5 ft. outside diameter, 24 ft. height). The user can select another tank size if desired.

*Embodied**Emissions 4.1.2-3*

5.7.8 Embodied emissions in long-distance transport infrastructure

Long-distance transport of crude in pipelines requires steel. The length of the US pipeline infrastructure is chosen as a model infrastructure, at 240,000 km [194]. The infrastructure is assumed to last 30 years, and transport 10×10^6 bbl/d averaged over its lifetime.

*Embodied**Emissions 5.1.1-2**Embodied**Emissions 5.1.7-8*

ANSI pipe schedules [49, Table 9.7] are used to tabulate thickness and weight per unit length for pipeline diameters from 12 to 48 in. (4 in. increments). Two standard thicknesses, designated STD and XH are tabulated, as these are available in all required sizes. By default, the assumed pipeline infrastructure is assumed to be made of 32 in. diameter, XH grade pipe (168 lb/ft).

*Embodied**Emissions 5.1.3-4*

The resulting default steel intensity is 278 bbl of oil transported per lbm of steel consumed in building long-distance pipelines.

*Embodied**Emissions 5.1.11*

We do not consider embodied emissions in oil tankers or trains in OPGEE v2.0b.

5.7.9 Shipment of oilfield capital equipment

All equipment and materials used to build oil and gas operations must be shipped from the site of production (e.g., well casing factory) to the oilfield site.

We first compute the total weight of oilfield equipment of four types modeled above:

*Embodied**Emissions 6.1*

- Steel;
- Cement;
- Fracturing sand;
- Fracturing water.

Default shipment distances assume that steel and fracturing sand are transported long distances (1000 mi) due to their specialized nature. Water and cement are assumed to be locally available (100 mi). If more specific information is available on the distances of material shipment, this should be used in place of defaults. By default, steel products and fracturing sand are shipped by rail, while fracturing water and cement are moved by truck.

*Embodied**Emissions 6.2**Embodied**Emissions 6.3*

Using the energy intensity of transport used elsewhere in the OPGEE model, the energy requirements of transporting each material are computed. To compute emissions, all energy is assumed provided by diesel fuel consumed in the appropriate vehicle.

*Embodied**Emissions 6.4-5*

5.8 Emissions factors

Emissions factors are required for the calculation of GHG emissions from combustion (fuel combustion) and non-combustion (venting and fugitives) sources.

Table 5.9: Combustion technologies and fuels included in OPGEE.

| | Natural gas | Diesel | Crude | Residual oil | Pet. coke | Coal |
|----------------------|-------------|--------|-------|--------------|-----------|------|
| Industrial boiler | ✓ | ✓ | ✓ | ✓ | ✓ | ✓ |
| Turbine | ✓ | ✓ | | | | |
| CC gas turbine | ✓ | | | | | |
| Reciprocating engine | ✓ | ✓ | | | | |

5.8.1 Combustion emissions factors

The emissions factors for fuel combustion are from CA-GREET [84]. Table 5.9 shows the technologies and fuels included. Gas species tracked include VOC, CO, CH₄, N₂O, and CO₂. Emissions are converted into carbon dioxide equivalent using IPCC GWPs [195] as shown in eq. (5.24).

$$EM_{CO_2eq,i} = EM_i \cdot GWP_i \quad [gCO_2eq] \quad (5.24)$$

where $EM_{CO_2eq,i}$ = emissions of species i in carbon dioxide equivalent [gCO₂eq]; EM_i = emissions of species i [g]; and GWP_i = GWP of species i [gCO₂eq./g]. GWPs are discussed in Section 8.1.

5.8.2 Non-combustion emissions factors

Section 5.9 describes how emissions factors for venting and some fugitives sources are generated from the ARB survey data [10]. Emissions factors from ARB are specified by gas component. The ARB survey data used to generate emissions factors for venting are shown in Table 5.10.

The emissions factors for venting by gas component were calculated using ARB survey data as:

$$EF_{CO_2Vent} = \frac{a_{EFV}}{c_{EFV}} 10^6 \quad \left[\frac{g}{event} \right], \text{ etc.} \quad (5.25)$$

$$EF_{CH_4Vent} = \frac{b_{EFV}}{c_{EFV}} 10^6 \quad \left[\frac{g}{event} \right], \text{ etc.}$$

where EF_{CO_2Vent} = emissions factor of CO₂ venting [g/event; g/mile-yr; g/MMscf]. For a description of a_{EFV} , b_{EFV} , and c_{EFV} parameters see Table 5.10.

Similar calculations were performed for emissions factors for fugitives from the sources listed in Table 5.11. Emissions factors for fugitives from other sources (valves, flanges, etc) are taken from API [12, p. 20].

Emissions factors for gas dehydrators are calculated on volume basis (i.e., in grams of CO₂ or CH₄ per MMscf processed gas). These data are derived from an updated version of the ARB survey cited above [11]. In this improved version of the survey, ARB staff S. Detwiler and J. Duffy separated dehydration systems with and without vapor recovery systems (VRS) to determine emissions factors with and without VRS. See Table 5.12.

Table 5.10: ARB data used in the calculation of venting emissions factors (unit specified below). Source: [10].

| Source | Total CO ₂ emissions (ton- ne/yr) a_{EF_V} | Total CH ₄ emissions (tonne/yr) b_{EF_V} | # units (event/yr, oth- erwise noted) c_{EF_V} |
|----------------------------------|--|--|--|
| Well workovers | | | |
| - Ultra-heavy | 0 | 0 | – |
| - Heavy | 405 | 1,428 | 12,889 |
| - Light | 225 | 575 | 5,424 |
| - Ultra-light | 9 | 65 | 599 |
| Well cleanups | | | |
| - Ultra-heavy | 0 | 0 | – |
| - Heavy | 103 | 90 | 956 |
| - Light | 113 | 201 | 1977 |
| - Ultra-light | 3 | 21 | 187 |
| Compressor startups | 4 | 69 | 1071 |
| Compressor blow-downs | 172 | 3,238 | 1071 |
| Gathering pipelines main-tenance | 2659 | 2490 | 2295 (mile) |
| Gathering pipelines pig-ging | 104 | 5 | 1417 |

Table 5.11: ARB data used in the calculation of fugitives emissions factors (unit specified below). Source: [10].

| Source | Total CO ₂ emissions (ton- ne/yr) a_{EF_F} | Total CH ₄ emissions (tonne/yr) b_{EF_F} | # units (event/yr, oth- erwise noted) c_{EF_F} |
|---------------------|--|--|--|
| Active wells | | | |
| - Ultra-heavy | 0 | 0 | – |
| - Heavy | 66 | 155 | 36,619 |
| - Light | 459 | 1,415 | 14,261 |
| - Ultra-light | 19 | 139 | 1,323 |
| Well cellars | | | |
| - Ultra-heavy | – | 3 | 22 |
| - Heavy | – | 933 | 7,461 |
| - Light | – | 850 | 4,998 |
| - Ultra-light | – | 369 | 2,168 |
| Gathering pipelines | 327 | 867 | 2,295 (mile) |
| Separators | 11 | 170 | 4,618 |
| Sumps and pits | – | 264 | 250 |

Table 5.12: ARB data for gas dehydrators, for systems with and without vapor recovery systems (VRS). Source: [11].

| Source | CO ₂ emissions (g/MMscf) | CH ₄ emissions (g/MMSCF) | Gas input volume (MMscf) |
|------------------------|--|--|-----------------------------|
| Venting - No VRS | 148 | 13,677 | 60,941 |
| Venting - VRS | 466 | 1,782 | 640,181 |
| Venting - All dehyd. | 439 | 2,816 | 701,123 |
| Fugitives - No VRS | 172 | 3,925 | 60,941 |
| Fugitives - VRS | 25,863 | 748 | 640,181 |
| Fugitives - All dehyd. | 23,630 | 1,024 | 701,123 |

Table 5.13: An example of EPA emissions factors for oil and gas production components (g/unit-yr). Source: [12].

| Source | CH ₄ | VOC emissions |
|--|-----------------|---------------|
| Non-leaking components (< 10,000 ppmv) | | |
| Valves | | |
| Gas service | 148 | 37 |
| Heavy oil service | 69 | 2 |
| Light oil service | 101 | 49 |
| Connectors | | |
| Gas service | 60 | 15 |
| Heavy oil service | 62 | 2 |
| Light oil service | 52 | 25 |
| Leaking components (> 10,000 ppmv) | | |
| Valves | | |
| Gas service | 590,678 | 147,025 |
| Heavy oil service | – | – |
| Light oil service | 465,479 | 225,134 |
| Connectors | | |
| Gas service | 159,029 | 39,584 |
| Heavy oil service | – | – |
| Light oil service | 141,668 | 68,519 |

As described in Section 4.4.2.6, venting from the amine unit is calculated from the gas balance of OPGEE by assuming that all CO₂ left in the gas stream after flaring, fugitives, and other venting is vented. In Gas Processing Path 6 (membrane-amine CO₂ EOR) the vented CO₂ is reinjected into the reservoir. The emissions factor for CH₄ fugitives from the AGR unit is 965 scf CH₄/MMscf of gas throughput [196, p. 23].

EPA emissions factors for fugitives from the components listed in Table 5.17 are reported by API as total hydrocarbons (THC) by service type, i.e. gas service, heavy oil service [12, p. 20]. As explained in Section 5.9.3.1 the THC emissions factors are calculated assuming that 25% of the components are associated with gas service and the remaining 75% are associated with oil service. An example of EPA emissions factors for oil and gas production components after speciation is shown in Table 5.13 for valves and connectors [12, p. 20]. Fugitives from non-leaking components are negligible. The user determines the percentage of leaking components in the ‘Venting & Fugitives’ worksheet.

Emissions factors for land use change are discussed in Section 4.2. Table 4.6 shows the emissions factors per unit of crude oil produced for low, medium, and high intensity development in low, medium, and high ecosystem productivity en-

vironments [6].

5.9 Venting and fugitive emissions

5.9.1 Introduction to venting, and fugitive emissions

Venting and fugitive emissions can be a significant source of GHG emissions from oil production operations. We use these definitions here:

Venting emissions Purposeful release of non-combusted hydrocarbon gases to the atmosphere. Venting emissions generally occur during maintenance operations and other intermittent, infrequent activities.

Fugitive emissions Non-purposeful or non-planned emissions of non-combusted hydrocarbon gases to the atmosphere. Fugitive emissions commonly result from leaking equipment and tanks.

Venting and fugitive emissions arise from oil field operations and devices. Sources include well workovers and cleanups, compressor startups and blowdowns, pipeline maintenance, gas dehydrators, AGR units, well cellars, separators (wash tanks, free knock outs, etc.), sumps and pits, and components (valves, connectors, pump seals, flanges, etc.). The heterogeneous nature of these sources makes venting and fugitive difficult to monitor and track.

5.9.2 Calculation of venting emissions

Two types of venting occur in production and processing facilities: (i) operational venting, and (ii) venting to dispose of associated gas where there is no infrastructure for the use of gas. Operational venting is associated with production, processing and maintenance operations such as well workovers and cleanups, compressor blowdowns, and gas processing units (AGR and glycol dehydrator). These operations necessitate the venting of some gas.

Venting associated with production and surface operations is estimated using data collected in the 2007 oil & gas GHG emissions survey in California, performed by California Air Resources Board (ARB) [10], and the API manual of petroleum measurement standards [77]. Some sources use updated factors from the updated California Air Resources Board survey [11]. Venting calculations for the Ryan-Holmes process use data from NETL [197].

5.9.2.1 Venting of associated gas as disposal mechanism (flaring substitute)

Venting to dispose of large quantities of gas is not common, due to safety concerns and environmental impacts. However, it may be practiced in some fields as an alternative to flaring (e.g., local regulations may prohibit flaring). Venting as an alternative to flaring is not environmentally acceptable because methane and volatile organic compounds (VOCs) have higher GWPs compared to carbon dioxide. The venting of produced gas is a user input and is presented by the venting-to-oil ratio or VOR in the 'Active Field' worksheet. This quantity is used to compute associated gas disposal venting emissions. The calculation of emissions from vented gas is as shown in eq. (5.38).

Venting & Fugitives 2.1.1

Table 5.14: Emissions data used in the estimation of operational venting. Data from California oil fields, 2007. Source: [10], except where otherwise noted.

| Source | Activity | Unit | Oil Prod. (bbl/yr) | Activity fac- tor | Unit |
|------------------------------------|----------------------|------------|-----------------------|-----------------------|--------------------|
| | a_{V_G} | | b_{V_G} | c_{V_G} | [event/bbl] |
| Well workovers | | | | | |
| - Ultra-heavy | 0 | [event/yr] | 614,683 | 0 | [event/bbl] |
| - Heavy | 12,889 | [event/yr] | 156,304,520 | 8.25×10^{-5} | [event/bbl] |
| - Light | 5,424 | [event/yr] | 61,524,698 | 8.82×10^{-5} | [event/bbl] |
| - Ultra-light | 599 | [event/yr] | 15,649,398 | 3.83×10^{-5} | [event/bbl] |
| Well cleanups | | | | | |
| - Ultra-heavy | 0 | [event/yr] | 614,683 | 0 | [event/bbl] |
| - Heavy | 956 | [event/yr] | 156,304,520 | 6.12×10^{-6} | [event/bbl] |
| - Light | 1977 | [event/yr] | 61,524,698 | 3.21×10^{-5} | [event/bbl] |
| - Ultra-light | 187 | [event/yr] | 15,649,398 | 1.19×10^{-5} | [event/bbl] |
| Compressors | $\approx 1071^a$ | [device] | 390326918 (Mscf) | 2.74×10^{-6} | [unit- yr/Mscf] |
| Gathering pipelines | 1218 ^b | [mile] | 234,093,299 | 5.20×10^{-6} | [mile- yr/bbl] |
| Pigging launcher open- ings | $\approx 850^a$ | [event/yr] | 234,093,299 | 3.63×10^{-6} | [event/bbl] |
| Pneumatic devices - Low bleed | 145,179 ^c | [devices] | 1891×10^6 | 0.03 | [device/bbl/y] |
| Pneumatic devices - High bleed | 269,618 ^c | [devices] | 1891×10^6 | 0.05 | [device/bbl/y] |
| Pneumatic chemical injection pumps | 28,702 ^c | [devices] | 1891×10^6 | 0.0055 | [device/bbl/y] |

a - Estimated from the total number of compressors which is shared by both the crude oil and dry gas businesses in California. We assume that the number of compressors is proportional to total natural gas production in California, both dry and associated. Data from updated California survey [11], Tables 2.5 and 15.1.

b - Estimated by summing the number of miles associated with the crude oil business. Miles associated with dry gas production and gas storage facilities are not counted. For central gas processing facilities 75% of the miles are allocated to the crude oil business. This assumption is based on the split between the types of gases produced in California where $\approx 75\%$ of the produced gas is associated gas [10].

c - Total number of pneumatic controllers and pneumatic chemical injection pumps in the US, from EPA device count estimates, divided by total US crude oil production (data from 2012) [198, Annex 3.6, Tables A-147, A-152].

5.9.2.2 Venting from general sources

Operational venting may be associated with units (e.g., compressors), events (e.g., well workovers), or distance of product transport (e.g., gathering pipelines). The amount of gas vented from various sources is calculated using the number of unit-years, mile-years, or events associated with the volume of oil produced. A unit-year (abbreviated unit-yr), for example, is one unit operating over a time period of one year.

Low- and High-bleed pneumatic device venting emissions are estimated using US EPA emissions factors [198], due to lack of pneumatic device adoption in California. If modeling production in a region where methane bleeding pneumatic devices are known to not used, these emissions factors should be reduced to 0.

The sources for general venting are listed in Table 5.14. The first step in calculating venting emissions from general sources is to estimate the number of unit-years, mile-years, or events associated with one barrel of oil, as shown in Table 5.14. The venting emissions from general sources are calculated as:

$$EM_{V_G} = \sum_s c_{V_G,s} Q_o EF_{V_s} \quad [\text{g/d}] \quad (5.26)$$

where EM_{V_G} = venting emissions from general sources as listed in Table 5.14 [g/d]; $c_{V_G,s}$ = activity factor per unit of oil produced [unit-years/bbl, event/bbl or mile-years/bbl]; Q_o = total rate of oil production [bbl/d]; and EF_{V_s} = vent emissions factors for source s [g/unit-yr, g/mile-yr, or g/event]. $c_{V_G,s}$ is calculated as shown in Table 5.14 by multiplying $a_{V_G,s}$ which is the total number of units, events or miles surveyed [mile, unit, or event/yr] with $b_{V_G,s}$ which is the reported oil production volumes [bbl/yr].

The emissions factors and therefore the emissions estimates are specific to gas components (e.g., CO_2). The emissions factors for the venting of CO_2 and CH_4 are also estimated using data from the ARB survey [10]. Calculations of emissions factors are explained in Section 5.8.

5.9.2.3 Venting from gas processing units

Other than the general venting emissions sources that are listed in Table 5.14 there are major venting sources which include venting from gas processing technologies like glycol dehydrators and amine acid gas removal (AGR) systems. The methods for calculating venting from glycol dehydration and amine AGR units are volume based. For the glycol dehydrator unit the venting emissions of both CO_2 and CH_4 are calculated based on the gas unit volume as:

$$EM_{V_{GD}} = Q_{GD} \cdot EF_{V_{GD}} \quad [\text{g/d}] \quad (5.27)$$

where $EM_{V_{GD}}$ = venting emissions from the glycol dehydrator unit [g/d]; Q_{GD} = volume throughput of the glycol dehydrator unit [MMscf/d]; and $EF_{V_{GD}}$ = vent emissions factors for glycol dehydrator [g/MMscf]. The emissions factors as noted above are calculated from the updated 2013 ARB survey data [11] as explained above. The approximate volume throughput of the glycol dehydrator is determined by the gas balance and is calculated as shown in eq. (4.67). A description of the gas balance is found in Section 5.1.

The calculation of CH_4 venting from the amine-based AGR unit is performed as outlined above for the glycol dehydrator:

$$EM_{V_{AGR}} = Q_{AGR} \cdot EF_{V_{AGR}} \quad [\text{g/d}] \quad (5.28)$$

where $EM_{V_{AGR}}$ = CH_4 venting emissions from the amine AGR unit [g/d]; Q_{AGR} = volume of the amine AGR unit [MMscf/d]; and $EF_{V_{AGR}}$ = vent emissions factor for AGR unit [g CH_4 /MMscf]. The calculation of the CO_2 emissions from the amine-based AGR unit is determined by the gas balance where all the CO_2 left in the gas after flaring, fugitives, and other venting is assumed to be absorbed and stripped in the amine treater. In the amine AGR located in Gas Processing Path 6 (dual amine-membrane process for CO_2 EOR) the CO_2 is reinjected into the reservoir. In the amine AGR located in Gas Processing Paths 3 and 5, the CO_2 is vented.

Venting emissions factors for the Ryan-Holmes unit are from NETL [197]. VOC venting from the Ryan-Holmes unit is calculated as:

$$EM_{V_{RHVOC}} = Q_{RH} \cdot EF_{V_{RHVOC}} \quad [\text{g/d}] \quad (5.29)$$

Venting & Fugitives
2.1.2

Venting & Fugitives
2.1.2

Venting & Fugitives
2.1.2

where $EM_{V_{RH_{VOC}}} = \text{VOC venting emissions from the Ryan-Holmes unit [g/d]}$; $Q_{RH} = \text{volume of the Ryan-Holmes unit feedstream [MMscf/d]}$; and $EF_{V_{RH_{VOC}}} = \text{VOC vented emissions factor for the Ryan-Holmes unit [g/MMscf]}$.

Ryan-Holmes unit CH_4 and CO_2 vented emissions are calculated by linearly scaling the VOC emissions calculated in Equation 5.29 based on the relative concentrations of the appropriate chemical species. Ryan-Holmes CH_4 vented emissions are calculated as:

$$EM_{V_{RH_{CH_4}}} = \frac{Y_{CH_4}}{Y_{VOC}} \cdot EM_{V_{RH_{VOC}}} \quad [\text{g/d}] \quad (5.30)$$

where $EM_{V_{RH_{CH_4}}} = \text{CH}_4 \text{ venting emissions from the Ryan-Holmes unit [g/d]}$; $Y_{CH_4} = \text{the molar share of CH}_4 \text{ in the overall feed stream [-]}$; $Y_{VOC} = \text{the molar share of VOC in the overall feed stream [-]}$; and $EM_{V_{RH_{VOC}}} = \text{VOC vented emissions from the Ryan-Holmes unit [g/d]}$.

Similarly, Ryan-Holmes CO_2 vented emissions are calculated as:

$$EM_{V_{RH_{CO_2}}} = \frac{Y_{CO_2}}{Y_{VOC}} \cdot EM_{V_{RH_{VOC}}} \quad [\text{g/d}] \quad (5.31)$$

where $EM_{V_{RH_{CO_2}}} = \text{CO}_2 \text{ venting emissions from the Ryan-Holmes unit [g/d]}$; $Y_{CO_2} = \text{the molar share of CO}_2 \text{ in the overall feed stream [-]}$; $Y_{VOC} = \text{the molar share of VOC in the overall feed stream [-]}$; and $EM_{V_{RH_{VOC}}} = \text{VOC vented emissions from the Ryan-Holmes unit [g/d]}$.

5.9.2.4 Venting from crude oil storage tanks

The estimation of venting emissions from storage tanks is based on an emissions factor generated using data from the ARB survey. The emissions factor for CH_4 emissions was calculated as 49.2 g CH_4 /bbl oil [10].

5.9.2.5 Venting emissions gathering

All the methods that have been discussed for the estimation of emissions from venting generate weight of gas species lost into the atmosphere (the balancing of the gas as is discussed in Section 5.1). Therefore weight is converted to volume using the densities of gas species (e.g., CH_4) [156]. The estimated weight of the gas species emissions is converted to [g/d] and divided by the species density [g/ft³].

After the weight and volume of emissions from each source is calculated, categorization of the emissions sources is required to allocate venting emissions to the different stages in OPGEE (e.g., 'Production & Extraction'). Table 5.15 lists the sources of venting emissions under each process stage. Crude oil transport is not included because it is a separate process.

The emissions volumes from each process stage are converted into CO_2 equivalent GHG emissions using the IPCC GWPs of the gas constituents [195].

5.9.3 Calculation of fugitive emissions

The estimation of fugitive emissions from various components is difficult due to the non-planned nature of the losses and the number of sources. This includes

Venting & Fugitives
2.1.2
Input Data
Table 1.2

Table 5.15: Categorization of venting emissions sources by process stage.

| Process stage | Venting emissions sources |
|-------------------------|--|
| Exploration | None |
| Drilling & development | None |
| Production & extraction | None |
| Oil field processing | Flaring substitute ^a Gas dehydrator AGR unit Ryan-Holmes unit Storage standing losses ^b Storage working losses ^b |
| Maintenance | Well workovers and cleanups Gathering pipelines maintenance and pigging Compressor blowdowns and startups |
| Waste disposal | None |

^a - Venting of associated gas as a flaring substitute is computed in 'Venting & Fugitives 2.1'.

^b - Standing and working losses are combined into a single emissions factor in 'Emissions Factors' Table 1.2

fugitive emissions from active wells, well cellars, gas processing units, gathering pipelines, sumps and pits, storage tanks (e.g., free knock out vessel) and various equipment (valves, connectors, flanges, etc). Fugitives associated with production and surface operations are estimated using data collected by ARB [10, 11], and emissions factors from the API workbook for oil and gas production equipment fugitive emissions [12].

The approach used to estimate fugitive emissions is similar to the approach used in the calculation of venting emissions. Fugitive losses are linked to various units (e.g., equipment and active wells), gathering pipeline miles, and volumes of gas processing units (e.g., AGR unit). Most fugitive losses are linked to units and equipment. The number of unit-years or mile-years associated with the total volume of oil produced is estimated using the ARB survey data [10].

Venting & Fugitives
2.2.1

5.9.3.1 Fugitives from general sources

Fugitive emissions from general sources are listed in Table 5.16. This table does not include all equipment fugitives. API research suggests that a good approximation of the number of components can be obtained by estimating the number of valves and pumps and then calculating the probable number of flanges, connectors, open-ended lines, and other components from the number of valves [12, p. 14]. During a field study of petroleum production operations, API found that the number of flanges is usually about the same as the number of valves, while the number of connectors (threaded pipes and tubing fittings) is about three times the number of valves. API also found that about 10% of all valves have one side that can be opened to the atmosphere (open-ended lines) and that the number of other components is approximately 5% of the number of valves. No correlation was found between the number of valves and the number of pumps [12, p. 14]. The number of valves and pump seals are estimated from the ARB survey data as shown in Table 5.16 and the number of remaining components is estimated from the number of valves using the API method.

As shown in Table 5.16 the number of unit-years or mile-years associated with one barrel of oil production is estimated using data from the ARB survey [10]. The number of remaining sources of fugitive emissions is estimated from the number

Table 5.16: Data used in the estimation of fugitives. Source: [10].

| Source | Activity | Unit | Oil prod. (bbl/yr) | Activity factor | Unit |
|--|--------------------|--------|-----------------------|-----------------------|---------------|
| | a_{FG} | | b_{FG} | c_{FG} | |
| Gathering pipelines ^a | 1218 | [mile] | 234,093,299 | 5.20×10^{-6} | [mile-yr/bbl] |
| Separators | $\simeq 3557^b$ | [unit] | 234,093,299 | 1.52×10^{-5} | [unit-yr/bbl] |
| Sumps & pits | 250 | [unit] | 234,093,299 | 1.07×10^{-6} | [unit-yr/bbl] |
| Valves - Light oil service (without open-ends) | $\simeq 251,589^c$ | [unit] | 77,174,096 | 3.26×10^{-3} | [unit-yr/bbl] |
| Valves - Heavy oil service (without open-ends) | $\simeq 324,935^c$ | [unit] | 156,919,203 | 2.07×10^{-3} | [unit-yr/bbl] |
| Pump seals - Light oil service | $\simeq 3,327^c$ | [unit] | 77,174,096 | 2.51×10^{-5} | [unit-yr/bbl] |
| Pump seals - Heavy oil service | $\simeq 3,942^c$ | [unit] | 156,919,203 | 4.31×10^{-5} | [unit-yr/bbl] |

a - Miles of pipeline. See Table 5.14.

b - Estimated by summing the number of separators associated with the crude oil business. Separators associated with dry gas production and gas storage facilities are not counted. For gas processing facilities, 75% of the separators are allocated to the crude oil business. This assumption is based on the split between the types of gases produced in California where $\approx 75\%$ of the produced gas is associated gas [10].

c - Estimated by summing the number of valves and pump seals associated with light and heavy crude oil service. Counts for light and heavy oil computed separately [11]. Data from ARB updated survey, Tables 2.3, 8.1 [11].

Table 5.17: Estimating the number of remaining components.

| Component | Number |
|-------------------------|----------------|
| Valves (with open ends) | N |
| Pumps | No correlation |
| Flanges | N |
| Connectors | $3N$ |
| Open-ends | $0.1N$ |
| Others ^a | $0.05N$ |

a - Includes compressor seals, diaphragms, drains, etc.

Table 5.18: Speciation fractions for total hydrocarbon (THC) emissions calculated using API emissions factors [%].

| Emissions component | Gas | Heavy oil | Light oil |
|---------------------|-------|-----------|-----------|
| Methane | 0.687 | 0.942 | 0.612 |
| VOC | 0.171 | 0.030 | 0.296 |

of valves as outlined in Table 5.17. Therefore the total number of unit-years or mile-years associated with the amount of oil produced in OPGEE and the fugitive emissions from the various sources listed in Tables 5.16 and 5.17 is calculated as:

$$EM_{F_G} = \sum_s c_{F_G,s} Q_o EF_{F_s} \quad [\text{g/d}] \quad (5.32)$$

where EM_{F_G} = fugitive emissions [g/d]; $c_{F_G,s}$ = number of unit-years or mile-years per barrel of oil and is calculated as shown in Table 5.16; Q_o = total rate of oil production entered by the user [bbl/d]; and EF_{F_s} = fugitive emissions factors for source s [g/unit-yr, g/mile-yr]. $c_{F_G,s}$ is calculated by multiplying $a_{F_G,s}$ which is the total number of units or miles surveyed [mile, unit] with $b_{F_G,s}$ which is the reported oil production volumes [bbl/yr]. For the estimation of fugitives from active wells and well cellars, the number of active wells (producing wells) is given in the 'Active Field' worksheet and the number of well cellars is assumed equal to the number of active wells.

The emissions factors generated from the ARB survey, and therefore the calculated emissions, are specific to gas components (e.g., CO₂). The calculation of the emissions factors is explained in Section 5.8. Emissions factors for equipment fugitives that are listed in Table 5.17 are taken from the API documentation [12, p. 20]. The emissions factors from API are not speciated. The speciation in Table 5.18 is used to allocate the total hydrocarbon (THC) emissions calculated using the API emissions factors to the main gas components, i.e. methane and VOC [12, p. 15].

As shown in Table 5.18, the fractions are different for fugitives from different streams. For the division of THC emissions, 75% of the components are assumed in oil service, and 25% in gas service. This assumption is based on an example from the API methods on the calculation of fugitive emissions from a crude oil production operations which co-produce natural gas [12, p. 16]. For oil service components the fraction is determined by the API gravity of the oil. For the calculation of the volume of VOC emissions the VOC is broken down into 31% C₂, 42% C₃, and 27% C₄. The fraction of C₅+ VOC components is negligible. This breakdown is based on average THC emissions speciation profiles [75, p. ES-2].

5.9.3.2 Fugitives from gas processing units

Other than the general fugitive emissions sources that are listed in Tables 5.16 and 5.17, fugitives sources include gas processing units like glycol dehydrator units, amine acid gas removal (AGR) units, and the Ryan-Holmes process. The methods for calculating fugitives from glycol dehydration, amine AGR units, and the Ryan-Holmes process are volume based.

For the glycol dehydrator and AGR units, the fugitive emissions of both CO₂ and CH₄ are calculated based on the gas unit throughput volume as:

Venting & Fugitives
1.2
2.2.1

Venting & Fugitives
1.2
2.2.1

Table 5.19: Categorization of fugitive emissions sources by process stage.

| Process stage | Fugitive emissions sources |
|---------------------------|---|
| Exploration | None |
| Drilling and development | None |
| Production and extraction | Active wells |
| | Well cellars |
| Oil field processing | Separators |
| | Gas dehydrator |
| | AGR unit |
| | Gathering pipelines |
| | Sumps and pits |
| | Components (valves, connectors, flanges, etc) |
| Maintenance | None |
| Waste disposal | None |

$$EM_{F_{GP}} = Q_{GP}EF_{F_{GP}} \quad [\text{g/d}] \quad (5.33)$$

where $EM_{F_{GP}}$ = fugitive emissions from the gas processing unit [g/d]; Q_{GP} = volume throughput of the gas processing unit [MMscf/d]; and $EF_{F_{GP}}$ = fugitive emissions factors for gas processing unit [g/MMscf]. The emissions factors are calculated from the ARB survey data [10] as explained in Section 5.8.2. The emissions factor for fugitive CH_4 emissions from AGR unit is taken from [196, p. 23]. The approximate volume of the gas processing unit is determined by the gas balance and is calculated as shown in eq. (4.67). A description of the gas balance is found in Section 5.1.

Fugitive emissions from the Ryan-Holmes process are calculated similarly, using a fugitive VOC emissions factor from NETL [197] and the volumetric throughput of the incoming feedstream. CH_4 and CO_2 fugitives emissions for the Ryan-Holmes process are then calculated by linearly scaling the VOC fugitives volume as performed in Equations 5.30 and 5.31 in section 5.9.2.3.

Produced water tank emissions occur in a manner similar to crude oil storage tank flashing losses, though at a smaller relative rate. Methane emissions from produced water tanks are lower than crude tank flashing losses because CH_4 has a stronger affinity for hydrocarbon oil than it does for water. Thus, more CH_4 is dissolved in the oil phase than the water phase. CH_4 fugitive emission factors from water tank is also included using reported data by Shires et al. [199].

5.9.3.3 Fugitive emissions gathering

All the methods that have been discussed for the estimation of fugitives end up generating mass of gas species lost into the atmosphere. The balancing of the gas is discussed in Section 5.1. Therefore mass is converted to volume using the densities of gas species [156]. After the mass and volume of emissions from each source is calculated, categorization of the emissions sources is required to allocate fugitive emissions to the different stages in OPGEE (e.g., 'Production & Extraction'). Table 5.19 lists the sources of fugitive emissions under each process stage. Fugitive emissions from crude oil transport are not included because it forms a separate process.

The emissions volumes of each process stage are converted into CO_2 equivalent GHG emissions using the IPCC GWPs [195].

5.9.4 Default values for venting and fugitive emissions

The default emissions factors and the number of associated unit-years, mile-years or events/yr are generated from the ARB survey data [10]. The estimation of the number of unit-years, mile-years or events/yr was previously discussed. The user is allowed to overwrite these defaults. As these defaults represent the average case in California, in some cases they might not be a good representation of the level of venting and fugitives in other areas of the world. This is particularly true where practices and environmental regulations are significantly different than California regulations. The average EPA emissions factors for fugitives from the various components listed in Table 5.17 are used as default [12, p. 20]. These defaults represent the average US case and can also be overwritten by the user to represent changes in equipment condition, practices, and environmental regulations.

Table 5.20: Default inputs for venting, flaring, and fugitive emissions.

| Param. | Description | Eq. no. | Default | Literature range | Unit | Sources | Notes |
|----------------|--|---------|-------------------------|------------------|---------------------------|-----------|-------|
| $c_{FG,s}$ | Number of fugitive source per oil barrel | - | Table 5.16 | - | [unit-yr/bbl] | [10] | a |
| $c_{VG,s}$ | Number of vent source per oil barrel | - | Table 5.14 | - | [event/bbl] | [10] | b |
| EF_{FGP} | Fugitive em. factors for gas proc. unit | - | Section 5.8 | - | [g/MMscf] | [10, 196] | |
| EF_{Fs} | Fugitive emissions factors for source s | - | Tables 5.11 & 5.13 | - | [g/unit-yr] | [10, 12] | c |
| $EF_{V,Amine}$ | Vent emissions factors for amine process | - | 0 | - | [gCH ₄ /MMscf] | [10] | d |
| $EF_{V,GD}$ | Vent emissions factors for gas dehydrator | - | Section 5.8 | - | [g/MMscf] | [10] | |
| $EF_{V,RH}$ | Vent emissions factors for Ryan-Holmes process | - | Section 5.8 | - | [g/MMscf] | [197] | |
| EF_{Vs} | Vent emissions factors for source s | - | Table 5.10 | - | [g/event] | [10] | e |
| EM_{FG} | Fugitive emissions general | (5.32) | - | - | [g/d] | | |
| EM_{FGP} | Fugitive emissions from gas proc. unit | (5.33) | - | - | [g/d] | | |
| $EM_{V,Amine}$ | Vent emissions from amine process | (5.28) | - | - | [g/d] | | |
| $EM_{V,GD}$ | Vent emissions from gas dehydrator | (5.27) | - | - | [g/d] | | |
| $EM_{V,RH}$ | Vent emissions from Ryan-Holmes process | (5.27) | - | - | [g/d] | | |
| EM_{VG} | Vent emissions general | (5.26) | - | - | [g/d] | | |
| $GW P_i$ | Global warming potential for species i | - | 'Input data' Table 2.1 | - | [gCO ₂ eq./g] | [195] | f |
| Π_i | Stoichiometric combustion ratios | - | Table 5.23 | - | [gCO ₂ /g] | - | g |
| Q_{Amine} | Volume of amine process | - | 'Gas Balance' | - | [MMscf/d] | | |
| Q_{RH} | Volume of Ryan-Holmes process | - | 'Gas Balance' | - | [MMscf/d] | | |
| Q_{GD} | Volume of gas dehydrator | - | 'Gas Balance' | - | [MMscf/d] | | |
| Q_o | Volume of oil production | - | 1500 | - | [bbl/d] | | |
| Q_{GP} | Volume of gas processing unit | - | 'Gas Balance' | - | [MMscf/d] | | |
| ρ_i | Gas density for species i | - | 'Input Data' Table 2.2 | - | [g/ft ³] | - | h |
| x_i | Mole fraction of gas composition | - | 'Gas Balance' Table 1.1 | - | [-] | [10] | i |

a - Most of the fugitives are associated with units. Therefore the most common unit for the number of sources per oil barrel is [unit-yr/bbl]. Other units include [mile-yr/bbl] for fugitives associated with pipeline miles.

b - Most venting is associated with events. Therefore the most common unit for number of sources per oil barrel is [event/bbl]. Other units include [unit-yr/bbl] and [mile-yr/bbl] for venting associated with units and pipeline miles, respectively.

c - Most of the fugitives are associated with units. Therefore the most common unit for fugitive emissions factors is [g/unit-yr]. Other units include [g/mile-yr] for fugitives associated with pipeline miles.

Continued on next page...

Continued from previous page

| Param. | Description | Eq. no. | Default | Literature range | Unit | Sources | Notes |
|----------|--|------------|---------|------------------|------|---------|-------|
| <i>d</i> | Venting of CO ₂ from the AGR units is calculated from the gas balance. | | | | | | |
| <i>e</i> | Most of the venting is associated with events. Therefore the most common unit for vent emissions factors is [g/event]. Other units include [q/unit-yr] and [g/mile-yr] for venting associated with units and pipeline miles, respectively. | | | | | | |
| <i>f</i> | 100-year GWPs from the IPCC Fourth Assessment Report [195]. | | | | | | |
| <i>g</i> | Standard combustion stoichiometry assuming complete combustion. | | | | | | |
| <i>h</i> | Standard gas densities [156] | | | | | | |
| <i>i</i> | Gas composition can vary. Default gas composition given from [10]. | | | | | | |

Table 5.21: Sources of flaring data and construction notes

| | Flaring volumes | Oil production volumes |
|------|--|---|
| 2010 | OPGEE 1.1e, 'Flaring' worksheet | BP 2016 Statistical Review of World Energy. If unavailable, EIA International Petroleum Production, data series "Total Petroleum and Other Liquids" |
| 2011 | OPGEE 1.1e, 'Flaring' worksheet | <i>ibid.</i> |
| 2012 | Dataset obtained from Chris Elvidge via Jim Duffy, California Air Resources Board, July 21st, 2015. Contains country-level totals from NOAA analysis | <i>ibid.</i> |
| 2013 | World Bank Global Gas Flaring Reduction Partnership, website accessed 5/30/2017 | <i>ibid.</i> |
| 2014 | <i>ibid.</i> | <i>ibid.</i> |
| 2015 | <i>ibid.</i> | <i>ibid.</i> |

5.10 Compressors

OPGEE contains many different compressors, as described in Section 4.3 (Production & Extraction) and Section 4.4 (Surface Processing). Compressor-related calculation steps, such as the determination of pseudocritical properties, acid gas correction factors, compressibility factors (z-factors), pressure, temperatures, and adiabatic work of compression are performed in this worksheet.

5.11 Flaring

Flaring is used to dispose of associated natural gas produced during bulk separation (see Section 4.4) when it cannot be used economically. Gas flaring resulted in emissions of 0.28 Gt CO₂ eq. in 2008, or about 1% of global GHG emissions [25].

Since 1994, NOAA National Geophysical Data Center has estimated flaring volume using satellite imagery [25]. The distribution of estimate flaring volume by country is highly skewed; in 2008 Russia, Nigeria, Iran, and Iraq were the country with the highest flaring volumes [25].

5.11.1 Calculation of flaring emissions

For the calculation of flaring emissions, the key input parameter is the flaring-to-oil ratio, or FOR [scf/bbl]. The FOR is converted into flaring volume using the volume of oil produced:

$$Q_F = \frac{FOR \cdot Q_o}{10^6} \quad [\text{MMscf/d}] \quad (5.34)$$

where Q_F = flaring volume [MMscf/d]; FOR = flaring-to-oil ratio [scf/bbl of oil]; and Q_o = volume of oil produced [bbl/d].

The OPGEE default FOR is given by country-level flaring data [200] and production volumes [201] for the years 2010 to 2015. A detailed listing of sources and compilation notes for flaring data is given in Table 5.21. The default flaring rate is retrieved from the 'Flaring' worksheet based on the field location specified in the 'Active Field' worksheet. The flaring rate in a specific oil field could be significantly higher or lower than the country-average. In the case no default is available for the specified field location, the world average is taken as the default value.

Flaring
1.3

Flaring
Table 4.1

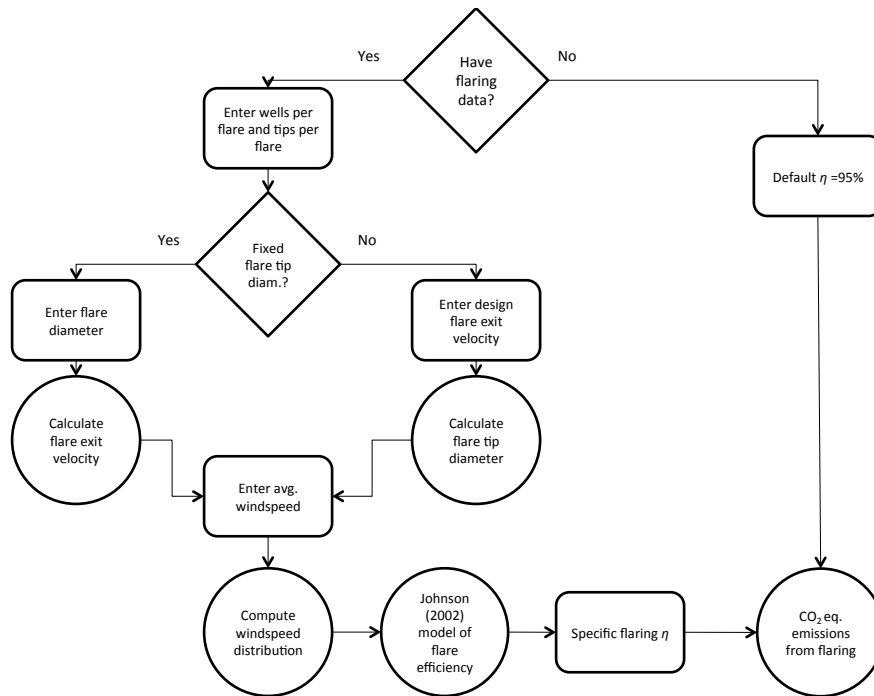


Figure 5.9: Flowchart illustrating the logic of the flaring computation worksheet.

Carbon-dioxide-equivalent flaring emissions are calculated from the flaring volume using the flare efficiency η_F . The flare efficiency is the fraction of flared gas that is combusted. The remaining gas undergoes fuel stripping and is emitted as unburned hydrocarbons.

Flaring
3.1

Flare efficiency varies with flare exit velocities and diameters, cross wind speed, and gas composition [23, 24]. For example, flare efficiencies in Alberta were estimated to range from 55% to $\geq 99\%$, with a median value of 95%, adjusted for wind speed distributions [23].

If the user does not have field specific information about the flare system design and average ambient wind conditions, then OPGEE populates the model with a default flare efficiency of 95%. If the user has the full amount of required data (see Table 5.22) then the user can determine the field-specific flaring efficiency.

Flaring
1.1

The logical progression of the flaring worksheet is shown as a flow-chart in Figure 5.9.

OPGEE uses a flare efficiency equation developed by Johnson and Kostiuik [202]:

Flaring 3.1

$$\eta_F = 1 - \frac{A \exp \left[\frac{BU_\infty}{(gVd)^{\frac{1}{3}}} \right]}{LHV^3} \quad (5.35)$$

Where $A = 156.4$ [MJ/kg], $B = 0.318$ [dimensionless], U_∞ is the wind velocity [m/s], g is the gravitational constant [m/s²], V is flare gas exit velocity [m/s], d is flare

Table 5.22: Data requirements for utilizing field-specific flaring calculation.

| Data requirement | Units |
|----------------------------------|----------------------|
| Oil production | [bbl/d] |
| Flaring intensity | [scf/bbl] |
| Number of flares | [#] |
| Number of flare tips per flare | [#] |
| Flare tip diameter | [in] |
| Lower heating value of gas (LHV) | [MJ/kg] or [Btu/scf] |
| Average wind speed | [mph] |

pipe exit diameter [m], and *LHV* is the lower heating value of the flare gas [MJ/kg]. The most impactful parameters on flare efficiency are wind speed, gas exit velocity, and LHV. For completeness, all parameters are discussed below.

A second parametric model by Gogolek was explored [203], but for ease of integration into OPGEE, the Johnson model was selected.

5.11.1.1 Constants

The Johnson and Kostiuk model, contains different values for *A* and *B* given for methane flares and propane flares (the two flare gasses tested in the experiments). We implement the constants for methane flares for two reasons: first, the primary gas component in most flares is methane, and second, there is no simple direct linear relationship that can be used to interpolate the *A* and *B* values when non-pure gas mixtures are flared.

5.11.1.2 Lower heating value

The flare gas LHV is calculated by multiplying the LHV for each component of the gas by that component's mass fraction. The mass fraction of each gas species is taken from the 'Gas Balance' worksheet, and the LHV for each species is taken from the 'Fuel Specs' worksheet. If the flare gas has significant non-combustibles like N₂ and CO₂, the LHV of the gas, and thus the flare efficiency, will be reduced.

Flaring
1.4

5.11.1.3 Flare gas exit velocity and diameter

There are cases where multiple wells feed to a single flare. There are also cases where each flare stack has multiple openings (flare tips) out of which gas exits. To calculate an efficiency, we are interested in the velocity of the gas coming out of each individual flare tip. As such, the user is asked to enter the number of wells per flare and the number of flare tips per flare. The volumetric flowrate of gas exiting through each opening is found by dividing the total flowrate for the field by the number of flare tips in the field.

Flaring
2.1.2
Flaring
2.1.4

Some flare tips have a variable orifice diameter, to allow for more even combustion properties under varying flow conditions. The user therefore first chooses whether they have a fixed diameter flare or a variable diameter flare. If the user chooses a variable tip diameter, then they choose a flow rate to size the flare to. Suggested maximum regulated flare exit velocity are given in the notes section of this entry. A US EPA regulatory standard is used. For onshore U.S. production, the EPA 60.18 40 CFR Ch.1 [204] regulation states that for flares with a LHV of between

Flaring
2.2.1

200 and 1,000 btu/scf, the maximum allowable gas exit velocity is 122 feet/sec. For flares with a LHV above 1,000 btu/scf, the maximum allowable gas exit velocity is 400 feet/sec [204].

Users with pipe diameter information can enter that information. The flare pipe exit diameter is used directly in the Johnson and Kostiuk model, and is also used to calculate the flare gas exit velocity. Flare gas exit velocity is calculated by dividing the mass flux of gas by the cross sectional area of the pipe.

Flaring

2.2.2.1

Flaring

2.2.3.2

Flaring

2.2.3.3

5.11.1.4 Volume of gas flared

If the user knows the volume of gas that is flared in their field, they can input these data. Otherwise, OPGEE estimates this number based on what country the user selected on the 'Active Field' worksheet.

Flaring

1.3

Flaring

Table 4.1

5.11.1.5 Wind Speed

The user must enter an average wind speed for their field. If the user is onshore in the United States, the user can select a local area from the dropdown list, and this will populate the wind speed cell with an average local wind speed. National Oceanic and Atmospheric Administration data on the average wind speed for hundreds of locations across the United States.

Flaring

2.3

Flaring

Table 4.2

Because the efficiency of combustion (5.35) has an exponential dependence on wind speed, a seemingly small increase in wind speed can significantly alter flare efficiency and thus emissions as well. As such, using a yearly average wind speed to calculate flaring efficiency can yield an inaccurate result. To resolve this, the Rayleigh probability distribution method has been adapted and applied from da Rossa [205]. Figure 5.10 illustrates the fit of the Rayleigh distribution to National Renewable Energy Laboratory wind data for 6 randomly chosen wind sites in the western United States.

The Rayleigh method estimates a wind velocity probability distribution based on what is known about wind speeds. In this case, the user input average (mean) wind speed. This method estimates a mode (most frequently occurring wind speed) using the relationship:

$$m_U = \frac{\mu_U}{\sqrt{\frac{\pi}{2}}} \quad (5.36)$$

where m_U is the mode of the windspeed [mph], and μ_U is the average (mean) wind-speed [mph].

The probability density curve for the Rayleigh distribution is calculated from the mode using the expression:

$$p(U) = \frac{U}{m_U} \exp \left[-\frac{1}{2} \left(\frac{U^2}{m_U^2} \right) \right] \quad (5.37)$$

where $p(U)$ is the probability of finding wind speeds of velocity U [mph].

To calculate an overall flaring efficiency, the efficiency of combustion at each wind speed along the probability density curve is calculated using (5.35), and efficiencies are summed by their fractional probability. Figure 5.11 shows the probability distribution for an average wind speed of 30 mph. Using the Johnson and

Table 5.23: Stoichiometric relationships for complete combustion.

| Fuel | Stoichiometric factor Π |
|--------------------------------|-----------------------------|
| CO ₂ | 1 |
| CH ₄ | 44/16 |
| C ₂ H ₆ | 88/30 |
| C ₃ H ₈ | 132/44 |
| C ₄ H ₁₀ | 176/58 |

Kostiuk (2002) model with these data, OPGEE calculates the flaring combustion efficiency.

Flaring
3.1

5.11.2 Emissions from flares

Emissions from non-combusted gas are calculated using the composition of associated gas from the 'Gas Balance' worksheet:

Flaring
3.2.2.1

$$EM_{F, str} = Q_F(1 - \eta_F) \sum_i x_i \rho_i GWP_i \quad [\text{tCO}_2\text{eq/d}] \quad (5.38)$$

where $EM_{F, str}$ = flaring emissions from stripped, non-combusted gas [tCO₂eq/d]; η_F = flaring efficiency [%]; Q_F = flaring volume [MMscf/d]; i = index of gas species CO₂, CH₄, and volatile organic compounds C₂H₆, C₃H₈ and C₄H₁₀; x_i = molar fraction of gas component i [mol/mol]; ρ_i = density of gas component i [g/ft³]; and GWP_i = GWP of gas component i [g CO₂ eq. /g gas].

Emissions from flare combustion products assume complete combustion:

Flaring
3.2.1.1

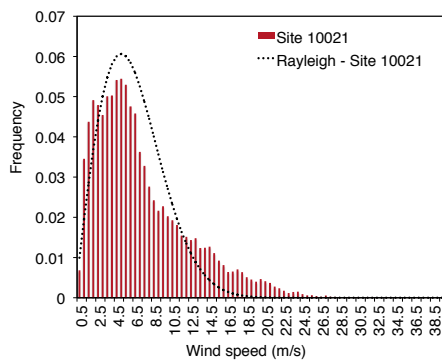
$$EM_{F, comb} = Q_F \eta_F \sum_i x_i \rho_i \Pi_i \quad [\text{tCO}_2\text{eq/d}] \quad (5.39)$$

where $EM_{F, comb}$ = flaring emissions from combusted gas [tCO₂eq./d]; Π_i = stoichiometric relationship between component i and product CO₂ for complete combustion [g CO₂/g gas]. Combustion factors are listed in Table 5.23.

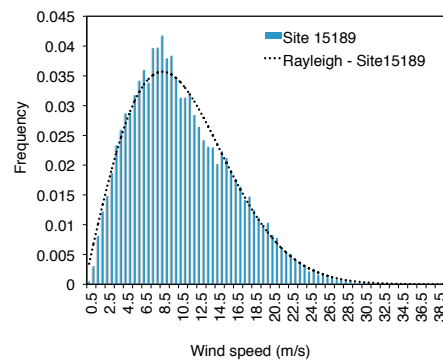
Total flaring emissions are the sum of stripped and combustion emissions:

Flaring
3.2

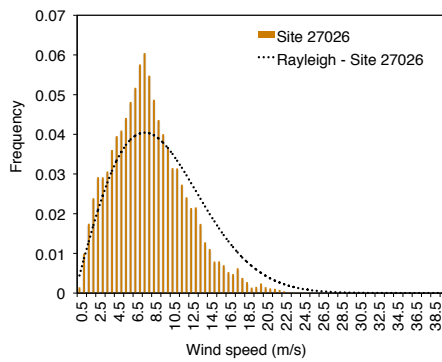
$$EM_{F, tot} = EM_{F, str} + EM_{F, comb} \quad [\text{tCO}_2\text{eq/d}] \quad (5.40)$$



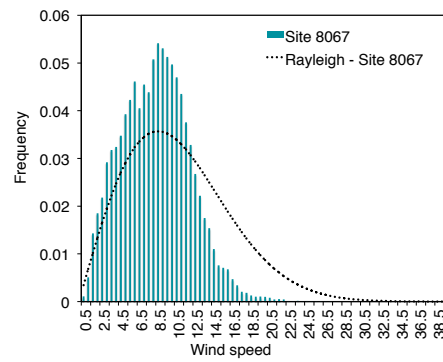
(a)



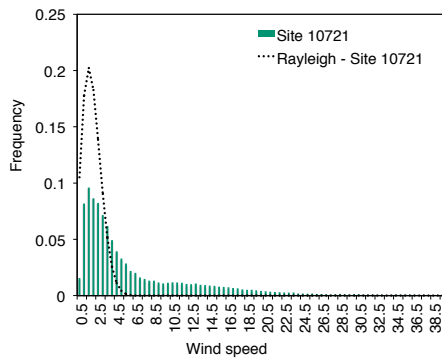
(b)



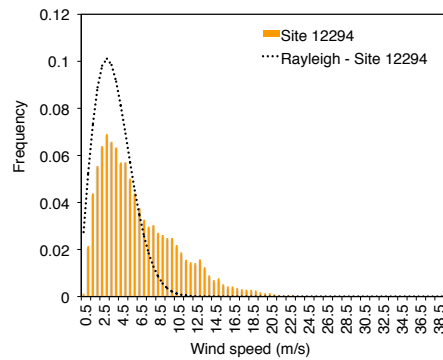
(c)



(d)



(e)



(f)

Figure 5.10: Rayleigh distribution fit to 6 wind speed datasets from western United States. Data source: NREL Western Wind Integration Dataset.

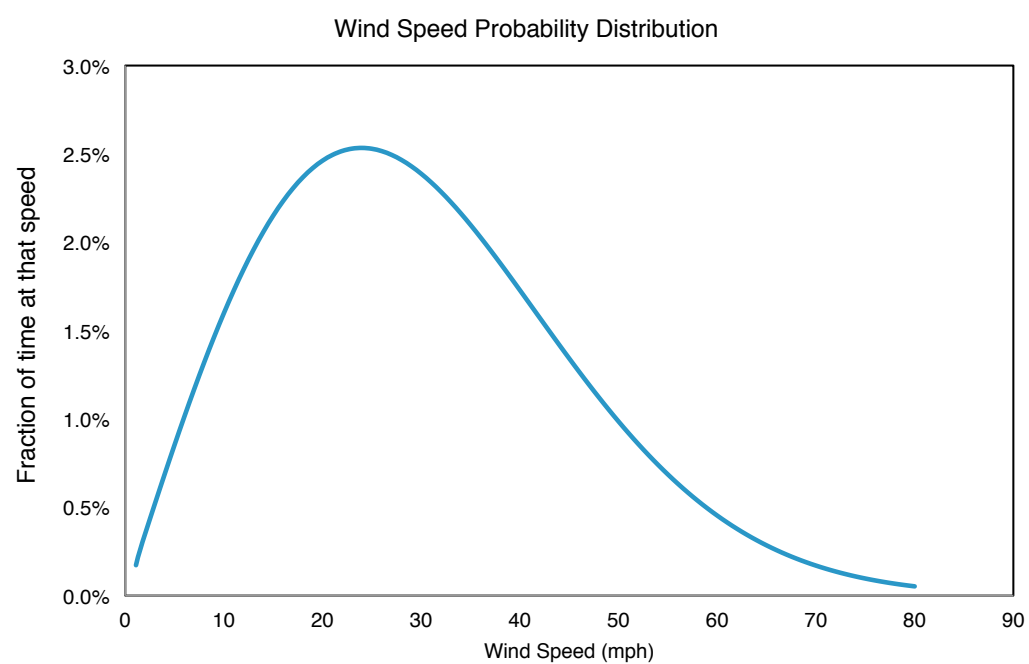


Figure 5.11: Example of OPGEE wind speed distribution for a 30 mph average windspeed input.

Table 5.24: Default inputs for venting, flaring, and fugitive emissions.

| Param. | Description | Eq. no. | Default | Literature range | Unit | Sources | Notes |
|---------------|--|---------|-------------------------|--------------------|--------------------------|---------------|-------|
| A | Flaring eff. pre-exponential constant | - | 156.4 | NA | [MJ/kg] | [202] | |
| B | Flaring eff. growth constant | - | 0.318 | NA | [-] | [202] | |
| d | Flare diameter | - | 3 | 0.25-24 | [in] | | |
| $EM_{F,comb}$ | Flare combustion emissions | (5.39) | - | - | [tCO ₂ eq/d] | | |
| $EM_{F,slr}$ | Flare stripping emissions | (5.38) | - | - | [tCO ₂ eq/d] | | |
| η_F | Flaring efficiency | - | 0.95 | 0.54 - ≥ 0.99 | [-] | [23, 24, 206] | a |
| FOR | Flaring-to-oil ratio | - | 177 | 11-3010 | [scf/bbl] | | |
| g | Gravitational constant | - | 9.8 | - | [m/sec ²] | | |
| GWP_i | Global warming potential for species i | - | 'Input data' Table 2.1 | - | [gCO ₂ eq./g] | [195] | b |
| LHV | Lower heating value of associated gas | - | - | - | [MJ/kg] | | b |
| Π_i | Stoichiometric combustion ratios | - | Table 5.23 | - | [gCO ₂ /g] | - | c |
| Q_F | Flaring volume | (5.34) | - | - | [MMscf/d] | | |
| Q_o | Volume of oil production | - | 1500 | - | [bbl/d] | | |
| ρ_i | Gas density for species i | - | 'Input Data' Table 2.2 | - | [g/ft ³] | - | d |
| U_∞ | Wind speed | - | NA | 0-100 | [mph] | | e |
| V | Flare exit velocity | - | NA | 0-100 | [m/s] | | f |
| x_i | Mole fraction of gas composition | - | 'Gas Balance' Table 1.1 | - | [-] | [10] | g |

a - Average efficiency for Alberta found to be ≈ 0.95 across 4 years of data using known wind distributions and flaring volumes [23]. Very low efficiencies are seen in high cross winds and with high fractions of non-combustible gas components (e.g., CO₂, N₂).

b - 100-year GWPs from the IPCC Fourth Assessment Report [195].

c - Standard combustion stoichiometry assuming complete combustion.

d - Standard gas densities [156]

e - The experimental wind conditions in the Johnson (2002) study only ranged from 4 to 38 mph. OPGEE presents a warning if a wind speed outside of this range is entered.

f - The flare exit velocities in the Johnson (2002) study only ranged from 0.5 to 4 m/s (low momentum flares). OPGEE presents a warning if a wind speed outside of this range is entered. For most flare design conditions, flare exit velocities (and momentum ratios) will be higher than this range, and flare efficiency will be at upper end of model results. Johnson suggest (pers. comm. 2012) that for conditions with momentum ratios above the experimental conditions, a default flaring efficiency of 99.8% be used.

g - Gas composition can vary. Default gas composition given from [10].

6 Gathering worksheets

This section explains three worksheets in OPGEE which are used to collect output from intermediate calculations in process stage and supplemental worksheets. This collected output is used to calculate the overall WTR energy consumption and GHG emissions of the study crude. These gathering worksheets are the ‘Energy Consumption’, ‘GHG Emissions’, and ‘Active Field’ worksheets.

6.1 ‘Energy Consumption’ gathering worksheet

In the ‘Energy Consumption’ gathering worksheet, energy use is summed in order of process stages, from Exploration to Waste disposal. For consistency, all energy inputs are summed on a daily basis, either as thermal energy (MMBtu/d) or as electrical energy (kWh/d). All energy types are classified using a fuel code. The primary energy types included are: 1A) Natural gas; 1B) Natural gas liquids; 2) Diesel fuel; 3) Electricity; 4) Crude oil.

First, the amount and type of fuel consumed by each process stage (e.g., Exploration, Drilling & Development, etc) is collected using nested if then statements. Second, the fuel consumption is summed by fuel type (e.g., natural gas, diesel) to calculate the gross energy consumption.

The gross energy consumption can include double counted energy. For example, the electricity consumed to drive a pump may be generated onsite and the energy consumed to generate that electricity would also be counted as natural gas or diesel, resulting in double counting.

The net energy consumption is calculated by fuel type. The net energy consumption is equal to the gross energy consumption for all fuels except for electricity. The net energy consumption of electricity is calculated as:

$$E_{el,net} = E_{el,gr} - E_{el,gen} \quad [\text{MMBtu}] \quad (6.1)$$

where $E_{el,net}$ = net electricity consumption [MMBtu/d]; $E_{el,gr}$ = gross electricity consumption [MMBtu/d]; and $E_{el,gen}$ = total electricity generated onsite [MMBtu/d]. The total electricity generated onsite includes electricity generated using an onsite generator or simple turbine and electricity co-generated in the steam generation system, if applicable. In other words, the net electricity consumption is equal to the electricity imported from the grid, if any.

Once the net energy consumption is calculated by fuel type the energy exports/imports are calculated by fuel type. Energy exports/imports are used to calculate indirect (offsite) energy consumption and GHG emissions by fuel type. Indirect energy consumption and GHG emissions are associated with the production and transport (production only in case of exports) of the fuel consumed directly. The

Energy
Consumption
Table 1
Energy
Consumption
Table 2

Energy
Consumption
Table 1

Energy
Consumption
Table 3

exports/imports of natural gas are calculated as:

$$E_{ng,exp} = E_{ng,gr} - E_{ng,fuel} + E_{ng,mu} - E_{ng,rec} \quad \left[\frac{\text{MMBtu}}{\text{d}} \right] \quad (6.2)$$

where $E_{ng,exp}$ = natural gas export/import [MMBtu/d]; $E_{ng,gr}$ = gross natural gas consumption [MMBtu/d]; $E_{ng,fuel}$ = natural gas produced as fuel after gas lifting/re-injection [MMBtu/d]; $E_{ng,mu}$ = make up natural gas for gas flooding [MMBtu/d], if applicable; and $E_{ng,rec}$ = natural gas recovered from venting and fugitives. The produced gas remaining to be used as a process fuel is equal to 0 MMBtu/d in the case of gas flooding where 100% of produced gas is re-injected. Negative $E_{ng,exp}$ represents gas exports. Positive $E_{ng,exp}$ represents gas imports.

The exports/imports of natural gas liquid (NGL) is calculated as:

$$E_{ngl,exp} = E_{ngl,gr} - E_{ngl,fuel} \quad \left[\frac{\text{MMBtu}}{\text{d}} \right] \quad (6.3)$$

where $E_{ngl,exp}$ = NGL export/import [MMBtu/d]; $E_{ngl,gr}$ = gross NGL consumption [MMBtu/d]; and $E_{ngl,fuel}$ = amount of NGL produced as fuel [MMBtu/d].

The import of diesel is equal to gross diesel consumption. The export of diesel does not apply because diesel is not produced in upstream operations. The export/import of electricity is equal to electricity net consumption as calculated in eq. (6.1). Positive net electricity consumption is equal to electricity imported from the grid and negative net electricity consumption is equal to electricity exported to the grid. Crude oil export/import does not apply because crude oil is the main product. Any crude oil used as a process fuel on site is subtracted from the amount produced and shipped (see Section 7).

Finally, the indirect energy consumption by fuel type is calculated. The indirect energy consumption is calculated as:

$$\begin{aligned} E_{k,ind} &= E_{k,exp} E_{k,FC} && \text{for } E_{k,exp} > 0 \\ E_{k,ind} &= E_{k,exp} E_{k,DS} && \text{for } E_{k,exp} < 0 \text{ and displacement} \\ E_{k,ind} &= 0 && \text{for } E_{k,exp} < 0 \text{ and allocation by energy value} \end{aligned} \quad (6.4)$$

where k refers to the fuel type; $E_{k,ind}$ = indirect energy consumption [MMBtu/d]; $E_{k,exp}$ = fuel export/import [MMBtu/d]; $E_{k,FC}$ = fuel cycle energy consumption [MMBtu/MMBtu]; and $E_{k,DS}$ = energy consumption of displaced system in case of fuel export [MMBtu/MMBtu]. For details on the energy consumption of fuel cycles and displaced systems, see Section 5.6.

6.2 'GHG Emissions' gathering worksheet

The GHG emissions gathering worksheet compiles and computes emissions of all emissions types across all process stages. The first step is the calculation of direct GHG emissions from the different components of the model. Direct GHG emissions are calculated as:

$$EM_{s,k} = E_{s,k,gr} EF_{s,k} \quad \left[\frac{\text{gCO}_2\text{eq}}{\text{d}} \right] \quad (6.5)$$

where s = emissions source (e.g., downhole pump driver); k = fuel type;
 $EM_{s,k}$ = direct GHG emissions from the consumption of fuel k in source s [gCO₂eq/d];

Energy
Consumption
Table 4

GHG
Emissions Table 1

and $E_{s,k,gr}$ = gross energy consumption of fuel k in source s [MMBtu/d]; and $EF_{s,k}$ = emissions factor of source s using fuel k [g CO₂ eq./MMBtu]. This equation does not apply to electricity, where direct GHG emissions are equal to 0 gCO₂eq./d.

Next, the GHG emissions from land use, flaring, and venting/fugitives are calculated by process stage. This includes gathering emissions calculated in each process stage and supplemental worksheets.

GHG

Emissions Table 1

The next step is the calculation of indirect GHG emissions by fuel import type. The indirect GHG emissions are calculated as:

GHG

Emissions Table 2

$$\begin{aligned} EM_{k,ind} &= E_{k,exp} EM_{k,FC} && \text{for } E_{k,exp} > 0 \\ EM_{k,ind} &= E_{k,exp} EM_{k,DS} && \text{for } E_{k,exp} < 0 \text{ and displacement} \\ EM_{k,ind} &= 0 && \text{for } E_{k,exp} < 0 \text{ and allocation by energy value} \end{aligned} \quad (6.6)$$

where k refers to the fuel type; $EM_{k,ind}$ = indirect GHG emissions from fuel consumption [gCO₂eq/d]; $E_{k,exp}$ = fuel export/import [MMBtu/d]; $EM_{k,FC}$ = fuel cycle GHG emissions [gCO₂eq/MMBtu]; and $EM_{k,DS}$ = GHG emissions from displaced system in case of fuel export [gCO₂eq/MMBtu]. For details on the GHG emissions of fuel cycles and displaced systems, see section 5.6.

Finally, the GHG emissions gathering worksheet considers the impact of CO₂ sequestration. Sequestration-related calculations are applicable only if gas flooding is selected as a production practice and CO₂ is selected as the flood gas. Table 3 is an overview of system-level calculations related to CO₂ sequestration.

GHG

Emissions Table 3

The CO₂ sequestration credited to the oilfield is included in the overall calculations in the 'Results' worksheet. It is calculated by first considering the source of the CO₂. If the CO₂ was acquired from a naturally occurring subterranean source then no sequestration credit accrues because this CO₂ was already sequestered. A sequestration credit is applicable only if the CO₂ originated from an anthropogenic source — it must have been captured during industrial process such as coal combustion.

Active Field
2.4.7.2

Furthermore, depending on the specific regulations and laws governing CO₂ sequestration, the credit may accrue either to the CO₂ capturing facility or to the oilfield operator injecting it into a reservoir. OPGEE also deducts CO₂ that is released due to long-term reservoir leakage and an oilfield operator's decision to conduct terminal phase blow-down operations. OPGEE's consideration of long-term leakage and operator blow-down is described in Section 4.3.2.8.

Production

If the carbon dioxide used for EOR is anthropogenic, then the overall CO₂ sequestration credit accruing to the oilfield is calculated as:

& Extraction
1.2.9.2, 1.2.9.3

$$CR_{CO_2} = P_{oilfield} \cdot (Seq_{CO_2} - Blow_{CO_2} - Leakage_{CO_2}) \quad \left[\frac{gCO_2}{d} \right] \quad (6.7)$$

where CR_{CO_2} = CO₂ sequestration credit assigned to the oilfield [gCO₂/d]; $P_{oilfield}$ = proportion of the overall sequestration credit assigned to the oilfield [-]; Seq_{CO_2} = CO₂ sequestration rate [gCO₂/d]; $Blow_{CO_2}$ = CO₂ lost from the reservoir from terminal blow-down operations [gCO₂/d]; and $Leakage_{CO_2}$ = the amount of CO₂ leaving the reservoir from long-term leakage [gCO₂/d].

7 'Active Field' gathering worksheet

In this worksheet the total energy consumption and GHG emissions for the most recently processed field are calculated and displayed in graphical form. Both the total energy consumption and total GHG emissions are calculated by process stage (e.g., Production & Extraction). First the total energy consumption is calculated as:

$$E_{tot} = \frac{E_{tot,dir} + E_{tot,ind} + EL_{VFF}}{E_{tot,out}} \quad [\text{MJ}/\text{MJ}_{out}] \quad (7.1)$$

Active Field 3.1.1.

- 3.7.1, Table 1

where E_{tot} = total energy consumption of the process $[\text{MJ}/\text{MJ}_{out}]$; $E_{tot,dir}$ = total direct energy consumption (calculated in the 'Energy Consumption' worksheet as net energy consumption) $[\text{MMBtu}/\text{d}]$; $E_{tot,ind}$ = total indirect energy consumption (calculated in the 'Energy Consumption' worksheet) $[\text{MMBtu}/\text{d}]$; EL_{VFF} = total energy loss from VFF emissions $[\text{MMBtu}/\text{d}]$; and $E_{tot,out}$ = total process energy output $[\text{MMBtu}/\text{d}]$. The total process energy output is calculated as:

Active Field 5.1.1.

- 5.9.1

$$E_{tot,out} = Q_o HV_o + E_{ngl,blend} - E_{co,net} \quad [\text{MMBtu}/\text{d}] \quad (7.2)$$

where $E_{tot,out}$ = total process energy output $[\text{MMBtu}/\text{d}]$; Q_o = volume of oil production $[\text{bbl}/\text{d}]$; HV_o = heating value of crude oil $[\text{MMBtu}/\text{bbl}]$;

$E_{ngl,blend}$ = amount of produced NGL that is added to crude oil $[\text{MMBtu}/\text{d}]$; and $E_{co,net}$ = net crude oil consumption, if applicable $[\text{MMBtu}/\text{d}]$. The heating value HV for the denominator crude oil can be selected as LHV or HHV.

Fuel Specs 1.1

If the allocation of co-products is done by energy value and not displacement then eq. (7.2) becomes:

$$E_{tot,out} = Q_o HV_o + E_{ngl,blend} - E_{co,net} + \left| \sum_k E_{k,exp} \right| \quad \text{and} \quad E_{k,exp} < 0 \quad (7.3)$$

where $\left| \sum_k E_{k,exp} \right|$ = absolute sum of all energy exports $[\text{MMBtu}/\text{d}]$.

Total energy consumption is allocated by process stage using the fraction of direct energy consumed in a stage (not including the energy consumption of electricity generation). The allocation of energy consumption to different process stages has no effect on the total energy consumption.

For each process stage, GHG emissions are broken down into three categories: (i) combustion/land use, (ii) VFF, and (iii) credit/debt. For combustion/land use emissions, the direct GHG emissions and land use GHG emissions associated with the process stage are summed in the 'GHG emissions' worksheet. The direct GHG emissions from electricity generation, if any, are divided between the production & extraction and surface processing stages based on the shares of total direct energy consumption between these stages.

GHG

Emissions Table 1

VFF emissions associated with a process stage are summed from the 'GHG emissions' worksheet. Indirect GHG emissions calculated in the 'GHG emissions' work-

GHG

Emissions Table 1

sheet represent the total net credit/debt, which is allocated by process stage using the same allocation method used for allocating the total energy consumption.

This sheet also includes CO₂ sequestration credited accruing to the oilfield, which are described in Section 4.3.2.8.

Finally, the total energy consumption and GHG emissions from the process stages of crude oil extraction and surface processing of associated fluids are integrated with the total energy consumption and GHG emissions of crude oil transport to the refinery to calculate the life cycle energy consumption and GHG emissions on a well-to-refinery basis. The life cycle GHG emissions, for example, are calculated as:

$$EM_{LC} = EM_{PP,tot} \epsilon_{CT} + EM_{CT,tot} \left[\frac{\text{gCO}_2\text{eq}}{\text{MJ}_{ref}} \right] \quad (7.4)$$

where EM_{LC} = life cycle GHG emissions [gCO₂eq/MJ_F]; $EM_{PP,tot}$ = total GHG emissions from the process stages of crude oil production and processing [gCO₂eq/MJ_{out}]; ϵ_{CT} = crude oil transport loss factor (calculated based on the amount of crude oil lost in transportation) [-]; and $EM_{CT,tot}$ = total GHG emissions from transport [gCO₂eq/MJ_{ref}]. 1 MJ_{out} is one MJ of energy output from crude oil production and processing; and 1 MJ_{ref} is one MJ at refinery gate.

The life cycle energy consumption and GHG emissions are shown in tabular and graphical formats with full GHG emissions breakdown. The total GHG emissions has a separate category for VFF emissions. The energy content of fuels lost to VFF emissions is not tracked as a separate category of energy consumption.

GHG

Emissions Table 2

Active Field

Tables 1.1 - 1.2

Figures 1.1 - 1.2

8 Fundamental data inputs

A variety of fundamental data inputs and conversions are required in OPGEE. These data inputs are included in the worksheets '*Input data*' and '*Fuel Specs*'. These inputs are described below, organized by broad class of property.

8.1 Global warming potentials

Global warming potentials (GWPs) for gases with radiative forcing are taken from the IPCC Fourth Assessment Report [195]. The GWPs used are the 100-year GWPs. *Input Data Table 2.1*

8.2 Properties of water and steam

The density of fresh water at 32 °F is used as the base density of water for lifting, boiling and other calculations in OPGEE. Thermodynamic properties of water and steam are required for steam generation calculations. The following data tables are required for use in steam generation calculations in OPGEE: *Input Data Table 5.1*

- Saturation properties as a function of temperature;
- Saturation properties as a function of pressure;
- Properties of compressed water and superheated steam.

8.2.1 Saturation properties as a function of temperature

Saturation properties of saturated water and steam as a function of saturation temperature are produced using Knovel steam tables [160, Table 1b]. Properties are derived for temperatures starting at 32 °F and in increments of 20 °F from 40 °F to the critical temperature of 705.1 °F. Properties included are liquid and vapor specific volume v [ft³/lb], specific enthalpy h [Btu/lbm], specific internal energy u (Btu/lbm), and specific entropy s [Btu/lbm °R] *Input Data Table 5.2*

8.2.2 Saturation properties as a function of pressure

Saturation properties of saturated water and steam as a function of saturation pressure are produced using Knovel steam tables [160, Table 1d]. Properties are derived for pressures starting at 15 psia in increments of 5 psia from 15 to 2500 psia. Identical properties are included as above. *Input Data Table 5.3*

8.2.3 Properties of compressed water and superheated steam

Properties of compressed water and superheated steam are compiled from Knovel steam tables [160, Table 2b]. Pressures are included from 100 to 1500 psia in increments of 100. The following temperatures are included: 32°F and in increments of 20 °F from 40 °F to 1500 °F. Identical properties are included as above.

Input

Data

Table 5.4

8.3 Properties of air and exhaust gas components

The composition of dry air and densities of gases required in OPGEE are derived from online tabulations [156]. Moisture in atmospheric air varies as a function of temperature and relative humidity. Assumed moisture content is 2 mol%.

Input

Data

Table 2.2

8.3.1 Enthalpies of air and exhaust gas components

The enthalpy of air and exhaust gas at various temperatures and atmospheric pressure is modeled as described above in the Steam Injection methods description (see Section 5.2). Coefficients for the specific heats of gases as a function of temperature are taken from literature tabulations [163, Table A2-E]. Specific heats are integrated to derive the enthalpy change between two temperatures for combustion products (exhaust gases) and inlet air/fuel mixtures.

Input

Data

Tables 4.1 - 4.7

8.4 Compositions and properties of fuels

8.4.1 Heating value of crude oil as a function of density

Crude oil heating values are a function of the chemical composition of the crude oil. Crude oil density can be used to determine the approximate heating value (gross and net heating value, or HHV and LHV) of crude oils. Gross and net crude oil heating values (in Btu per lb and Btu per gallon) are presented as a function of API gravity and are given for API gravities from 0 to 46 °API [90, Table 11]. These heating values are converted to SI units and specific gravity for broader applicability.

Fuel Specs Table

1.1

8.4.2 Crude oil chemical composition as a function of density

Crude oil chemical compositions (C, H, S, (O+N)) are given as a function of the density of crude oil [90, Table 9]. Values are interpolated between those given in the table using a relationship for fraction H as a function of API gravity. O + N contents are assumed to sum to 0.2 wt.%. Sulfur content ranges from 5 wt% to 0.5 wt.%, with approximate concentrations derived from Figure 5.2. Carbon mass fraction is computed by difference.

Fuel Specs Table

1.2

8.4.3 Heat of combustion of gaseous fuel components

A variety of properties were collected for gaseous fuel components, including N₂, Ar, O₂, CO₂, H₂O, CH₄, C₂H₆, C₃H₈, n-C₄H₁₀, CO, H₂, H₂S, and SO₂ [207, Chapter 17] [162]. For simplicity, N₂, Ar and all other inert species are lumped and given properties of N₂. The following properties were collected for each species:

Fuel Specs Table

1.3

- Molar mass [g/mol, mol/kg];

- Moles of C and H per mole of each species (for stoichiometric combustion calculations);
- Higher and lower heating value (HHV, LHV) on a volumetric [Btu/scf], gravimetric [Btu/lbm] and molar basis [Btu/mol, Btu/lbmol]. For completeness, gravimetric energy densities in SI units [MJ/kg] are also included.

8.4.4 Refined and processed fuels heating values

The heating values and densities of refined and processed fuels are taken from the CA-GREET model [84] for a variety of fuels.

*Fuel Specs Table
4.1*

9 OPGEE limitations

9.1 Scope limitations

OPGEE includes within its system boundaries over 100 emissions sources from oil and gas production. The current version of the model (OPGEE v2.0b) includes in the system boundaries emissions sources from all major process stages (e.g., drilling and development, production and extraction, surface processing). However, emissions are subject to significant cutoffs, wherein very small emissions sources are neglected as (likely) insignificant in magnitude. Therefore, some emissions sources from exploration, maintenance, and waste disposal are not explicitly modeled. This cutoff is applied because it would be infeasible (and counter-productive) for regulators or producers to model the magnitude of every emissions source.

Production technologies included in OPGEE are: primary production, secondary production (water flooding), and major tertiary recovery technologies (steam injection). Some production technologies are not included in the current version of OPGEE: polymer and chemical EOR, CO₂ EOR, miscible HC flooding, solar thermal steam generation, insitu combustion, subsurface electric heaters, and cold heavy oil production with sand (CHOPS) are not currently included.

9.2 Technical limitations

9.2.1 Production modeling

OPGEE assumes single phase fluid flow in the calculation of the pressure drop between the well reservoir interface and the well head. In reality, there is a simultaneous flow of both fluid (oil and water) and vapor (associated gas). Results show that pressure drop calculated using a two phase flow model can be significantly lower than that calculated using a single phase flow linear model [53]. The deviation of our single phase flow assumption from reality is expected to increase at high GOR.

In the modeling of TEOR, OPGEE does not model changes in viscosity of the oil in lifting calculations [70]. The concept of TEOR is based on reducing the viscosity of the oil, which decreases the lifting energy requirement. This effect is likely to be small because the bulk of the energy consumption in TEOR is from steam generation and not lifting.

9.2.2 Surface processing

It is infeasible in a model such as OPGEE to account for the many possible variations in surface processing. The goal is to include the most frequently applied processes in the industry, while still retaining some flexibility to model varying operating modes (e.g. placement of flow heater in the oil-water separation scheme).

The energy consumption of the demethanizer unit is calculated using energy factors that are generated from a default configuration [153]. Energy factors are calculated in unit energy per kmol of gas feed. Therefore, energy consumption is sensitive to inlet gas composition. However, the use of a default configuration does not allow accounting for the effect of changes in NGL recovery (e.g., 80% ethane recovery). The user can change the amount of NGL produced by changing the fractions of NGL recovered in the ‘*Surface Processing*’ worksheet but this does not have an effect on the demethanizer energy consumption calculations. Emissions from a demethanizer unit are of small significance and therefore do not warrant a full engineering synthesis which can be reconfigured based on user inputs.

9.2.3 Data limitations

9.2.3.1 VFF data

Flaring rates (MMscf per bbl of oil) used in OPGEE are calculated using country level data, which cannot account for variations in field characteristics and practices [200, 201]. Most fugitive and venting emissions in OPGEE are calculated using emissions factors derived from California Air Resources Board (ARB) industry survey data [10]. Challenges include completeness and quality of data collected in the survey (as is common with all survey results). Also, the data are specific to California where environmental regulations and practices are different than other regions.

It was not possible to obtain operational venting and fugitives emissions factors for the chiller unit and the membrane unit. Operational venting and fugitives are not calculated for these units.

9.2.3.2 Default specifications

The accuracy of OPGEE results is fundamentally related to data inputs available. All inputs to OPGEE are assigned default values that can be kept as is or changed to match the characteristics of a given oil field or crude blend/MCON. If only a limited amount of information is available for a given field, most of the input values will remain equal to defaults. In contrast, if detailed-level data are available, a more accurate emissions estimate can be generated.

Some defaults require more flexible (“smart”) default specifications. The water-oil ratio (WOR) is a major parameter in influencing GHG emissions. OPGEE includes a statistical relationship for water production as a function of reservoir age. The default exponential relationship is a moderate case parameterized with a variety of industry data. Nevertheless, this relationship does not work well in predicting WOR for giant fields with very high per well productivity (e.g., Ghawar in Saudi Arabia).

The GOR varies over the life of the field. As the reservoir pressure drops, increasing amounts of gas evolve from oil (beginning at the bubble point pressure if the oil is initially under-saturated). This tends to result in increasing producing GOR over time. Also, lighter crude oils tend to have a higher GOR. Because of this complexity, a static single value for GOR is not desirable. OPGEE uses California producing GORs to generate GORs for three crude oil bins based on API gravity. All data required to generate empirical correlations for GOR are not likely to be available.

9.3 Future work

In the future we will use more detailed engineering sub-models and more comprehensive data analyses to eliminate the limitations of OPGEE model. OPGEE will be expanded to include innovative production technologies such as solar steam generation. Larger data sets are collected to improve the correlations of WOR and GOR defaults. Another important initiative is the calculation of field-level flaring rates using high resolution satellite data [208]. This is believed to have significant impact on the accuracy of results from OPGEE. Work-in progress include generating and updating venting and fugitives emissions factors using technical reports.

A Terminology: Acronyms and abbreviations

Table A.1: Acronyms and abbreviations.

| Acronym or abbreviation | Description |
|-------------------------|---|
| ABS | Absorbents |
| AGR | Acid gas removal |
| AIR | Air stripping |
| AL | Aerated lagoons |
| ANS | Alaska North Slope |
| API | American Petroleum Institute |
| ARB | California Air Resources Board |
| AS | Activated sludge |
| BHP | Brake horsepower |
| CHOPS | Cold heavy oil production with sand |
| CSS | Cyclic steam stimulation |
| CWL | Wetlands |
| DAF | Dissolved air flotation |
| DEA | Di-ethanol amine |
| DGA | Diglycolamine |
| DMF | Dual media filtration |
| DOGGR | State of California Department of Conservations Division of Oil, Gas and Geothermal Resources |
| EDR | Electrodialysis reversal |
| EGOR | Onsite electricity generation to oil ratio |
| EOR | Enhanced oil recovery |
| EPA | Environmental Protection Agency |
| ERCB | Alberta Energy Resources Conservation Board |
| FOR | Flaring to oil ratio |
| FWKO | Free-water knockouts |
| GAC | Granular activated carbon |
| GGFR | Global Gas Flaring Reduction Partnership at the World Bank |
| GHG | Greenhouse gases |
| GLR | Gas to liquid ratio |
| GOR | Gas to oil ratio |
| REET | Greenhouse Gases, Regulated Emissions, and Energy Use in Transportation Model |
| GT | Gas turbine |
| GWP | Global warming potential |
| HHV | Higher heating value |
| HRSG | Heat recovery steam generator |
| HYDRO | Hydrocyclones |
| IPCC | Intergovernmental Panel on Climate Change |
| LCA | Life cycle assessment |
| LHV | Lower heating value |
| MEA | Monoethanolamine |
| MF | Microfiltration |
| NF | Nanofiltration |
| NGL | Natural gas liquid |

Continued on next page...

Continued from previous page

| Acronym or ab- breviation | Description |
|------------------------------|---|
| NOAA | National Oceanic and Atmospheric Administration |
| OPGEE | Oil Production Greenhouse Gas Emissions Estimator |
| ORG | Organoclay |
| OTSG | Once-through steam generators |
| OZO | Ozone |
| RBC | Rotating biological contactors |
| RO | Reverse osmosis |
| RVP | Reid vapor pressure |
| SAGD | Steam assisted gravity drainage |
| SCO | Synthetic crude oil |
| SOR | Steam to oil ratio |
| SSF | Slow sand filtration |
| TDS | Total dissolved solids |
| TEG | Triethylene glycol |
| TEOR | Thermal enhanced oil recovery |
| TF | Trickling filters |
| THC | Total hydrocarbon |
| UF | Ultrafiltration |
| VFF | Venting, flaring and fugitives |
| VOC | Volatile organic compounds |
| VOR | Venting to oil ratio |
| W&S | Standing and working losses |
| WOR | Water to oil ratio |
| WTR | Well to refinery |

B Mathematical terms and definitions

Mathematical terms and subscripts are defined in Table B.1. Parameters and variables serve as the key signifiers in the formulae. A variety of subscripts are used in the mathematics, and can be divided into:

1. Process stages, represented by a a two- or three-letter capitalized symbol (e.g., DD = Drilling & Development)
2. Sub-processes, represented by two- or three-letter capitalized symbol (e.g. GP = Gas processing)
3. Process flows or environments, represented by lower-case symbols (e.g., a = air)
4. Technologies or technology components, represented by capitalized symbols (e.g., GD = glycol dehydrator)
5. Primary fuels and energy carriers, represented by one- to three-letter lower-case symbols (e.g., di = Diesel fuel)
6. Modifiers, represented by lower-case symbols or word fragments (e.g., avg = average)
7. Gas species, represented by capitalized species formulae (e.g., O_2 = oxygen)

In general, a term in the equation will follow the above order as in:

$$[Param][PROCESS][SUB-PROCESS][flow][TECHNOLOGY][fuel][modifier(s)][SPECIES] \quad (B.1)$$

if an element is not needed, it is simply excluded. To create a (relatively extreme) example, one might have: $p_{OTSG,ng,avg,in}$, which represents average inlet natural gas pressure to the once-through steam generator. Most equation elements will not require this many elements.

Table B.1: Mathematical symbols and subscripts.

| Symbol | Description |
|--|---|
| Parameters and variables | |
| α | Solar absorbance |
| δ | Change |
| ϵ | Loss |
| η | Efficiency |
| γ | Specific gravity |
| λ | Fraction or share |
| ρ | Density |
| $a, b, c, d \dots$ | Constants in fitting equations or from data |
| C | Capacity |
| C | Concentration |
| D | Diameter |
| API | Degrees API |
| e | Energy (per unit of something) |
| E | Energy quantity |
| EF | Emissions factor |
| EL | Energy loss |
| EM | Emissions |
| f | Friction factor |
| f | Fraction of a quantity |
| FOR | Flaring oil ratio |
| GOR | Gas oil ratio |
| GWP | Global warming potential |
| h | Height |
| h | Enthalpy |
| H | Head |
| I | Solar insolation |
| I | Process intensity factor |
| l | Load factor |
| m | Mass |
| MW | Molecular weight |
| N | Number of something |
| p | Pressure |
| P | Power |
| Q | Flow rate |
| R | Ratio |
| r | Radius |
| RVP | Reid vapor pressure |
| T | Temperature |
| U | Effectiveness |
| v | Velocity |
| V | Volume |
| W | Work |
| w | Mass fraction |
| WOR | Water oil ratio |
| x | Mole fraction |
| y | Binary variable |
| Y | Process yield factor |
| Process stages (Index = j) | |
| EX | Exploration |
| DD | Drilling & Development |
| PE | Production & Extraction |
| SP | Surface Processing |
| MA | Maintenance |
| CT | Crude Transport |

Continued on next page...

Continued from previous page

| Symbol | Description |
|--|---|
| <i>SI</i> | Steam Injection |
| <i>EL</i> | Electricity |
| <i>FC</i> | Fuel cycle |
| <i>VFF</i> | Venting, flaring and fugitives |
| <i>LC</i> | Life cycle |
| <i>DS</i> | Displaced system |
| <i>PP</i> | Process stages of curde oil production and processing |
| Sub-processes (Index = j) | |
| <i>EX</i> | Extraction |
| <i>GP</i> | Gas processing |
| <i>ISC</i> | In situ thermal production via CSS |
| <i>ISD</i> | In situ thermal production via SAGD |
| <i>ISF</i> | In situ thermal production via steamflood |
| <i>MI</i> | Integrated mining & upgrading |
| <i>MN</i> | Non-integrated mining & upgrading |
| <i>UP</i> | Upgrading |
| Process flows & Environment (Index = i) | |
| <i>a</i> | Air |
| <i>atm</i> | Atmosphere |
| <i>e</i> | Exhaust |
| <i>f</i> | Fuel |
| <i>fg</i> | Flood gas |
| <i>g</i> | Gas |
| <i>l</i> | Liquid |
| <i>o</i> | Oil |
| <i>w</i> | Water |
| <i>ws</i> | Water as steam |
| Technologies (Index = j) | |
| <i>AGR</i> | General term for an acid gas removal process |
| <i>Amine</i> | Amine-based process |
| <i>B</i> | Barge |
| <i>BP</i> | Booster pump |
| <i>C</i> | Compressor |
| <i>CD</i> | Crude dehydrator |
| <i>Chiller</i> | Chiller unit |
| <i>CP</i> | Circulation pump |
| <i>D</i> | Driver |
| <i>DR</i> | Drill rig |
| <i>EG</i> | Electricity generator |
| <i>F</i> | Flaring |
| <i>F</i> | Fan |
| <i>F</i> | Fugitives |
| <i>G</i> | Generator |
| <i>GD</i> | Gas dehydrator (glycol dehydrator) |
| <i>GP</i> | Glycol pump |
| <i>GS</i> | Generator set |
| <i>GT</i> | Gas turbine |
| <i>HRSG</i> | Heat recovery steam generator |
| <i>M</i> | Motor |
| <i>OTSG</i> | Once-through steam generator |
| <i>P</i> | Pipeline |
| <i>R</i> | Rail |
| <i>R</i> | Roof |
| <i>RE</i> | Reciprocating engine |
| <i>RH</i> | Ryan-Holmes process |
| <i>RP</i> | Reflux pump |

Continued on next page...

Continued from previous page

| Symbol | Description |
|------------|------------------------|
| <i>S</i> | Stabilizer |
| <i>SMR</i> | Steam-methane-reformer |
| <i>T</i> | Tanker |
| <i>T</i> | Tank |
| <i>TR</i> | Truck |
| <i>V</i> | Vent |
| <i>W</i> | Well |

Fuels and energy carriers (Index = *k*)

| | |
|------------|--|
| <i>ag</i> | Associated gas |
| <i>bit</i> | Bitumen |
| <i>c</i> | Coal |
| <i>ck</i> | Coke |
| <i>co</i> | Crude oil |
| <i>db</i> | Diluted bitumen |
| <i>di</i> | Diesel |
| <i>dl</i> | Diluent |
| <i>el</i> | Electricity |
| <i>ng</i> | Natural gas |
| <i>ngl</i> | Natural gas liquids |
| <i>pg</i> | Process gas (upgrader by-product, similar to refinery still gas) |
| <i>pag</i> | Processed associated gas |
| <i>ro</i> | Residual oil |
| <i>sco</i> | Synthetic crude oil |
| <i>sg</i> | Still gas |

Modifiers

| | |
|-------------|-------------------------------------|
| <i>avg</i> | Average |
| <i>atm</i> | Atmospheric |
| <i>b</i> | Base |
| <i>wf</i> | Bottomhole (well-formation) |
| <i>comb</i> | Combusted |
| <i>dir</i> | Direct |
| <i>d</i> | Discharge |
| <i>ent</i> | Entrained |
| <i>exp</i> | Exported |
| <i>gen</i> | Generated |
| <i>gr</i> | Gross |
| <i>heat</i> | Heated |
| <i>im</i> | Imported |
| <i>ind</i> | Indirect |
| <i>inj</i> | Injected (as in an injected stream) |
| <i>in</i> | Input |
| <i>l</i> | Lost |
| <i>mu</i> | Make-up |
| <i>max</i> | Maximum |
| <i>min</i> | Minimum |
| <i>net</i> | Net |
| <i>new</i> | New |
| <i>ot</i> | Other |
| <i>out</i> | Output |
| <i>rem</i> | Removed |
| <i>req</i> | Required |
| <i>res</i> | Reservoir |
| <i>rec</i> | recovered |
| <i>ref</i> | refinery |
| <i>s</i> | Stages |
| <i>sc</i> | Standard conditions |
| <i>str</i> | Stripped |

Continued on next page...

Continued from previous page

| Symbol | Description |
|---------------------------------------|------------------|
| <i>s</i> | Suction |
| <i>th</i> | Thermal |
| <i>tot</i> | Total |
| <i>to</i> | Turn over |
| <i>wh</i> | Wellhead |
| <i>trav</i> | traverse |
| <i>lift</i> | lifting |
| Gas species (Index = <i>i</i>) | |
| C | Carbon |
| CO2 | Carbon dioxide |
| H2 | Hydrogen |
| H2O | Water |
| H2S | Hydrogen sulfide |
| N2 | Nitrogen |
| O2 | Oxygen |

C Tabulated sources for each production stage

The full classification of emissions sources for each production stage is given below in Tables C.1 to C.7.

Each emissions source is classified according to process, sub-process, and specific emissions source. Any variants of that emissions source are listed (if they have material effects on emissions or energy consumption). A sensitivity code is given from 1 to 4 stars (* to ***) based on judgement of the likely magnitude of the source. Lastly, the table indicates whether or not an emissions source is included (incl. = 1 means that the source is included).

Table C.1: Emissions sources from exploratory operations. For inclusion: 0 = not included, 1 = included.

| Main stage | Process | Sub-process | Emissions source | Variants | Sensitivity code | Estimated magnitude | Incl. |
|-----------------------------|-------------------------|---------------------------|--|----------|------------------|---------------------|-------|
| Exploration | Seismic exploration | Terrestrial seismic | Vehicular emissions | - | * | < 0.01 g | 0 |
| | | | Data processing | - | * | < 0.01 g | 0 |
| | | | Consumed materials (charges etc.) | - | * | < 0.01 g | 0 |
| | | | Land use impacts | - | * | < 0.01 g | 0 |
| | | Oceanic seismic | Ship emissions | - | * | < 0.01 g | 0 |
| | | | Data processing | - | * | < 0.01 g | 0 |
| | | | Consumed materials | - | * | < 0.01 g | 0 |
| | | | Prime mover emissions | - | * | < 0.01 g | 0 |
| | Exploratory drilling | Terrestrial drilling | Land clearing and construction | - | * | < 0.01 g | 0 |
| | | | Vents and upset emissions | - | * | < 0.01 g | 0 |
| | | | Drilling flares | - | * | < 0.01 g | 0 |
| | | | Casing and cement | - | * | < 0.01 g | 0 |
| | | | Other material consumption (e.g., frac sand) | - | * | < 0.01 g | 0 |
| | | | Land use impacts | - | * | < 0.01 g | 0 |
| | | | Indirect land use impacts (opening of inaccessible land) | - | * | < 0.01 g | 0 |
| | | | Prime mover emissions | - | * | < 0.01 g | 0 |
| | | Offshore drilling | Drilling flares | - | * | < 0.01 g | 0 |
| | | | Vents and upset emissions | - | * | < 0.01 g | 0 |
| | | | Casing and cement | - | * | < 0.01 g | 0 |
| | | | Energy consumption (other than prime mover) | - | * | < 0.01 g | 0 |
| Waste handling and disposal | Mud and fluid handling | Fracturing fluid disposal | Fugitives from mud | - | * | < 0.01 g | 0 |
| | | | Disposal of mud | - | * | < 0.01 g | 0 |
| | | | Processing and disposal of fracturing fluid | - | * | < 0.01 g | 0 |
| | | | Processing of produced water | - | * | < 0.01 g | 0 |
| | Produced water disposal | | Disposal of produced water (remote or on-site reinjection) | - | * | < 0.01 g | 0 |
| | | | | - | * | < 0.01 g | 0 |

Table C.2: Emissions sources from drilling operations.

| Main stage | Process | Sub-process | Emissions source | Variants | Sensitivity code | Estimated magnitude | Incl. |
|--------------------------|-------------------------------|----------------------------|---|----------|------------------|---------------------|-------|
| Drilling and development | Developmental drilling | Terrestrial drilling | Prime mover emissions | - | ** | 0.1 g | 1 |
| | | | Drilling flares | - | * | ≤ 0.01 g | 0 |
| | | | Vents and upset emissions | - | ** | 0.1 g | 0 |
| | | | Land use impacts | - | ** | 0.1 g | 1 |
| | | | Clearing and construction | - | * | ≤ 0.01 g | 0 |
| | | | Casing and cement embodied emissions | - | * | ≤ 0.01 g | 0 |
| | | | Other materials consumption (e.g., frac sand) | - | * | ≤ 0.01 g | 0 |
| | | | Prime mover emissions | - | ** | 0.1 g | 1 |
| | | | Drilling flares | - | * | ≤ 0.01 g | 0 |
| | | | Vents and upset emissions | - | ** | 0.1 g | 0 |
| | Processing capital investment | Oceanic drilling | Casing and cement embodied emissions | - | * | ≤ 0.01 g | 0 |
| | | | Separator assembly | - | * | ≤ 0.01 g | 0 |
| | | | Separator fabrication | - | * | ≤ 0.01 g | 0 |
| | | | Separator transport | - | * | ≤ 0.01 g | 0 |
| | | | Raw materials manufacture | - | * | ≤ 0.01 g | 0 |
| | | | Various drilling emissions from reinjection wells (see above) | - | * | ≤ 0.01 g | 0 |
| | | | Pump assembly | - | * | ≤ 0.01 g | 0 |
| | | | Pump fabrication and raw materials manufacture | - | * | ≤ 0.01 g | 0 |
| | | | Pump transport | - | * | ≤ 0.01 g | 0 |
| | | | Tank assembly | - | * | ≤ 0.01 g | 0 |
| | Storage capital investment | Storage capital investment | Tank fabrication | - | * | ≤ 0.01 g | 0 |
| | | | Tank transport | - | * | ≤ 0.01 g | 0 |
| | | | Raw materials manufacture | - | * | ≤ 0.01 g | 0 |
| | | | Land use impacts | - | * | ≤ 0.01 g | 0 |
| | | | Pipeline assembly | - | * | ≤ 0.01 g | 0 |
| | | | Pipe fabrication | - | * | ≤ 0.01 g | 0 |
| | | | Pipe transport | - | * | ≤ 0.01 g | 0 |
| | | | Raw materials manufacture | - | * | ≤ 0.01 g | 0 |
| | | | Land use impacts | - | * | ≤ 0.01 g | 0 |
| | | | Other infrastructure fabrication and assembly | - | * | ≤ 0.01 g | 0 |

Table C.3: Emissions sources from production and extraction operations.

| Main stage | Process | Sub-process | Emissions source | Variants | Sensitivity code | Estimated magnitude | Incl. |
|---------------------------|---------------|----------------------------|--|---------------------------|------------------|---------------------|-------|
| Production and extraction | Lifting | Pumping | Combustion for pump driver | - | *** | 1 g | 1.0 |
| | | | Electricity for pump driver | - | *** | 1 g | 1.0 |
| | | Gas lift | Casing and wellhead fugitive emissions | - | *** | 1 g | 1.0 |
| | | | Compressor prime mover emissions | - | *** | 1 g | 1.0 |
| | Injection | Gas injection | Compression electricity emissions | - | *** | 1 g | 1.0 |
| | | | Casing and wellhead fugitive emissions | - | *** | 1 g | 1.0 |
| | | | External gas processing (e.g. N2 production) | - | *** | 1 g | 1.0 |
| | | | Gas compression energy | - | *** | 1 g | 1.0 |
| | | Water injection | [-] Gas sequestration credit (CO2 flood) | - | *** | 1 g | 0.0 |
| | | | Water pumping energy | - | *** | 1 g | 1.0 |
| | | Steam injection | Water pre-treatment | - | * | <= 0.01 g | 0.0 |
| | | | OTSG fuel combustion | NG, produced oil | **** | 10 g | 1.0 |
| | | | Turbine gas consumption (combined cycle) | Low, med, high efficiency | **** | 10 g | 1.0 |
| | Polymer flood | Polymer flood | HRSG duct firing (combined cycle) | - | *** | 1 g | 1.0 |
| | | | [-] Electricity co-production offsets (combined cycle) | Grid mix variation | **** | 10 g | 1.0 |
| | | | Steam pumping energy (if any) | - | * | <= 0.01 g | 0.0 |
| | | | Polymer embodied energy | - | * | <= 0.01 g | 0.0 |
| | | Surfactant/other injection | Polymer mixing | - | * | <= 0.01 g | 0.0 |
| | | | Polymer/water mixture pumping energy | - | * | <= 0.01 g | 0.0 |
| | | | Surfactant/other embodied energy | - | * | <= 0.01 g | 0.0 |
| | | Surfactant/other injection | Surfactant/other mixing | - | * | <= 0.01 g | 0.0 |
| | | | Surfactant/other mixture pumping energy | - | * | <= 0.01 g | 0.0 |
| | | | Surfactant/other mixture pumping energy | - | * | <= 0.01 g | 0.0 |

Table C.4: Emissions sources from surface processing operations.

| Main stage | Process | Sub-process | Emissions source | Variants | Sensitivity code | Estimated magnitude | Incl. |
|-----------------------------------|---------------------------------|--------------------------------|---|--------------------------------|------------------|---------------------|-------|
| Separation and surface processing | Fluid separation | Oil-water-gas separation | Oil-water-gas separation | - | ** | 0.1 g | 1 |
| | | | Oil-water-gas separation with heater-treaters | - | ** | 0.1 g | 1 |
| | | | Associated gas venting | Variations in flare efficiency | **** | 10 g | 1 |
| | | | Associated gas flaring | Variations in flare efficiency | **** | 10 g | 1 |
| | Solid/fluid separation | Solid separation from fluids | Solids removal from separation | - | * | ≤ 0.01 g | 0 |
| | | | Produced gas dehydration | - | * | ≤ 0.01 g | 1 |
| | Gas processing | Gas processing | Produced gas venting and flaring | - | *** | 1 g | 1 |
| | | | Produced water cleanup | - | ** | 0.1 g | 1 |
| | Water treatment and disposal | Water treatment | Produced water handling and pumping | - | ** | 0.1 g | 1 |
| | | | Produced water reinjection | - | *** | 1 g | 1 |
| | Storage (as part of separation) | Water reinjection and disposal | Produced water disposal | - | ** | 0.1 g | 1 |
| | | | Storage pumping energy | - | * | ≤ 0.01 g | 0 |
| | | Storage | Tank assembly and installation | - | * | ≤ 0.01 g | 0 |
| | | | Evaporative and fugitive emissions | - | ** | 0.1 g | 1 |
| | | | Tank materials manufacture | - | * | ≤ 0.01 g | 0 |
| | | | Land use impacts | - | * | ≤ 0.01 g | 0 |

Table C.5: Emissions sources from maintenance operations.

| Main stage | Process | Sub-process | Emissions source | Variants | Sensitivity code | Estimated magnitude | Incl. |
|---------------------------|-------------------|---------------------------|---|----------|------------------|---------------------|-------|
| Maintenance and workovers | Well workover | Terrestrial well workover | Workover rig energy use | - | * | ≤ 0.01 g | 0 |
| | | | Fugitive emissions during workover | - | ** | 0.1 g | 1 |
| | | | Embodied energy in consumed replacement parts | - | * | ≤ 0.01 g | 0 |
| | | Offshore well workover | Workover rig energy use | - | * | ≤ 0.01 g | 0 |
| | | | Fugitive emissions during workover | - | ** | 0.1 g | 1 |
| | Other maintenance | Other maintenance | Embodied energy in consumed replacement parts | - | * | ≤ 0.01 g | 0 |
| | | | Solids removal from separation | - | * | ≤ 0.01 g | 0 |

Table C.6: Emissions sources from waste treatment and disposal operations.

| Main stage | Process | Sub-process | Emissions source | Variants | Sensitivity code | Estimated magnitude | Incl. |
|------------------------------|--|---------------------------------------|--|----------|------------------|---------------------|-------|
| Waste treatment and disposal | Water processing waste | Water treatment waste disposal | Subsurface disposal of concentrated WW residuals | - | * | ≤ 0.01 g | 0 |
| | | | Surface disposal of separated solids | - | * | ≤ 0.01 g | 0 |
| | | | Surface disposal of concentrated WW residuals | - | * | ≤ 0.01 g | 0 |
| | Other waste separation and disposal | Other waste separation and processing | Other waste separation and processing | - | * | ≤ 0.01 g | 0 |
| | | | Other waste storage | - | * | ≤ 0.01 g | 0 |
| | | Other waste disposal | Spills and other upsets | - | * | ≤ 0.01 g | 0 |
| | | | Other waste transport | - | * | ≤ 0.01 g | 0 |
| | | | Other waste disposal (non-hazardous) | - | * | ≤ 0.01 g | 0 |
| | Solid waste disposal and project decommissioning | Solid waste disposal | Other waste disposal (hazardous) | - | * | ≤ 0.01 g | 0 |
| | | | Solid waste separation and processing | - | * | ≤ 0.01 g | 0 |
| | | | Solid waste transport and disposal | - | * | ≤ 0.01 g | 0 |
| | | End of life and decommissioning | Demolition and decommissioning | - | * | ≤ 0.01 g | 0 |
| | | | Scrap and waste disposal | - | * | ≤ 0.01 g | 0 |
| | | | [-] Credit for waste recycling (embodied energy) | - | * | ≤ 0.01 g | 0 |

Table C.7: Emissions sources from transport.

| Main stage | Process | Sub-process | Emissions source | Variants | Sensitivity code | Estimated magnitude | Incl. |
|-------------------------|--------------------------------|-----------------------|--|----------|------------------|---------------------|-------|
| Crude product transport | Pipeline transport | Pipeline transport | Combustion for pump prime mover | - | *** | 1 g | 1 |
| | | | Electricity for pump use | - | *** | 1 g | 1 |
| | | | Process upsets (one-time events) | - | * | ≤ 0.01 g | 1 |
| | | | Leaks (pipeline losses) | - | *** | 1 g | 1 |
| | | | Construction equipment energy use | - | * | ≤ 0.01 g | 0 |
| | Pipeline construction | Pipeline construction | Embodied energy in pipeline materials (cement and steel) | - | * | ≤ 0.01 g | 0 |
| | | | Land use impacts | - | * | ≤ 0.01 g | 0 |
| | | | Combustion in tanker prime mover (bunker fuels) | - | *** | 1 g | 1 |
| | | | Loading and unloading pumping | - | * | ≤ 0.01 g | 1 |
| | | | Flares | - | * | ≤ 0.01 g | 1 |
| | Tanker transport | Tanker transport | Vents, leaks and upsets | - | * | ≤ 0.01 g | 1 |
| | | | Embodied energy in tanker materials (steel) | - | * | ≤ 0.01 g | 0 |
| | | | Construction energy | - | * | ≤ 0.01 g | 0 |
| | | | Storage pumping energy | - | * | ≤ 0.01 g | 0 |
| | | | Tank assembly and installation | - | * | ≤ 0.01 g | 0 |
| | Storage (as part of transport) | Storage | Evaporative and fugitive emissions | - | ** | 0.1 g | 1 |
| | | | Tank materials manufacture | - | * | ≤ 0.01 g | 0 |
| | | | Land use impacts | - | * | ≤ 0.01 g | 0 |

D Bulk assessment macro error correction

The bulk assessment machinery is capable of fixing errors, performing iterative calculations and adjusting input parameters where necessary. It is not practical to perform these computational tasks manually when assessing a large number of projects (100+). The built-in macro ensures consistent treatment across all fields. Errors that are addressed in the macro include:

- Discrepancies between country-average default flaring rate and entered GOR (e.g., flaring module predicts more flaring than field has available);
- Discrepancies between default fugitive emissions of gaseous components and gas available from production;
- Requirement to iteratively solve for the gas composition in the wellbore in the case of gas lift;
- Error with productivity index resulting in negative bottomhole pressures;
- Error resulting from very large frictional lifting penalties due to too-small assumed wellbore;
- Requirement to iteratively solve for gas reinjected to result in 0 gas export.

Figure D.1 shows the logic of errors fixing and entry adjustments related to GOR and gas composition. Other errors and adjustments are shown in Figure D.2. One of the most common errors encountered in running OPGEE is the gas composition error which can result in more than one case of data inconsistency. First, the macro checks to ensure that GOR is at least 10 to satisfy the requirements for leaks in the other sections of the model (not shown in flow chart). Then, the macro tackles the most common gas-related errors are related to flaring and fugitive emissions. First, relying on country-average flaring rates in combination with field-specific GOR can result in flaring more gas than that which is produced. As shown in Figure D.1 the gas composition error is fixed by either increasing GOR to match flaring or decreasing flaring to match GOR. The choice between the two options is based on the input data quality. If flaring volume is default then flaring is adjusted. If GOR is default then GOR is adjusted. If both flaring volume and GOR are user inputs then GOR is adjusted because we assume that the flaring rate, being measured by satellite, is more likely to be accurate than the default GOR.

Another problem is having insufficient CO₂ and VOC in the gas stream to match default system losses from venting and fugitives (see Figure D.1 “Gas Comp Error?”). If this occurs, the GOR is increased by 10 scf/bbl until sufficient gas is available to provide emissions estimates.

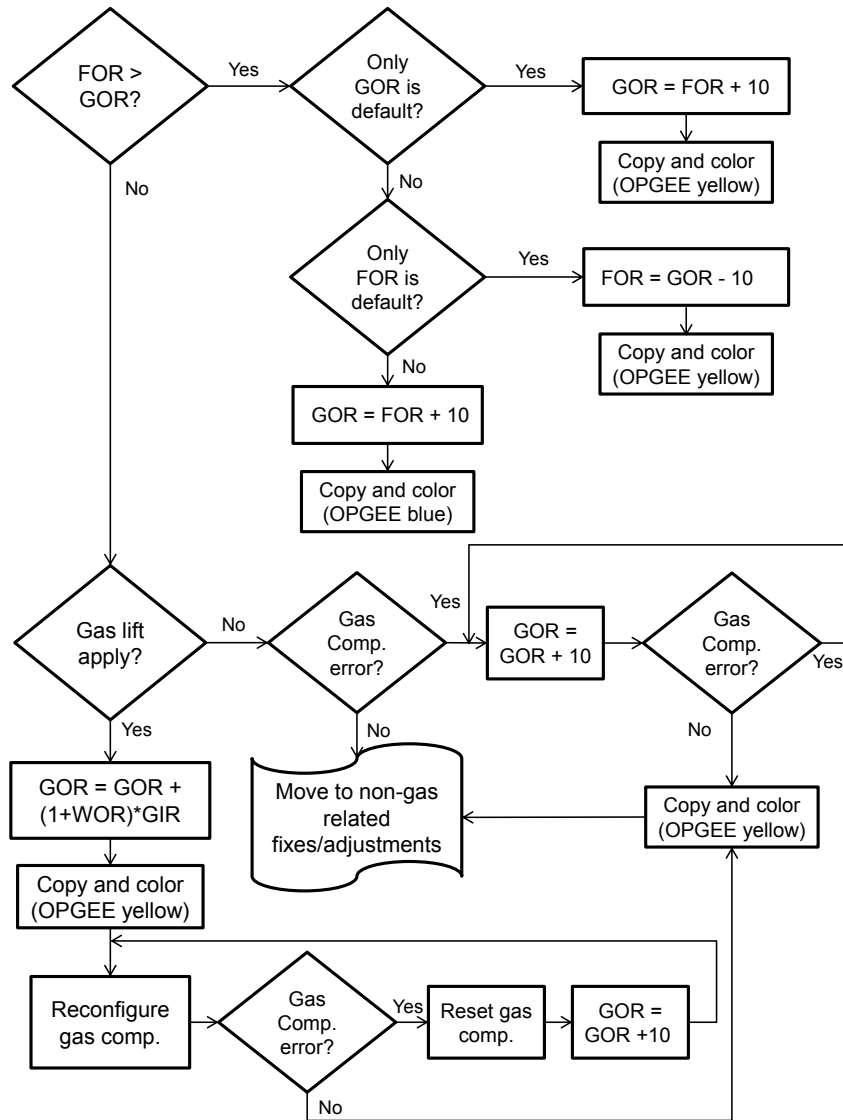


Figure D.1: The errors fixing/entries adjustment logic.

In the case of gas lift, the gas composition in the wellbore is not the reservoir gas composition. The product gas is injected into the well stream, re-processed and re-injected again in a continuous cycle. Therefore the gas at the wellhead separator is a mixture of both the reservoir and product gases. The bulk assessment machinery reconfigures the gas composition by combining the product and reservoir gases in consecutive iterations until the gas composition stabilizes. As shown in Figure D.1 before reconfiguring the gas composition the GOR is adjusted to add the amount of gas injected into the well stream.

Figure D.2 shows the error fixes and adjustments not related to GOR or gas composition.

The second most common error encountered in running OPGEE is the productivity index (PI) error which results when the user or default PI value does not satisfy the minimum bottomhole pressure requirement (0 psi). The bulk assessment

fixes the PI error by incrementally increasing the PI value until the error resolves.

After this, the macro checks for the friction pressure traverse (p_f) as a fraction of total pressure traverse (p_{trav}). In cases where the friction pressure traverse accounts for more than 25% of the total pressure traverse, it is assumed that this is not a realistic system design (e.g., designers would account for and reduce large friction penalties due to effects on lifting costs). Such assumptions are supported by the literature, where the nominal range of the friction pressure traverse is assumed not to exceed 25% of the total pressure traverse [91]. To address this problem, the bulk assessment macro widens the well diameter (D) in increments of 0.25 in. until the friction pressure traverse is $\leq 25\%$.

Finally, if the user chooses to set gas export to zero as opposed to default setting where remaining gas is exported, the bulk assessment machinery increases the gas reinjection fraction by increments of 0.5% until no remaining gas is exported. **To set gas export to ≈ 0 scf the user must enter -1 in the fraction of remaining gas reinjected.**

Colors are used to highlight where the bulk assessment fills in or adjusts data. OPGEE *green color* represents default values. OPGEE *yellow color* represents adjusted parameters. And OPGEE *red color* represents warnings in case the adjusted parameter exceeds literature range / design standards (e.g., >4.5 inch production well diameter) [53, p. 106].

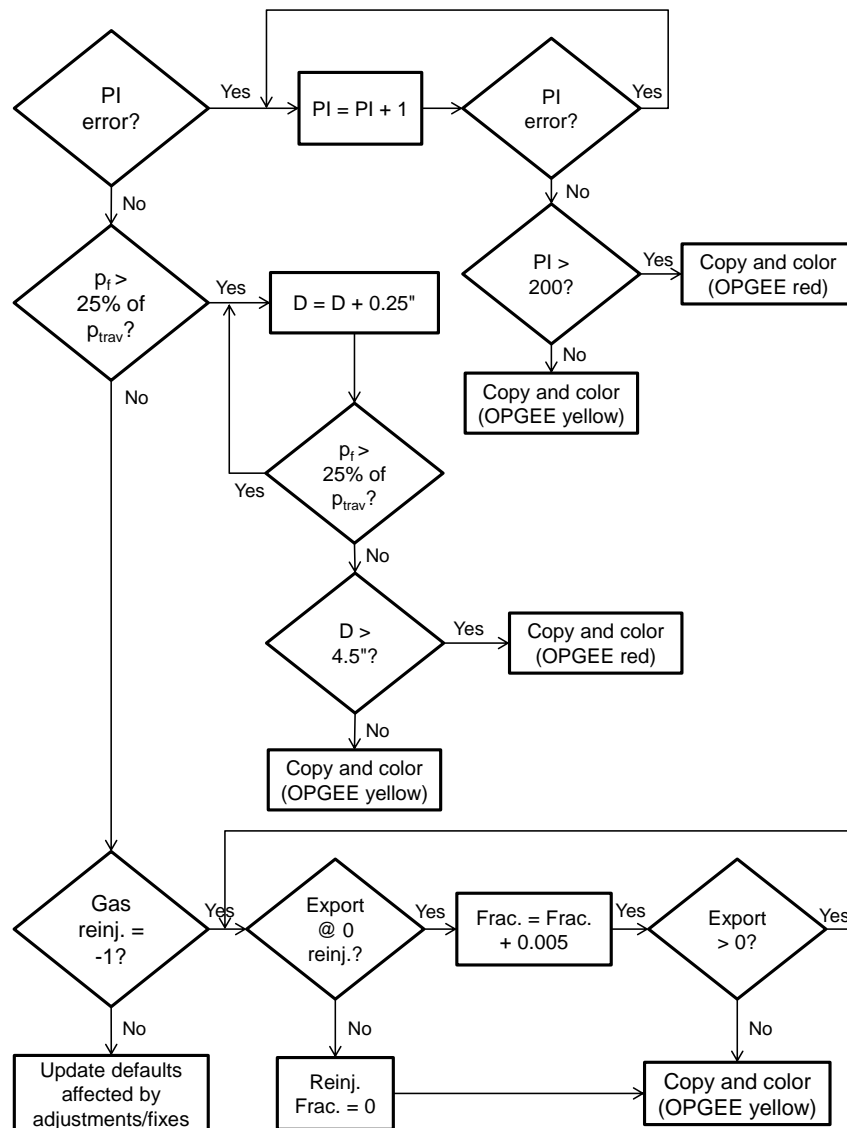


Figure D.2: The errors fixing/entries adjustment logic for non-GOR, gas composition related entries.

E Changes and updates from previous versions of OPGEE

E.1 Changes and updates from OPGEE v2.0a to OPGEE v2.0b

- Flaring volumes are now updated for OPGEE 2.0b, including flaring volumes from 2010 to 2015. See worksheet "Flaring" for significant modifications.
 - Flaring volumes are updated using NOAA/GGFRP information for country-level flaring volumes over the years 2010-2015.
 - Oil production data is now updated to BP Statistical Review of World Energy, 2016 volume, for all available countries. Data are collected 2010-2015, in thousands of bbl per day.
 - Oil production data for countries not available in BP Statistical Review of World Energy (mostly minor producing countries) are updated using EIA international energy statistics for 2010-2015
- Solar thermal has now been implemented in OPGEE 2.0b as part of a re-implemented steam generation module. The user can now change the fraction of steam generated using solar thermal, on inputs sheet 1.4.13
- We have implemented duct firing in OPGEE 2.0b, as part of a re-implemented steam generation module. The user can now turn on duct firing on the Steam Generation worksheet, item 1.2.7.2.3 The comment about cogeneration crediting is unclear, will reach out to CAPP for more comments.

E.2 Changes and updates from OPGEE v1.1 Draft E to OPGEE v2.0a

- Exploration emissions added
 - Added emissions from seismic exploration efforts, non-productive drilling ("dry holes") and scientific/exploratory wells
- Transport changes
 - Included transport energy use in "Energy consumption" gathering sheet
 - Included transport emissions in "GHG emissions" gathering sheet
 - Included indirect emissions associated with producing energy carriers used in transport, which were neglected in OPGEE 1.1 method of including transport outside of gathering sheets
 - Included truck transport using heavy-duty diesel vehicle from GREET1_2013 model

- Embodied energy added
 - Sheet which models embodied energy in oilfield materials and consumables is added.
 - Embodied emissions worksheet from A.R. Brandt (2015) "Embodied energy and GHG emissions from material use in conventional and unconventional oil and gas operations". Environmental Science & Technology. DOI: 10.1021/acs.est.5b03540
- CO2 EOR feature added
 - Changes throughout model to include CO2 EOR
 - New CO2 accounting table on GHG emissions gathering sheet
 - New compressor work calculations on "Compressor" supplemental sheet
 - New gas balance pathways in "Gas Balance" worksheet
 - New gas processing technologies including membranes and Ryan-Holmes
- Heavy oil and bitumen upgrading added
 - "Upgrading" supplemental worksheet added
 - Upgrading section added to surface processing worksheet
- New analysis features added
 - Change start and end field to allow assessment of subset of fields

E.3 Changes and updates from OPGEE v1.1 Draft D to OPGEE v1.1 Draft E

E.3.1 Steam Injection changes

- Feedwater temperature revised to 140°F to account for recycle of hot produced water
- HRSG exhaust temperature corrected to 350°F

E.4 Changes and updates from OPGEE v1.1 Draft C to OPGEE v1.1 Draft D

E.4.1 Bulk assessment changes

- The overall error check in Bulk Assessment worksheet was not functional in previous versions. In this version, the Bulk Assessment macro checks for the overall error.
- The 'Bulk Assessment' worksheet has been split into two worksheets. Data for many fields should be entered in 'Bulk Assessment - Inputs' worksheet.
- The new 'Bulk Assessment - Results' worksheet reports results and allows monitoring of changes which are automatically applied to the user input variables entered in the 'Bulk Assessment - Data' worksheet.

- The Bulk Assessment macro is fixed to correctly solve for fraction of the remaining gas re-injected required to set the export gas to zero.
- In input data worksheet, row 1896, a new section 8 is added. This table works with the Bulk Assessment macro to verify that the Excel calculation mode is set to "Automatic" which is a requirement for Bulk Assessment worksheet to function correctly. This was overlooked in previous versions.

E.4.2 Fugitive emissions changes

- Modeling of gas dehydration system fugitives and venting are updated with improved California survey data. Now emissions factors are disaggregated depending on whether vapor recovery systems are applied.
- The number of valves, which are used to scale other components, are updated from new California survey data.
- The number of pump seals are updated using new California survey data.
- Pneumatic devices (controllers and chemical injection pumps) added as venting sources, using US EPA emissions intensities. Gas balance changes
- In 'Gas Balance' worksheet the rate of the fuel gas consumption (calculated in Energy Consumption worksheet) is added.
- A warning is added in 'User Inputs & Results' worksheet (I97). This warning is activated when the fraction of the remaining gas reinjected is adjusted to a value that causes the non-reinjected portion of the remaining gas become less than fuel gas demand for on-site use
- In the previous versions when gas lift is the method of recovery and FOR is higher than GOR then OPGEE gives error message on the gas composition.

E.4.3 Documentation and clarity improvements

- In 'Gas Balance' worksheet the 'Fuel Gas/Export' label is changed to 'Fuel gas consumed + export'.
- Typos in 'User Inputs & Results' are corrected: In row 297 and 298, AN19 and AN28 changed to AP19 and AP28

E.5 Changes and updates from OPGEE v1.1 Draft B to OPGEE v1.1 Draft C

- Electricity module substantially revised to allow for variable power source efficiencies Drivers reworked with user-defined functions to greatly simplify calculation of driver energy use.
- Bitumen extraction and upgrading sheet updated to GHGenius version 4.03, utilizing GHGenius fuel use directly, or GHGenius LHVs where direct fuel consumption not available. This avoids incongruity between GREET and GHGenius LHV/HHV ratios.

- In bulk assessment macro, the location of `?Outputs.Range("J97").Value = 0?` is changed. In the previous version (after revision of the electricity module), when the fraction of remaining gas re-injected was set to -1 in bulk assessment work sheet, a type mismatch error would occur.
- In gas balance work sheet `?Process fuel / Export?` is changed to `?Process fuel consumed + Export?`.

E.6 Changes and updates from OPGEE v1.1 Draft A to OPGEE v1.1 Draft B

E.6.1 Gas balance and gas properties

- Gas balance sheet fixed so that gas compositions of $C_4 = 0\%$ do not trigger gas balance error. This required changing the accounting of fugitive emissions gas composition. Now, if the associated gas processing vents of C_4 are greater than the input of C_4 to gas processing, then no C_4 is assumed vented. Otherwise, the original C_4 venting equation holds. See cell 'Gas Balance' U14.
- Densities of gas changed: standard conditions are changed to 60F and 1 atm. The user can now select the definition of standard conditions. See 'Input Data' section 6: Definition of Standard Condition.
- Density of VOC is computed directly from VOC composition, rather than assuming density is equal to density of ethane (C_2). See 'Gas Balance' Table 1.4.

E.6.2 Production emissions

- Air separation unit work is now populated with literature data for N_2 separation for Cantarell field [101, 102]. The Cantarell field N_2 plant produces 1200 MMSCF/d of N_2 using 500,500 hp of compression power, resulting in power intensity of 417 hp/MMSCF/d. This includes both compression for air separation and compression to field pressure of 1685 psia. OPGEE calculations for compression from OPGEE default of 125 psia to 1685 psia is 185 hp/MMSCF/d. Thus, separation work is calculated as 232 hp/MMSCF/d, or 0.15 kWh/m³ N_2 . See 'Production & Extraction' section 2.7.3. Any additional compression to take N_2 to field pressure is computed in 'Production & Extraction' section 2.7.4.
- A warning is now generated if no artificial lift is specified but reservoir pressure is not enough to provide artificial lift. See cell 'User Inputs & Results' N75.

E.6.3 Venting and fugitives

- Error corrected in 'Venting & Fugitives' section 1.2.8. Fraction of leaking components changed from 25% to a formula that provides a default based

on API gravity. These defaults provided by API studies of leaking components [38]. The percentage of leaking components is outlined in ‘Input Data’ section 7. From Tables 1-1 and 2-1 in API Standard 4589 [38], leaking components were found to be 0.86% in light crude oil service and 0.01% in heavy crude oil service. Because using these values directly causes a sharp discontinuity in crude carbon intensity at 20° API, OPGEE includes an intermediate case between 15° API and 25° API, with a leakage rate equal to the average of light crude oil and heavy crude oil service (0.43%).

- A conversion factor was fixed in computation of emissions from fugitive leaks. An error in ‘Venting & Fugitives’ cell F212:G212 resulted in division by 1,000,000 rather than division by 365. This effect offsets the reduction in leaking components.
- Corrected error in formula in ‘Venting & Fugitives’ cells F212 and G212. An offset error in these two cells was corrected so that cell reference H86 was changed to H87 and H87 was changed to H88.

E.6.4 Other corrections and error fixes

- GHG emissions worksheet error corrected. ‘GHG Emissions’ cell H22 previously called an incorrect emissions factor.
- Cells ‘Bitumen Extraction & Upgrading’ M38 and M40 were corrected to address error in VFF accounting. Cell M138 was changed to:

$$M52 * M57 * F288 / C240 + \dots \quad (E.1)$$

from:

$$M52 * M57 * F288 + \dots \quad (E.2)$$

where cell C240 scales the emissions per bbl of bitumen produced by the volumetric gain or loss upon upgrading to SCO. Cell M140 on the same sheet was changed similarly.

- Error in steam production calculations for default column fixed (did not affect user calculations). The function for default (not user) steam mixture fluid enthalpy in ‘Steam Injection’ section 1.2.11 referenced the wrong cell.

E.7 Changes and updates from OPGEE v1.0 to OPGEE v1.1 Draft A

E.7.1 Overall model organization

- Added worksheet to track model changes
- Changed color themes to OPGEE custom color theme

E.7.2 User inputs & results worksheet

- Organized user inputs worksheet for the implementation of new macro for the bulk assessment
- Allowed removal of gas processing units on the user inputs worksheet
- Added ocean tanker size to user inputs worksheet
- Added volume fraction of diluent as a user input
- Added a separate emissions category for diluent life cycle emissions
- Removed the allocation of off-site GHG emissions (credits/debts)
- Added a separate emissions category for total off-site GHG emissions

E.7.3 Defaults and smart defaults

- Rounded no. of injection wells to the nearest 1 well

E.7.4 Data and input parameters

- Modified land use change emissions factors to account for 30 year analysis period
- Added petroleum coke life cycle energy consumption and GHG emissions

E.7.5 Error checks

- Corrected the '*Gas Balance*' gas composition overall error check
- Added error check to ensure that downhole pump and gas lift do not co-exist (results in miscalculation of required lifting work)
- Added error check to ensure that user input for volume fraction of diluent is not less than the volume fraction of NGL produced onsite as crude oil blend

E.7.6 New model functionality

- Added improved flaring efficiency calculation worksheet
- More detailed demethanizer model now includes energy consumed by demethanizer
 - Added demethanizer input data
 - Added N₂ and H₂S gas densities to input data worksheet
 - Calculated gas feed into demethanizer in kmol
 - Updated gathering worksheets to include energy consumption and emissions of demethanizer

E.7.7 Bulk assessment macro changes

- Developed a new macro which runs the bulk assessment for unlimited number of fields and has a built in logic for errors fixing
- Bulk assessment macro now has the following features:
 - Works with limited datasets, and fills in defaults or smart defaults where applicable
 - Resolves errors by changing programmatically the well diameter, productivity index, GOR etc. See Section 3.7 for details.
 - Uses colors to highlight where the macro fills in or alters data
- Processing configuration flexibility
 - Dehydrator can be switched ON/OFF
 - AGR unit can be switched ON/OFF
 - Demethanizer can be switched ON/OFF
- Diluent blending and upgrading for non oil sands heavy crudes
 - Developed the option of diluent blending after production. The model now accounts for indirect GHG emissions associated with importing NGL for use as diluent. Added an ERROR check to make sure that the diluent volume fraction is the minimum as indicated by model inputs (minimum is NGL produced onsite as crude oil blend).
 - Calculated non-integrated upgrader emissions and energy consumption for non-bitumen pathways using upgrading data from bitumen worksheet
 - Added emissions and energy consumption of non-integrated upgrader (if applicable) to conventional oil GHG emissions

E.7.8 Corrections and improvements

- Changed heater/treater calculations using default oil emulsion (14% emulsified water)
- Corrected the AGR unit venting emissions calculation
- Heating value basis in Bitumen Extraction & Upgrading worksheet is changed from HHV basis to LHV basis to address error in emissions computation
- Fixed treatment of imported vs. on site energy at bitumen production facilities and clarified use of fuel cycle emissions for imported fuels
- Diluted bitumen pathways now exhibit sensitivity in flaring and fugitive emissions computations to level of diluent blending. Upstream flaring and fugitive emissions from diluent life cycle are tracked in the *'Fuel Cycle'* worksheet, and therefore should not be double counted in the *'Bitumen Extraction & Upgrading'* worksheet.

- Improved compressor model (compressor now between 1 and 5 stages)
- Corrected two typo mistakes in the bulk assessment worksheet (scf/bbl liquid for gas lift injection and C4+ instead of C4 for gas composition)
- Corrected flaring emissions calculations (use preprocessing gas composition)

E.7.9 Documentation and model explanation

- Highlighted changes to heater/treater calculations
- Improved description of offsite credits/debts
- Fixed error in documentation of small sources
- Labeling of '*Bitumen Extraction & Upgrading*' Table 4.10 fixed
- Fixed numbering in Bitumen Extraction & Upgrading worksheet

E.8 Changes from OPGEE v1.0 Draft A to OPGEE v1.0

Draft version A of the model was released on June 22nd, 2012 for public review and commenting. A public workshop which was held on the July 12th, 2012 at California Air Resources Board, Sacramento. In this appendix the comments received at this meeting and at other times are addressed as described below.

E.8.1 Major changes

- The version released to the public is now the same as the “pro” version of the model. The public version of the model now contains the macro to run up to 50 fields at one time. See worksheet '*Bulk Assessment Tool*', which allows the user to run multiple cases at once.
- Complex storage tank emissions calculations were removed from OPGEE v1.0 Draft A and replaced with a single parameter. At this time, it was judged that the scale of tank emissions (relatively small) and the complexity with which they were addressed (high complexity) were incommensurate. This is especially the case given the large numbers of parameters needed for the storage tank emissions model, many of which would not likely be available to users of the model. In place of the complex tank calculations, an average tank emissions factor from California data is included.
- The '*User Inputs & Results*' worksheet was significantly expanded to allow easier running of the model with less need to access the detailed calculation worksheets. Parameters added to the '*User Inputs & Results*' worksheet include: fraction of steam generated via cogeneration for thermal EOR; field productivity index; and well production tubing diameter.
- An option is now added to deal with the co-production of oil and other products (NGLs, gas, etc.): OPGEE v1.0 Draft A only treated co-production

with system boundary expansion, while in OPGEE v1.0 Draft B, allocation of emissions by energy content is allowed. In system boundary expansion (also known as co-product displacement or co-product credit method), an alternative production method for the co-produced product is assessed and the resulting emissions are credited to the main product as if the co-product directly displaces material produced elsewhere. In allocation, the emissions are divided between products and co-products in proportion to some measure of output (often energy, mass, or monetary value). The user can now choose the co-product treatment method on the *'Fuel Cycle'* worksheet.

- OPGEE was updated with data from the CA-GREET variant of the GREET model. This update allows better congruence with other California LCFS calculations, which rely on the CA-GREET model. The data inputs changed include fuel properties and upstream (fuel cycle) emissions for use in co-product displacement calculations.
- All calculations were updated to use lower heating values instead of higher heating values. The user can still choose the heating value metric for the denominator energy content of the final result (e.g., g/MJ LHV or g/MJ HHV crude oil delivered to refinery).
- Water injection pressure is now calculated using reservoir pressure and an injectivity index (bbl/psi-well). This is more in line with the calculation of work to lift fluids.

E.8.2 Minor changes

- The user guide is expanded with additional descriptions of the input parameters on the *'User Inputs & Results'* worksheet to reduce uncertainty about the definitions of parameters. These descriptions are included in Section 3.6.1.
- More explanation is given in tables regarding parameters that are outside of literature ranges (e.g., pump and compressor efficiency).
- More attention is drawn to the overall model error check indicator to alert the user to possible errors in model inputs.
- An error is reported when a user puts in an incorrectly spelled country name. This prevents spurious default to average flaring emissions rates that might occur due to simple input errors.
- To address transmission losses between pumps and prime movers, pump efficiency is slightly reduced. This is believed to be a minor factor, and data are not currently available to separate transmission losses from other losses.
- The value for flaring emissions on the *'User Inputs & Results'* worksheet (J99 in OPGEE v1.0 Draft A) is now used to compute flaring emissions.
- The friction factor is now included as a 'User Free' cell instead of a fixed default. This will allow the user to reduce the friction factor in cases of very high well flow rates (flow character in turbulent regime).

- Water reinjection pump suction pressure is added as a parameter to allow for high pressure oil-water separation and resulting reduced pump work.
- Conversion factor from grams to pounds changed to 453.59 g/lb from 453.
- The units that accompanied cell '*Bitumen Extraction & Upgrading*' M164 in OPGEE v1.0 Draft A, are corrected from g/bbl to g/MJ.
- GWP values are allowed to vary for examining differences using 20 and 100 year GWPs.

Bibliography

1. Katz, D.L.; Standing, M.B. Density of Natural Gases. *Transactions of the American Institute of Mining, Metallurgical and Petroleum Engineers* **1942**, *146*, 140–149.
2. Standing, M.B. *Volumetric and phase behavior of oilfield hydrocarbon systems*; Society of Petroleum Engineers of AIME: Dallas, TX, 1977.
3. Beck, S.; Collins, R. Moody diagram. Technical report, University of Sheffield, 2008.
4. Skone, T.J.; R., J.; Cooney, G.; Jamieson, M.; Littlefield, J.; Marriott, J. Gate-to-Gate Life Cycle Inventory and Model of CO₂-Enhanced Oil Recovery. Technical Report DOE/NETL-2013/1599, U.S. Department of Energy, National Energy Technology Laboratory, 2013.
5. Manning, F.S.; Thompson, R. *Oilfield processing of petroleum, Volume 1: Natural gas*; PennWell: Tulsa, OK, 1991.
6. Yeh, S.; Jordann, S.M.; Brandt, A.R.; Turetsky, M.; Spatari, S.; Keith, D.W. Land use greenhouse gas emissions from conventional oil production and oil sands. *Environmental Science & Technology* **2010**, *44*, 8766–8772.
7. Haynes, H.; Thrasher, L.; Katz, M.; Eck, T. An Analysis of the Potential for Enhanced Oil Recovery from Known Fields in the United States–1976 to 2000. Technical report, National Petroleum Council, 1976.
8. McAllister, E. *Pipeline rules of thumb handbook, 7th edition*; PennWell: Tulsa, OK, 2009.
9. Vlasopoulos, N.; Memon, F.; Butler, D.; Murphy, R. Life cycle assessment of wastewater treatment technologies treating petroleum process waters. *Science of the Total Environment* **2006**, *367*, 58–70.
10. Lee, S. 2007 Oil and Gas Industry Survey Results: Draft Report. Technical report, California Environmental Protection Agency, Air Resources Board, 2011.
11. Detwiler, S. 2007 Oil and Gas Industry Survey Results - Final Report (Revised). Technical report, October 2013.
12. API. Calculation Workbook For Oil And Gas Production Equipment Fugitive Emissions. Workbook API publication number 4638, American Petroleum Institute, 1996.
13. Keesom, W.; Unnasch, S.; Moretta, J. Life cycle assessment comparison of North American and imported crudes. Technical report, Jacobs Consultancy and Life Cycle Associates for Alberta Energy Resources Institute, 2009.
14. Rosenfeld, J.; Pont, J.; Law, K.; Hirshfeld, D.; Kolb, J. Comparison of North American and imported crude oil life cycle GHG emissions. Technical report, TIAX LLC. and MathPro Inc. for Alberta Energy Research Institute, 2009.

15. Howarth, G. Carbon Intensity of Crude Oil in Europe Crude. Technical report, Energy-Redefined LLC for ICCT, 2010.
16. Skone, T.J.; Gerdes, K.J. Development of baseline data and analysis of life cycle greenhouse gas emissions of petroleum-based fuels. Technical Report DOE/NETL-2009/1346, Office of Systems, Analyses and Planning, National Energy Technology Laboratory, 2008.
17. Gerdes, K.J.; Skone, T.J. Consideration of crude oil source in evaluating transportation fuel GHG emissions. Technical Report DOE/NETL-2009/1360, National Energy Technology Laboratory, 2009.
18. Brandt, A.R. Variability and Uncertainty in Life Cycle Assessment Models for Greenhouse Gas Emissions from Canadian Oil Sands Production. *Environmental Science & Technology* **2011**, *46*, 1253–1261.
19. Charpentier, A.D.; Bergerson, J.; MacLean, H.L. Understanding the Canadian oil sands industry's greenhouse gas emissions. *Environmental Research Letters* **2009**, *4*, 14.
20. Charpentier, A.; Kofoworola, O.; Bergerson, J.; MacLean, H. Life Cycle Greenhouse Gas Emissions of Current Oil Sands Technologies: GHOST Model Development and SAGD Application. *Environmental Science & Technology* **2011**, *45*, 9393–9404.
21. Brandt, A.R.; Unnasch, S. Energy intensity and greenhouse gas emissions from California thermal enhanced oil recovery. *Energy & Fuels* **2010**, DOI: 10.1021/ef100410f.
22. (S&T)². GHGenius, model version 4.0c. Technical report, (S&T)² consultants, for Natural Resources Canada, <http://www.ghgenius.ca/>, 2012.
23. Johnson, M. Flare efficiency & emissions: Past & current research. Global Forum on Flaring and Venting Reduction and Natural Gas Utilisation, 2008.
24. Johnson, M.; Wilson, D.; Kostiuik, L. A fuel stripping mechanism for wake-stabilized jet diffusion flames in crossflow. *Combustion Science and Technology* **2001**, *169*, 155–174.
25. Elvidge, C.; Ziskin, D.; Baugh, K.; Tuttle, B.; Ghosh, T.; Pack, D.; Erwin, E.; Zhizhin, M. A fifteen year record of global natural gas flaring derived from satellite data. *Energies* **2009**, *2*, 595–622.
26. Wang, M. GREET Model 1.8d. Computer program, Argonne National Laboratory, <http://greet.es.anl.gov/>, 2010.
27. Abella, J.; Bergerson, J. Model to investigate energy and greenhouse gas emissions implications of refining petroleum: Impacts of crude quality and refinery configuration. *Environmental Science & Technology* **2012**, *46*.
28. EPA. AP-42: Compilation of air pollutant emissions factors, Fifth edition. Technical report, Environmental Protection Agency, 1995.
29. Shires, T.M.; Loughran, C.J. Compendium of Greenhouse Gas Emissions Methodologies for the Oil and Gas Industry. Technical report, American Petroleum Institute, 2004.
30. Azar, J.; Samuel, G.R. *Drilling engineering*; PennWell: Tulsa, OK, 2007.
31. Devereux, S. *Practical well planning and drilling manual*; PennWell: Tulsa, OK, 1998.

32. Gidley, J.L.; Holditch, S.A.; Nierode, D.E.; Veatch, R.W.J. *Recent advances in hydraulic fracturing*; SPE Monograph Series, volume 12, Society of Petroleum Engineers: Richardson, TX, 1989.
33. Lapeyrouse, N.J. *Formulas and calculations for drilling, production and workover, 2nd edition*; PennWell: Tulsa, OK, 2002.
34. Mitchell, R.F. Volume II: Drilling Engineering. In *Petroleum Engineering Handbook*; Lake, L.W., Ed.; Society of Petroleum Engineers: Richardson, TX, 2006.
35. Mitchell, R.F.; Miska, S.Z. *Fundamentals of drilling engineering*; Society of Petroleum Engineers: Richardson, TX, 2011.
36. Wilson, M.J.; Frederick, J.D. *Environmental Engineering for Exploration and Production Activities*; SPE Monograph Series, Society of Petroleum Engineers: Richardson, TX, 1999.
37. API. An engineering assessment of volumetric methods of leak detection in above-ground storage tanks. Technical Report API Publication 306, American Petroleum Institute, 1991.
38. API. Fugitive hydrocarbon emissions from oil and gas production operations. Technical Report API Publication 4589, American Petroleum Institute, 1993.
39. API. Emissions factors for oil and gas production operations. Technical Report API Publication 4615, American Petroleum Institute, 1995.
40. API. Fugitive emissions from equipment leaks II: Calculation procedures for petroleum industry facilities. Technical Report API Publication 343, American Petroleum Institute, 1998.
41. API. Manual of petroleum measurement standards: Chapter 19 - Evaporative-loss measurement - Section 2 - Evaporative loss from floating-roof tanks. Technical Report Formerly API Publication 2517 & 2519, American Petroleum Institute, 2003.
42. API. Evaporation loss from low-pressure tanks. Technical report, American Petroleum Institute, 2006.
43. API. Flare details for general refinery and petrochemical service. Technical Report API/ANSI Standard 537, American Petroleum Institute, 2008.
44. API. Pressure-relieving and depressuring systems. Technical Report ANSI/API Standard 521, Fifth edition, American Petroleum Institute, 2008.
45. API. Compilation of air emission estimating methods for petroleum distribution and dispensing facilities. Technical Report API Publication 1673, American Petroleum Institute, 2009.
46. API. Specification for vertical and horizontal emulsion treaters. Technical Report API Specification 12L, American Petroleum Institute, 2009.
47. API. Specification for indirect type oilfield heaters. Technical Report API Specification 12K, American Petroleum Institute, 2009.
48. API. Specification for oil and gas separators. Technical Report API Specification 12J, American Petroleum Institute, 2009.
49. Arnold, K. *Petroleum Engineering Handbook, Volume III: Facilities and construction engineering*; Society of Petroleum Engineers: Richardson, TX, 2007.

50. Chilingarian, G.V.; Robertson, J.; Kumar, S. *Surface operations in petroleum production I*; Elsevier: New York, 1987.
51. Chilingarian, G.V.; Robertson, J.; Kumar, S. *Surface operations in petroleum production II*; Elsevier: New York, 1989.
52. Cholet, H. *Well production practical handbook*; Editions Technip: Paris, 2000.
53. Clegg, J.D. Volume IV: Production operations engineering. In *Petroleum Engineering Handbook*; Lake, L.W., Ed.; Society of Petroleum Engineers: Richardson, TX, 2007.
54. Fanchi, J.R. Volume I: General engineering. In *Petroleum Engineering Handbook*; Lake, L.W., Ed.; Society of Petroleum Engineers: Richardson, TX, 2007.
55. GPSA. *GPSA Engineering Data Book, 12th edition*; Gas Processors Suppliers Association: Tulsa, OK, 2004.
56. Holstein, E.D. Volume Va: Reservoir Engineering and Petrophysics. In *Petroleum Engineering Handbook*; Lake, L.W., Ed.; Society of Petroleum Engineers: Richardson, TX, 2007. OPGEE.
57. Holstein, E.D. Volume Vb: Reservoir Engineering and Petrophysics. In *Petroleum Engineering Handbook*; Lake, L.W., Ed.; Society of Petroleum Engineers: Richardson, TX, 2007.
58. Leffler, W.L.; Martin, R. *Oil and gas production in nontechnical language*; PennWell: Tulsa, OK, 2006.
59. Manning, F.S.; Thompson, R. *Oilfield processing, Volume 2: Crude oil*; PennWell: Tulsa, OK, 1995.
60. Stewart, M.; Arnold, K. *Gas-liquid and liquid-liquid separators*; Gulf Equipment Guides, Gulf Professional Publishing: Burlington, MA, 2008.
61. Stewart, M.; Arnold, K. *Emulsions and oil treating equipment: Selection, sizing, and troubleshooting*; Gulf Professional Publishing: Burlington, MA, 2009.
62. Stewart, M.; Arnold, K. *Produced water treatment field manual*; Gulf Professional Publishing: Waltham, MA, 2011.
63. Takacs, G. *Modern sucker rod pumping*; PennWell: Tulsa, OK, 1993.
64. Takacs, G. *Sucker rod pumping manual*; PennWell: Tulsa, OK, 2003.
65. Craig, F.F. *The reservoir engineering aspects of waterflooding*; SPE Monograph Series, volume 3, Society of Petroleum Engineers: Richardson, TX, 1993.
66. Jarrell, P.M.; Fox, C.; Stein, M.; Webb, S. *Practical aspects of CO₂ flooding*; SPE Monograph Series, volume 22, Society of Petroleum Engineers: Richardson, TX, 2002.
67. Prats, M. *Thermal recovery*; Henry L. Doherty Series, Volume 7, Society of Petroleum Engineers: Richardson, TX, 1985.
68. Rose, S.C.; Buckwalter, J.F.; Woodhall, R.J. *Design engineering aspects of waterflooding*; SPE Monograph Series volume 11, Society of Petroleum Engineers: Richardson, TX, 1989.
69. Warner, H. Volume VI: Emerging and peripheral technologies. In *Petroleum Engineering Handbook*; Lake, L.W., Ed.; Society of Petroleum Engineers: Richardson, TX, 2007.

70. Green, D.W.; Willhite, G.P. *Enhanced oil recovery*; Henry L. Doherty Memorial Fund of AIME, Society of Petroleum Engineers: Richardson, TX, 1998.
71. Khatib, Z.; Verbeek, P. Water to value - Produced water management for sustainable field development of green and mature fields, 2002.
72. Neff, J.M.; Hagemann, R.E. Environmental challenges of heavy crude oils: Management of liquid wastes. 2007 SPE E&P Environmental and Safety Conference, 2007, Vol. SPE 101973.
73. Reed, M.; Johnsen, S. *Produced water 2: Environmental issues and mitigation technologies*; Plenum Press: New York, NY, 1996.
74. Veil, J.A.; Puder, M.G.; Elcock, D.; Redweik, R.J.j. A white paper describing produced water from the production of crude oil, natural gas, and coal bed methane. Technical report, National Energy Technology Laboratory, 2004.
75. API. Correlation equations to predict Reid vapor pressure and properties of gaseous emissions for exploration and production facilities. Technical Report API Publication 4683, American Petroleum Institute, 1998.
76. API. Fugitive emissions from equipment leaks I: Monitoring manual. Technical Report API Publication 342, American Petroleum Institute, 1998.
77. API. Manual of petroleum measurement standards: Chapter 19 - Evaporative loss measurement - Section 1 - Evaporative loss from fixed-roof tanks. Technical report, American Petroleum Institute, 2008.
78. API. Marine vapor control training guidelines. Technical Report API Recommended Practice 1127, American Petroleum Institute, 1993.
79. API. Venting atmospheric and low-pressure storage tanks. Technical Report ANSI/API Standard 2000, American Petroleum Institute, 2009.
80. API. Ship, barge, and terminal hydrocarbon vapor collection manifolds. Technical Report API Recommended Practice 1124, American Petroleum Institute, 1995.
81. API. Fugitive emission factors for crude oil and product pipeline facilities. Technical Report API Publication 4653, American Petroleum Institute, 1997.
82. Miesner, T.O.; Leffler, W.L. *Oil & gas pipelines in nontechnical language*; PennWell: Tulsa, OK, 2006.
83. Szilas, A. *Production and transport of oil and gas: Part B - Gathering and transport*; Elsevier: New York, NY, 1985.
84. Wang, M. CA-GREET Model v1.8b. Computer program, Argonne National Laboratory, 2009.
85. Vafi, K.; Brandt, A.R. GHGfrack: An open-source model for estimating greenhouse gas emissions from combustion of fuel in drilling and hydraulic fracturing. *Environmental Science & Technology* **2016**: In review.
86. Vafi, K.; Brandt, A. GHGfrack: Model documentation. Technical report, Stanford University, 2016.
87. Vafi, K.; Brandt, A.R., A.R. GHGfrack v1.0 model code. Technical report, Stanford University, 2016.

88. Brandt, A.R. Embodied energy and GHG emissions from material use in conventional and unconventional oil and gas operations. *Environmental Science & Technology* **2015**.
89. Yeh, S. 2012 updates to calculations on land use emissions. Technical report, University of California, Davis, 2012.
90. Schmidt, P.F. *Fuel oil manual*, 4th ed.; Industrial Press: New York, 1985.
91. Takacs, G. *Gas lift manual*; PennWell: Tulsa, OK, 2005.
92. Span, R.; Lemmon, E.W.; Jacobsen, R.T.; Wagner, W.; Yokozeki, A. A Reference Equation of State for the Thermodynamic Properties of Nitrogen for Temperatures from 63.151 to 1000 K and Pressures to 2200 Mpa. *Journal of Physical and Chemical Reference Data* **2000**, 29, 1361–1433.
93. Span, R.; Wagner, W. A New Equation of State for Carbon Dioxide Covering the Fluid Region from the Triple-Point Temperature to 1100 K at Pressures to 800 Mpa. *Journal of Physical and Chemical Reference Data* **1996**, 25, 1509–1596.
94. Lemmon, E.W.; Jacobsen, R.T.; Penoncello, S.G.; Friend, D.G. Thermodynamic Properties of Air and Mixtures of Nitrogen, Argon, and Oxygen from 60 to 2000 K at Pressures to 2000 MPa. *Journal of Physical and Chemical Reference Data* **2000**, 29, 331–385.
95. Schmidt, R.; Wagner, W. A New Form of the Equation of State for Pure Substances and its Application to Oxygen. *Fluid Phase Equilibria* **1985**, 19, 175–200.
96. Lemmon, E.W.; Huber, M.L.; McLinden, M.O. *NIST Standard Reference Database 23: Reference Fluid Thermodynamic and Transport Properties - REFPROP*. National Institute of Standards and Technology, Standard Reference Data Program, Gaithersburg, MD, 9.1 ed., 2013.
97. McCain, W.D. *Properties of Petroleum Fluids*, 2nd ed.; PennWell, 1990.
98. Stewart, W.F.; Burkhardt, S.F.; Voo, D. Prediction of Pseudocritical Parameters for Mixtures **1959**. Presented at the AIChE Meeting, Kansas City, MO.
99. Wichert, E.; Aziz, K. Calculate Z's for sour gases. *Hydrocarbon Processing* **1959**, 51, 119–122.
100. UNEP. Electrical Energy Equipment: Compressors and Compressed Air Systems. Technical report, United Nations Environment Programme, 2006.
101. Bocker, N.; Grahl, M.; Tota, A.; Haussinger, P.; Leitgeb, P.; Schmucker, B., Ullmann's Encyclopeida of Industrial Chemistry; Wiley, 2013; chapter Nitrogen.
102. Kuo, J.; Luna-Melo, J.; Perez, P. World's largest N₂ generation plant. *Oil & Gas Journal* **2001**.
103. Orr Jr, F.; Silva, M. Effect of oil composition on minimum miscibility pressure-part 2: correlation. *SPE Reservoir Engineering* **1987**, 2, 479–491.
104. Oxy Denver Unit CO₂ Subpart RR Monitoring, Reporting and Verification (MRV) Plan. Report submitted by Occidental Petroleum to U.S. Environmental Protection Agency, available online at https://www.epa.gov/sites/production/files/2015-12/documents/denver_unit_mrv_plan.pdf, 2015. Accessed April 2016.

105. Oxy CO₂ EOR Project. Presentation submitted by Occidental Petroleum to California Energy Commission, available online at http://www.energy.ca.gov/sitingcases/hydrogen_energy/documents/others/2012-06-20_OEHI_Project_Overview_workshop_presentation.pdf, 2012. Accessed April 2016.
106. Kang, M.; Baik, E.; Miller, A.R.; Bandilla, K.W.; Celia, M.A. Effective permeabilities of abandoned oil and gas wells: Analysis of Data from Pennsylvania. *Environmental science & technology* **2015**, *49*, 4757–4764.
107. Celia, M.A.; Nordbotten, J.M.; Court, B.; Dobossy, M.; Bachu, S. Field-scale application of a semi-analytical model for estimation of CO₂ and brine leakage along old wells. *International Journal of Greenhouse Gas Control* **2011**, *5*, 257–269.
108. Benson, S.; Cook, P., IPCC Special Report on Carbon Dioxide Capture and Storage; IPCC, 2005; chapter Chapter 5: Underground Geologic Storage.
109. Stevens, S.; Kuuskraa, V.; Taber, J. Sequestration of CO₂ in depleted oil and gas fields: Barriers to overcome in implementation of CO₂ capture and sequestration. *International Energy Agency Greenhouse Gas R&D Programme* **1999**.
110. Leach, A.; Mason, C.; van 't Veld, K. Co-optimization of enhanced oil recovery and carbon sequestration. *Resource and Energy Economics* **2010**, pp. 893–912.
111. Guo, B.; Lyons, W.C. *Petroleum production engineering, a computer-assisted approach*; Gulf Professional Publishing, 2007.
112. Cengel, Y.A.; Turner, R.H. *Fundamentals of thermal-fluid sciences*; McGraw-Hill, 2005.
113. Caterpillar. Oil & Gas Production Power Spec Sheets. Technical report, Caterpillar Oil & Gas Resource Center, 2012.
114. GE. GE Motors Catalog 1.3. Technical report, General Electric, 2011.
115. AER. ST39: Alberta Mineable Oil Sands Plant Statistics. Technical report, Alberta Energy Regulator, 1970-2002, 2008-2012.
116. AER. ST43: Alberta Mineable Oil Sands Plant Statistics – Annual. Technical report, Alberta Energy Regulator, 2003-2007.
117. AER. Alberta Energy Regulator: Personal communication, Toronto ON, 2016. Technical report, Alberta Energy Regulator, 2016.
118. COSIA. COSIA Mining and Extraction Reference Facility – Energy and Material Balance – PFT. Technical report, Canadian Oil Sands Innovation Alliance, 2015.
119. COSIA. COSIA Mining and Extraction Reference Facility – Energy and Material Balance – NFT. Technical report, Canadian Oil Sands Innovation Alliance, 2015.
120. AEMERA. Fugitive GHG Emissions for SGER Oil Sands Facilities: 2011-2014. Technical report, Alberta Environmental Monitoring, Evaluation, and Reporting Agency, Lower Athabasca, 2015.
121. Johnson, M.; Crosland, B.; McEwen, J.; Hager, D.; Armitage, J.; Karimi-Golpayegani, M.; Picard, D. Estimating fugitive methane emissions from oil sands mining using extractive core samples. *Atmospheric Environment* **2016**, *144*, 111–123.
122. (S&T)². GHGenius, model version 4.03. Technical report, (S&T)² consultants, for Natural Resources Canada, 2013.

123. Consultancy, J.E. A greenhouse gas reduction roadmap for oil sands. Technical report, CCEMC, 2012.
124. O&GJ. 2010 Worldwide Oil Field Production Survey. Technical Report Microsoft Excel dataset, Oil & Gas Journal, PennWell publishers, 2009.
125. Simmons, M.R. *Twilight in the desert: The coming Saudi oil shock and the world economy*; John Wiley & Sons, 2005.
126. Simmons, M.R. The world's giant oilfields. Technical report, Simmons & Company International, 2006.
127. Deffeyes, K.S. *Hubbert's peak: The impending world oil shortage*; Princeton University Press: Princeton, NJ, 2001; p. 208.
128. Deffeyes, K.S. *Beyond oil: The view from Hubbert's peak*; Hill and Wang: New York, 2005.
129. O&GJ. A worldwide look at reserves and production. Technical Report Microsoft Excel dataset, Oil & Gas Journal, PennWell publishers, 2009.
130. CDC-DOGGR. 2010 Annual Report of the State Oil & Gas Supervisor. Technical report, California Department of Conservation, Department of Oil, Gas and Geothermal Resources, 2011.
131. AOGCC. Oil and Gas Pools - Statistics Pages. Technical Report http://doa.alaska.gov/ogc/annual/current/annindex_current.html, Alaska Oil and Gas Conservation Commission, 2012.
132. CDC-DOGGR. California Oil and Gas Fields, Volume III - Northern California. Technical report, California Department of Conservation, Division of Oil Gas and Geothermal Resources, 1982.
133. CDC-DOGGR. California Oil and Gas Fields, Volume II - Southern, Central Coastal, and Offshore California. Technical report, California Department of Conservation, Division of Oil Gas and Geothermal Resources, 1992.
134. CDC-DOGGR. California Oil and Gas Fields, Volume I - Central California. Technical report, California Department of Conservation, Division of Oil Gas and Geothermal Resources, 1998.
135. CDC-DOGGR. Online production and injection database. Technical report, California Department of Conservation, Division of Oil, Gas, and Geothermal Resources, <http://opi.consrv.ca.gov/opi/opi.dll>.
136. CDC-DOGGR. Monthly oil and gas production and injection report (January-December). Technical report, California Department of Conservation, Department of Oil, Gas and Geothermal Resources, 2010.
137. Guzmann, M.S. Review of a Forgotten Technology With High Potential-The World Largest Nitrogen Based IOR Project in the Supergiant Field Cantarell, Mexico. SPE Russian Oil and Gas Exploration & Production Technical Conference and Exhibition. Society of Petroleum Engineers, 2014.
138. Pyo, K.; Damian-Diaz, N.; Powell, M.; Nieuwkerk, V. CO₂ flooding in Joffre Viking pool. Canadian International Petroleum Conference. Petroleum Society of Canada, 2003.

139. Malone, T.; Kuuskraa, V. CO₂-EOR Offshore Resource Assessment. Technical Report DOE/NETL-2014/1631, U.S. Department of Energy, National Energy Technology Laboratory, 2014.
140. Johnston, J. Weeks Island gravity stable CO₂ pilot. SPE Enhanced Oil Recovery Symposium. Society of Petroleum Engineers, 1988.
141. Abdel-Aal, H., F.M.; Aggour, M. *Petroleum & Gas Field Processing*; CRC, 2003.
142. U.S. Department of Energy, N.E.T.L. NETL Life Cycle Inventory Data - Unit Process: Gas Stream Chilling, 2012.
143. U.S. Department of Energy, N.E.T.L. NETL Life Cycle Inventory Data - Unit Process: Membrane Separation of CO₂ and Hydrocarbons, 2012.
144. U.S. Department of Energy, N.E.T.L. NETL Life Cycle Inventory Data - Unit Process: Ryan Holmes Gas Separation, 2012.
145. Pacheco, D.; MacLean, H.L. Oil Sands Technology Upgrading Model (OSTUM) model documentation. Technical report, University of Toronto, 2016.
146. Kidnay, A.J.; Parrish, W.R.; McCartney, D. *Fundamentals of Natural Gas Processing*; CRC Press: Boca Raton, FL, 2011.
147. Parro, D. Membrane CO₂ Separation Proves Out At Sacroc Tertiary Recovery Project. *Oil & Gas Journal* **1984**, pp. 85–88.
148. Parro, D. Membrane Technology Matters. *Oil & Gas Journal* **2002**, pp. 43–47.
149. Khan, M.; Manning, W. Practical Designs for Amine Plants. Technical report, Petroenergy Workshop, Houston, TX, 1985.
150. Jones, V.; Perry, C. Fundamentals of gas treating. Gas Conditioning Conference, 1973.
151. Rojey, A.; Jaffret, C. *Natural gas: production, processing, transport*; Editions Technip, 1997.
152. Milligan, E. Evaluation of Permit Application No. 2005-100-TVR, Whiting Oil and Gas Corporation, Dry Trail Gas Plant (SIC 1321), NE/4 of Section 14, T5N, R13E, Texas County, 2007.
153. Nawaz, M.; Jobson, M. Synthesis and optimization of demethanizer flowsheets for low temperature separation processes. *Distillation Absorption* **2010**, pp. 79–84.
154. Dillon, J. Treatment technology review and assessment for petroleum process waters. PhD thesis, Imperial College, 2003.
155. COSIA. COSIA In situ reference facility - SAGD. Technical report, Canadian Oil Sands Innovation Alliance, 2014.
156. The Engineering Toolbox. Technical report, www.engineeringtoolbox.com, 2012.
157. Moritis, G. CO₂ miscible, steam dominate enhanced oil recovery processes: EOR survey. *Oil & Gas Journal* **2010**, 108, 36+.
158. Baibakov, N.; Garushev, A. *Thermal methods of petroleum production*; Developments in Petroleum Science 25, Elsevier, 1989.
159. Donaldson, E.C.; Chilingarian, G.V. *Enhanced oil recovery, processes and operations*; Vol. 17B, *Developments in Petroleum Science*, Elsevier: Amsterdam, 1989.

160. Knovel. Knovel Steam Tables. Technical report, Available from www.knovel.com, 2006, Accessed 2012.
161. Tackett, H.H.; Cripe, J.A.; Dyson, G. Positive displacement reciprocating pump fundamentals - Power and direct acting types. Proceedings of the twenty-fourth international pump users symposium, 2008.
162. Ganapathy, V. *Industrial boilers and heat recovery steam generators: Design, applications and calculations*; Marcel Dekker: New York, 2003.
163. Cengel, Y.A.; Boles, M. *Thermodynamics: An engineering approach*, 5th ed.; McGraw-Hill: New York, 2006.
164. Buchanan, I.; Westphalen, D.; Davies, S.; Chawla, N.; Gieseman, J. SAGD Energy Efficiency Study. Technical report, Jacobs Consultancy, Prepared for Alberta Energy Research Institute, 2009.
165. Speight, J.G. *The chemistry and technology of petroleum*; Chemical Industries, Marcel Dekker: New York, 1994.
166. Swafford, P. Understanding the quality of Canadian bitumen and synthetic crudes. Technical report, Spiral Software, 2009.
167. Cantera: An object-oriented software toolkit for chemical kinetics, thermodynamics, and transport processes. Technical report, <http://code.google.com/p/cantera/>, 2012.
168. Siemens. Industrial gas turbines: The comprehensive product range from 5 to 50 megawatts. Technical report, Siemens AG, 2012.
169. Badeer, G. GE Aeroderivative Gas Turbines - Design and Operating Features. Technical report, GE Power Systems, 2012.
170. Gas Turbine World: 2010 GTW Handbook. Technical report, Fairfield, CT, 2010.
171. Kim, T. Comparative analysis on the part load performance of combined cycle plants considering design performance and power control strategy. *Energy* **2004**, 29, 71–85.
172. Ganapathy, V. Heat-recovery steam generators: Understand the basics. *Chemical Engineering Progress* **1996**.
173. Wang, J.; O'Donnell, J.; Brandt, A.R. Potential solar energy use in the global petroleum sector. *Energy* **2016**.
174. Sandler, J.; Fowler, G.; Cheng, K.; Kovscek, A.R. Solar-generated steam for oil recovery: Reservoir simulation, economic analysis, and life cycle assessment. *Energy Conversion and Management* **2014**, 77, 721–732.
175. Palmer, D.; O'Donnell, J.; Walter, B. Solar enhanced oil recovery application to Kuwait's heavy oil fields. *SPE Kuwait oil and gas show and conference* **2015**.
176. ERCB. ST53: Alberta Crude Bitumen In Situ Production Monthly Statistics, 2010. Technical report, Energy Resources Conservation Board, 2011.
177. CDC-DOGGR. 2009 Annual Report of the State Oil & Gas Supervisor. Technical report, California Department of Conservation, Department of Oil, Gas and Geothermal Resources, 2010.

178. ERCB. ST53: Alberta Crude Bitumen In Situ Production Monthly Statistics, 2009. Technical report, Energy Resources Conservation Board, 2010.
179. company authors, V. In situ progress reports to Alberta Energy Regulator. Technical report, Alberta Energy Regulator, Various.
180. Turbines, S. Gas Turbine Generator Sets. Technical report, Solar Turbines, 2012.
181. Caterpillar. 3512C Offshore Drilling Module. Technical report, Caterpillar Oil & Gas Resource Center, 2012.
182. ISO. ISO 14040: Environmental management - Life cycle assessment - Principles and framework, 2006.
183. ISO. ISO 14044: Environmental management - Life cycle assessment - Requirements and guidelines, 2006.
184. Centre, E. EcoInvent v.3.0 Dataset. Technical report, Swiss Centre for Life Cycle Inventories, 2014.
185. Wang, M. GREET Model 2_2012. Computer program, Argonne National Laboratory, <http://greet.es.anl.gov/>, 2012.
186. Nguyen, J. *Drilling: Oil and Gas Field Development Techniques*; Editions Technip, 1996.
187. Vetcogray. Specialty Connectors & Pipe: For land, platform, jackup, floater and deepwater applications. Technical report, Vetcogray: a GE oil & gas business, http://site.ge-energy.com/businesses/ge_oilandgas/en/literature/en/downloads/specialty_connectors.pdf, 2008, accessed April 2014.
188. API. API Tubing Table. Technical report, American Petroleum Institute, <http://www.oilproduction.net/files/005-apitubing.pdf>, Accessed April 2014.
189. Inc., A.D. Oilfield Data Handbook. Technical report, Apex Distribution Inc., <http://www.monarchapex.com/pdf/Oilfield>
190. Brandt, A.R.e.a. Energy Intensity and Greenhouse Gas Emissions from Crude Oil Production in the Bakken Formation: Input Data and Analysis Methods. Technical report, Argonne National Laboratory, 2015.
191. Corporation, S.E. Two & Three Phase Vertical & Horizontal Separators & Gas Scrubbers. Technical report, Surface Equipment Corporation, <http://www.surfaceequip.com/two-three-phase-vertical-horizontal-separators-gas-scrubbers.html>, 2014.
192. Exterran. Production Solutions: Glycol Dehydration Unit. Technical report, Exterran Holdings Inc., <http://www.exterran.com/Content/Docs/Products/Glycol-Dehydration-Unit-English-Letter.pdf>, 2012.
193. API. Specification for shop welded tanks for storage of production liquids. Technical Report API Specification 12F, American Petroleum Institute, 1994.
194. CIA. The World Factbook. Technical report, Central Intelligence Agency, <https://www.cia.gov/library/publications/the-world-factbook/>, 2013.
195. Solomon, S.; Qin, D.; Manning, M.; Chen, Z.; Marquis, M.; Averyt, K.B.; Tignor, M.; Miller, H.L., Eds. *Contribution of Working Group I to the Fourth Assessment Report of the Intergovernmental Panel on Climate Change 2007*; Cambridge University Press, 2007.

196. Management, N.R. Methane Emissions from the NG Industry. Technical report, Environmental Protection Agency, 1996.
197. Dilmore, R. An Assessment of Gate-to-Gate Environmental Life Cycle Performance of Water-Alternating-Gas CO₂ -Enhanced Oil Recovery in the Permian Basin. Technical Report DOE/NETL-2010/1433, U.S. Department of Energy, National Energy Technology Laboratory, 2010.
198. USEPA. Inventory of US greenhouse gas emissions and sinks: 1990-2012, Annex 3. Technical report, United States Environmental Protection Agency, 2014.
199. Shires, T.; Loughran, C.; Jones, S.; Hopkins, E. Compendium of greenhouse gas emissions methodologies for the oil and natural gas industry. Technical report, Prepared by URS Corporation for the American Petroleum Institute, Washington DC., 2009.
200. NOAA. Global Gas Flaring Estimates. Technical report, National Geophysical Data Center, 2010.
201. EIA. International Energy Statistics - Petroleum. Technical report, U.S. Energy Information Administration, 2010.
202. Johnson, M.R.; Kostiuik, L. A parametric model for the efficiency of a flare in cross-wind. *Proceedings of the Combustion Institute* **2002**, 29, 1943–1950.
203. Gogolek, P. Methane emissions factors for biogas flares. *Industrial combustion* **2012**, p. 17.
204. EPA. EPA Flaring Regulation. Technical Report 60.18 40CFR Ch.1, US Environmental Protection Agency, 2010.
205. da Rossa, A. *Fundamentals of Renewable Energy Processes*; Vol. Version 3, Elsevier Inc., 2012.
206. Johnson, M.; Kistiuk, L. Efficiencies of low-momentum jet diffusion flames in cross-winds. *Combustion and Flame* **2000**, 123, 189–200.
207. Kutz, M., Ed. *Mechanical Engineer's Handbook*, 3rd ed.; Vol. 4, John Wiley & Sons, 2006.
208. Elvidge, C.D. Satellite Data Estimation of Gas Flaring Volumes. Technical report, NOAA, 2012.